

Lecture Notes in Civil Engineering

Rafid Al Khaddar
N. D. Kaushika
S. K. Singh
R. K. Tomar *Editors*

Advances in Energy and Environment

Select Proceedings of TRACE 2020

 Springer

Lecture Notes in Civil Engineering

Volume 142

Series Editors

Marco di Prisco, Politecnico di Milano, Milano, Italy

Sheng-Hong Chen, School of Water Resources and Hydropower Engineering,
Wuhan University, Wuhan, China

Ioannis Vayas, Institute of Steel Structures, National Technical University of
Athens, Athens, Greece

Sanjay Kumar Shukla, School of Engineering, Edith Cowan University, Joondalup,
WA, Australia

Anuj Sharma, Iowa State University, Ames, IA, USA

Nagesh Kumar, Department of Civil Engineering, Indian Institute of Science
Bangalore, Bengaluru, Karnataka, India

Chien Ming Wang, School of Civil Engineering, The University of Queensland,
Brisbane, QLD, Australia

Lecture Notes in Civil Engineering (LNCE) publishes the latest developments in Civil Engineering - quickly, informally and in top quality. Though original research reported in proceedings and post-proceedings represents the core of LNCE, edited volumes of exceptionally high quality and interest may also be considered for publication. Volumes published in LNCE embrace all aspects and subfields of, as well as new challenges in, Civil Engineering. Topics in the series include:

- Construction and Structural Mechanics
- Building Materials
- Concrete, Steel and Timber Structures
- Geotechnical Engineering
- Earthquake Engineering
- Coastal Engineering
- Ocean and Offshore Engineering; Ships and Floating Structures
- Hydraulics, Hydrology and Water Resources Engineering
- Environmental Engineering and Sustainability
- Structural Health and Monitoring
- Surveying and Geographical Information Systems
- Indoor Environments
- Transportation and Traffic
- Risk Analysis
- Safety and Security

To submit a proposal or request further information, please contact the appropriate Springer Editor:

- Pierpaolo Riva at pierpaolo.riva@springer.com (Europe and Americas);
- Swati Meherishi at swati.meherishi@springer.com (Asia - except China, and Australia, New Zealand);
- Wayne Hu at wayne.hu@springer.com (China).

All books in the series now indexed by Scopus and EI Compendex database!

More information about this series at <http://www.springer.com/series/15087>

Rafid Al Khaddar · N. D. Kaushika · S. K. Singh ·
R. K. Tomar
Editors

Advances in Energy and Environment

Select Proceedings of TRACE 2020

 Springer

Editors

Rafid Al Khaddar
Department of Civil Engineering
Liverpool John Moores University
Liverpool, UK

S. K. Singh
Department Civil and Environmental
Engineering
Delhi Technological University
New Delhi, Delhi, India

N. D. Kaushika
Indian Institute of Technology Delhi
New Delhi, Delhi, India

R. K. Tomar
Amity School of Engineering
and Technology
Amity University
Noida, Uttar Pradesh, India

ISSN 2366-2557

ISSN 2366-2565 (electronic)

Lecture Notes in Civil Engineering

ISBN 978-981-33-6694-7

ISBN 978-981-33-6695-4 (eBook)

<https://doi.org/10.1007/978-981-33-6695-4>

© The Editor(s) (if applicable) and The Author(s), under exclusive license to Springer Nature Singapore Pte Ltd. 2021

This work is subject to copyright. All rights are solely and exclusively licensed by the Publisher, whether the whole or part of the material is concerned, specifically the rights of translation, reprinting, reuse of illustrations, recitation, broadcasting, reproduction on microfilms or in any other physical way, and transmission or information storage and retrieval, electronic adaptation, computer software, or by similar or dissimilar methodology now known or hereafter developed.

The use of general descriptive names, registered names, trademarks, service marks, etc. in this publication does not imply, even in the absence of a specific statement, that such names are exempt from the relevant protective laws and regulations and therefore free for general use.

The publisher, the authors and the editors are safe to assume that the advice and information in this book are believed to be true and accurate at the date of publication. Neither the publisher nor the authors or the editors give a warranty, expressed or implied, with respect to the material contained herein or for any errors or omissions that may have been made. The publisher remains neutral with regard to jurisdictional claims in published maps and institutional affiliations.

This Springer imprint is published by the registered company Springer Nature Singapore Pte Ltd.

The registered company address is: 152 Beach Road, #21-01/04 Gateway East, Singapore 189721, Singapore

Preface

The present global objective in civil engineering is to meet the ever-growing demand to handle rising population, various energy–environmental concerns and safety of structures and its inhabitants. The 3rd International Conference on “Trends and Recent Advancement in Civil Engineering” (TRACE) was hosted by Department of Civil Engineering during 20th and 21st August 2020 at Amity University, Uttar Pradesh, Noida, India.

TRACE 2020 focused on advances and rapid evolution of various areas in civil engineering. The conference witnessed participation and presentation of research papers (topical reviews and original articles) from academia, industry expert and researchers from R&D centres from India and abroad. The conference proceedings was classified into three titles:

- Advances in Energy and Environment
- Advances in Geotechnics and Structural Engineering
- Advances in Water Resources and Transportation Engineering

The title *Advances in Energy and Environment* covers papers on contemporary renewable energy and environmental technologies which include water purification, water distribution network, use of solar energy for electricity production, waste management, greening of buildings and air quality analysis. In all twenty-three papers have been selected for publication. It is believed that this collection will be useful to fairly wide spectrum of audience like researchers, application engineers and industry managers.

Liverpool, UK
New Delhi, India
New Delhi, India
Noida, India

Rafid Al Khaddar
N. D. Kaushika
S. K. Singh
R. K. Tomar

Acknowledgements

The conference was organized to fulfil the vision of honourable Dr. Ashok K. Chauhan, Founder President of Ritnand Balved Education Foundation (RBEF), and under the able leadership of honourable Dr. Atul Chauhan, Chancellor, Amity University, Uttar Pradesh, Noida, India. I am also thankful to Honorable Vice Chancellor, Dr. Balvinder Shukla for giving us platform and all the support required for successful conduct and our Jt. HOI's for guiding us by providing vital inputs. I am honored to organize this prestigious conference which connected world's foremost industries with top most academia.

I express my sincerest thanks to all the lead speakers and authors for their original research papers contribution. I also express thanks to all the reviewers for their cooperation in the review process. I am happy to express my deep sense of gratitude to our publication sponsor Springer Nature for publishing the conference proceedings.

I express my gratitude towards all our sponsors: Academic Partners: Liverpool John Moores University, UK; Tribhuvan University, Nepal and Rowan University, USA; Industry Partner: J K Cement Ltd., Defense Infrastructure Planning and Management (DIPM) Council of India; Knowledge Partners: Institution of Civil Engineers, India; Bentley Systems India Pvt. Ltd., Women in Science & Engineering (WISE), India and Indian Geotechnical Society (IGS), Delhi.

Finally, I compliment my team for their hard work and enthusiasm to make TRACE 2020 a success story. I am confident that TRACE 2020 will allow exciting and meaningful conversations, partnerships and collaborations in construction technology and infrastructure growth.

Dr. R. K. Tomar
General Chair, TRACE 2020
Head, Department of Civil Engineering, Amity
School of Engineering and Technology
Amity University
Noida, Uttar Pradesh, India

Contents

Proposed Modification of Solar Still Using PCM for Purification of Ground Water	1
Harsha Yadav, Apurv Yadav, and Asha Anish Madhavan	
An Approach for Reclamation of Salinity Affected Lands for Bio-energy Production	9
Himanshu Tyagi and Anupriya Goyal	
Optimal Design of Water Distribution Network by Reliability Considerations	17
Ashish Mishra, Ishan Sharma, and Rakesh Mehrotra	
Potable Water Production by Single Slope Active Solar Distillation Unit—A Review	31
Ashok Kumar Singh, Dalvir Singh, M. K. Lohumi, B. K. Srivastava, H. P. Gupta, and R. Prasad	
Heavy Metal Assessment in Urban Particulate Matter in Industrial Areas of Vadodara City	43
S. A. Nihalani, A. K. Khambete, and N. D. Jariwala	
An Improved Approach for Accurate Weather Forecasting	55
Shubham Aggarwal, S. Hasnain Pasha, Sunil Kumar Chowdhary, Chetna Choudhary, Shiva Mendiratta, and Pramathesh Majumder	
Planning Approach with “Better Than Before” Concept: A Case Study of Library Building at SVNIT, Surat, Gujarat, India	63
Krupesh A. Chauhan and Bhagyashri H. Sisode	
Wastewater Allocation and Pricing Model for the Efficient Functioning of CETP Serving a Textile Industrial Cluster	85
Bhoomi Shah, Deepak Chaurasia, and Ajit Pratap Singh	
A Low-Cost Decentralized Grey Water Recycling System for Toilet Flushing	95
N. Bhanu Sree	

Water Demand as Fuzzy Random Variable in the Analysis of Water Distribution Networks	103
Prerna Pandey, Shilpa Dongre, and Rajesh Gupta	
Integrating Geospatial Interpolation Techniques and TOPSIS to Identify the Plausible Regions in India to Harness Solar Energy	115
Aditya Kumar Dupakuntla and Harish Puppala	
Utilization Potential of Iron Ore Tailing Waste in Various Applications	125
S. R. Bharath, N. Lavanya, H. B. Bharath Kumar, R. K. Chaitra, and Rahul Dandautiya	
Sustainable Landfill Site Selection for Construction and Demolition Waste Management Using GIS and AHP	135
Bhoomi Shah	
Stationary Source Emissions and Impact Assessment on Ambient Air Quality: A Case Study of Delhi Region	143
Debarshi Ghosh and Madhuri Kumari	
Use of WaterGEMS for Hydraulic Performance Assessment of Water Distribution Network: A Case Study of Dire Dawa City, Ethiopia	151
Bahar Adem Beker and Mitthan Lal Kansal	
Comparative Analysis and Prediction of Ecological Quality of Delhi	163
Syed Zubair, Shailendra Kumar Jain, and Shivangi Somvanshi	
Defluoridation of Drinking Water–Fluoride Wars	179
G. Gayathri, M. Beulah, H. J. Pallavi, and K. Sarath Chandra	
A Review of Electric Power Generation from Solar Ponds Using Organic Rankine Cycle and Air Turbine	189
Gaurav Mittal, Desh Bandhu Singh, Gaurav Singh, and Navneet Kumar	
Major Flows for Lead (Pb) Within an Academic Campus	201
Akash Agarwal, Amit Kumar, and Sanyam Dangayach	
Comparative Analysis of Different Vegetation Indices of Noida City Using Landsat Data	209
Richa Sharma, Lolita Pradhan, Maya Kumari, and Prodyut Bhattacharya	
Review of Biomass Technologies and Practices for Cooking in India	223
Harshika Kumari	
Present Status, Conservation, and Management of Wetlands in India	235
Vandana Shan, S. K. Singh, and A. K. Haritash	

Annual Rainfall Prediction Using Artificial Neural Networks 257
Anjaney Singh, Amit Dua, and A. P. Singh

About the Editors

Dr. Rafid Al Khaddar has extensive experience in Water and Environmental Engineering, with special expertise in wastewater treatment methods. He graduated from the University of Basra, Iraq, as a civil engineer, and obtained his Masters and Ph.D. in Civil Engineering Hydraulics from the University of Strathclyde, Glasgow, UK. He is currently Professor and Head of the Department of Civil Engineering at Liverpool John Moores University where he manages 27 staff and 900 students, who are enrolled in various courses such as HNC, B.Eng., M.Eng., M.Sc. and Ph.D. The Department runs fully accredited degrees by the Institution of Civil Engineers in the UK, and he led a number of these accreditations. He has maintained a very strong link with the UK Water and Environmental industry in order to stay involved with any new developments in the aforementioned fields. He was President of the Chartered Institution of Water and Environmental Management (CIWEM) in 2015–2016. He is also Fellow of the Institution and Honorary Vice President of the Institution. He has developed a number of collaborative programmes with International Universities with the University of Babylon (Iraq), International College for Business and Technology (Sri Lanka) and Oryx Global University (Qatar). He has published over 170 publications in peer-reviewed journals and international conferences. He has managed to attract over £1.5 Million in research and consultancy funding since the year 2000.

Dr. N. D. Kaushika, Formerly Professor, Centre for Energy Studies, Indian Institute of Technology Delhi, and subsequently Director of reputed engineering institutions in Delhi and National Capital Region, is a specialist in renewable energy and environment. He is a recipient of the Hariom Prerit S. S. Bhatnagar Research Endowment Award for research in energy conservation in 1987. Currently, he is Visiting Research Professor at the Institute of Technological Engineering and Research of SOA University, Bhubaneswar, India. He is an author of five books and has contributed articles in several reputed journals and book chapters in several books by international publishers.

Dr. S. K. Singh is Professor and Dean, at Delhi Technological University (DTU), Delhi. He has obtained his Ph.D. from BITS, Pilani, and M.Tech. from IIT (BHU), Varanasi, and B.E. from Gorakhpur University having first division with distinction throughout. He is engaged in teaching, research, administration and consultancy for the last 31 years and is presently Professor of Civil and Environmental Engineering for the last 20 years at DTU, Delhi. He is also Independent Director, WAPCOS Limited (A Mini Ratna-I PSU, GOI). He has guided 12 Ph.D.s, about 65 M.Tech. theses and more than 150 UG Projects. He has participated in various national and international conferences, published more than 214 research papers in national and international journals of repute and authored 04 books. He has provided technical assistance as Member to groups of experts, set up for determining polluting industries in NCT of Delhi; examining proposals for establishing degree/diploma level technical institutions in NCT of Delhi; evaluation of projects for the Department of Science and Technology (DST), Ministry of Environment and Forest, GOI; Member of Board of Governors, CSMRS, Ministry of Water Resources, GOI; Chairman, Departmental Promotion Committee, IASRI (ICAR) New Delhi; Member, University Court, University of Delhi; Expert Member, Equivalence Committee, UPSC, New Delhi; Advisor, Selection Committee for recruitment at UPSC, New Delhi; Technical Expert for various committees of MoEFCC, GOI; Expert Member, DST, GOI; Member, Expert Committee, CAPART, Ministry of Rural Development, Government of India. He has received felicitations and awards by professional bodies such as APJ Abdul Kalam Award 2016, Rashtriya Shiksha Gaurav Puraskar 2014; International Felicitatation and WEC-IIIEE-IAEWP Environmental Award; Rashtriya Samman Puraskar 2005; Excellent Services Award; Clean Up The Earth Award; Eminent Personality Award.

Dr. R. K. Tomar received his Ph.D. from the Indian Institute of Technology (IIT) Delhi and is currently, Head of the Department of Civil Engineering, Amity School of Engineering and Technology, Amity University, India. His research interests include artificial intelligence applications in buildings and sustainable built environment. He has a combined experience of 30 years in industry and academia in various capacities. He has published several research articles in international peer-reviewed journals. He is also guiding students for Ph.D. in the field of Energy and Built Environment.

Proposed Modification of Solar Still Using PCM for Purification of Ground Water



Harsha Yadav , Apurv Yadav , and Asha Anish Madhavan 

Abstract The advent of industrialization increased the problems of water scarcity and groundwater degradation. Solar stills are robust devices to produce fresh water from contaminated. The low productivity of these devices limits their widespread commercial usage. This drawback could be enhanced by the utilization of phase change nanocomposite materials. This paper proposes a design for the modification of solar still by using both nanocomposites and solar photovoltaic energy. The integration of both these approaches will enhance the effectiveness of the process and will increase the productivity of solar stills.

Keywords Groundwater · Solar still · Heat storage · Phase change materials · Nanoparticles

1 Introduction

Overexploitation of groundwater due to industrial development leads to its degradation and increases its salinity [1]. This reduces the already depleting freshwater present in the land. Potable water scarcity is one of the greatest challenges around the world, because of the increasing water demand and the decreasing availability of pure natural water resources [2]. Many commercial water purifying plants are used that run on the energy supplied by diesel or electricity generated from fossil fuels [3]. This also leads to an increase in pollution and global warming. Hence more and more renewable energy-based techniques are considered [4]. Biodiesels are also being considered to power purification systems and new biodiesels are being explored [5, 6]. The most promising method for the purification of water is the use of solar stills [7]. Since long solar distillation has been considered as an economical and an easy to implement method for brackish water treatment [8]. Around 2.3 MJ/kg

H. Yadav (✉)

Indian Institute of Technology, New Delhi, Delhi 110016, India
e-mail: harsha.civil32@gmail.com

A. Yadav · A. A. Madhavan
Amity University Dubai, Dubai 345019, UAE

amount of energy is required for the evaporation of water [9]. Although it is more strenuous than reverse osmosis, it is advantageous that it does not need energy in terms of electrical power but as heat; dense medium distillation can be also conducted and it is almost no maintenance device [10]. In practical application, solar distillation is much cheaper than reverse osmosis.

2 Solar Stills

A solar still is an insulated container of water covered by a transparent glass from the top. The glass is slanted generally at an angle equal to the latitude location [11]. The sunlight enters this container through the glass and heats the water. The water evaporated and the vapors condense on the inner side of the glass surface and then the droplets trickle down to a collector tray. The contaminants are left behind at the bottom of the container. All types of solar stills follow the common basic working principle. A fundamental schematic of solar still is shown in Fig. 1.

The efficiency of the solar still, η , is given by

$$\eta = I_{\text{utilized}} / I_{\text{incident}} \quad (1)$$

where I_{utilized} is the ratio of the amount of solar radiation utilized for evaporation and.

I_{incident} is the total amount of radiation incident on the still.

The approximate daily output (l/day) from solar still can be found by

$$P = \eta I_G A / 2.3 \quad (2)$$

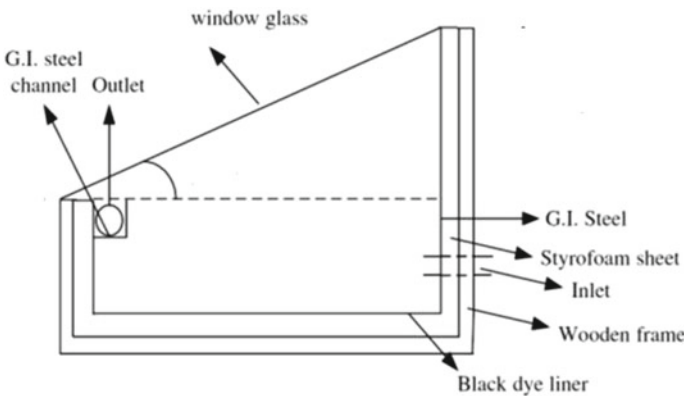


Fig. 1 Single basin solar still printed with permission from Elsevier [12]

where P is the daily output, A is the aperture area of the solar still in m^2 , and I_G denotes the global solar irradiation in MJ/m^2 [13]. Although it is a robust, simple, and reliable device, and it has low productivity. Therefore, many researchers have focused on limiting this drawback [14, 15]. The output of a solar still can be increased by increasing its operating hours. The most promising method is the use of phase change materials (PCM) as absorbers in solar still.

3 Phase Change Materials Integrated Solar Stills

The most effective method of improving productivity was found out to be storing of sun's heat energy during the day and its release at night when there is no sun. Phase change materials (PCM) are energy storage materials that possess the properties of isothermal heat storage and retrieval [16]. Radhawan [17] incorporated a PCM absorber layer in a stepped solar still. A uniform still temperature and daily efficiency of 57% were obtained. El-Sebaei et al. [18] did a similar experiment in a simple solar still investigate its performance. The still operation continued during the night also and high efficiency of 85.2% was attained. PCM was found to be effective in both the systems. As the difference in temperature between the basin water and tilted glass cover is increased, it led to higher heat transfer rates. Also, a substantial amount of the heat is accumulated by the PCM in comparison to the heat rejection to surroundings in case of simple still. During the night, PCM is hotter in comparison to the basin water; therefore, the flow of heat takes place from PCM to water, consequently evaporating the water. This increases the nocturnal productivity of the still. PCM integration in a solar still is shown in Fig. 2.

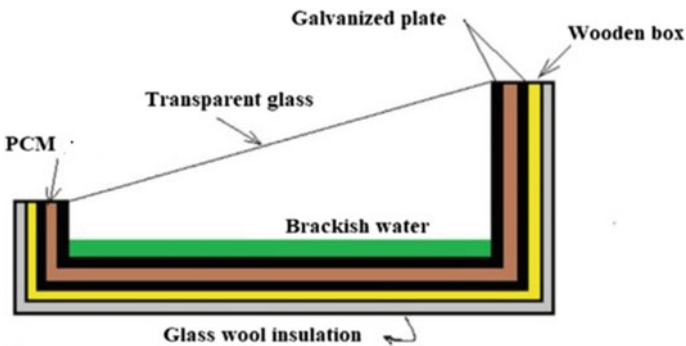


Fig. 2 Solar still with PCM integration printed with permission from Elsevier [19]

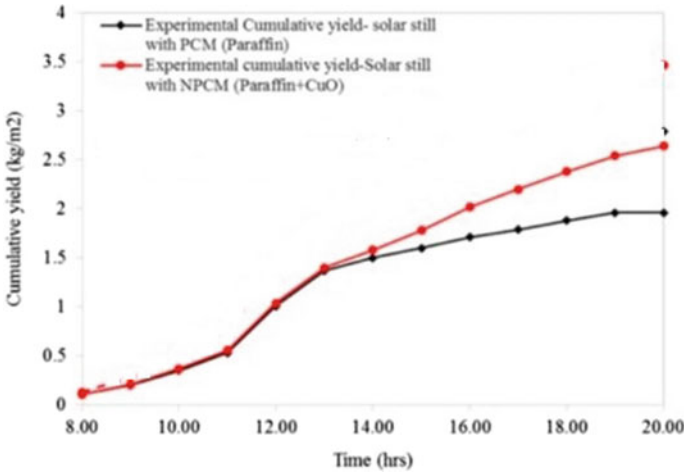


Fig. 3 Increased productivity of solar still by nanoparticle enhanced PCM printed with permission from Elsevier [25]

4 Nanoparticle Enhanced Phase Change Materials

However, the application of PCM does not provide the desired results at night due to their poor thermal conductivity. This limitation could be eliminated by the inclusion of nanoparticles in PCM [20]. Adding highly conductive nanoparticles in PCM increases the effective thermal conductivity of composites and paves a way for higher heat transfer rates [21–23]. The addition of alumina nanoparticles in the absorber PCM of a dual-slope solar still increased its productivity by 12% [24]. Rufuss et al. [25] discovered that the impregnating copper oxide nanoparticles in paraffin PCM used as an absorber layer in a solar still improves the still productivity by 35%. The performance of the solar still with and without nanoparticles in PCM is shown in Fig. 3.

Carbon-based nanomaterials have proven to be more effective in PCM as apart from high thermal conductivity they possess an additional perk of low density [26, 27].

5 Proposed Design

Hot inlet water supply is beneficial for the productivity of solar still [28]. Many integrations have been used with the solar stills to heat the water before it enters the still [29]. Groundwater can be pumped to the solar still with the help of solar panels. The rise in solar panel temperature decreases its efficiency; therefore, its cooling will increase its output [30]. This work proposes the integration of a modified solar

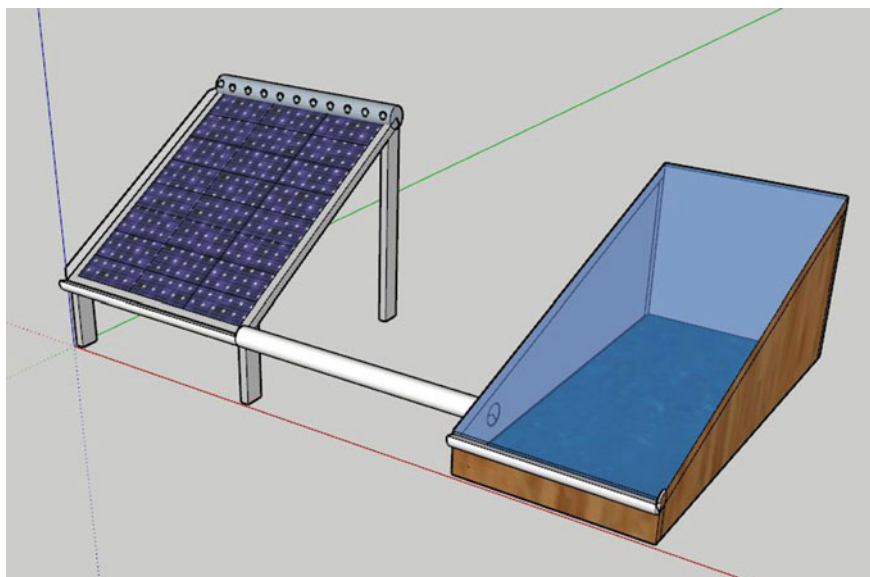


Fig. 4 Proposed solar panel integrated solar still design

panel with the solar stills as presented in Fig. 4. The design involves the installation of cooling pipes akin to a solar thermal collector at the back of the panel. These pipes will receive the cooling water from the groundwater which will be pumped with the help of a DC pump powered by the panel itself. The water running through the metal pipes in contact with the panel will absorb heat from the panel and reduce the excess temperature. This heated water will enter the solar still and get collected in the basin. Due to the high water temperature, the evaporation rate will be higher than the normal setup.

Also, a paraffin PCM layer enhanced with carbon-based nanoparticle will be fitted at the bottom of the basin to act as an energy storage layer. In nocturnal hours, the operation of the solar panel will cease and water can no longer receive heat from sunlight. However, the heating of water will continue due to stored heat in the PCM as discussed in the previous section.

6 Conclusion

The salinity of groundwater is a global issue that renders it unfit for human consumption. Solar still is a method of purification of water but pumping water into it requires electrical power. Also, the productivity of solar still is very low. This work proposes a modification in the design of a solar still for the purification of groundwater. The supply of groundwater and purification will be powered by solar photovoltaic and

solar thermal energy, respectively. This system will be self-sufficient and the setup can be installed in remote or rural areas. Further modification and validation through the experimental setup will increase in prospects of this design.

References

1. Khan FA, Pal N, Saeed SH (2018) Review of solar photovoltaic and wind hybrid energy systems for sizing strategies optimization techniques and cost analysis methodologies. *Renew Sustain Energy Rev* 92:937–947
2. Kumar S, Yadav A (2018) Comparative experimental investigation of preheated thumba oil for its performance testing on a CI engine. *Energy Environ* 29(4):533–542
3. Indian GDP from agriculture. <https://tradingeconomics.com/india/gdp-from-agriculture>
4. Singh A (2015) Soil salinization and waterlogging: a threat to environment and agricultural sustainability. *Ecol Ind* 57:128–130
5. Gregory PJ, Hester R, Harrison R (2012) Soils and food security: challenges and opportunities. In: *Soils and food security*. RSC Publishing, London, 1–30
6. Sorour MH, El Defrawy NMH, Shaalan HF (2003) Treatment of agricultural drainage water via lagoon/reverse osmosis system. *Desalination* 152(1–3):359–366
7. Zarzo D, Campos E, Terrero P (2013) Spanish experience in desalination for agriculture. *Desalination Water Treatment* 51(1–3):53–66
8. Rahardianto A, McCool BC, Cohen Y (2008) Reverse osmosis desalting of inland brackish water of high gypsum scaling propensity: kinetics and mitigation of membrane mineral scaling. *Environ Sci Technol* 42(12):4292–4297
9. Burn S, Hoang M, Zarzo D, Olewniak F, Campos E, Bolto B, Barron O (2015) Desalination techniques—a review of the opportunities for desalination in agriculture. *Desalination* 364:2–16
10. Stuber MD, Sullivan C, Kirk SA, Farrand JA, Schillaci PV, Fojtasek BD, Mandell AH (2015) Pilot demonstration of concentrated solar-powered desalination of subsurface agricultural drainage water and other brackish groundwater sources. *Desalination* 355:186–196
11. Selvaraj K, Natarajan A (2018) Factors influencing the performance and productivity of solar stills—a review. *Desalination* 435:181–187
12. Scrivani A, El Asmar T, Bardi U (2007) Solar trough concentration for fresh water production and waste water treatment. *Desalination* 206(1–3):485–493
13. Samuel DH, Nagarajan PK, Arunkumar T, Kannan E, Sathyamurthy R (2016) Enhancing the solar still yield by increasing the surface area of water—a review. *Environ Progress Sustain Energy* 35(3):815–822
14. Rajaseenivasan T, Tinnokesh AP, Kumar GR, Srithar K (2016) Glass basin solar still with integrated preheated water supply—theoretical and experimental investigation. *Desalination* 398:214–221
15. Shalaby SM, El-Bialy E, El-Sebaili AA (2016) An experimental investigation of a v-corrugated absorber single-basin solar still using PCM. *Desalination* 398:247–255
16. Sharma A, Tyagi VV, Chen CR, Buddhi D (2009) Review on thermal energy storage with phase change materials and applications. *Renew Sustain Energy Rev* 13(2):318–345
17. Radhwan AM (2005) Transient performance of a stepped solar still with built-in latent heat thermal energy storage. *Desalination* 171(1):61–76
18. El-Sebaili AA, Al-Ghamdi AA, Al-Hazmi FS, Faidah AS (2009) Thermal performance of a single basin solar still with PCM as a storage medium. *Appl Energy* 86(7–8):1187–1195
19. Chaichan MT, Kazem HA (2018) Single slope solar distillator productivity improvement using phase change material and Al₂O₃ nanoparticle. *Sol Energy* 164:370–381
20. Yadav A, Barman B, Kumar V, Kardam A, Narayanan SS, Verma A, Madhwal D, Shukla P, Jain VK (2017) A review on thermophysical properties of nanoparticle-enhanced phase change

- materials for thermal energy storage. In: *Recent trends in materials and devices*. Springer, Cham, 37–47
21. Yadav A, Barman B, Kumar V, Kardam A, Narayanan SS, Verma A, Madhwal D, Shukla P, Jain VK (2016) Solar thermal charging properties of graphene oxide embedded myristic acid composites phase change material. *AIP Conf Proc* 1731(1):030030. AIP Publishing
 22. Yadav A, Barman B, Kardam A, Narayanan SS, Verma A, Jain VK (2017) Thermal properties of nano-graphite-embedded magnesium chloride hexahydrate phase change composites. *Energy Environ* 28(7):651–660
 23. Yadav A, Verma A, Bhatnagar PK, Jain VK, Kumar V (2019) Enhanced thermal characteristics of NG based acetamide composites. *Int J Innov Technol Exploring Eng* 8(10):4227–4331
 24. Sahota L, Tiwari GN (2016) Effect of Al₂O₃ nanoparticles on the performance of passive double slope solar still. *Sol Energy* 130:260–272
 25. Rufuss DDW, Iniyani S, Suganthi L, Davies PA (2017) Nanoparticles enhanced phase change material (NPCM) as heat storage in solar still application for productivity enhancement. *Energy Procedia* 141:45–49
 26. Yadav A, Verma A, Narayanan SS, Jain VK, Bhatnagar PK (2018) Carbon based phase change nanocomposites for solar energy storage. *AGU Fall Meeting Abstracts*, GC23D-1226
 27. Yadav A, Kumar V, Verma A, Bhatnagar PK, Jain VK (2020) Expedited heat transfer rate of mesoporous carbon enhanced PCM. *Lecture notes in mechanical engineering*. In Press
 28. Yadav A, Shivhare MK (2020) Nanoparticle enhanced PCM for solar thermal energy storage. In: *2020 advances in science and engineering technology international conferences (ASET)*. IEEE, 1–3
 29. Sharshir SW, Peng G, Wu L, Essa FA, Kabeel AE, Yang N (2017) The effects of flake graphite nanoparticles, phase change material, and film cooling on the solar still performance. *Appl Energy* 191:358–366

An Approach for Reclamation of Salinity Affected Lands for Bio-energy Production



Himanshu Tyagi and Anupriya Goyal

Abstract Vast arable tracts are suffering from soil alkalinity/salinity. Such marginal lands need to be rehabilitated through eco-friendly and socio-economically viable technologies. The approach being presented here suggests rejuvenation of such wastelands through plantation of salt-resistant trees like *Jatropha* and *Pongamia pinnata* which are also known for being a biodiesel source. This model is not only effective in recovering salty soils but can go a long way in making villages bioenergy hub.

Keywords Wasteland · Soil salinity · Biodiesel · *Jatropha* · *Pongamia pinnata*

1 Introduction

Due to finite land resources, land and energy security is of utmost importance. But with ever-increasing human needs, the supply of land and land-linked products is far lagging behind their disproportionate demand [1]. In population-rich nations like India, this shortfall has resulted in over exploitation of land resources and continuous decline in per capita cultivable land due to formation of numerous patches of degraded lands affected by desertification, erosion, salinity, water logging, etc. [2].

For instance, approximately 6309.10 km² area in India is affected from varying degrees of salt problems attributable to climate change and anthropogenic influences [2]. As can be observed from Table 1, these wastelands are spread predominantly over Indian states/union territories of Andhra Pradesh, Bihar, Daman and Diu, Gujarat, Haryana, Jammu and Kashmir, Karnataka, Maharashtra, Odisha, Punjab, Rajasthan, Tamil Nadu, Telangana, Uttar Pradesh, and West Bengal [2].

H. Tyagi (✉) · A. Goyal
Department of Civil Engineering, Indian Institute of Technology Delhi, New Delhi, India
e-mail: tyagiben@gmail.com

Table 1 Salinity-affected states/union territories of India

State/union territory	Area affected by strong/medium salinity/alkalinity (In sq. km)
Andhra Pradesh	1150.03
Bihar	1.33
Daman and Diu	3.13
Gujarat	763.52
Haryana	65.62
Jammu and Kashmir	181.34
Karnataka	398.36
Maharashtra	52.41
Odisha	26.27
Punjab	20.66
Rajasthan	799.01
Tamil Nadu	279.78
Telangana	434.99
Uttar Pradesh	2129.61
West Bengal	3.04
Total	6309.10

Source Wasteland Atlas of India—2019

2 Soil Salinity and Its Origins

The salinity-affected lands have surplus soluble salts and high exchangeable Sodium [3]. Such lands have predominance of sodium carbonates and bicarbonates [4]. Alkaline soils can be identified through white or grayish-white salt efflorescence in dry seasons [5]. These soils appear in different shades of white tone with fine to coarse texture on false color composite satellite images [6]. *Prosopis juliflora*, *Acacia nilotica*, *Capparis aphylla*, *Cynodon dactylon*, etc., are indicator plants for these areas [6]. Based on the physio-chemical properties and the salt characteristics, salinity-affected soils are categorized as saline, sodic and saline-sodic [7].

Soil salinity primarily happens due to capillary movement of water through the soil profile during extreme climatic conditions, leaving a coating of accumulated salts on the surface. Chemical weathering of rocks results in release of dissolvable salts that get deposited in the lower soil layers via downward movement of soil water [8]. But these salts again move up to the soil surface when the water evaporates. This way salts also get deposited in the root zone during water table fluctuations. Further, scanty rainfall and high temperature of arid regions do not allow leaching of soluble weathered products [9]. Additionally, excessive irrigation through poor quality water and use of basic fertilizers like sodium nitrate may also develop soil salinity [10].

3 Adverse Effects of Salinity

Salt-affected marginal lands do not give decent crop yields and experience water stagnation due to poor drainage [11]. Salinity also affects the water quality and makes soil erosion prone due to weak vegetation [12]. It also results in sedimentation issues and spoils infrastructure.

4 Management of Salt-Affected Areas

Saline wastelands can only be revitalized by removal of salts from the root zone. Adequate leaching requirement in irrigation efficiency can prevent soil from turning saline. Artificial drainage may be provided in places where use of leaching is limited. Drip and sprinkler irrigation systems can also be engaged to dilute the salt content by high soil moisture [13]. Furthermore, application of organic mulch slows surface evaporation and may decrease salt movement by evaporative water [14]. Though very tedious, scraping off highly saline patches can also be employed.

Because of high pH in saline soils, many plant nutrients are fixed up in unavailable forms. So, manure application can remove this deficiency of organic matter and improve soil fertility. If saline soil contains a little amount of sodium, gypsum is needed to displace sodium [15]. Further, molasses can be applied on the affected soils as on fermentation it produces organic acids that can reduce alkalinity [16]. The use of some acidifying fertilizers can also help in reducing the salt toxicity.

In addition to the above-mentioned remedial measures, plantation of salt-resistance crops may also help in rehabilitating the salty soils [17–20]. Trees like *Jatropha*, *Pongamia pinnata*, *Arjun*, *Palash*, and certain types of babool (Australian babool, babool, vilayati babool) are known for being tolerant to the saline conditions [21–23].

5 Suggested Model

In fast-developing countries which have limited fossil resources, it is imperative to explore new avenues of sustainable energy for uninterrupted progress of the nation. Recovered wastelands possess enormous potential for supporting energy needs, especially in rural areas [24, 25]. Therefore, in this communication, a case is being made to revive saline wastelands through cultivation of established salt-resistant trees like *Jatropha* and *Pongamia pinnata* which can double up as a biofuel source too. The adoption of this innovative technology will not only bring wastelands back to their productive capabilities, but will also support agro-forestry and energy needs.

Ahamed et al. [26] reviewed biodiesel production from abundantly available non-edible oils of *Jatropha*, *Karanja*, and *Castor* and found biodiesel to be an ideal

substitute for diesel as it does not necessitate engine adjustment. Both *Jatropha* and *Pongamia pinnata* are native to subtropical environments and can grow on different soil types within temperature range of 5–50 °C [26, 27]. Mature trees can endure water logging and slight frost too. They have a height of about 15–25 m and yield of around 20–25 kg [27, 28]. The derived oil has good calorific value, and even the deoiled cake and residual fruit shells possess decent energy [29–31]. Besides, they have a relatively short gestation period years and long economic life [27, 28]. Typical process of biodiesel production can be seen in Fig. 1.

The governments in India are sentient of the fiscal prospects of the wastelands. For instance, while there is still ambiguity about biodiesel production in most of the states, states like Chhattisgarh, Madhya Pradesh, Rajasthan, and Uttarakhand are leading by an example in endorsing *Jatropha* biofuel by leasing marginal lands to businesses for trivial amounts and have also setup biofuel development authorities

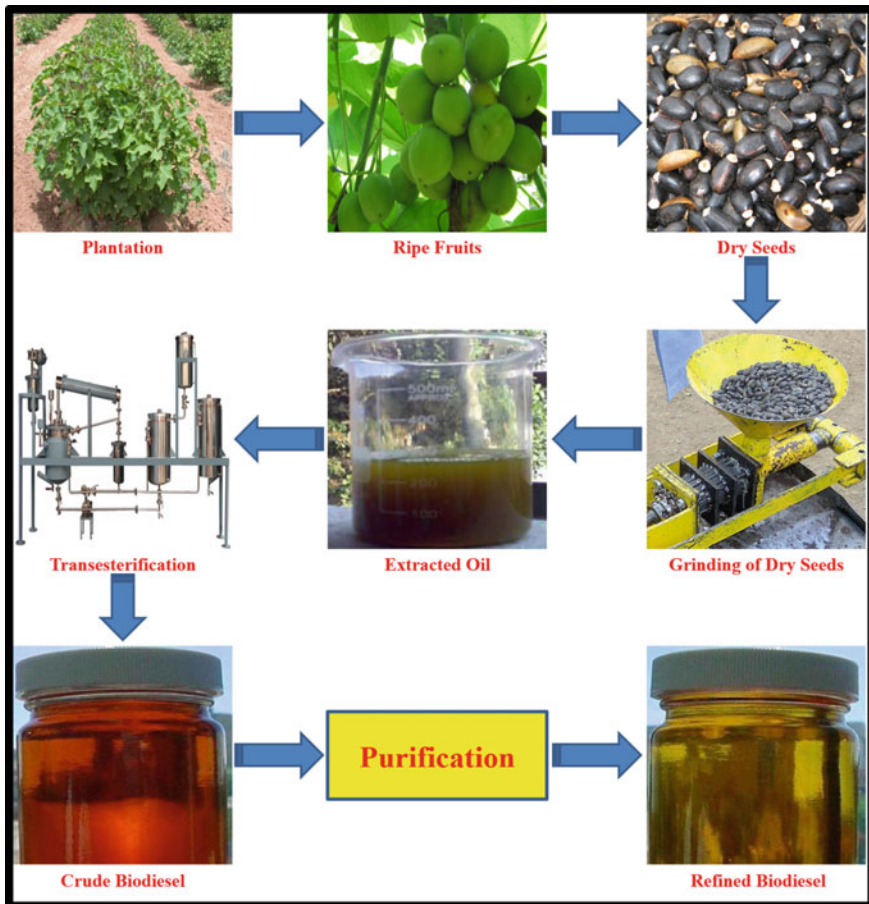


Fig. 1 Typical biodiesel production process

to encourage biofuel plantation [32]. In 2006, Chhattisgarh Biofuel Development Authority (CBDA) planted 160 million saplings throughout the state in its endeavor to become bioenergy self-sufficient and since 2010 generates a revenue of INR 40 billion/year by selling *Jatropha* seeds [33].

6 Conclusion

It can be said that the idea being recommended through this paper possesses enormous potential for supporting energy needs and can resolve multitude of concerns like joblessness and exodus of rural denizens by empowering villagers to lead a monetary self-reliant and dignified life. In a country like India where the government has a vision to grow 7.5 million tonnes biofuel per year and consequently generate jobs for 5 million people [34], the proposed approach can be a revolutionary measure if implemented after rigorous scientific studies and solid policy backup [35]. The principal advantage of this technique lies in the fact that biodiesel generation does not compete with food production as these proposed trees can be grown on lands which were rendered useless. Therefore, this model is not only sustainable in recovering salty soils but can go a long way in making rural areas a bioenergy hub.

References

1. Karnataka State Remote Sensing Applications Centre. Wasteland Atlas. Government of Karnataka, India. <https://karunadu.karnataka.gov.in/ksrsac/atlas-wasteland.html>
2. Department of Land Resources and National Remote Sensing Centre (2019) Wasteland Atlas of India-2019. Department of Land Resources, Ministry of Rural Development, Government of India, New Delhi and National Remote Sensing Centre, Indian Space Research Organisation, Department of Space, Government of India, Hyderabad
3. Central Soil Salinity Research Institute (2015) Vision 2050. Central Soil Salinity Research Institute, Indian Council of Agricultural Research, Ministry of Agriculture and Farmers Welfare, Government of India, Karnal
4. Department of Land Resources and National Remote Sensing Centre (2011) Wasteland Atlas of India-2011. Department of Land Resources, Ministry of Rural Development, Government of India, New Delhi and National Remote Sensing Centre, Indian Space Research Organisation, Department of Space, Government of India, Hyderabad
5. Dagar JC, Singh AK, Arunachalam A (2014) Agroforestry systems in India: livelihood security & ecosystem services. Springer, India
6. Goyal A, Tyagi H (2017) Spatial mapping of salinity affected lands. In: Proceedings of the international conference on remote sensing and GIS for applications in geosciences. Aligarh Muslim University, Aligarh, p 25
7. Indian Council of Agricultural Research (2010) Degraded and Wastelands of India. Indian Council of Agricultural Research Ministry of Agriculture and Farmers Welfare, Government of India, New Delhi
8. Shivay YS (2011) Saline and alkali soils and their management for effective utilization. *Kurukshetra J* 60:8–12

9. Verheye W (2009) Soils of arid and semi-arid areas. Land use land cover and soil sciences. EOLSS Publishers, Oxford
10. Kumar A (2004) A text book of environmental science. APH Publishing, New Delhi
11. Bhattacharya AK (2007) Drainage. <https://nsdl.niscair.res.in/jspui/bitstream/123456789/543/1/Drainage%20-%20FORMATTED.pdf>
12. Department of Environment and Resource Management (2011) Salinity management handbook. Department of Environment and Resource Management, The State of Queensland, Brisbane. <https://publications.qld.gov.au/storage/f/2013-12-19T04%3A10%3A23.754Z/salinity-management-handbook.pdf>
13. Abrol IP, Yadav JSP, Massoud FI (1988) Salt-affected soils and their management. FAO Soils Bulletin 39, Food and Agriculture Organization of the United Nations
14. Chalker-Scott L (2007) Impact of mulches on landscape plants and the environment-a review. J Environ Horticult 25:239–249
15. Hodges SC (2010) Soil fertility basics. Soil science extension, North Carolina State University. <https://www2.mans.edu.eg/projects/heapf/ilppp/cources/12/pdf%20course/38/Nutrient%20Management%20for%20CCA.pdf>
16. Sharma BK, Kaur H (1994) Soil and noise pollution. Krishna Prakashan Mandir, Meerut
17. Ladeira B (2012) Saline agriculture in the 21st century: using salt contaminated resources to cope food requirements. J Bot
18. Ashraf MY, Awan AR, Mahmood K (2012) Rehabilitation of saline ecosystems through cultivation of salt tolerant plants. Pak J Bot 44:69–75
19. Biswas A, Biswas A (2014) Comprehensive approaches in rehabilitating salt affected soils: a review on Indian perspective. Open Trans Geosci 1:13–24
20. Hasanuzzaman M, Nahar K, Alam MM, Bhowmik PC, Hossain MA, Rahman MM, Prasad MNV, Ozturk M, Fujita M (2014) Potential use of halophytes to remediate saline soils. BioMed Res Int
21. Thapliyal A, Malik A, Teixeira da Silva JA (2006) Application of fly ash in reclamation of wastelands through plantations and floriculture. Floricul Ornament Plant Biotechnol 288–297
22. Niu G, Rodriguez D, Mendoza M, Jifon J, Ganjegunte G (2012) Responses of *Jatropha curcas* to salt and drought stresses. Int J Agronomy
23. Dagar JC, Minhas P (2016) Agroforestry for the management of waterlogged saline soils and poor-quality waters. Springer, India
24. Sharma SK, Dagar JC, Singh GB (2010) Biosafor-biosaline (agro) forestry: remediation of saline wasteland through production of renewable energy, biomaterials and fodder. Central Soil Salinity Research Institute, Indian Council of Agricultural Research, Ministry of Agriculture and Farmers Welfare, Government of India, Karnal
25. Sarin A (2012) Biodiesel: production and properties. Royal Society of Chemistry Publishing, Cambridge
26. Ahamed MS, Dash SK, Kumar A, Lingfa P (2020) A critical review on the production of biodiesel from *Jatropha*, *Karanja* and castor feedstocks. In: Ghosh S, Sen R, Chanakya H, Pariatamby A (eds) Bioresource utilization and bioprocess. Springer, Singapore
27. Pradhan RC (2010) Centre design and development of low cost post harvest equipments for *Jatropha*. Ph.D. Thesis, Centre for Rural Development and Technology, Indian Institute of Technology Delhi, New Delhi
28. Muralidharan M, Mathew P, Thariyan S, Subrahmanyam JP, Subbarao PMV (2004) Use of pongamia biodiesel in CI engines for rural application. In: Proceedings of the 3rd international conference on automotive and fuel technology. Allied Publishers, New Delhi, pp 199–204
29. Kesari V, Das A, Rangan L (2010) Physico-chemical characterization and antimicrobial activity from seed oil of *Pongamia pinnata*, a potential biofuel crop. Bio Mass and Bioenergy. 34:108–115
30. Eipeson WS, Manjunatha JR, Srinivas P, Kanya TS (2010) Extraction and recovery of karanja: a value addition to karanja (*Pongamia pinnata*) seed oil. Ind Crops Prod 32:118–122
31. Mukta N, Sreevalli Y (2010) Propagation techniques, evaluation and improvement of the biodiesel plant. Ind Crops Prod 31:1–12

32. Mishra SN (2014) Design of resource use: case of Jatropha based biodiesel in India. *J Rural Develop* 33:1–13
33. Biofuel in India. https://en.wikipedia.org/wiki/Biofuel_in_India
34. De Fraiture C, Giordano M, Liao Y (2008) Biofuels and implications for agricultural water use: blue impacts of green energy. *Water Policy* 10:67–81
35. Gopakumar L (2020) Jatropha cultivation in South India—policy implications. In: Mauerhofer V, Rupo D, Tarquinio L (eds) *Sustainability and law*. Springer, Cham

Optimal Design of Water Distribution Network by Reliability Considerations



Ashish Mishra , Ishan Sharma, and Rakesh Mehrotra

Abstract Water distribution networks (WDNs) are quite complex systems in such a manner that it is not easy to obtain the most reliable and efficient systems due to the complexity of algorithms generated using linear programming. Many studies dealt in the past with the objective of least cost design where reliability was quantified as a constraint. This study provides a multiobjective approach for assessing the performance and reliability of an urban residential area Surjamal Vihar, New Delhi. The schematic network is constructed using commercial software Bentley WaterGEMS V8i, which is also used to simulate the results. Linear programming algorithm approach is used to analyze the network for the design, considering the reliability of the network. Results are discussed at the end of the study suggesting certain modifications in the network design to achieve optimization of the distribution system, including constraints related to hydraulic feasibility, satisfaction of nodal demands, and requirement of nodal pressures.

Keywords Urban water supply · Water distribution networks (WDNs) · Optimization · Reliability

1 Introduction

A water distribution system is a vital part of the modern urban infrastructure. With global rise in population and raised living standards, there is a constant demand for the development and modification of such systems [1–4]. Transients in a water

A. Mishra (✉)

Department of Hydrology, Indian Institute of Technology Roorkee, Roorkee, Uttarakhand 247667, India

e-mail: ashish.mshr3@gmail.com

I. Sharma

Department of Water Resources Development and Management, Indian Institute of Technology Roorkee, Roorkee, Uttarakhand 247667, India

R. Mehrotra

Department of Civil Engineering, Delhi Technological University, New Delhi 110042, India

distribution system are a common practice in the daily operation and management [5]. Numerous studies reveal that a linearized approach is used beyond its limits of applicability to solve the nonlinear optimal operation of groundwater distribution systems [6], which has been proved to be unreliable in several past studies. Optimal design of a water supply system by taking into account its reliability is the prime focus of this study. Several models have been used to investigate the optimal size of reliable water distribution network (WDN) and applied to a hypothetical system [7]. Design here involves model simulation of actual water distribution network involving constraints like pipe diameters, pipe length for the reliable system, and introduction of sluice valve to satisfy the nodal demands within the allowable limits. Computer models that can simulate the hydraulics of water distribution systems have been available for many years [8]. Such models have been adopted in the past decade for optimal operation of water supply system. This study focuses on simulation of water distribution system with the application of linear programming. Optimal operational management of the system is the prime objective of the study, and to achieve this, it involves few assumptions like the topography of the region is taken as flat. The per capita demand for urban region is recommended as 135 LPCD recommended by CPHEEO, but taking into account the peak factor as 3.0 it is taken as 165 LPCD. Since our study is for domestic water supply, certain variables have not been taken into account. Nodal pressure varies with the purpose of water supply. Network simulation is obtained with the help of commercial software Bentley WaterGEMS. Globally adopted types of network systems adopted for water supply are dead end system, grid iron system, ring system, and radial system. Grid iron type of system with intermittent supply is adopted for this study. Data availability is a major issue while studying such systems, government organizations, and stakeholders can be approached to get access of such data. The present-day water distribution networks are complex and involve heavy costs in the construction, management, and maintenance. Due to these reasons, a need to improve their operational management by minimizing cost maximizing the benefit accrued from them is strongly recommended [9]. Urban drinking water before reaching source undergoes a stringent treatment process. After this, it travels a long path through old, deteriorated, leaking, and corroded system of pipes. Apart from this, waterlines carrying water for more than 20 odd hours are not pressurized. During no flow conditions, the gradient in pipelines also creates a vacuum, which may result in pulling up of unhygienic material, in case of leaking joints which is common in urban distribution systems. Therefore, the losses in systems due to leakage are to be taken into account while establishing the infrastructure. The urban distribution systems consist of several components like pipes, overhead, or underground tanks, valves or pumps. Reliability in a system is stochastic approach of performance for a system. It is difficult to determine the probability of such system, and hence various models are developed in past to study it as a stochastic approach of performance [1, 10]. In recent years, researchers have tried to predict the behavior of the water distribution systems under pressure-deficient conditions [11]. Metamodels using genetic algorithms have been used in the past to simulate the water distribution models, and these models are capable of handling nonlinear functions that govern the flow [12].

In the view of the above, this study aims to provide a multiobjective approach for assessing the performance and reliability of a WDN, which will be helpful for its optimal design. This is necessary for proper management of water, particularly in a developing country like India as it faces the challenge of equitable water distribution [13–16]. The problems have even worsened by rising issues of water availability, mainly due to rapid population growth and looming climate change [16–18]. Therefore, the performance and reliability assessment of a WDN is a timely research work.

2 Methodology

The methodology applied to this study can be broadly classified into two parts, first is the application of linear programming in the WDN study and other is designing and analysis of network in commercial software of Bentley WaterGEMS software. Several attempts have been made in past decade and the reliability surrogates are compared [19].

2.1 Linear Programming

The aim of this study is to identify the pipe sizes of varying diameters and their associated lengths to obtain the optimal operation of a system for its reliable performance while satisfying the criteria of hydraulic feasibility and reliability requirements, alongside monitoring the quality of drinking water from the treatment plant to the consumers tap is critical to ensure compliance with national standards and/or WHO guideline levels [20]. The optimization technique to obtain acceptable service during peak demands involving pipe costs has been in practice in the recent past [21]. Optimization technique helps to identify the best-fit diameters for network line to achieve optimum results. In this method, pipe lengths are the assumed unknown parameters for any link and are denoted by the symbol X_{jk} . The objective function in Eq. (1) helps to identify the unknown parameters by minimizing it.

Objective function:

$$\text{Minimize } C = \sum_{j=1}^{NLn(j)} \sum_{k=1} C_{jk} \cdot X_{jk} \quad (1)$$

Computation of length: This function (2) assures that the total sum of individual pipe lengths is equal to the total length of pipeline at the nodes or pipes. The two pipes meeting at a point is called a node.

$$\sum_{k=1}^{n(j)} X_{jk} = L_j, \quad \text{For all links } j \quad (2)$$

Head loss computation: The min and max permissible head at all demand nodes should be within satisfactory limits.

$$H_0 - \sum_{j \in p(n)} \sum_{k=1}^{n(j)} J_{jk} \cdot X_{jk} \geq H_{n \min}, \quad \text{for all nodes } n \quad (3)$$

Analysis of loop: The total head loss should be zero for a closed-loop system.

$$H_0 - \sum_{j \in p(n)} \sum_{k=1}^{n(j)} J_{jk} \cdot X_{jk} \leq H_{nmax}, \quad \text{for all nodes } n \quad (4)$$

$$\sum_{j \in p(b)} \sum_{k=1}^{n(j)} J_{jk} \cdot X_{jk} = 0 \quad (5)$$

Check for non-negative pressure at junction:

$$X_{jk} \geq 0, \quad \text{For all } j \text{ and } k \quad (6)$$

Reliability analysis: Eq. (7) measures the reliability of the expected number of average breaks within a given time period.

$$\sum_{k=1}^{n(j)} r_{jk} \cdot X_{jk} \leq R_j, \quad \text{For all links } j \quad (7)$$

where C_{jk} is the cost of pipe of diameter 'k' in junction or link 'j' (dollar/km), C is the total cost expenses (in dollars), H_{nmin} and H_{nmax} are the minimum and maximum permissible head at node 'n' (m), respectively, H_0 represents the head at the source (original), J_{jk} refers to the hydraulic gradient for pipe diameter 'k' in link 'j' (m/km), L_i is total length of link 'j' (km), $n(j)$ is the number of pipe diameters in link 'j', NL is total links in the system, $p(n)$ represents number of links in the path from source to node n , r_{jk} represents number of breaks per km per year, R_j is the maximum allowable number of failures per year in link 'j', and X_{jk} is the pipe length of diameter 'k' in link 'j' (in kms).

3 Study Area and Network Design

The study area taken into account is a residential cluster in New Delhi of area 5 ha or 0.05 km² approximately, with population estimate 5200 people in approximately 265 households. Figure 1 shows the satellite image of study area derived using Google Earth search engine. The total length of pipeline in the area is estimated to be 1615 m. The network is designed for demand estimate is taken as 165 LPCD recommended by CPHEEO in their guidelines. Total 30 pipes, 26 nodes, and 9 sluice valves are proposed for the network with one reservoir at 22 m elevation and 6 million liters capacity (6000 m³). Ductile iron (DI) pipes are used for the construction of pipes. The diameter of the pipelines may vary depending upon the nodal demand. Flow supplied is taken as 42 LPS, and peak factor considered 3.0 for the design life of 30 years.

In India, as per the guidelines listed by the Central Public Health and Environmental Engineering Organization (CPHEEO), the peak factor can vary from 3 to 12 depending upon the type of supply. The network has been designed in WaterGEMS as shown in Fig. 2. The working mechanism of WaterGEMS software by Bentley can be broadly classified as (i) drawing the network using the layout plan or satellite image for the study area. Once the network is drawn (ii) the input parameters are entered like reservoir capacity, pipe length, pump details, and other input values for a water distribution network. (iii) Steady-state analysis is then run for the input values followed by (iv) extended period simulation (EPS) (v) network design in WaterGEMS is validated. If the network is satisfactory with the output values, it is considered as final else, (vi) modification of data for the network is done.

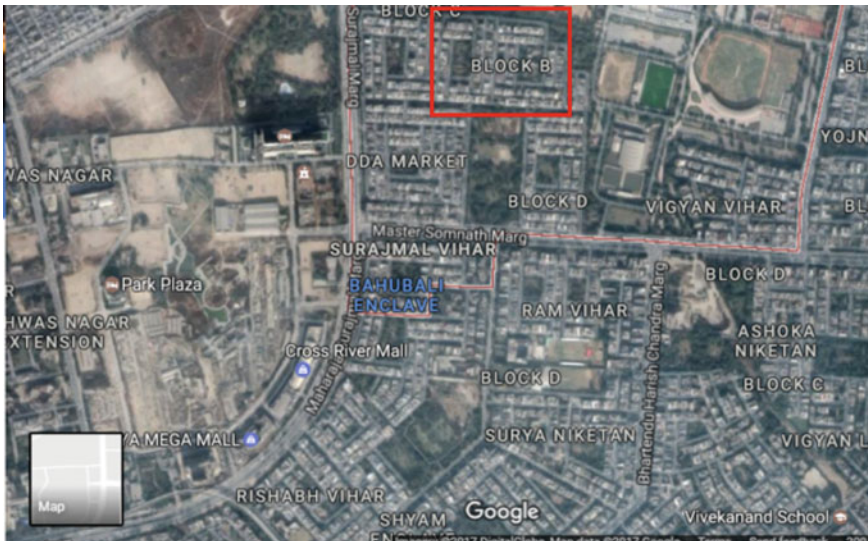


Fig. 1 Satellite image of the study area (marked with red)

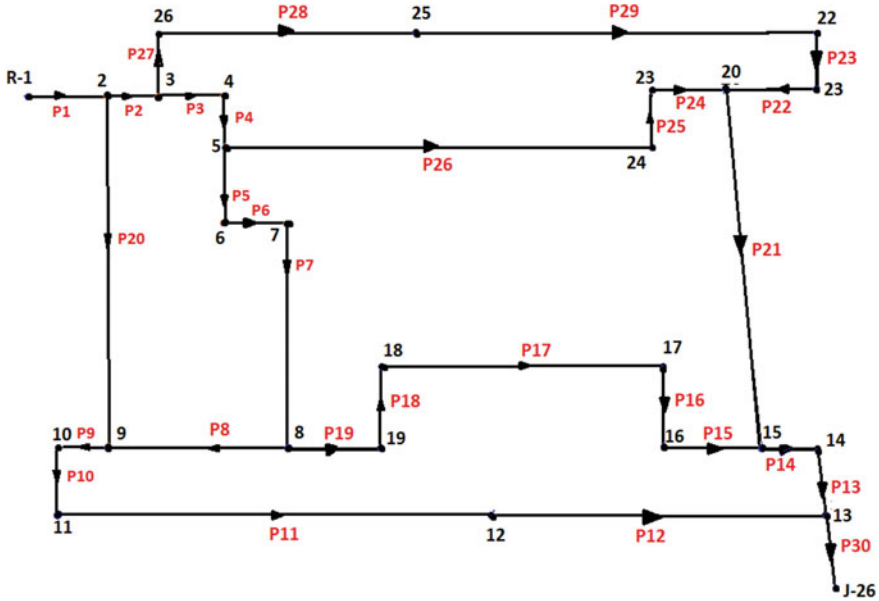


Fig. 2 Network design using Bentley WaterGEMS V8

The study area is located in a densely populated area of New Delhi, known as Surajamal vihar. The WDN to be designed for approximately 5000 inhabitants, and the work is carried out by Delhi Development Authority (DDA).

3.1 Population Forecasting and Water Demand

Population forecasting and calculation of water demand is a vital factor in network design of water supply. Operational management design requires the precise forecast of water supply based on population forecasting. The design life of the reservoir in this study is 30 years, so the population forecasting is will be based on geometric method. Further, the per capita demand will be extrapolated with the population estimate of design life geometric method is employed for population forecasting in this study. Studies involving redundancy in the upgradation of existing a network have been carried out in the past [22]. Table 1 depicts the change in population growth over 1941–2011, whereas Table 2 depicts the geometric method-based population forecasting and future demands. Figure 3 represents the freshwater withdrawal by source for 1950–2010 with respect to the population trends.

$$[(P = P (2016) + (1 + r)^n)] \tag{8}$$

where P is the population, r is the growth rate, and n is the number of decades.

Table 1 Population growth of Delhi NCT (*Source* Census report 2013) [23]

Year	Population	Growth rate
1941	140,227	
1951	203,659	0.452
1961	295,375	0.450
1971	442,481	0.498
1981	649,085	0.467
1991	764,586	0.178
2001	956,107	0.251
2011	1,206,917	0.262

Table 2 Demand based on population forecasting of study area using geometric method

Year	Population	Growth rate (r)	Demand (MLD)
2016	5200		0.85
2026	6780	0.35	1.11
2036	8790	0.40	1.45
2046	11,420	0.42	1.97

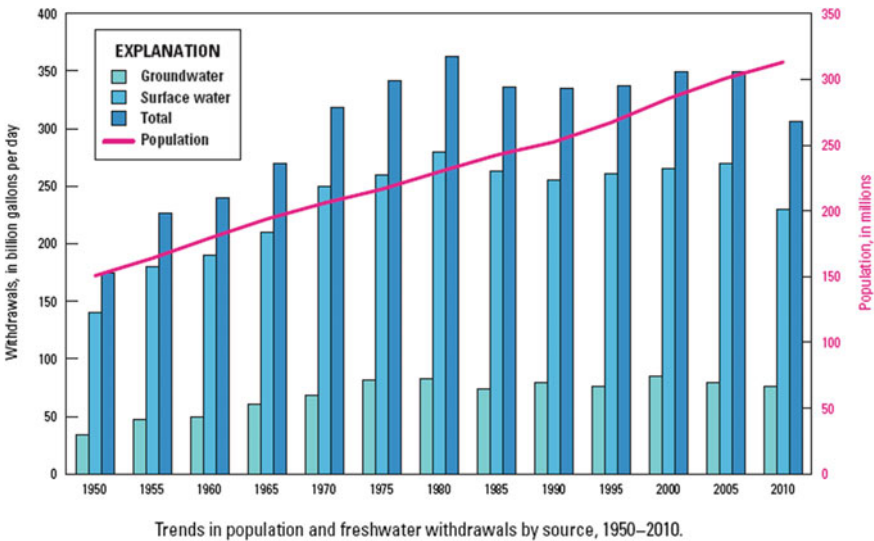


Fig. 3 Change in trend in population and freshwater withdrawals by source for 1950–2010

Reservoir Capacity.

Trend analysis of water supply–demand makes it evident that the total demand will increase multifold in the forthcoming years; therefore, the reservoir design should be feasible for the design life of 30 years and satisfy the nodal demands. Using

forecasting techniques and trend analysis, the installed capacity of the reservoir should be 6 million liters or 6000 m³ per day. The per capita demand of the each household is considered as 165 LPCD (liters per capita per day) as suggested by CPHEEO.

4 Results and Discussion

4.1 Network Validation

The water network is designed in commercial version of Bentley WaterGEMS that requires validation. The validation process takes place for different parameters, including length and diameters of pipes. This validation process is done using the flex table feature of WaterGEMS, which tabulates the complete network. The distribution system in this study is designed as a GRIDIRON type network, with intermittent supply.

Validation of flow of supply through nodes and conduits is also carried out using flex table. The flow validation flex table identifies the interrelationship between Hazen-William’s coefficient (C), pipe material, and flow supplied. On the basis of demand estimates for the inhabitants of study region, the reservoir capacity is taken as 42 L per second with a peak factor of 3.0. The variation of flow in the network is depicted in Fig. 4.

Validation of Velocity and head loss, flow and head loss validation, further to satisfy the nodal demands at the user end. CPHEEO advised minimum velocity as 0.6 m per second to reduce the risk of corrosion and deposition, while 1.42 m per second as the maximum to reduce the risk of water hammer. The flow velocity variation in the pipeline is shown in Fig. 5. But in certain cases these limits can vary depending upon the size of conduits and type of supply. But frictional losses are taken into account as 1 m/km per m/s velocity for given C and Manning’s coefficient of roughness. Modified Hazen-William formula (MHW) provides more accurate results by overcoming the limitations. The value of roughness coefficient for pipe material is 100 in this study. As a result, flow velocity is obtained in the range of 0.00–1.42 m

Fig. 4 Variations of flow through the network

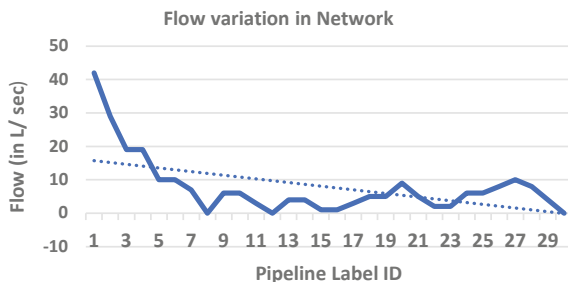


Fig. 5 Variation of flow velocities in conduits

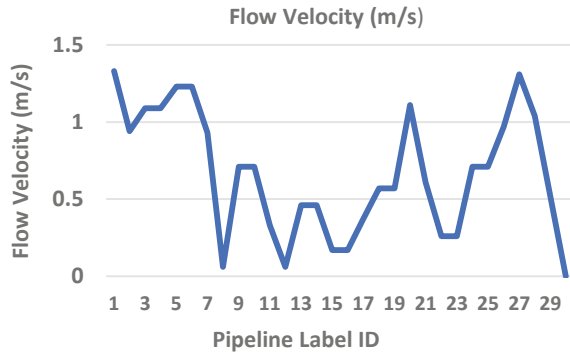
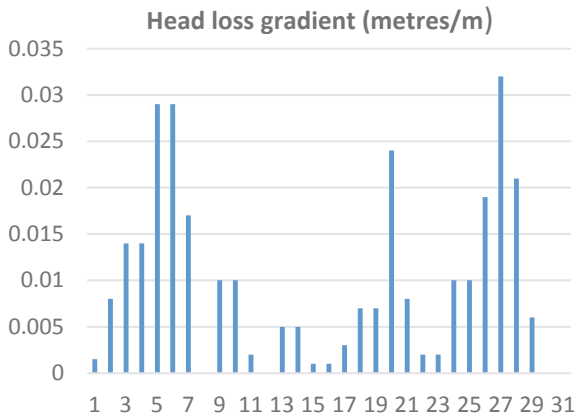


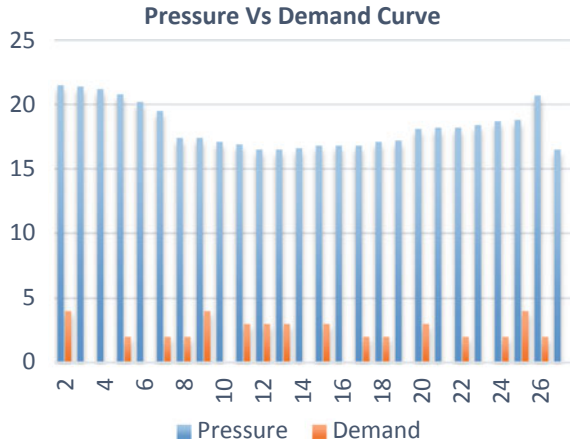
Fig. 6 Head loss gradient variations in the network



per seconds and head loss gradient is obtained in the range of 0.000–0.035 m/m. The system shows satisfactory performance in terms of the head loss gradient in Fig. 6.

Validation of water pressure (m-H₂O) and hydraulic head, the two most important parameters in the design network are hydraulic head and water pressure. Water hammer pressure has always been a major cause of concern in the design of water distribution systems. If not controlled it can cause serious damage to the pipelines and reduce the design life of the system. CPHEEO recommends that however, in case of function and surge pressure exceeding 1.1 times of internal design pressure, specific protection and safety measures are to taken. It also states that in no case, the combined value of maximum operation pressure and surge pressure should not exceed the hydrostatic design pressure. The elevation of reservoir in the present study is 22 m. The hydraulic head and pressure at the junction are satisfied for reliable network. Pressure at junctions, nodes if exceeded, can cause water hammer phenomenon resulting in breakdown of system. High demand junctions have high pressure values shown in Fig. 7, hence safety measures like sluice valves can be provided.

Fig. 7 Pressure versus demand curve



4.2 Color Coding of Network

With the application of color coding technique, the WDN was classified on the basis of parameters, viz. diameter, flow velocity, head loss gradient, and water pressure on the junction depicted in Fig. 8, respectively. User input function allows us to color code the network as per the specifications. Figure 8a defines the flow velocity, as

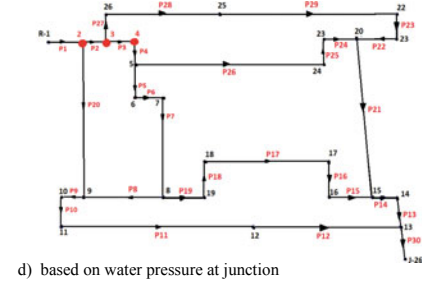
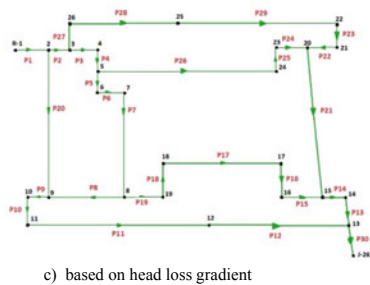
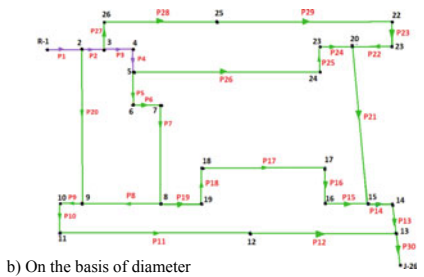
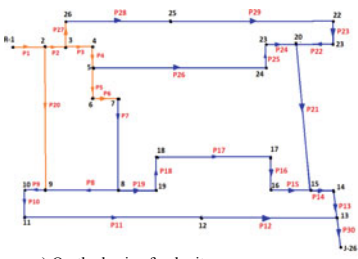


Fig. 8 Color coding of the network on the basis of **a** flow velocity, **b** diameter, **c** head loss gradient, and **d** water pressure at junction

recommended by CPHHEO is 1.32 m/s. The objective is to identify pipelines having velocities more than 1.32 m/s, which is the allowable velocity of flow in the WDN. Therefore, pipelines P1 to P5P20 and P 28 are the pipelines where flow velocity is greater than the permissible limit. While Fig. 8b depicts the conduits with diameter above 100 mm were considered as redundant or insufficient to carry the large volume of water supply, the algorithm identified four such pipelines namely P₁–P₄ that were color coded as blue, while the green colored pipelines were within satisfactory limits. The permissible had loss gradient in the network which is equal or less then 1 m per km as recommended by CPHEEO, so Fig. 8c identifies the head loss gradient and is clear that WDN follows this design criteria. Further, the CPHEEO recommends the allowable limit of pressure gradient which is supposed to be less than the total hydraulic head of the reservoir. For present study, reservoir hydraulic head is 22 m, and therefore, according to design recommendations by CPHEEO, the allowable limit should be within the range of 7–21.5 m H₂O. From Fig. 8d, it is evident that three pressure junctions J-2,3,4 are at risk; therefore, those junctions are color coded as red while those within permissible limit as blue. Therefore, with the application of color coding, the network can be analyzed for the satisfactory performance of network components viz., conduits, junctions, nodes and pumps. Further, necessary modifications can be implemented based on this analysis.

4.3 Modifications of the Data

The validation parameters and results of the network designed in Bentley WaterGEMS software are discussed in the previous sections, and the network was also validated for parameters like head loss gradient, water pressure at junctions, the pressure which is crucial for the supply to reach at the consumer end. Validation results showed that a number of pipelines were not satisfying the design criteria therefore it requires modification.

The diameter of pipelines P₁–P₄ has been upgraded to 200 m, whereas to satisfy the flow velocity and pressure criteria sluice valves have been introduced into the system. Sluice valves are designed for gradual opening, i.e., 30 degree, 50 degree, or 360 degree turns of the handle, to prevent water hammer in the pipelines. In this study, nine sluice valves are introduced into the pipelines P₁, P₃, P₇, P₁₁, P₁₇, P₂₀, P₂₆, and P₂₈ one in each pipeline to reduce the risk of water hammer. The following section discusses the conclusion of the study and gaps for future studies.

5 Conclusions and Scope for Future Work

In conclusion, the WDN design in this study provides effective framework for steady and unsteady conditions. The results obtained may provide guidelines for the operational management of modern urban water distribution networks or similar infrastructure like sewerage system. The operational solutions obtained in this study are limited to the transients and constraints involved are generated by pump and reservoir operations and these results may vary if the prevailing conditions are modified like the type of supply or the material of pipeline. Hence, the proposed methodology in this study cannot be considered as general tool to design distribution networks, but can be considered as initial step to study the interrelationship between water supply network and unsteady flow effects in WDN. Modelers and designers must take reliability and efficiency of the system into account.

Future studies should lay emphasis on the improvements of the algorithms developed using linear programming algorithms, used in this study. The given study can be also extended to develop a least cost design using cost benefit analysis approach. Node isolation approach for network improvement could be included in the decision making process for future studies, especially in cases of financial constraints. Detection of accidental contamination or chlorine disinfection approach of a water distribution network can also be included as another objective for this study. Conceptually, a complete novel study can be carried out in the WDN to detect internal deterioration of water quality. The proposed method could be also be further extended for least cost and resilience studies involving constraints with design objectives like the pump energy, pipe material, reservoir capacity, water quality, chlorine contamination, and peak factor variation with change in population. And fire-fighting capacity and results can be validated using existing models of WDNs and similar infrastructure with the aim of enhancing their performance and resilience in handling complex transients, as only reliability of the system are considered in this study.

Acknowledgements The authors would like to thank the Delhi Development Authority, Delhi (DDA), for providing constant guidance and valuable data support for the study region.

References

1. Ostfeld A, Oliker N, Salomons E (2014) Multiobjective optimization for least cost design and resiliency of water distribution systems. *J Water Res Planning Manage* 140(12):04014037
2. WHO (2006) Guidelines for Drinking-water Quality. In: Recommendations, third edn., vol. 1. World Health Organisation, Geneva
3. Swain S, Verma MK, Verma MK (2018) Streamflow estimation using SWAT model over Seonath river basin, Chhattisgarh, India. In: *Hydrologic modeling*. Springer, Singapore, pp 659–665
4. Swain S, Sharma I, Mishra SK, Pandey A, Amrit K, Nikam V (2020) A framework for managing irrigation water requirements under climatic uncertainties over Beed District, Maharashtra,

- India. In: World environmental and water resources congress 2020: water resources planning and management and irrigation and drainage. ASCE, pp 1–8
5. Huang Y, Zheng F, Duan HF, Zhang Q (2020) Multi-objective optimal design of water distribution networks accounting for transient impacts. *Water Res Manage* 1–18
 6. Pezeshk S, Helweg OJ, Oliver KE (1994) Optimal operation of ground-water supply distribution systems. *J Water Res Planning Manage* 120(5):573–586
 7. Walski TM, Brill Jr ED, Gessler J, Goulter IC, Jeppson RM, Lansey K et al (1987) Battle of the network models: epilogue. *J Water Res Planning Manage* 113(2):191–203
 8. Sakarya ABA, Mays LW (2000) Optimal operation of water distribution pumps considering water quality. *J Water Res Planning Manage* 126(4):210–220
 9. Prasad TD, Park NS (2004) Multiobjective genetic algorithms for design of water distribution networks. *J Water Res Planning Manage* 130(1):73–82
 10. Wu W, Simpson AR, Maier HR, Marchi A (2012) Incorporation of variable-speed pumping in multiobjective genetic algorithm optimization of the design of water transmission systems. *J Water Res Planning Manage* 138(5):543–552
 11. Ang WK, Jowitt PW (2006) Solution for water distribution systems under pressure-deficient conditions. *J Water Res Planning Manage* 132(3):175–182
 12. Broad DR, Dandy GC, Maier HR (2005) Water distribution system optimization using metamodells. *J Water Res Planning Manage* 131(3):172–180
 13. Swain S, Patel P, Nandi S (2017) A multiple linear regression model for precipitation forecasting over Cuttack district, Odisha, India. In: 2017 2nd international conference for convergence in technology (I2CT), pp 355–357
 14. Aadhar S, Swain S, Rath DR (2019) Application and performance assessment of SWAT hydrological model over Kharun river basin, Chhattisgarh, India. In: World environmental and water resources congress 2019: watershed management, irrigation and drainage, and water resources planning and management, pp 272–280
 15. Swain S, Nandi S, Patel P (2018) Development of an ARIMA model for monthly rainfall forecasting over Khordha district, Odisha, India. In: Recent findings in intelligent computing techniques. Springer, pp 325–331
 16. Dayal D, Swain S, Gautam AK, Palmate SS, Pandey A, Mishra SK (2019) Development of ARIMA model for monthly rainfall forecasting over an Indian River Basin. In: World environmental and water resources congress 2019: watershed management, irrigation and drainage, and water resources planning and management. ASCE, pp 264–271
 17. Swain S, Patel P, Nandi S (2017) Application of SPI, EDI and PNPI using MSWEP precipitation data over Marathwada, India. In: 2017 IEEE international geoscience and remote sensing symposium (IGARSS). IEEE, pp 5505–5507
 18. Swain S, Mishra SK, Pandey A (2020) Assessment of meteorological droughts over Hoshangabad district, India. In: IOP conference series: earth and environmental science, vol. 491(1). IOP Publishing, p 012012
 19. Raad DN, Sinske AN, Van Vuuren JH (2010) Comparison of four reliability surrogate measures for water distribution systems design. *Water Res Res* 46(5)
 20. Aisopou A, Stoianov I, Graham NJ (2012) In-pipe water quality monitoring in water supply systems under steady and unsteady state flow conditions: A quantitative assessment. *Water Res* 46(1):235–246
 21. Filion YR, Jung BS (2010) Least-cost design of water distribution networks including fire damages. *J Water Res Planning Manage* 136(6):658–668
 22. Gupta R, Kakwani N, Ormsbee L (2015) Optimal upgrading of water distribution network redundancy. *J Water Res Planning Manage* 141(1):04014043
 23. Delhi NCT Report (2013) Delhi Jal Board guidelines for urban drinking water supply, and recommendations for water treatment. <https://www.delhijalboard.com>

Potable Water Production by Single Slope Active Solar Distillation Unit—A Review



Ashok Kumar Singh, Dalvir Singh, M. K. Lohumi, B. K. Srivastava, H. P. Gupta, and R. Prasad

Abstract A solar energy operated still unit, i.e., SDU is a recommended system which is much suitable to treat the brackish water with the use of heat of the Sun. The process of distillation is same as nature makes rain. The earliest use of solar systems for the purpose of water treatment was liberally used in 1551, and further the corresponding advanced still was used in 1882 by Arab alchemists and Charles Wilson, respectively. So, they started the new age of potable water production techniques and quite useful as the whole world facing the water scarce situations which are becoming more severe day by day. In this study, a wide classification and review of published research work have been done that is based on the concentrated and vacuum-type tube collectors connected solar still systems. This article covers various modifications which have been made in single slope distillation unit especially based on the compound parabolic concentrator and evacuated tube collectors.

Keywords Solar still · Single slope · Water productivity · Water yield

1 Introduction

The current situation in the world is quite tough in terms of the water quality and water quantity both because population is growing very fast, and the corresponding demand for the potable water is proportionally increasing day by day. So, the inhabitants are directly or indirectly related to this worse situation related to the water supply and demand. As the naturally available water is limited to reach as well as limited to use, the used water is further released in the form of brackish water in large quantity that also contaminates the freshly available water to our nearby sources. So, it is quite necessary to overlook such kind of aspects, i.e., the large amount of brackish water

A. K. Singh (✉) · D. Singh · M. K. Lohumi · H. P. Gupta
Department of Mechanical Engineering, Galgotias College of Engineering and Technology,
Greater Noida, Uttar Pradesh 201306, India
e-mail: agashok26@gmail.com

B. K. Srivastava · R. Prasad
Department of Applied Sciences, Galgotias College of Engineering and Technology, Greater
Noida, Uttar Pradesh 201306, India

© The Author(s), under exclusive license to Springer Nature Singapore Pte Ltd. 2021
R. Al Khaddar et al. (eds.), *Advances in Energy and Environment*, Lecture Notes in Civil
Engineering 142, https://doi.org/10.1007/978-981-33-6695-4_4

should be treated to make it a pure one in parallel occurrences, and solar still system is a quite suitable technology for that purpose [1]. In this field, many works have been done like reviews for the economy perspective and payout times, etc. [2], different performing observations related to the system efficiencies [3], newly revealed system performances [4, 5], conventionally simple design stills and its performances [6, 7] and further advanced designs that has implementation of various efficient materials along with or even without nano-formed metal oxides and its applications in still systems [8, 9]. The evacuated tube collectors (ETC) integrated systems are one of the interesting systems due to its better performance appearance in the system in terms of the higher-temperature establishment and corresponding increase in the distillate as well, and same observations have been studied by many researchers [10, 11]. In addition to these observations, some additional elements having concentrators associated with the system have been analyzed by the researchers [12, 13] and also reviewed for material conscious economic analysis [14] and performances of different stills [15].

Such solar systems in a larger scale are used in many countries for the generation of potable water and electricity as well such as USA and Arab countries had been established with solar energy conditioned water plants having 400 m³ in a day potable water production capacity [16]. Solar still systems have better results and also more pure than the water obtained from other systems such as reversed osmosis water [17]. Further, solar still system performance is directly based on the solar exposure incident over the basin, and it was found that the roof over type SDU with diffuse operated channels performs better rather than conventional one as this design is much capable of maintaining higher basin temperature [18].

The better performance of the system will be further optimized by utilizing effective number of solar collectors, exposed basin area, etc. [19] In consequence with the increase in collector numbers, corresponding increase in the yield output appears but this increment will be interrupted after the optimized value of the yield output from the system. Further, a solar system has been developed to treat the most saline water, i.e., warmer seawater and found the system performance gets doubled and tripled at 25 and 45 °C. Such performance of the system was because of the combined effect of the atmospheric temperature, wind velocity, solar exposure (basin area) and the solar intensity over the system [20]. It is also recommended that the use of latent heat available to the water vapor can be further utilized to improve the systems performance [21].

It has been observed that for large annual freshwater, the most favorable inclination dedicated to FP solar receivers are twenty degrees and fifteen degrees for the still glass covers [22]. Better values of freshwater production appear during the months of April, May and October; this is due to favorable meteorological conditions. As one increases the mass of water, net yearly output will decrease due to the storage effect. Also, a solar system will be improved in its performances under the intensified solar insolation and by using a radiative cooling system [23]. A limitation related to the performance observed is representing the decrease in its overall efficiency for the corresponding increase in the systems temperature as comprised to the basin temperature. This is so because, improvement in the stills temperature also

increases the thermal losses of the still toward the atmosphere of either sides. The still productivity also improves by increasing the ambient temperature, as it improves the overall system performance and greater temperature difference in between the water and ambient.

So, above all, the remotely located areas of societies will suffer the conventional power supply to operate the electrical appliances also, these areas are mostly unavailable, and supply generated by fossil fuels is very costly too. Hence, the distillation units should use an alternate source of energy such as energy from the Sun. Being the conventional water purification processes energy demanding, Bourouni et al. [24] have offered an analysis on a new system for water treating under the consideration of air vapor condensation (AEC) in association with solar thermal receivers. By coupling a distillation unit functioning by AEC with solar units, they have optimized the unitary cost of the pure water.

The objective of present study is to review the single-phased SDU and ETC, CPC or concentrators associated solar stills and based on material conscious performances. And, based on the review, a confined conclusion with suggestive future scope has been given.

2 Merits and Demerits of Solar Still

2.1 Merits

- a. The solar-powered systems are almost free regarding maintenance.
- b. The passively operated units are generally free from moving parts and vice versa for active solar stills and accordingly maintenance cost applies.
- c. The mineral values are quite less, so better in use to such respective applications, otherwise for the drinking purpose it is required to add sort of mineral amounts as compared to others.
- d. Yield produced for the given area is appreciably high in case of active SDU.

2.2 Demerits

- a. Yield produced for the given area is quite low in case of passive SDU.
- b. Maintenance cost is high for active solar still systems.
- c. The vapor leakages are quite general for the system at its joints.
- d. The maintenance personals are usually system known one, that is why it is easy to operate.

3 CPC Inbuilt Systems

The CPC inbuilt systems are highly concentrated devices due to converging ability of the distracted solar energy toward the targeted basin areas where the water masses are supposed to be evaporated for the distillation processes. This segment is specified toward the applicable combinations in the presented solar inbuilt systems with CPC as follows.

The efficient system as shown in Figs. 1 and 2 has been analyzed for its feasible performances in association with the CPC and FLR for the large water production in the large-scale potable water production power plant along with power generation as well. They have selected many typical sites within these partner countries. As the compound parabolic concentrator (CPC) has better reflectivity for a typical solar angle that can be focused on the focal point of the parabola, the concentrated heat is the main concern the system [25].

Further, a still system in association with CCC, TSS, as shown in Fig. 3 has been studied and also compared with the conventional systems on yield basis and found the better results for the combinations of CCC concentrator assisted to the system. The result was better due to the higher concentration ratio occurrences in these combinations [26].

Then, CT-SDU associated still system was studied, and integration of PCM makes the overall system more effective in terms of the appreciable performing parameters. So, PCM improves the system's performance due to its heat absorption and corresponding heat recovery nature in off shine time [27].



Fig. 1 Parabolic trough collectors [25]

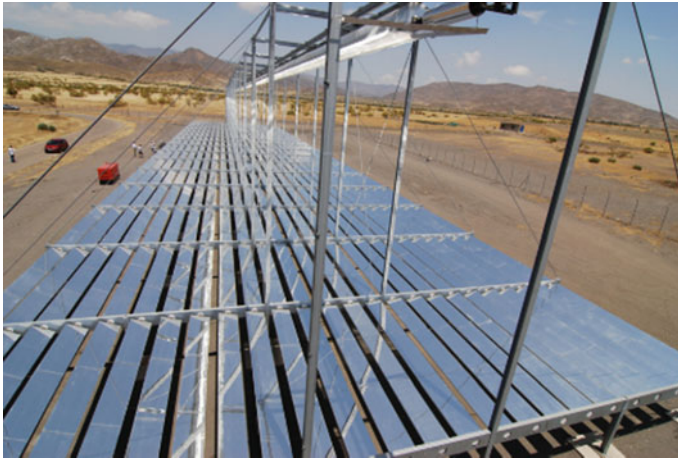


Fig. 2 Linear Fresnel reflector [25]

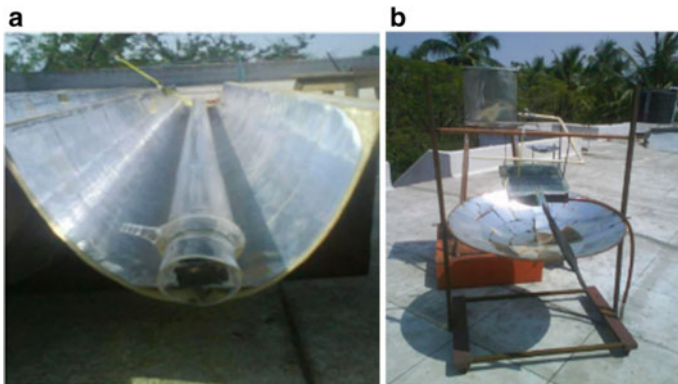


Fig. 3 a CCC solar still [26], b CPC-TSS-SDU [26]

The further corresponding study related to the TS, CPC and CTS in association with the still systems has been represented in Fig. 4 that shows the confined concentration of solar energy toward the still water. The system associated with CPC-CT to the pyramid structured still produces the better results as compared to the other combinations, as the larger area provided by the cover helps the improved yield output [28].

After that, a system with fractional covering of with PVT and integrated with the CPC has been analyzed for its lifetime operation, payback time, etc., for the double slope covering systems. Based on the observations, the single-phased still shows the inferior results than the -aced solar stills, as the still preferably double-faced system offers the extended area as well the larger water mass supports the performance of the system [29].

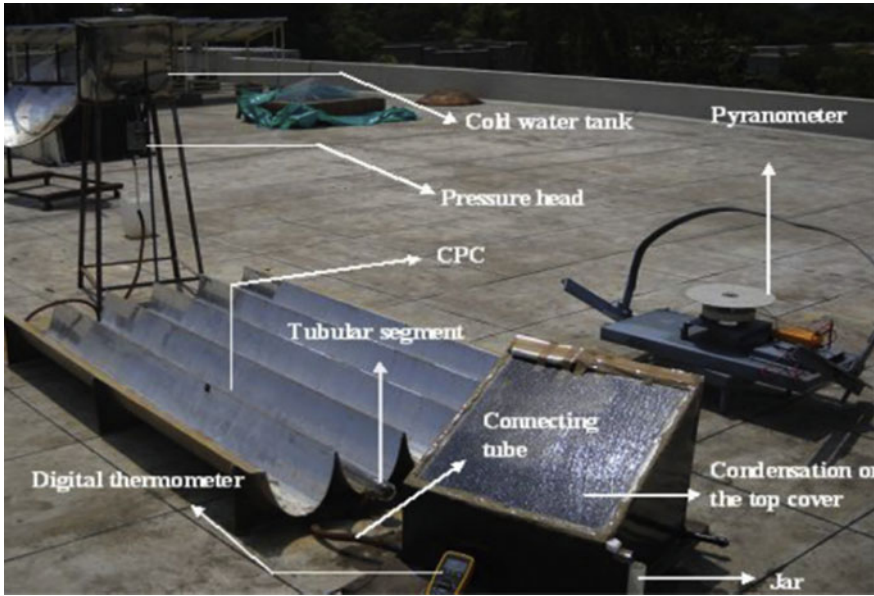


Fig. 4 CPC-CTSS-SDU [28]

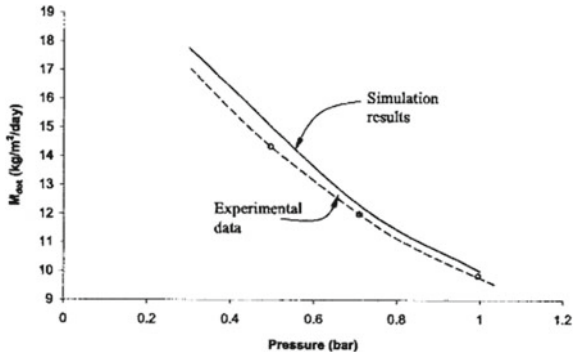
Moreover, the systems associated with the PV modules and concentrators of parabolic profile attached to stills have been observed to find the optimum yield performance and corresponding energy and exergy performances through the system. Based on the observed values of the system, it is easily predicted that the double exposed cover still system performs better having the optimum water height into the basin as 0.31 m or somehow greater than that and performed results are better due to the higher capabilities of sensible heating of the water and further utilization of it in the corresponding production of potable water.

4 ETC Inbuilt Systems

The ETC inbuilt systems are highly performed devices due to converging ability of the distracted solar energy toward the targeted basin areas under the confined tubular chamber of evacuated cross section where the water masses are supposed to receive the accumulated heat for the distillation processes. This segment is specified toward the applicable combinations in the presented solar inbuilt systems with ETC as follows.

In this context, a multi-step or staged basin system equipped with the confined tubular section having the evacuated section inside attached with the still system as shown in Fig. 5 was analyzed and compared with a conventionally operated solar still system and found the appreciable amount of distilled water into the collection jar.

Fig. 5 Yield versus internal pressure curve



The results are so observed due to the efficient heating of water inside the ETC tube and successfully conveyed to the basin water for the further desalination process, and also the result was so because evaporation rate is lower at high pressure [30].

And Fig. 6 shows a still connected with ETC having the heat reconsideration aspects inside the still system that improves the overall system performance as well considerably [31]. Further, it has been observed as the system runs properly within the daytime and increased output appeared for the peak solar radiations toward that system, and advanced improvement in the system’s performance in terms of yield appeared while the cold water overflowed to the covering of the system [32] as the cold water increases the intermediate temperature differences between two surfaces, i.e., water and glass.

After that still with ETC connection as referred in Fig. 7 represents a sophisticated combination of separate solar water heater interconnected with still chamber for the further utilization of hot water in desalination purpose. The combined system is



Fig. 6 Five-staged SDU-ETC [31]



Fig. 7 Solar still assisted ETC heat chamber [33]

deliberately performing the simultaneous operations related to water heating and desalination processes efficiently. And, the results obtained by this system have been matched with experimental values. It is noticed that the temperatures and yield have been enhanced [33].

Later on, still system with ETC and different types of PCM materials, its combinations and performing comparisons has been done in this study as represented in Fig. 8. In this study, it is an experimental type, and results are in favor of the black color or black basin linear. The result was so improving due to the better heat receiving and storing capabilities in comparison with others, and this system is also capable of desalinating the high saline water with high efficiency [34].

Then after, a new design of solar still that consists of ETC integrated a heat absorbing capable pipe inside it and recommended as a new version of ETC, i.e., with heat pipe and much more sufficient in instant solar heat receiving and as well as heat transmitting for the further use of desalination processes. This system results comparatively better output with higher efficiency as well as the corresponding distillate productivity under the solar peak hour conditions [35].

Also, a new design assisted a vacuum or low-pressure generating pump system assisted to the still system of two-side facing or opened to receive the solar radiations inside the basin chamber. The value addition due to low-pressure generating pump and the overall performance of the system improves accordingly. Further, the additional heat absorbing materials like stole gravel or pebble make the overall system a step ahead in the performance and corresponding yield in comparison with other systems of combinations. It also concludes the calcium stones which gives the highest freshwater output due to the good porosity of stones by which more solar energy is stored [36].

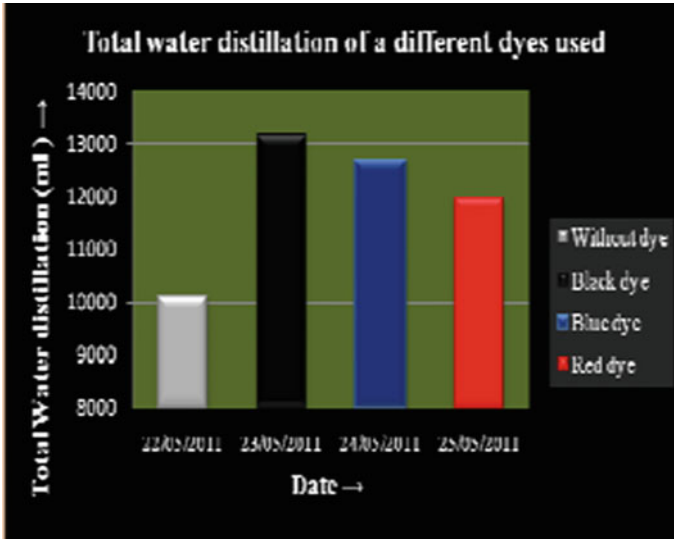


Fig. 8 Total water distillation using different dyes [34]

Further, a multistage still design assisting five numbers of staging steps in the basin chamber along with the parallel operated solar collectors along with the system has been modeled and analyzed and found more productive yield than other still systems or the combining still systems. Further, as the result was quite high, so the economy of the system and the productive cost of the yield appeared appreciably low in comparison with others [37].

Finally, a serried combinations of different still systems have been analyzed experimentally under the associative combinations of ETC, inclined stepped basin chamber that has a capability to remove the excessive or over floated salt or deposited salt over the basin water [38]. Also, Singh and Samsher [39] analyzed the energy matrix and enviroeconomics for the solar still associated with ETC and found better results with less ill effects on environment due to lower CO₂ emissions and lifelong working due to self-sustainability. Further, Singh and Samsher [40, 41] observed for different combinations of ETC in SDU and recommended better future for such associations to improve the overall performance of the system with further study of active solar stills [42] in view of performance improvements related to the overall system.

5 Conclusion and Future Scope

So, the present observations are clearly representing that there is a research gap for the utilization of self-sustainable use of these technologies or in a passive scenario for the production of potable water. However, a concise review of SDU incorporated

with ETC and concentrators has been discussed. As of importance point of view, both the elements are its own specialty depending upon the material utilized to make it smarter in the respective field.

CPC can produce higher heat due to concentrating the solar heat from a wide area to a focused absorber but higher heat has a drawback of higher heat losses. On the other hand, ETC has least heat losses in terms of radiation losses only due to its evacuated glaze layer fabrication, and the smart selective absorber coating sandwiched in between the glaze or moreover coated over the inner glaze outer surface of the tube makes the system much effective.

The overall system must be installed in such a way that gives the optimum performance of each elements utilized in it with least heat losses. Suitable materials should be adopted that have sensitive response toward heat transmission without any system disturbances as thermal expansion, heat absorption, chemical reaction or other side effects on the system that affects the system performance directly or indirectly. Moreover, the passive solar stills have much more capabilities to make the operations easier for a long period of time due to low maintenance, less embodied energy, self-sustainability, etc. Solar still compatible design with optimum performing combinations is required to maintain the gap in supply of freshwater against the corresponding demand of that by various fields of society.

References

1. Faegh M, Shafii MB (2017) Experimental investigation of a solar still equipped with an external heat storage system using phase change materials and heat pipes. *Desalination* 409:128–135
2. Singh AK, Singh DB, Mallick A, Kumar N (2018) Energy matrices and efficiency analyses of solar distiller units: a review. *Sol Energy* 173:53–75
3. Tiwari GN, Sahota L (2016) Review on the energy and economic efficiencies of passive and active solar distillation systems. *Desalination*. (in press)
4. Singh DB, Singh AK, Kumar N, Dwivedi VK, Yadav JK, Singh G (2019) Performance analysis of special design single basin passive solar distillation systems: a comprehensive review, advances in engineering design. *Lecture notes in mechanical engineering*. Springer, pp 301–310
5. Singh AK, Singh DB, Mallick A, Harender, Sharma SK, Kumar N, Dwivedi VK (2019) Performance analysis of specially designed single basin passive solar distillers incorporated with novel solar desalting stills: a review. *Solar Energy* 185:146–164
6. Singh AK, Chattopadhyaya S, Singh DB, Kumar N (2017) Performance study for active solar stills based on energy metrics: a short review. *JoRACHV* 4(3):21–26
7. Singh AK, Singh DB, Kumar N, Dwivedi VK, Singh G, Kumar R (2019) Basin-type solar distiller associated with PVT collectors—a comprehensive review, advances in energy and built environment. *Lect Notes Civil Eng Springer* 36:253–260
8. Singh AK, Singh DB, Dwivedi VK, Kumar N, Yadav JK (2019) A review of performance enhancement in solar desalination systems with the application of nanofluids. *ICACCCN*, pp 814–819
9. Samsheer D, Singh DB, Singh AK, Kumar N (2019) Solar distiller unit loaded with nanofluid—a short review, advances in interdisciplinary engineering. *Lecture notes in mechanical engineering*. Springer, pp 241–247
10. Tang R, Yang Y, Gao W (2011) Comparative studies on thermal performance of water-in-glass evacuated tube solar water heaters with different collector tilt-angles *Solar Energy* 85:1381–1389

11. Kabeel AE, Khalil A, Elsayed SS, Alatyar AM (2015) Modified mathematical model for evaluating the performance of water-in-glass evacuated tube solar collector considering tube shading effect. *Energy* 89:24–34
12. Shafii MB, Jahangiri Mamouri S, Lotfi MM, Jafari Mosleh H, A modified solar desalination system using evacuated tube collector. *Desalination* 396:30–38 (2016)
13. Jafari Mosleh H, Jahangiri Mamouri S, Shafii MB, Hakim Sima A (2015) A new desalination system using a combination of heat pipe, evacuated tube and parabolic through collector. *Energy Convers Manage* 99:141–150
14. Sanserwal M, Singh AK, Singh P (2020) Impact of materials and economic analysis of single slope single basin passive solar still: a review. *Mater Today Proc* 2:1643–1652
15. Singh AK, Singh DB, Dwivedi VK, Tiwari GN, Gupta A (2020) Water purification using solar still with/without nano-fluid: a review. *Mater Today Proc* 21:1700–1706
16. Seri WL (1981) Solar energy water desalination in the United States and Saudi Arabia
17. Tleimat BW, Howe ED (1982) Comparative productivity of distillation and reverse osmosis desalination using energy from solar ponds. *Trans ASME J Sol Energy Eng* 104(4):299–304
18. Elsayed MM (1983) Comparison of transient performance predictions of a solar operated diffusion type still with a roof type still. *J SolEnergy Eng* 105:23–28
19. Kumar S, Tiwari GN (1998) Optimization of collector and basin areas for a higher yield for active solar stills. *Int J Desalination* 116:42–54
20. Assouad Y, Lavan Z (1988) Solar desalination with latent heat recovery. *J Sol Energy Eng* 110(1):14
21. Tiwari GN, Sinha S (1993) Parametric studies of active regenerative solar still. *Energy Convers Manage* 34(3):209–218
22. Kumar S, Tiwari GN, Singh HN (2000) Annual performance of an active solar distillation system. *Desalination* 127(1):79–88
23. Haddad OM, Al-Nimr AM, Maqableh A (2000) Enhanced solar still performance using a radiative cooling system *Renewable Energy* 21(3–4):459–469
24. Bourouni K, Bouden C, Chaibi M (2003) Feasibility investigation of coupling a desalination prototype functioning by Aero-Evapo-Condensation with solar units. *Int J Nucl Desalin* 1(1):116–131
25. Moser M, Trieb F, Kern J, Allal H, Cottret N, Scharfe J, Savoldi E (2011) The MED-CSD project: potential for concentrating solar power desalination development in Mediterranean countries. *J SolEnergy Eng* 133(3):031012
26. Arunkumar T, Velraj R, Ahsan A, Khalifa AJN, Shams S, Denkenberger D, Sathyamurthy R (2016) Effect of parabolic solar energy collectors for water distillation. *Desalination Water Treat* 57(45):21234–21242
27. Arunkumar T, Velraj R, Denkenberger D, Sathyamurthy R, Vinothkumar K, Porkumaran K, Ahsan A (2016) Effect of heat removal on tubular solar desalting system. *Desalination* 379:24–33
28. Arunkumar T, Velraj R, Denkenberger DC, Sathyamurthy R, Kumar KV, Ahsan A (2016) Productivity enhancements of compound parabolic concentrator tubular solar stills. *Renewable Energy* 88:391–400
29. Singh DB, Tiwari GN (2016) Effect of energy matrices on life cycle cost analysis of partially covered photovoltaic compound parabolic concentrator collector active solar distillation system. *Desalination* 397:75–91
30. Singh AK (2020) An inclusive study on new conceptual designs of passive solar desalting systems. *Heliyon* 7:e05793
31. Schwarzer K, Da Silva MEV, Schwarzer T (2011) Field results in Namibia and Brazil of the new solar desalination system for decentralised drinking water production. *Desalination Water Treat* 31(1–3):379–386
32. Mousa H, Arabi MA (2013) Desalination and hot water production using solar still enhanced by external solar collector. *Desalination Water Treat* 51(4–6):1296–1301
33. Dev R, Tiwari GN (2012) Annual performance of evacuated tubular collector integrated solar still. *Desalination Water Treat* 41(1–3):204–223

34. Patel MI, Meena PM, Inkia S (2013) Effect of dye on distillation of a single slope active solar still coupled with evacuated glass tube solar collector. *IJERA* 1(3):456–460
35. Jahangiri MS, Gholami DH, Ghiasi M, Shafii MB, Shiee Z (2014) Experimental investigation of the effect of using thermosyphon heat pipes and vacuum glass on the performance of solar still. *Energy* 75:501–507
36. Panchal HN, Shah PK (2015) Enhancement of distillate output of double basin solar still with vacuum tubes. *J King Saud Univ Eng Sci* 27(2):170–175
37. Reddy KS, Sharon H (2017) Energy-environment-economic investigations on evacuated active multiple stage series flow solar distillation unit for potable water production. *Energy Convers Manage* 151:259–285
38. Patel MI, Meena PM, Inkia S (2011) Experimental investigation on single slope-double basin active solar still coupled with evacuated glass tubes. *IJAERS* 2249–8974
39. Singh AK (2020) Material conscious energy matrix and enviro-economic analysis of passive ETC solar still. *Mater Today Proc.* <https://doi.org/10.1016/j.matpr.2020.05.117>
40. Singh AK A review study of solar desalting units with evacuated tube collectors. *J Cleaner Prod* <https://doi.org/10.1016/j.jclepro.2020.123542>
41. Singh AK (2020) Analytical study of evacuated annulus tube collector assisted solar desalination system: a review. *Sol Energy* 207:1404–1426
42. Singh AK, Yadav RK, Mishra D, Prasad R, Gupta LK, Kumar P (2020) Active solar distillation technology: a wide overview. *Desalination* 493:114652

Heavy Metal Assessment in Urban Particulate Matter in Industrial Areas of Vadodara City



S. A. Nihalani, A. K. Khambete, and N. D. Jariwala

Abstract Air pollution related to particulate matter is becoming a crisis of chief concern these days in urban areas. The concentration of ambient particulates is recently grabbing attention all over the world, owing to its harmful effects on people. The prime health risks linked with particulate pollution are breathing problems like asthma and long-term effects leading to premature death in the case of people with respiratory problems. This can essentially be attributed to mounting exposure to urban fine particulates termed as PM_{2.5}. In the past several decades, exhaustive monitoring for ambient heavy metals focussing on long-term temporal trends and chemical characterisation has been done all over the world. The significant aspect of air pollution control depends on recognising the accurate sources of the pollutant. Sampling and monitoring for three sites at PCC industrial area in Vadodara for PM₁₀₀, PM₁₀, and PM_{2.5} including heavy metals have been carried out. PM₁₀₀ concentrations were observed to be between 214 and 398 $\mu\text{g}/\text{m}^3$, PM₁₀ was found to be between 70 and 93 $\mu\text{g}/\text{m}^3$, and PM_{2.5} concentration was in the range 10–35 $\mu\text{g}/\text{m}^3$. Highest concentrations of Fe, Zn, Cu, Ni, Pb, Cd, Hg, and Cr were found to be 10.86, 6.78, 0.995, 0.151, 0.077, 0.057, 0.025, and 0.014 $\mu\text{g}/\text{m}^3$, respectively. The chief sources of particulates and heavy metals at the site were emissions from industrial processes, traffic emissions, and re-suspension dust. It can be inferred that it is necessary to perform a detailed and exhaustive assessment of air pollutants and heavy metals in the study area.

Keywords Urban particulates · Heavy metal assessment · Suspended particulate matter

S. A. Nihalani (✉)

Department of Civil Engineering, SVNIT, Surat and Parul University, Vadodara, India

e-mail: seema.nihalani@paruluniversity.ac.in

A. K. Khambete · N. D. Jariwala

Department of Civil Engineering, SVNIT, Surat, India

e-mail: anjali_khambete3@yahoo.co.in

N. D. Jariwala

e-mail: ndj@ced.svnit.ac.in

1 Introduction

In developing countries like India, rapid industrialisation, urbanisation, and population explosion have led to an increase in fossil fuel combustion leading to a greater concentration of particulate matter and gaseous air pollutants [1]. The common air pollutants generally include total suspended particulate matter, respirable suspended particulates, carbon monoxide, sulphur dioxide, and nitrogen dioxide [2]. From the different air pollutants, urban particulates are considered to be of major concern due to its critical impact on air quality in an urban area and as well as a rural area [3]. Particulate matter is termed as a complex fusion of liquid or solid particulates that may vary in size. Airborne particulates are classified into coarse, fine, and ultrafine particles based on their aerodynamic diameters [4]. The natural sources of particulates may be dust, soil, or other crustal elements from, roads, mines, or volcanoes. The major anthropogenic sources of particulate matter may be industrial processes, fossil fuel burning, agricultural residue, or municipal solid waste incineration, construction activities, and emissions from paved and unpaved roads [5].

2 Sources and Effects of Heavy Metals Linked with Particulate Matter

Heavy metals are regarded as one of the most precarious groups of anthropogenic pollutants in the environment. This shall be attributed to their toxicity and persistent nature in the environment. Various studies have shown considerable links between health effects and different constituents of particulates like aluminium, arsenic, bromine, carbon, elemental carbon, chromium, copper, organic selenium, iron, lead, sulphate, mercury, nickel, nitrate, potassium, sodium, titanium, vanadium, and zinc, etc. Metals specifically cadmium, copper, and lead are capable of accumulating in the human body for a comparatively longer time period. The presence of heavy metals in urban particulates in significant concentration can lead to adverse health effects in human beings [6]. High levels of airborne heavy metals like lead, cadmium, and few organic pollutants may lead to neurological and behavioural problems in children. Lead is termed to be a community air pollutant. It is associated with increased blood lead in adults. Long-term exposure to Pb can lead to health problems such as tooth decay, anaemia, indigestion, and bone marrow alterations.

3 Study Area

Vadodara city is located in the central-eastern mainland region of Gujarat. Vadodara lies roughly between 22° 17' North latitude and 73° 15' East longitudes. The district covers an area of 7794 km² and accounts for 3.79% of the total geographical area of the state. Vadodara is considered a cosmopolitan city located on the banks of river Vishwamitri and to the South East of the city Ahmedabad [7]. Since all the major roads and railway lines connecting Delhi, Mumbai, and Ahmedabad pass through Vadodara, it is also known as the “Gateway to the Golden Corridor”. Due to urbanisation, various residential areas earlier have not been converted to the commercial areas, industrial areas, leading to severe air pollution. Since the late sixties and early seventies, the city has seen a spurt of industrial growth with the large refinery, petrochemicals, and fertilisers units being developed along with other downstream chemical units, and several ancillary units have been set up through the city in several industrial estates, which dot the city landscape. The major industries in the city include chemicals, petrochemicals, pharmaceuticals, and biotechnology. The monitoring locations were designed keeping the topography of the study area, wind speed as well as wind direction in mind [8].

From the several industrial areas, it was preferred to select the IOCL industrial area for study purposes since it houses various chemicals and pharmaceuticals. Three sampling locations were selected. One sampling station was selected on the upstream side of the industrial area, which is Koyali village, and two sampling stations were selected on the downstream of the industrial area that is Karachia and Ranoli villages. The annual wind rose diagram is shown in Fig. 1, and the sampling locations are shown in Fig. 2 and tabulated in Table 1.

4 Methodology

4.1 Sampling and Concentration of Particulate Matter

- Sampling was done at the stations for monitoring PM100, PM10, and PM2.5 using HVS, respirable dust sampler, and PM2.5 samplers.
- All three samplers were run simultaneously for 24 h in the open air, and flow rate was recorded [9].
- After the required time of sampling, the filter papers were taken out and stored carefully in envelopes within the desiccator.
- The filter papers were conditioned at 20–30 °C temperature and relative humidity between 40 and 50% [10].
- For all the three samplers, the initial weight (W_i) was taken for the filter papers.
- After sampling, the filter papers were again conditioned at 20–30 °C temperature and relative humidity between 40 and 50%.
- For all the three samplers, the final weight (W_f) was taken for the filter papers.

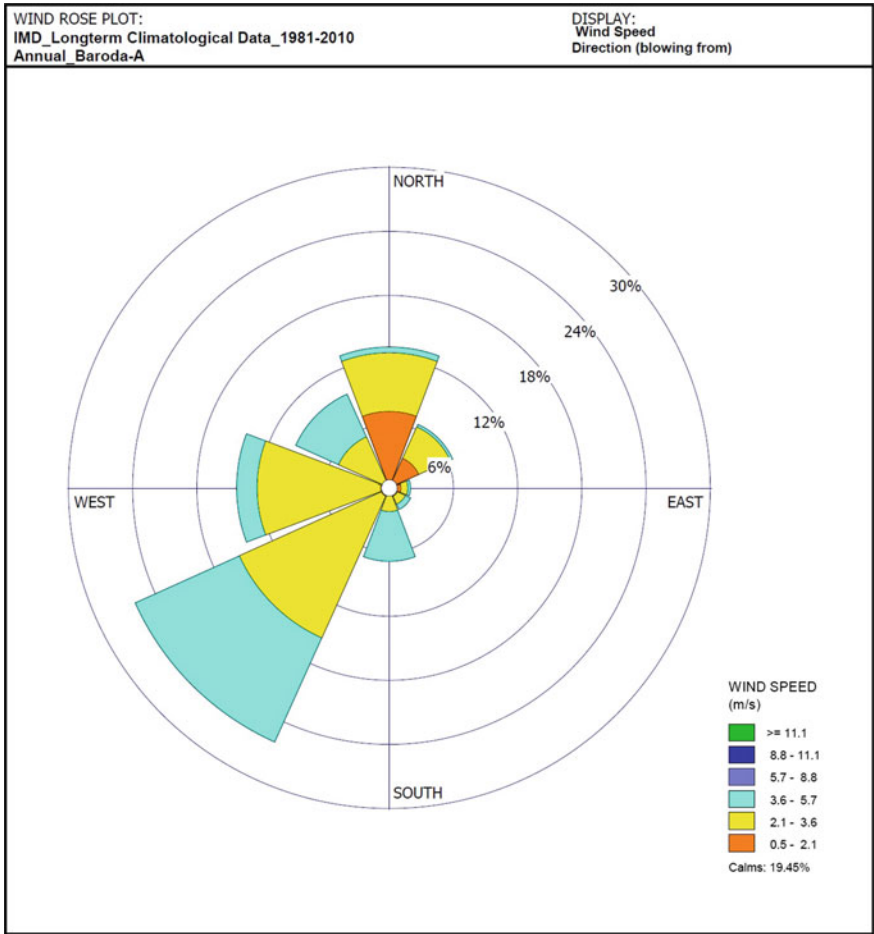


Fig. 1 Annual wind rose diagram

Calculations of the Mass of Particulate Matter

$$RSPM(\mu g/m^3) = (W_f - W_i) \times 10^6 / V$$

where

- V air volume sampled in m^3 .
- W_f final filter weight in g.
- W_i initial filter weight in g.

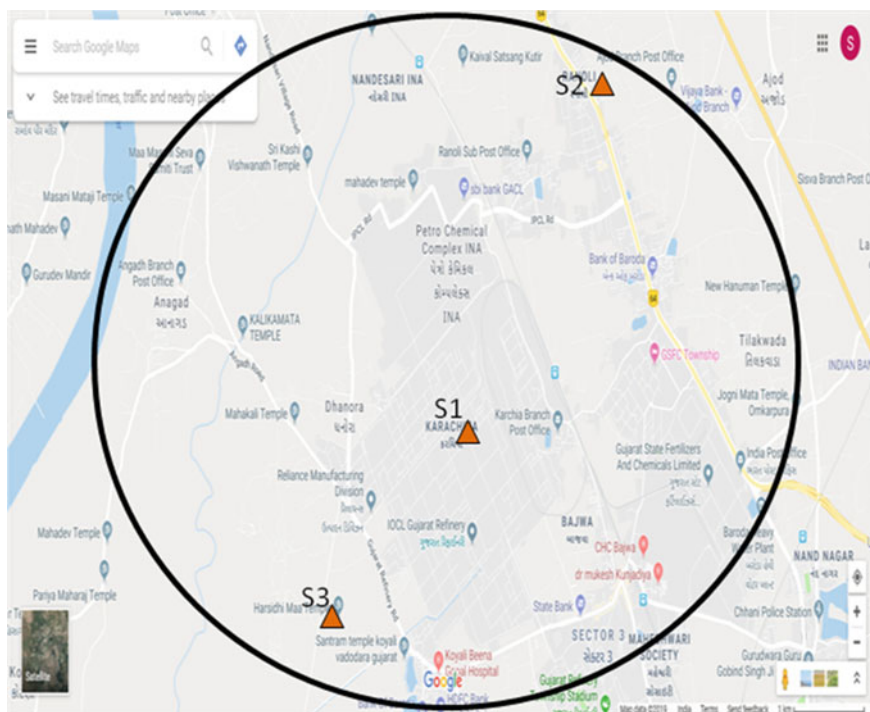


Fig. 2 Sampling locations in study area

Table 1 Details of sampling locations

Sr. No.	Station No.	Location	Rationale	Area category
1	AQ01	Karachia	d/w	Industrial
2	AQ02	Ranoli	d/w	Industrial
3	AQ03	Koyali	u/w	Industrial

4.2 Heavy Metal Analysis

- The size of the filter paper used for measurement of PM₁₀₀/PM₁₀ was adequate for further analysis for trace elements. Hence, toxic heavy metals, namely As, Cu, Cd, Cr, Hg, Fe, Mn, Ni, Pb, and Zn were analysed [11]. This method includes acid digestion of filter paper followed by chemical analysis using atomic absorption spectrometry.
- The exposed part of the filter was cut into three equal pieces. Once a piece of this filter paper was cut into small pieces and dip in a beaker having 100 ml acid (3% HNO₃ & 8% HCl) solution and beaker heated on the heating mantle for 10–15 min, till the volume reduces to 20 or 30 ml. Acid digestion was needed for

the metal estimation by AAS [12]. The contents of the beaker are cooled using filter paper, and the final volume made 100 ml be distilled water for estimation of heavy metal.

- Standard metal solutions were prepared in the optimum concentration range present by appropriate dilution of the CRM (certified reference metal) of As, Cu, Cd, Cr, Hg, Fe, Mn, Ni, Pb, and Zn solutions of 1000 ppm.
- The heavy metal determination was carried out using a Varian Spectra AA-220, atomic absorption spectrophotometer in the air-acetylene flame mode with background correction and hollow cathode lamps.

Calculations of Heavy Metals

The mass concentration of lead is expressed in micrograms per cubic metre in the air sample to the nearest $0.1 \mu\text{g}/\text{m}^3$ using equation

$$\text{Pb}(\text{conc}) = [\text{Pb}(\text{sm}) - \text{Pb}(\text{B1})] \times V1/V$$

where

- Pb (conc) mass concentration of particulate lead in $\mu\text{g}/\text{ml}$.
 Pb (Sm) concentration of particulate lead, in $\mu\text{g}/\text{ml}$ in the sample solution.
 Pb (B1) concentration of particulate lead, in $\mu\text{g}/\text{ml}$ in blank solution.
 V1 total volume of digested sample in ml, and.
 V volume of sampled air in m^3 .

5 Regulatory standards

The National Ambient Air Quality Standards are ambient air quality standards put in place by the Ministry of Environment and Forests and applicable nationwide [13]. These standards specify major pollutants along with their concentrations, averaging time and assessment procedures, etc. [14] National ambient air quality standard (NAAQS) for particulates and heavy metals is represented in Table 2, and standard heavy metal concentrations are given in Table 3.

6 Results

Three locations, namely Karachia, Ranoli, and Koyali were selected based on the wind rose diagram for the summer season. Koyali is located upstream of PCC industrial area and Karachia and Ranoli on downstream. PM100, PM10, and PM2.5 were measured at the same time at each location during the first and second weeks of June 2019. Further, on the filter papers used for sampling of PM100 and PM10, heavy metals were analysed using standard procedure. The concentrations of PM100,

Table 2 National ambient air quality standards—New Delhi 18 November 2009

Pollutant	Time-weighted average	Ambient air concentration	
		Industrial, residential, rural, and other areas	Ecologically sensitive area
Particulate matter—PM ₁₀ , $\mu\text{g}/\text{m}^3$	Annual * 24 h **	60 100	60 100
Particulate matter—PM _{2.5} , $\mu\text{g}/\text{m}^3$	Annual * 24 h **	40 60	40 60
Lead (Pb), $\mu\text{g}/\text{m}^3$	Annual * 24 h **	0.50 1.0	0.50 1.0
Arsenic (As), ng/m^3	Annual *	06	06
Nickel (Ni), ng/m^3	Annual *	20	20

Table 3 Standard heavy metals concentrations in ambient air

Sr. No.	Heavy metal	Standard concentration $\mu\text{g}/\text{m}^3$	Reference
1.	Cd	0.005	WHO, AAQC
2.	Pb	0.500	NEPC, AAQC
3.	Cr	0.010	TCEQ
4.	Ni	0.0038	WHO
5.	Cu	1.000	TCEQ
6.	Zn	100	EQA
7.	Mn	0.15	WHO

AQC Ambient Air Quality Criteria Act 1994, *EQA* Environmental Quality Act 1974, *NEPC* National Environmental Protection Council, *WHO* World Organisation Health, *TCEQ* Texas Commission on Environmental Quality

PM₁₀, and PM_{2.5} are shown in Fig. 3, and the heavy metal concentrations are shown in Table 4.

7 Discussion of Results

- The concentration of PM₁₀ was found to be between 214 and 398 $\mu\text{g}/\text{m}^3$ greater than the NAAQS standard of 230 $\mu\text{g}/\text{m}^3$.
- PM₁₀ concentrations were observed to be between 70 and 93 $\mu\text{g}/\text{m}^3$, less than the NAAQS standard of 100 $\mu\text{g}/\text{m}^3$.

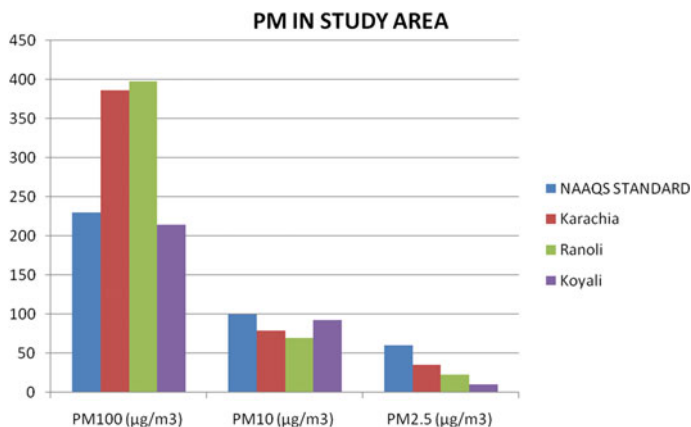


Fig. 3 Particulate matter status in the study area

Table 4 Heavy metal concentration in the study area

Sampling location			Karachia		Ranoli		Koyali	
Sr. No.	Heavy Metals	IS std	PM100	PM10	PM100	PM10	PM100	PM10
1	Arsenic (As)	0.006	ND*	ND*	ND*	ND*	ND*	ND*
2	Copper (Cu)	1	0.995	0.754	0.044	0.042	0.124	0.037
3	Cadmium (Cd)	0.005	ND*	ND*	ND*	ND*	0.057	ND*
4	Chromium (Cr)	0.01	0.014	0.01	0.008	0.006	0.011	0.009
5	Mercury (Hg)	50	0.025	0.017	0.003	0.003	0.004	0.001
6	Iron (Fe)	10	10.86	3.59	5.45	2.79	6.16	5.34
7	Manganese (Mn)	0.15	ND*	ND*	ND*	ND*	ND*	ND*
8	Nickel (Ni)	0.02	0.151	0.091	0.09	0.114	0.122	0.089
9	Lead (Pb)	1	ND*	ND*	ND*	ND*	0.077	0.03
10	Zinc (Zn)	10	2.19	4.1	6.78	3.5	5.19	4.39

- The average PM_{2.5} concentrations were found to be between 10 and 35 µg/m³ less than the NAAQS standard of 60 µg/m³.
- The highest concentrations for Cu, Cd, Cr, Hg, Ni, Pb, Fe, and Zn were found to be 0.995, 0.057, 0.014, 0.025, 0.151, 0.077, 10.86, and 6.78 µg/m³, respectively, in PM₁₀₀.
- The highest concentrations for heavy metals Cu, Cr, Hg, Ni, Pb, Fe, and Zn were found to be 0.754, 0.01, 0.017, 0.114, 0.03, 5.34, and 4.39 µg/m³, respectively, in PM₁₀.

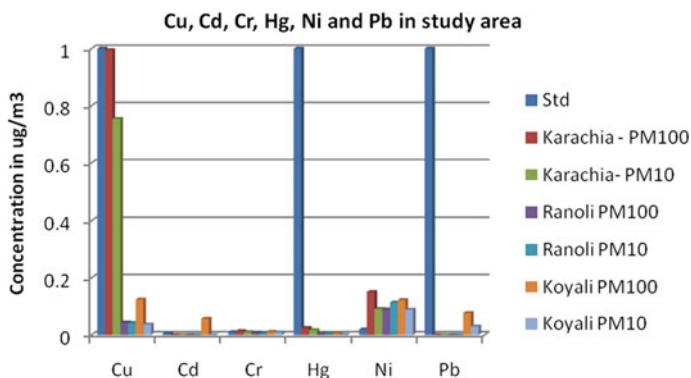


Fig. 4 Cu, Cd, Cr, Hg, Ni, and Pb in the study area

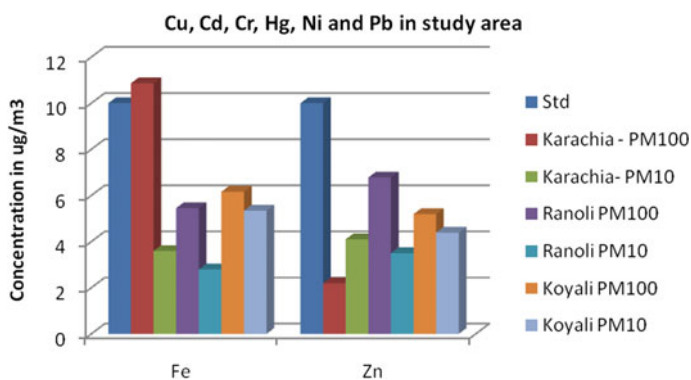


Fig. 5 Fe and Zn in the study area

- Figures 4 and 5 show the heavy metals concentrations in ambient particulates in the study area.
- The presence of copper indicates a probable source as vehicular emissions or coal combustion.
- The presence of chromium suggests emissions from coal and oil combustion.
- Presence of mercury points towards discharge from hydroelectric, mining, pulp, and paper industries.
- The presence of iron indicates emissions from soil or crustal sources.
- Presence of nickel points towards emissions from petroleum and coal combustion.
- The presence of zinc suggests emissions from the combustion of coal or coal-fired boiler.
- The presence of lead only at Koyali indicates proximity to traffic junction in addition to an industrial source.
- The absence of arsenic and manganese at all sites points towards the absence of steel smelting industries or coal combustion in the study area.

- The absence of cadmium at all sites except Koyali suggests the absence of probable sources of cadmium, which are steel, plastic, and pigment production.

8 Conclusion

The current study determines heavy metal levels in ambient particulates in Vadodara industrial area. The average PM_{2.5} concentrations were found to be between 10 and 35 $\mu\text{g}/\text{m}^3$ less than the NAAQS standard of 60 $\mu\text{g}/\text{m}^3$. Against the NAAQS standard of 100 $\mu\text{g}/\text{m}^3$, PM₁₀ concentrations were found to be between 70 and 93 $\mu\text{g}/\text{m}^3$. The concentration of PM₁₀₀ was found to be between 214 and 398 $\mu\text{g}/\text{m}^3$. In addition, all the six samples contained one or more metals at a concentration higher than the limit or guideline set by either CPCB or WHO [15]. Several of the detected metals, particularly chromium and arsenic, are carcinogenic to humans [16]. The detected heavy metals also give some indications as to the sources of particulate pollution [17]. High levels of copper, cadmium, chromium, nickel, and lead in particulates can be linked to industrial emissions, while high levels of iron and zinc can be linked to coal burning and ferrous metal melting [18]. High chromium and nickel can also be linked to traffic emissions. The heavy metal concentrations were observed to be more in PM₁₀₀ as compared to PM₁₀. The highest concentrations were found to be 0.995, 0.057, 0.014, 0.025, 0.151, 0.077, 10.86, and 6.78 $\mu\text{g}/\text{m}^3$ for Cu, Cd, Cr, Hg, Ni, Pb, Fe, and Zn in PM₁₀₀, respectively. The highest concentrations of heavy metals were found to be 0.754, 0.01, 0.017, 0.114, 0.03, 5.34, and 4.39 $\mu\text{g}/\text{m}^3$ for Cu, Cr, Hg, Ni, Pb, Fe, and Zn in PM₁₀, respectively. It is also a strong justification for more comprehensive monitoring programs of air pollution levels in middle-level cities like Vadodara, as well as the need for a renewed focus on the identification and control of sources for the toxic heavy metals associated with urban particulates.

References

1. Banerjee T, Srivastava RK (2011) Evaluation of environmental impacts of integrated industrial estate—Pantnagar through the application of air and water quality indices. *Environ Monit Assess* 172:547–560
2. Batra S, Gargava P, Kamyotra JS, Dube R (2010) An integrated approach to urban air quality management. *Studies on Pollution Mitigation*. CPCB 9–21
3. Kulshrestha A, Satsangi PG, Masih J, Taneja A (2009) Metal concentration of PM_{2.5} and PM₁₀ particles and seasonal variations in urban and rural environment of Agra, India. *Sci Total Environ* 407(24):6196–6204
4. Kumar R, Joseph AE (2006) Air pollution concentrations of PM 2.5, PM 10, and NO 2 at ambient and kerbside and their correlation in Metro City—Mumbai. *Environ Monitor Assess* 119(1–3):191–199
5. Bhuyan B, Gupta R (2014) Assessment of urban air quality in Guwahati city, India using air quality index. *ZENITH Int J Multidis Res* 4(10):90–99
6. Giri D, Adhikary P, Murthy V (2008) The influence of meteorological conditions on PM₁₀ concentrations in Kathmandu Valley. *Int J Environ Res* 2:49–60

7. Nihalani S, Kadam S (2019) Ambient air quality assessment for Vadodara City using AQI and exceedance factor. Available at SSRN 3464926.
8. Srimuruganandam B, Nagendra SMS (2010) Analysis and interpretation of particulate matter—PM10, PM2.5, and PM1 emissions from the heterogeneous traffic near an urban roadway. *Atmosph Pollut Res* 1(3):184–194
9. Dubey B, Pal AK, Singh G (2012) Trace metal composition of airborne particulate matter in the coal mining and non-mining areas of Dhanbad Region, Jharkhand India. *Atmosph Pollution Res* 3(2):238–246
10. Sarasamma JD, Narayanan BK (2014) Air quality assessment in the surroundings of KMML industrial area, Chavara in Kerala, South India. *Aerosol Air Q Res* 14(6):1769–1778
11. Rao SS, Rajamani NS, Reddi EUB (2015) Assessment of heavy metals in respirable suspended particulate matter at residential colonies of Gajuwaka industrial hub in Visakhapatnam. *Int J Geol Agricul Environl Sci* 3(5):56–64
12. Mishra AK, Maiti SK, Pal AK (2013) Status of PM10 bound heavy metals in ambient air in certain parts of Jharia coalfield, Jharkhand India. *Int J Environ Sci* 4(2):141
13. Mishra AA, Kori R, Saxena A, Upadhyay N, Shrivastava PK, Kulshreshtha A, Sen S (2019) Air Quality Index of Bhopal City, Madhya Pradesh, India. *Int J Environ Monitoring Protect* 6(1):1
14. Rajamanickam R, Nagan S (2018) Assessment of air quality index for cities and major towns in Tamil Nadu, India. *J Civil Environ Eng* 8(2)
15. Nihalani SA, Moondra N, Khambete AK, Christian RA, Jariwala ND (2020) Air quality assessment using fuzzy inference systems, Advanced engineering optimization through intelligent techniques. Springer, Singapore, pp 313–322
16. Nihalani SA, Khambete AK, Jariwala ND (2020) Receptor modelling for particulate matter: review of Indian scenario. *Asian J Water Environ Pollut* 17(1):105–112
17. Nihalani SA, Khambete AK, Jariwala ND (2020) Review of source apportionment of particulate matter for Indian scenario. In: *Emerging trends in civil engineering*. Springer, Singapore, pp 209–218
18. Nihalani SA, Khambete AK, Jariwala ND (2020) Source apportionment of particulate matter—a critical review for Indian scenario. In: *Environmental processes and management*. Springer, Cham, pp 249–283

An Improved Approach for Accurate Weather Forecasting



Shubham Aggarwal, S. Hasnain Pasha, Sunil Kumar Chowdhary, Chetna Choudhary, Shiva Mendiratta, and Pramathesh Majumder

Abstract As recurrence and the impact of some weather events are increasing, therefore it needs to tackle such events is the concern. Climate change is one of the factors causing such increase in magnitude and frequency of extreme weather events. Weather forecasting system can help in managing such events. Daily weather forecasting and monitoring promote resource management and disaster preparedness. This research focused on the daily weather conditions of cities of different countries like Shanghai, Manila, Tokyo, Kolkata and Mexico. Weather conditions of these cities were monitored and recorded from different weather forecasting Web sites daily. Based on this recorded data, an improved weather forecasting model can be developed through statistical analysis of temperature, wind speed, quantitative precipitation of extreme weather events happened among these cities in recent decades. Using Minitab statistical software, the accurate weather providing Web site was analyzed. The deviation of these readings helped in analyzing how accurate is the reading provided by the weather forecasting Web sites concerning the calculated mean of the readings.

Keywords Weather · Forecasting · Management · Minitab · Standard deviation

S. Aggarwal · S. H. Pasha (✉) · S. K. Chowdhary · C. Choudhary · S. Mendiratta · P. Majumder
Amity University, Uttar Pradesh, Noida, India
e-mail: hasnain.pasha@gmail.com

S. Aggarwal
e-mail: shubham.saini48@gmail.com

S. K. Chowdhary
e-mail: skchowdhary@amity.edu

C. Choudhary
e-mail: cchoudhary@amity.edu

1 Introduction

Weather is the atmospheric conditions of a particular location and time. Application of science and technology to predict the weather conditions is known as weather forecasting. Temperature, wind speed, rain, atmospheric pressure, humidity, etc., are the major attributes that affect the weather condition of a particular region. Predicting accurate weather conditions has always been the most challenging task. Factors like climate change and global warming predict to be more difficult and challenging. Rapid growth in population in India and their policies of adopting urbanization has led to increasing various socioeconomic impacts due to extreme weather events such as cyclones, flood, hailstorm, heat and cold waves, drought and thunderstorms.

Many of today's weather forecasting systems rely on observations and analysis done by meteorologists using conventional principles. As many new models are being developed for weather forecasting every year but most of them do not provide accurate values. The need is to use the correct algorithms for effective and accurate prediction of weather information. Also, different online weather forecasting stations provide different weather conditions, therefore the need to develop a model that can guide a user to the best possible source from where accurate weather conditions can be fetched and arise. Weather forecasting proves to be useful in various info-science fields like disaster management, early warning system in an airport or naval system, helping farmers in protecting their crops against any extreme weather conditions. Today's weather forecasting system includes a combination of various technologies, computer models, trends and patterns knowledge, observations, etc. Utilizing these technology's accuracy of weather forecasting can be calculated for five days in advance.

2 Data Preprocessing

Daily weather conditions of some extreme weather-affected cities of the world were monitored and recorded. This research focused on the daily weather conditions in Shanghai, Manila, Tokyo, Kolkata and Mexico. The weather conditions of these cities were monitored and recorded daily for up to 20 days. Weather conditions were recorded based on current temperature, quantitative precipitation and wind speeds. The data were formulated in the form of a table. The columns represent five cities of different countries affected by weather events, and the rows show weather forecasting Web sites. [1–5] To compare variations in the recorded weather conditions, we selected top weather forecasting Web sites—Accu-weather, Intellicast, WeatherBug, weather underground and Yahoo weather.

3 Literature Review

This section of paper investigates some recent researches in weather forecasting domain that have been done. It overviews the models, techniques, management processes that have already been implemented in this domain.

Norwegian Vilhelm Bjerknes and LF Richardson initiated numerical weather prediction in the early 1990s. This was much related to the initial value problem of statistics in mathematics. Models used for accurate weather prediction were based on linear regression. These models were easy and simple to understand. Multiple regression model was formulated further to improve the accuracy. In [6], research defines a solution to weather forecast using MapReduce framework. Researchers describe how data set and patterns of recent years help in the prediction of storm and support vector machine (SVM) helped in classifying the data.

In [7], the researchers performed a statistical analysis of weather conditions using historical weather forecast data of the National Oceanic and Atmospheric Administration [NOAA]. Important findings were that there were significant variations in forecast accuracies, observed probabilities of precipitation were significantly lower than forecasted one, and forecasting organizations generally predict wind speeds by a large margin for days when wind speed exceeds 20 mph.

In [8], the authors developed various models to predict daily weather forecast in cities like Albay and Tiwi. multilayer feed forward artificial neural network (MLFANN) architecture model was developed and trained with resilient propagation (RPROP) algorithm. The research also evaluated the artificial neural network (ANN) model capability in weather forecasting.

Structural and time series-based weather prediction algorithms can be used with IoT devices in this domain [9] 10. Support vector regression, linear regression, multiple linear regression (MLR) and auto-regressive integrated moving average (ARIMA) are some of these algorithms. Using them, the author observes the behavior of forecasting algorithms. In [11–13], multiple linear regression (MLR) equations are used for developing a model for weather prediction. The author used the coefficients of these regression equations for generating a prediction pattern for the weather.

This study focuses on developing a model that could help in providing most accurate weather information among the selected weather forecasting Web sites and create a warning system by examining the weather conditions of these cities during extreme weather events in recent decades.

4 Methodology

Statistical analysis is performed on the weather readings recorded for 20 days. Among these different weather forecasting Web sites, the best one was chosen based on the total deviation. Also, historical weather data of these cities during extreme

weather events were examined, and their attributes such as wind speed, quantitative precipitation were analyzed.

Using Minitab statistical software, a statistical analysis has been done. The mean of the current temperature from different weather providing Web sites has been calculated, and based on these calculations, deviations were calculated for a different Web site. All the deviations for different cities by a particular Web site were summed. And based on this obtained deviation least deviated value was figured out among different obtained deviation for a particular date.

5 Result and Analysis

The weather data for current temperature for this research have been recorded for five different cities since September 21, 2018–October 10, 2018, for a total 20 days from five different weather providing Web sites. The value under each Web site representing column represents the sum of the deviations of the five selected cities.

Steps in obtaining deviation:

1. Consider the recorded data for calculating deviation.
2. Firstly, the mean temperature was calculated for five different cities taken by summing the readings obtained by different Web sites (Fig. 1 Sample data set).
3. Deviation table is made by calculating the deviation from recorded temperature. (Deviation = Recorded temperature- Mean temperature).
4. Table 1 was obtained by summing the deviation obtained from five selected cities for a particular Web site.
5. Using Minitab statistical software, an analysis has been done, and the least deviation providing Web site was found (Fig. 2).

This analysis has been done on the recorded current temperature. Minitab analysis report shows four different statistics based on which the least deviated weather providing Web site was found. It can be seen that Intellicast weather providing Web site has 51.3 least total deviations. Also, the average deviation of this Web site was found to be minimum among these five Web sites that is 2.565. Also, the minimum and maximum deviation of Intellicast is minimum ranging from 1–4 as compared

23-Oct-18	The recorded temperature in Celsius					Deviation Table					Total Deviation
	Shanghai	Manila	Tokyo	Kolkata	Mexico	Shanghai	Manila	Tokyo	Kolkata	Mexico	
Accu-Weather	23	29	23	35	21	1.8	0.3	0.2	0.6	0.6	3.5
Intellicast	22	30	23	34	20	0.8	0.7	0.2	0.4	0.4	2.5
WeatherUnderground	22	30.5	24	35	19	0.8	1.2	0.8	0.6	1.4	4.8
Weather Bug	20	28	23	34	21	1.2	1.3	0.2	0.4	0.6	3.7
Yahoo Weather	19	29	23	34	21	2.2	0.3	0.2	0.4	0.6	3.7
Mean	21.2	29.3	23.2	34.4	20.4						

Fig. 1 Sample Dataset

Table 1 Sum of deviations from the mean value (for the current temperature)

Date	Accu-weather	Intellicast	Weather Underground	WeatherBug	Yahoo weather
September 21, 2018	2.2	4	2.6	3	4.5
September 22, 2018	4.7	2.6	1	1.6	6.2
September 23, 2018	3	3.6	2	7	5.5
September 24, 2018	1.7	1	2.6	2.2	2
September 25, 2018	2.4	3.8	4.2	2.4	6
September 26, 2018	4.4	2.6	6.6	2.4	8.4
September 27, 2018	1.6	1.6	3	1.2	3.8
September 28, 2018	5.6	3.4	5.8	3.6	4.8
September 29, 2018	3.5	2.5	4.8	3.7	3.7
September 30, 2018	3	3.2	1.8	2.8	2.4
October 01, 2018	3.2	2.2	3.8	3.6	2.8
October 02, 2018	3.4	2.2	3.2	3.6	6
October 03, 2018	4	2	2	2.2	3
October 04, 2018	4.6	3	5	3.8	8.4
October 05, 2018	3.2	1.4	3.8	3	5
October 06,2018	5.2	3.6	3.8	3	6
October 07, 2018	4.4	1.8	3.8	3.2	2.4
October 08, 2018	1.6	3	3.6	3.8	4.8
October 09,2018	3	1.4	4.8	3.6	2
October 10, 2018	3.2	2.4	7	6.4	5



Fig. 2 Minitab analysis report

to other Web sites. Therefore, from this analysis, we concluded that the Intellicast provides the least deviated weather reading and is most accurate than other Web sites. Yahoo weather Web site on the other hand shows 92.7 maximum total deviation, as well as the other statistics were very high as compared to other Web sites. So, Yahoo weather results to be least accurate in providing weather information.

Table 2 shows major disastrous weather events in these cities in the past few decades. In the Philippines, three major extreme weather events have been seen in history. Typhoon Durian, Ike, Haiyan were the most disastrous events that cause more than 10,000 deaths in total, millions of homeless and damages to property. All of them proved to be the worst typhoon of the century in the Philippines having an average speed above 250 kph. Also, the frequency of these typhoons is maximum in November month. In Mexico, hurricane Wilma and Patricia were the major events causing over 100 deaths, and the frequency of these disasters was maximum in October month. Both hurricanes with average wind speed above 300 kph result in heavy rainfall with an average height of 900 mm. In Kolkata, cyclone storm bob 04 and Alia caused heavy rainfall with an average wind speed of 110kph, and the estimated fatalities were above 150. Both the cyclones existed for two days. In 2016, Shanghai faced 370 mm heavy rainfall causing 160 deaths and flood.

The impact of such weather events does not seem to decrease. But the graph of deaths due to these events shows a significant fall. This is due to enhanced weather forecasting and warning systems, better disaster management strategies introduced

Table 2 Major disastrous weather events in recent decades

City/country	Event	Date	Wind speed	Precipitation	No. of deaths
Philippines	Typhoon	(Nov 25-Dec 6), 2006	195–250kph		
	(Durian) Typhoon	(Aug 26-Sep 6), 1984	165–230kph		1492
	(Ike) Typhoon	(3–11 Nov), 2013	230–315kph		6241
	(Haiyan) Hurricane	(16–27 Oct), 2005	295kph	1633.98 mm	< 87
Mexico	(Wilma) Hurricane	(20–24 Oct), 2015	345 kph	193 mm	< 10
	(Patricia) Cyclone	(10–12 Nov), 2002	100kph	110 mm	173
Kolkata	Storm BOB 04 Cyclone	(26–27 May), 2009	110kph-120kph		149
	(Alia) Heavy	(10 July), 2016		370 mm	160
Shanghai	Rainfall Tsunami	(11 March), 2011			1000 <
Japan	Tsunami	(17 Jan), 1995			6000

Source www.imd.gov.in/pages/services_cyclone.php
<https://www.reuters.com/article/us-climatechange-lima-losses>
https://en.wikipedia.org/wiki/Typhoons_in_the_Philippines
<https://climatescorecard.org/2017/04/08/mexico-extreme-weather-event/>
<https://reliefweb.int/report/china/current-extreme-weather-events>

all over the world and researches in this field. Using data of Table 2, we can design a warning system that can warn in advance if the forecasted weather conditions of the day are near to or matching the weather conditions of above extreme weather events. This helps in managing the impact of a disaster in advance and alarming the agencies and disaster management forces to tackle.

6 Conclusion

This study shows how accurate weather conditions are provided by different weather forecasting Web sites, and research on extreme and disastrous weather events in these cities in last few decades helps in knowing the weather conditions favorable for disaster and helps in managing the disaster earlier by generating warnings. Intellicast Web site was found to be the most accurate weather providing Web site based on deviation from the mean for current temperature through statistical analysis as weather forecasting plays a vital role in all our day-to-day activities.

Therefore, it is an important area of research in human life. So, an improved approach for accurate weather forecasting was shown based on a comprehensive statistical analysis.

References

1. www.accuweather.com
2. www.intellicast.com
3. <https://www.weatherbug.com/>
4. <https://www.wunderground.com>
5. <https://www.yahoo.com/news/weather>
6. Zhu AW, Pi H (2014) A method for improving the accuracy of weather forecasts based on a comprehensive statistical analysis of historical data for the contiguous United States.
7. Navadia S, Yadav P, Thomas J, Shaikh S (2017) Weather prediction: a novel approach for measuring and analyzing weather data. In: 2017 international conference on I-SMAC (IoT in social, mobile, analytics and cloud)
8. Sobrevilla KLMD, Quiñones AG, Lopez KVS, Azaña VT (2016) Daily weather forecast in Tiwi, Albay, Philippines using artificial neural network with missing values imputation. ISSN: 978-1-5090-2597-8/16/\$31.00c 2016
9. Sulaiman MN, Atan SR (2009) An effective fuzzy C-mean and type-2 logic for weather forecasting. *J Theoret Appl Inform* 5(5)
10. Shabariram CP, Kannammal KE, Manojgraphakar T (2016) Rainfall analysis and rainstorm prediction using MapReduce Framework. IN: International conference on computer communication and informatics (ICCCI). Coimbatore, INDIA, ISSN: 978-1-4673-6680-9/16/\$31.00
11. Bashir, HM, Chavan G (2018) An integrated approach for weather forecasting over the internet of things: a brief review. In: I-SMAC international conference (I-SMAC 2018)
12. Krishna GV (2015) An integrated approach for weather forecasting based on data mining and forecasting analysis. *Int J Comput Appl*
13. Paras SM (2016) A simple weather forecasting model using mathematical regression. *Indian Res J Extens Educ*

Planning Approach with “Better Than Before” Concept: A Case Study of Library Building at SVNIT, Surat, Gujarat, India



Krupesh A. Chauhan and Bhagyashri H. Sisode

Abstract Across the different parts of the world, the concept of green building is catching the attention of the architects, urban and town planners, engineers and even ordinary people. According to the experts, high-performance green buildings are the ones that benefit the environment as well as human beings by minimum waste generation at all the stages of its life cycle while being cost-effective, sustainable and providing comfort to the humans. This paper explains the planning of the new library building at Sardar Vallabhbhai National Institute of Technology (SVNIT), Surat. SVNIT, Surat, is located in Surat city that has the tropical savanna climate, moderated actively by the Sea to the Gulf of Cambay. This is the first building of the institute that was planned and constructed by following the Green Rating for Integrated Habitat Assessment (GRIHA) guidelines to obtain a minimum of three stars. Various parameters such as planning parameters, building material parameters and building envelope were all addressed during its planning process. All the building planning principles, viz. aspect, prospect, grouping, roominess, ventilation, lighting, sanitation, etc., were considered while planning the building. This paper delineates the step-by-step process of planning a library of the national institute in Indian conditions to obtain high performance in the future. Also, the new library is compared with the old library that was built in 1961. The new library building is an example of a green and sustainable building. Its usage in designing library and learning spaces leads to limited yet significant literature on the design of green libraries is based on GRIHA guidelines.

Keywords Green building · Library · Planning · GRIHA rating system

K. A. Chauhan (✉) · B. H. Sisode
SVNIT, Surat, India
e-mail: kac@ced.svnit.ac.in

B. H. Sisode
e-mail: bhagyashrisisode14@gmail.com

1 Introduction

The green building, as defined by American Society for Testing and Materials (ASTM) International (2001), is “A building that provides the specified building performance requirements while minimizing disturbance to and improving the functioning of local, regional, and global ecosystems both during and after its construction and specified service life”. Furthermore, “A green building optimizes efficiencies in resource management and operational performance; and minimizes risks to human health and the environment”.

Green Rating for Integrated Habitat Assessment (GRIHA) Green Building Rating System, conceived by “The Energy and Resources Institute” (TERI) and developed jointly by the Ministry of New and Renewable Energy, Government of India, is based on nationally accepted energy and environmental principles. Over 300 projects across India of varying scale and function are being built based on GRIHA guidelines [1]. Specifically, GRIHA focuses on the sustainability of projects after they are constructed by requiring ongoing reporting of performance factors as part of GRIHA recognition. GRIHA utilizes a 1–5 star rating system that focuses on energy/power consumption, water consumption, water generation and renewable energy integration [2].

The new central library at Sardar Vallabhbhai National Institute of Technology, Surat, was considered for case study. The parameters used in its planning and the data considered are elucidated in the “planning approach” section of the paper.

The Sardar Vallabhbhai National Institute of Technology, Surat (established in 1961), is one of the premier institutes of national importance and fully financed and controlled by the Government of India, New Delhi. It has experienced faculty and dynamic research scholars’ team and office staff.

The planning of the new library building was done while considering the guidelines of GRIHA, India, to build the green building. By addressing the orientation of the building, daylight saving was achieved along with the reduced air-conditioning load. Furthermore, the excavated earth from the construction site was used to develop the landscape around to reduce the to and fro vehicle movement.

2 Need of Study

In the technologically outpaced world like today, more emphasis is laid on providing comfort to the users. Due to which more energy is consumed, more the consumption of energy more is the operation and maintenance cost that is borne by the users or the organization. Also, the resources used increase considerably contributing to uprisng the carbon print and water print. All these are the contributing factors to global warming. In order to maintain and improve the climatic conditions, it thus becomes inevitable to reduce the consumption of resources. As more as 70% of buildings are there when looked upon the land use on the society level and 45% of

buildings when the city is considered. Moreover, a normal human living in an urban area spends almost 22 h in an indoor confined area. Thus, the planning approach plays an extremely vital role to use optimum resources along with providing comfort to the users.

3 Study Area

Surat, situated on the banks of river Tapi and the coast of the Arabian Sea, is in the Gujarat state of India. It is a high ranking industrial city of the country with a strong network of roads and flyovers. The campus of SVNIT, Surat, is located within the South West Zone of Surat city. The institute was initially established as Regional Engineering College (REC) in 1961 and was upgraded as a National Institute of Technology (NIT) with the status of “Deemed University” in 2002. The new library was constructed in recent years with full advanced facilities and green concept. The map of Surat city and the master plan of SVNIT, Surat, are shown in Figs. 1 and 2, respectively.

The library has been understood as, “A built-environment that ensures efficiency in the utilization of site through compact planning and conservation of land as a natural



Fig. 1 Map of Surat



Fig. 2 Master plan of SVNIT, Surat

resource; thus creating an environment that inculcates the spirit of learning embedded in its space planning and architecture”. It can also be defined as, “A timeless space that respects and dwells with biodiversity and sustainability as a lifestyle rather than an imposition, by inherent design gestures encouraging conducive microclimate through daylight utilization”. Sidney Sheldon perfectly describes: “Libraries store the energy that fuels the imagination. They open up windows to the world and inspire us to explore and achieve, and contribute to improving our quality of life”.

4 Objective

The objective of this research paper is to study the planning approach of the new library building with better than before concept.

5 Scope of Study

The scope of the study was limited to the new library building, SVNIT, Surat, and GRIHA guidelines.

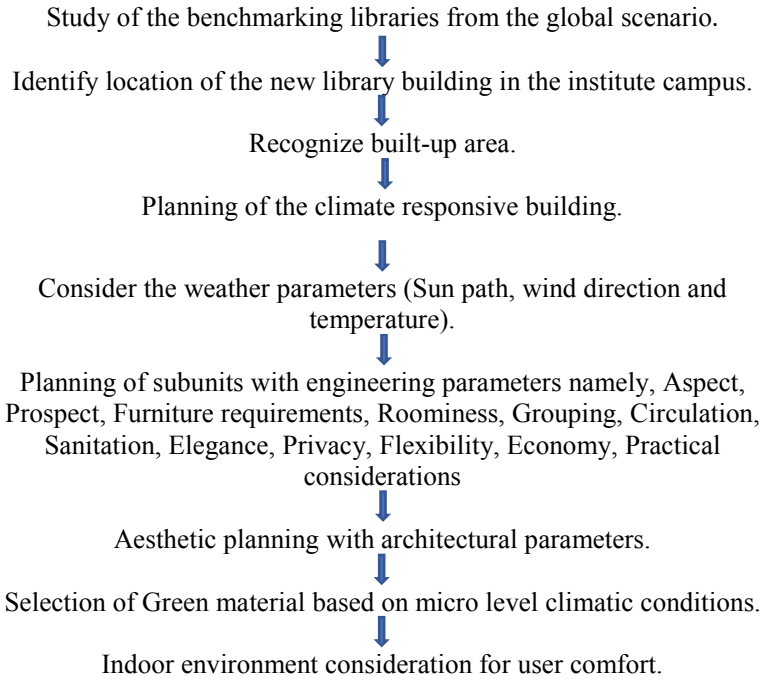


Fig. 3 Methodology flowchart

6 Methodology

The methodology for planning the green building with “Better than Before” approach is as described in Fig. 3. The flowchart shows the step-by-step procedure of planning that can be implemented to plan any type of building.

7 Planning Approach

The planning approach plays a vital role in getting the desired outcome [3]. The “Better than Before” planning approach aims at planning the building so that it has high efficiency and sustainability. By incorporating the climatic conditions and following the GRIHA guidelines, the planning can be done in much better way as compared to that in the past where only a few considerations were there pertaining to the sustainability and environment. The following steps elucidate the planning of the new library building at SVNIT, Surat.



Fig. 4 Exterior view of the Philip Exeter Library, USA

7.1 Learning from the Benchmarks

To plan the library with all the optimization, four benchmark libraries were studied. They are Philip Exeter Library at New Hampshire, United States of America (USA); London School of Economics and Political Science (LSE) Library at London, United Kingdom (UK); Delft University of Technology (TU Delft) Library at Delft, Netherlands; and Parliament Library at New Delhi, India, all of which are shown in Figs. 4, 5, 6 and 7, respectively. The best output is obtained when one considers the positives from the legends. To plan the new library building at SVNIT, Surat, the inspiration was taken from the benchmark libraries of the world.

7.2 Design Data for New Library Building

According to the Indian Standard (IS 1553: 1989), space required per reader is 2.33 m². While planning, it was estimated that there will be 1000 readers present at a time. Also, during the examination period, reading room is open 24 × 7, and hence, it was so planned to have almost 200–230 students at a time. The design had to include separate reading area for newspapers, magazines and books. Along with there had to be the provision of the digitization section in the digital library.



Fig. 5 LSE Library, London, UK



Fig. 6 TU Delft Library, Netherlands

7.3 *Selecting the Most Appropriate Building Form*

The building form selected for the new library building was square form. Square is the most primary geometry to grow out of the conditions of orthogonality. Each



Fig. 7 Parliament Library, New Delhi

square is related to the previous one by a factor of 2. Square is rationally symmetrical in four positions about the centre. Also, there are number of benefits for the square form as stated in the Hindu Mythology. Furthermore, when central open to sky is provided in the square form of building, the light is dispersed equally in all directions. Figure 8a shows the compositions that illustrate reflective and rotational symmetries within the squares, and Fig. 8 b shows the comparison of the square and rectangular building form.

The square shape represents “unmanifested energy” as per Vaastu sciences of Hindu Mythology. It creates energy source of positive nature. As square shape has four straight lines, which are equal in size, Vaastu believes it to be the “most perfect shape that is sacred and balanced in nature”.

Shape of the building is one of the major factors that plays vital role in green building analysis. Analysis of building shape can be done by various stimulatory models and manual methods. One of the methods is as follows:

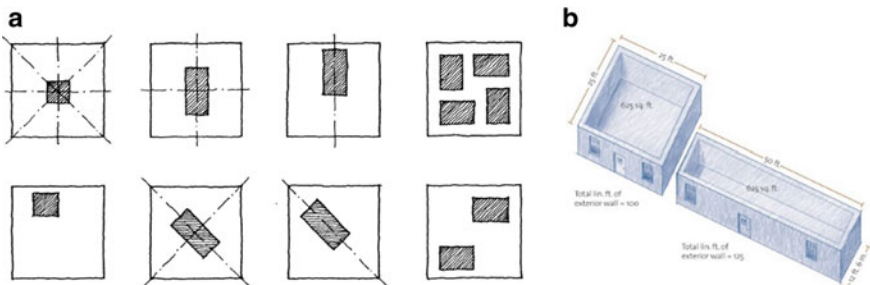


Fig. 8 a Compositions illustrate reflective and rotational symmetries within the squares. b Comparison of the square and rectangular building form

Shape Coefficient

$$C_f = \frac{S_e}{V}(m^2/m^3) \quad (1)$$

where S_e is the envelope surface area, and V is the inner volume of the building.

For library building,

Sides = 54.8 m.

Height = 48 m.

For library building,

$$\begin{aligned} C_f &= \{4(54.8 \times 48)\}/(54.8 \times 54.8 \times 48). \\ &= 0.076. \\ &\approx 7.6\% \end{aligned}$$

The result obtained by using the Eq. (1) shows that the shape is efficient energy responsive envelope. As there are number of benefits, square shape was chosen to plan the library.

7.4 Location of the New Library Building with Respect to the Campus

The planners must address the site location to create minimum disturbance to the existing surroundings including trees. The plot of the new library building was selected so that it is almost in the centre of the academic buildings and the hostels of the students, which would provide ease to the students (Fig. 9). Also, this location has the minimum external noises.

7.5 Location of the Built-Up Area

It can be seen in Fig. 10 that a particular portion of the selected site was chosen so that the maximum number of already existing trees can be saved and minimum harm is caused to nature. This location, along with benefiting the environment, also benefits in reducing the trip length and time that benefits the students. Also, following the criteria 2 and 3 of GRIHA manual [4], the excavated soil was reused to form contours and for landscaping in the site premises.

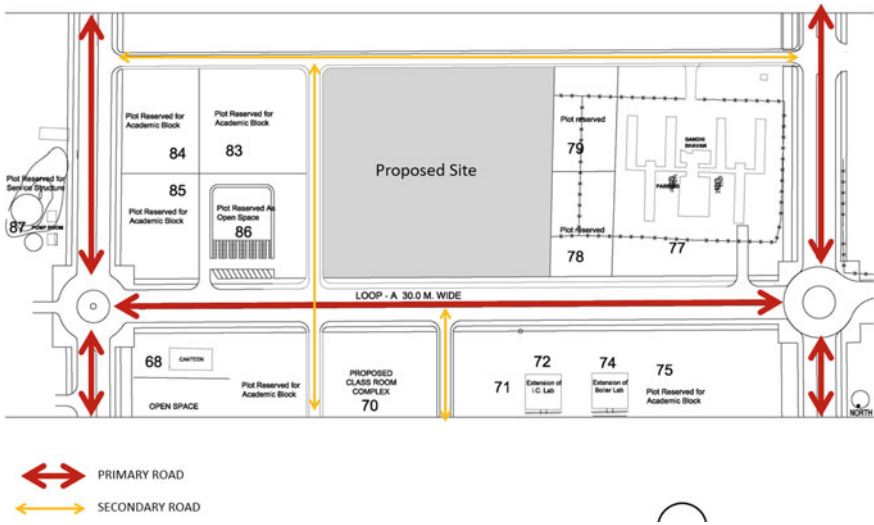


Fig. 9 Identification of the location for the library in the campus

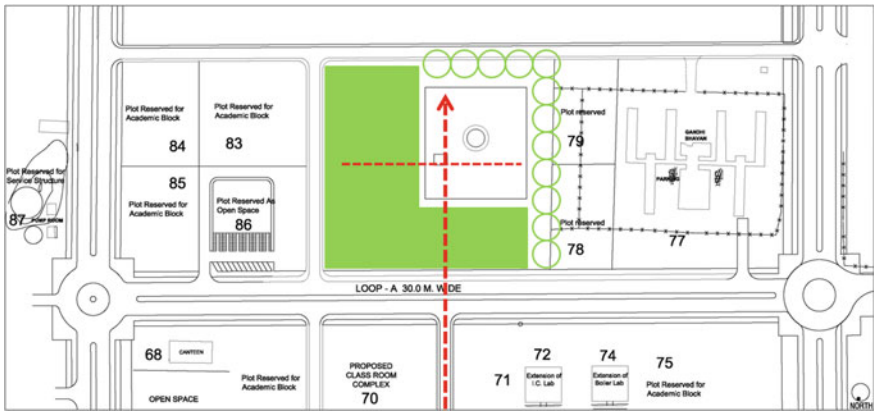


Fig. 10 Location of the built-up area

7.6 Climatic Considerations

To provide comfort to the users, it is inevitable to plan the building as per the climate. Surat has a tropical savanna climate, moderated strongly by the Sea to the Gulf of Cambay. The summer begins in early March. April and May are the hottest months, the average maximum temperature being 37 °C (99 °F). Monsoon begins in late June, and the city receives about 1,200 mm (47 inches) of rain by the end of September, with the average maximum being 32 °C (90 °F) during those months. Winter starts in

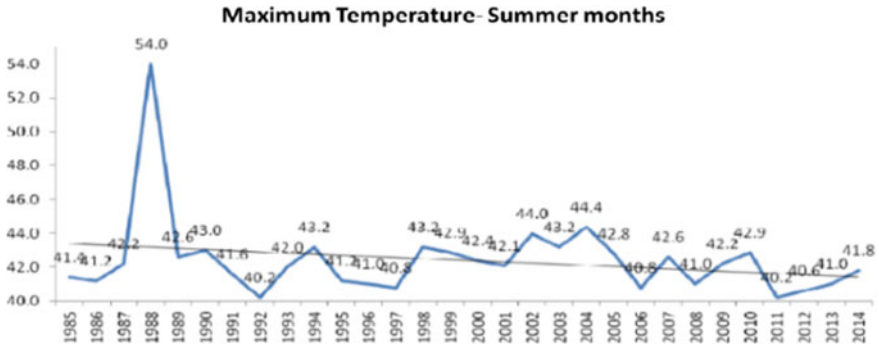


Fig. 11 Summer temperature (1985–2014)

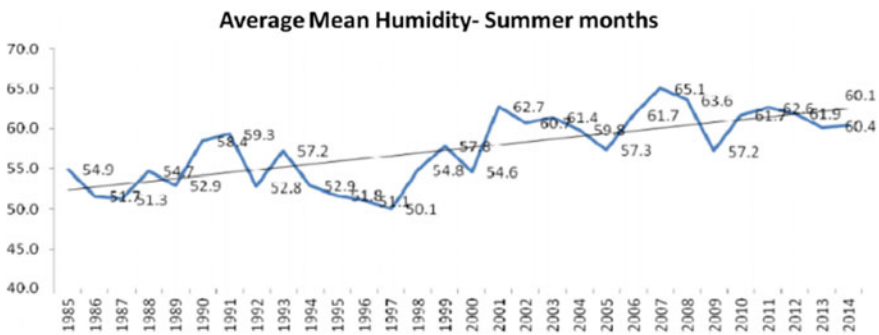


Fig. 12 Summer humidity (1985–2014)

December and ends in late February, with average mean temperatures of around 23 °C (73 °F) and negligible rain [5]. The following figures depict the summer temperature and humidity from 1985–2014, respectively, in Figs. 11 and 12.

Figures 13 and 14 show the sun path and the wind direction of the library building. These play extremely important role while planning the location of the sub-units, windows, materials to be used, etc.

7.7 Strategies to Design Green Building

In order to plan the energy-efficient building, various points must be addressed along with considering the climatic conditions in the area, firstly, to reduce the amount of heat reaching the building by providing shading at proper locations through projections or by plantation [6]. Also, for this, the shades when planned considering the orientation play a vital role. Secondly, to control the heat absorption through walls and roof, the choice of materials used to build walls and roof plays a significant

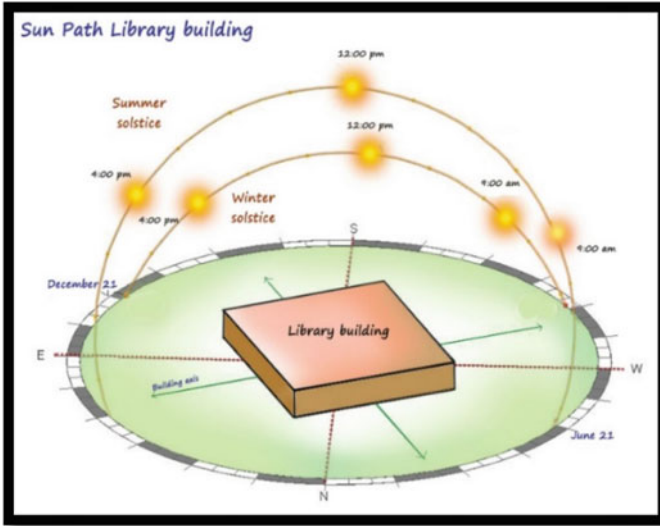


Fig. 13 Sun path of library building



Fig. 14 Wind flow

role to keep embodied energy low [6]. Add-on insulation should be judiciously used. Furthermore, heat gain can be controlled by using roof finishes with high solar reflective index or by shading the roof. Thirdly, to minimize the internal heat gain and improve the daylight, for this, the fixtures and appliances with low equipment power density [6] and with efficient Bureau of Energy Efficiency (BEE) rating should be used and by efficient planning of the artificial lighting, and lastly, to cool the building by using low-energy heating, ventilation and air-conditioning (HVAC) technologies. All the stated four strategies were considered while planning the new library building.

7.8 Floor-Wise Building Unit Planning

The planning was done while addressing various building principles, viz aspect, prospect, furniture requirements, roominess, grouping, circulation, sanitation, elegance, privacy, flexibility, economy and practical considerations [7]. The orientations of the building and sun path were considered while addressing the placement of service blocks, reading rooms, etc. Services such as toilet blocks and chiller plant are provided on the south side of the building (Fig. 15).

To utilize the daylight to its maximum, provision of dome skylight is provided. The daylight from the dome skylight is dispersed on all the floors equally as there is an open to sky (OTS) in the centre of the library as shown in Figs. 16, 17 and 18. The provision of OTS not only helps in getting the natural light, but also helps in creating oneness among different floors. Furthermore, three stair cases are provided for the easy vertical circulation and safety purposes.

The reading space and services are provided on all the floors. The first floor has the waiting area, cabins for the library and admin staff, space for procurement and cataloguing, book bank, conference room, faculty reading lounge and a separate girls reading room. The second floor has the waiting space, special book area, reprography, book binding space, issue counter, stack area and circulation. The third floor has the server room, digital library, discussion room and separate reading space for research scholars. The stacks were separated for text books, reference books, book bank and dissertation/ thesis, out of which the latter two do not have open access. The area and activity distribution are shown in the Figs. 19 and 20.

7.9 Planning of the Building Envelope

In the south direction where there is provision of services, wall is provided, whereas in the other three directions, glasses are used to separate the outer environment from the inside of the library (Fig. 21). It was so planned so as to utilize maximum daylight. As only the light is required, not the heat, fringe vertical blind curtains are provided to avoid the glare and heat that can be operated manually making it a smart building. The other purpose of the glass walls is that one can get the vision of outside. The roof

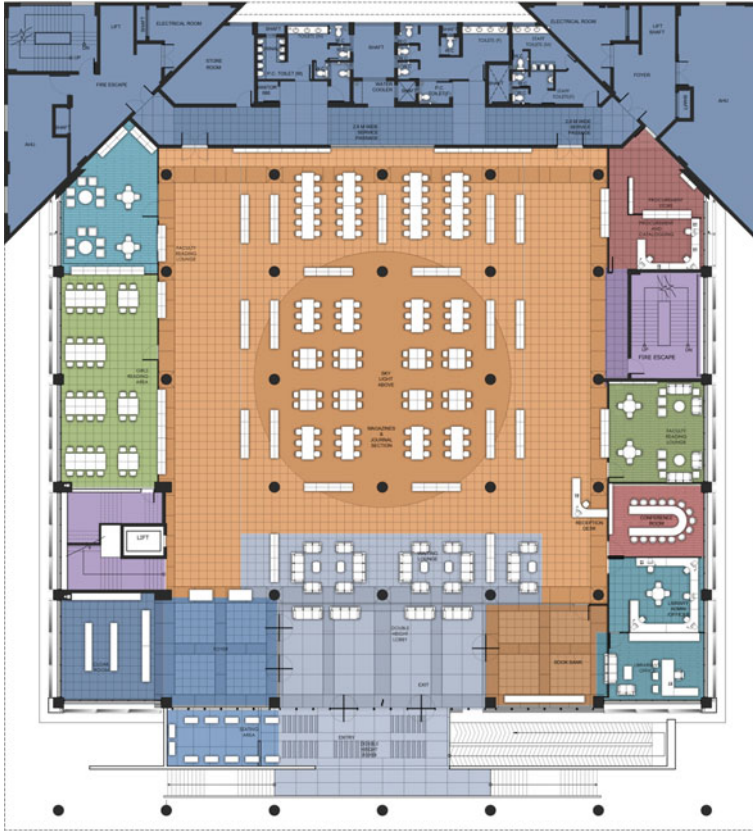


Fig. 15 Plan of the first floor

is exposed to the direct heat of the sun which results in heat gain. To prevent this, the solar panels are installed on the terrace, which serves the purpose of utilizing the renewable source of energy along keeping the roof cool (Fig. 22).

7.10 Selection of the Building Materials

It is very important to select the proper material for building as it adds on to the durability, heat gain and transfer and capital. The wall in the south direction is made of autoclaved aerated concrete (AAC) bricks. In contrast to this, the old library building had traditional red brick walls which were heavy and costly. Use of the AAC blocks also nullifies the need to paint the wall. The glass used to create the glass wall in other three directions is such that it prevents the glare and heat of sun.

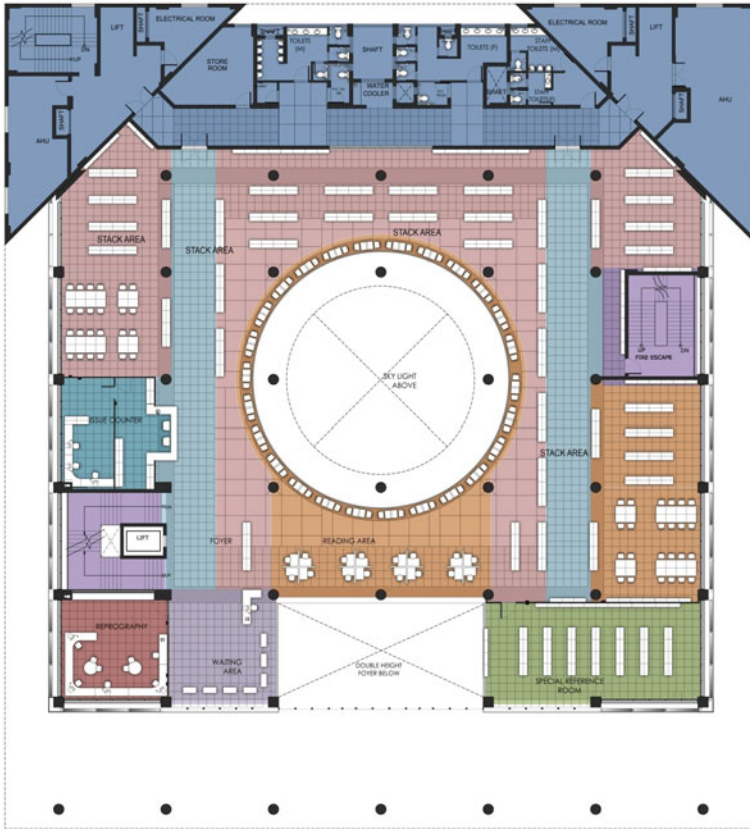


Fig. 16 Plan of the second floor

The criteria 17 of the GRIHA guidelines [4] encourages to utilize low-energy materials or products to a minimum of 70% of the total quantity of all interior finishes. When looked upon the material used for flooring, rubber was selected to minimize the noise level and provide maximum silence to the readers. Also, it should be noted that as there will be more movement and noise in the service block, the wall in the south direction has the sound absorbents in it. The indoor noise levels, thermal comfort requirements and artificial lighting lux level are within the acceptable limits as specified in National Building Code (NBC) 2005. It meets the minimum requirements of Central Pollution Control Board (CPCB) and National Ambient Air Quality Standard (NAAQS) for the quality of fresh air [8, 9]. Facilities as per Harmonized Guidelines and space standards for the barrier-free built environment for the disabled and elderly people for public buildings provided.

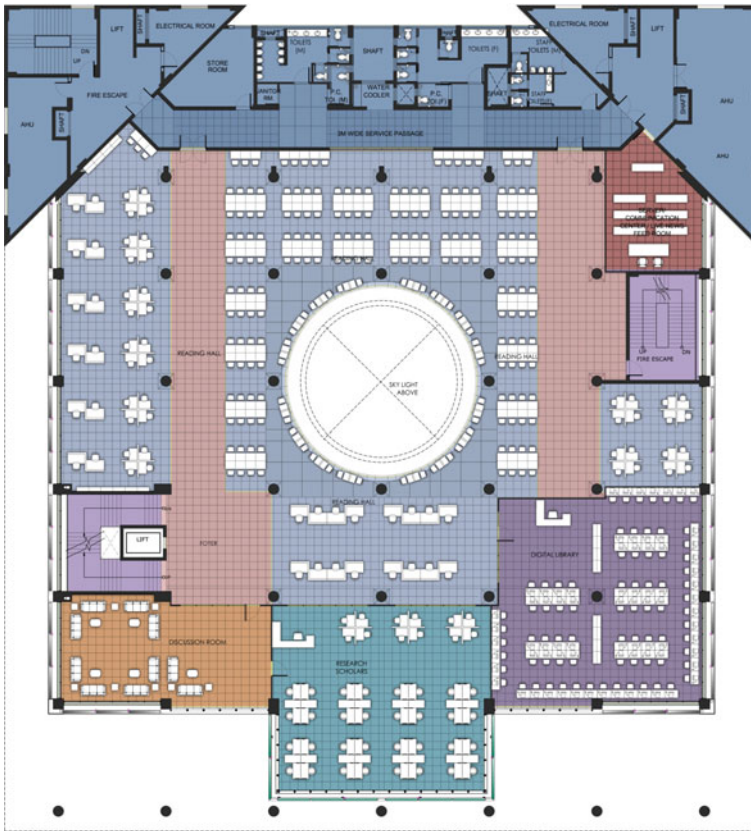


Fig. 17 Plan of the third floor

7.11 Energy-Efficient Building

To design the energy-efficient building, the glass walls, dome skylight and solar panels play a vital role. The use of artificial lights considerably reduces because of the glass walls and the dome skylight, meeting the requirement of useful daylight illuminance (UDI) for 90% of the potential daylight time in a year.

To add on to the efficiency of the building, 1000 KW capacity solar panels are installed on the terrace of the building (Fig. 22) that helps in producing enough electric energy to run the appliances in the building. According to the criteria 6 of the GRIHA manual [4], at least 25% of the total number or 15% of the total connected load of outdoor lighting fixtures (whichever is higher) should be powered by the solar energy. The installed solar panels efficiently fulfils criteria 6 and 18 of lighting and the use of renewable resources, respectively. This provision also helps in keeping the roof cool by absorbing less heat of the sun where the area of the terrace is covered

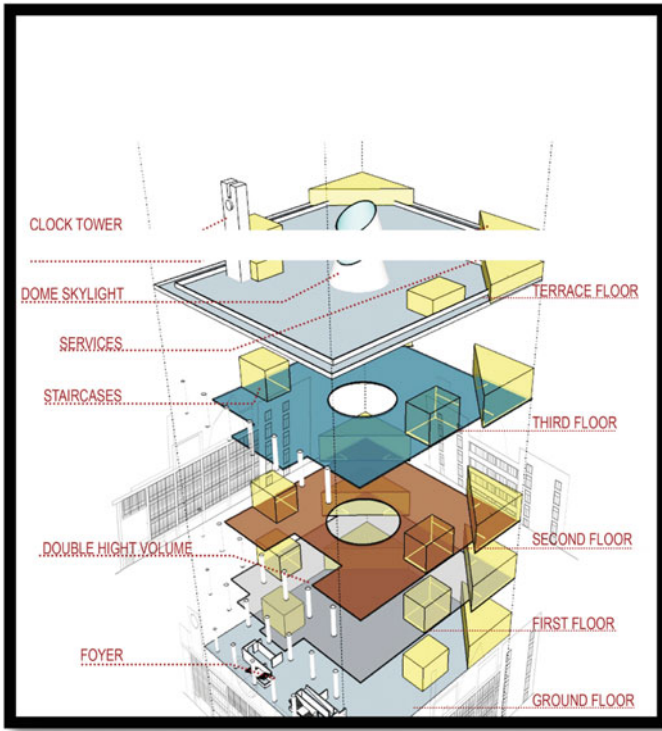


Fig. 18 Square form of library building with all layers

Fig. 19 Area distribution

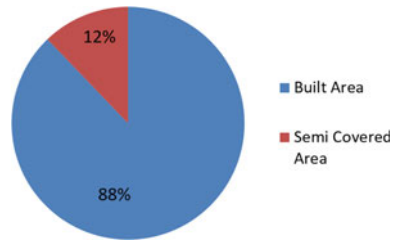
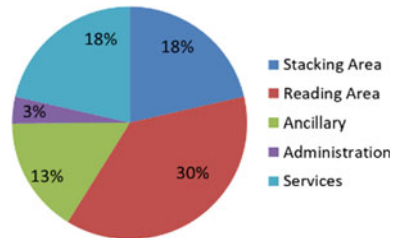


Fig. 20 Activity distribution



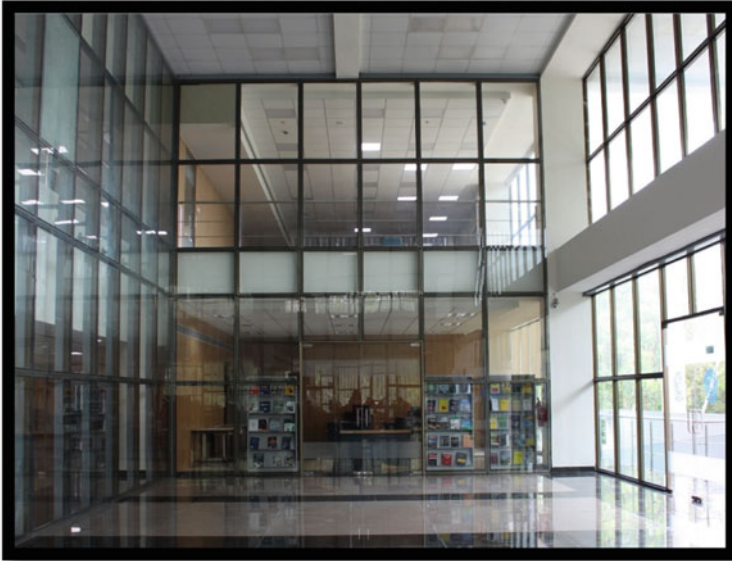


Fig. 21 Use of glass



Fig. 22 Installation of solar panels on the terrace

with the solar panels. The institute also has the tie-up with Gujarat Electric Board (GEB). This helps in switching to the power source when required.

Furthermore, design includes the provision of the rain water harvesting. There is an underground tank where the water from the roof top is collected. This water is utilized for flushing, washing and irrigation purpose.

7.12 Outcome

Addressing all the criteria of the GRIHA manual, the outcome of the detailed planning process was the energy-efficient and high-performance green building as shown in Figs. 23 and 24.

The total site area of the library building is 18,286 sq. m. which includes library building, pumping station, green spaces and parking space. The distance of library building from the main gate of campus is around 607.5 m. The built-up area of the library building is 11,115 sq. m. including parking, three floors and a terrace facing north-west direction.

The old central library of SVNIT, Surat, was planned with the traditional methods in 1960s. Previously, the planning parameters lacked the inclusion of the green and sustainable building concept. However, with the advancement in the technology



Fig. 23 Front and side view of the library

Fig. 24 Interior of the library



and developments in the field of construction industry, the materials used for the construction, the parameters considered for the planning, the consideration of the environment, etc., factors that make the building green and sustainable are now considered meticulously. Looking at the case study, it can be seen that the care is taken to preserve the environment and produce minimal waste throughout the life cycle of the building. This justifies that the Better than Before concept of planning is crucial and helpful not only for the humans but also for the environment.

8 Conclusion

The planning of the building has been done with special considerations for the performance of the building envelope in terms of window to wall ratio, window to floor ratio as well as daylighting and ventilation, to achieve better results in the indoor air quality and performance of the overall building. The building envelope performance has been met by analysing the site and locational aspects of the building at proposal stage and pre-design stage to achieve the optimum space and location for the building to be placed in such a manner that the orientation, internal space allocations, design of the building, etc., are done by ensuring minimum effect on the existing green cover spaces around the building plot. The pathways along the buildings are also designed

to limit the effect of construction to minimum, thus reducing the felling of trees on site.

As the building was planned, keeping in mind to achieve minimum 3 star GRIHA rating, the planning and design aspects of the building were chosen accordingly. The shape of the building was prepared in such a way that equal daylighting and ventilation were received on all parts of the building, thus creating a “symmetrical and balanced” condition for the building envelope. The built-up area of the library building is 11.115 m², where around 1000 readers can be occupied in the reading room at a time.

This building demonstrates the example of a “user-centric” green building, which adapts and provides for the students based on their activities and enables the students to achieve a prosperous, peace and calm place to study and grow for their future. This building is considered as a pilot project for the institute. Looking at the innumerable benefits of the green building, planning and construction of such buildings should be encouraged at the corporate level.

Looking at the proven benefits of constructing such green buildings, if more such smart buildings are built, then it will help in conserving the environment along with providing comfort to the users which is the need of the hour.

This study is the part of an ongoing research project. When the planning phase of the building was ongoing, GRIHA guidelines were to be followed as per the government guidelines. However, now there are separate guidelines of CPWD that are to be followed for the planning and construction of the new buildings.

Acknowledgements We express our heartfelt gratitude to SVNIT, Surat, for providing an opportunity to carry out research on the New Library Building of the Institute. We are also thankful to NBCC (India) Limited (formerly known as the National Buildings Construction Corporation Ltd.) for handling and managing the whole project, and Atelier [D]sync for their valuable architectural inputs. I, Dr. Krupesh A. Chauhan, wants to convey my sincere acknowledgements to SVNIT, Surat, and Estate section for choosing me as a team member in the committee and NBCC (India) Limited and Atelier [D]sync for being cooperative at all stages of the project.

References

1. Council, Indian Green Building (2015) IGBC green new buildings rating system—Version 3.0. India
2. Smith RM (2015) Green building in India: a comparative and spatial analysis of the LEED-India and GRIHA rating systems. *Asian Geographer* 32(2):73–84
3. Kang Y et al (2013) Comparison of preproject planning for green and conventional buildings. *J Construct Eng Manage* 139(11):04013018
4. MNRE T (2010) GRIHA manual, volume 1: introduction to national rating system-GRIHA. IN: An e-evaluation tool to help design, build, operate, and maintain a resource-efficient built environment. New Delhi, India
5. Desai VK et al (2015) Temperature and humidity variability for Surat (coastal) city India. *Int J Environ Sci* 5(5):935–946
6. UNEP Sustainable buildings and construction for India: policies, practices and performance. https://www.teriin.org/eventdocs/files/sus_bldg_paper_1342567768.pdf

7. Li F et al (2014) Research on social and humanistic needs in planning and construction of green buildings. *Sustain Cities Soc* 12:102–109
8. World Health Organization (2010) WHO guidelines for indoor air quality: selected pollutants
9. Wyon DP, Pawel W (2006) Indoor air quality effects on office work, *Creating the Productive Workplace*. pp 193–205
10. Singh MK, Mahapatra S, Atreya SK (2010) Green building design: a step towards sustainable habitat. *Natl Conf Renewable Energy 2010(NCRE2010)*:257–268
11. Wong NH, Jan WLS (2003) Total building performance evaluation of academic institution in Singapore. *Build Environ* 38(1):161–176

Wastewater Allocation and Pricing Model for the Efficient Functioning of CETP Serving a Textile Industrial Cluster



Bhoomi Shah , Deepak Chaurasia , and Ajit Pratap Singh 

Abstract Textile industry produces a quarter of the global industrial wastewater effluent, and most of the pollutants get added in the dyeing and printing processes of fabric production. Due to improper disposal and non-stringent policies, there is visible pollution of river bodies, degraded environmental flows and groundwater contamination. Since the cost of treatment to acceptable quality standards is high, industries operate by using cheaper water sources like lifting groundwater or bypassing the common effluent treatment plants (CETPs). Also, industries with small-scale production cannot bear the high cost levied on them by the authorities to recover the collective cost incurred by CETP. Thus, it is necessary to ensure that discharge and concentration of effluent sent to CETP by member industries are manageable, and industries pay as per their effluent quality and quantity. In this study, for the textile industrial cluster in Balotra, Rajasthan, in India, the zero liquid discharge (ZLD) technique has been proposed. Subsequently, the optimal allocation of effluent discharges for member industries in study region has been formulated. Using the industrial outflow data obtained from government agreements, the optimization relation between concentration, flow and cost has been implemented. The result obtained is the number of industries and their full or fractional wastewater share depending upon the value of fractional allocation (25, 33, 50, 66, 75 or 78%). This study can serve as an alternative to the existing ad hoc method of taxing member industries for wastewater treatment and lead to a win-win situation for industries, CETPs and the environment.

Keywords Textile industry · Wastewater · ZLD · Fractional allocation

B. Shah (✉) · D. Chaurasia · A. P. Singh
BITS Pilani, Rajasthan 300331, India
e-mail: h20180046@pilani.bits-pilani.ac.in

© The Author(s), under exclusive license to Springer Nature Singapore Pte Ltd. 2021
R. Al Khaddar et al. (eds.), *Advances in Energy and Environment*, Lecture Notes in Civil Engineering 142, https://doi.org/10.1007/978-981-33-6695-4_8

1 Introduction

Indian textile industry is the second largest in the world being the main producer of cotton, staple fibre and filament yarn. In ‘processing mills’, grey cloth is converted into fabric products by bleaching, mercerizing, dyeing, printing and washing. This is a water-intensive industrial sector since these mills consume 60–80% of total water used for cloth production. The World Bank estimates that almost 20% of global industrial water pollution originates from the treatment and dyeing of textiles. Not all the hazardous chemicals that are used in printing remain on the final fabric but get drained through the effluent discharged from the production factory into nearby river bodies and municipal sewers. Improper disposal of wastewater from textile industries due to inefficient treatment facilities and high cost of compliance to the treatment standards has largely contributed to the pollution of water bodies. This is observed mainly in the dyeing mills of Tamil Nadu, Rajasthan, Uttar Pradesh, Punjab, Gujarat and Maharashtra. To address this issue, the Union Ministry of Environment, Forest and Climate Change (MoEF&CC) [1] proposed the implementation of zero liquid discharge (ZLD) scheme, shown in Fig. 3. The non-uniformity in enforcement of ZLD scheme and the cost of groundwater extraction being cheaper than the salt recovery process of ZLD have led industries to find ways to escape the government regulations.

Rajasthan has emerged as a pre-eminent centre for the domestic textile industry covering the entire production chain, from spun yarn up to finished garments. At present, there are about 5000 composite and processing mills in Rajasthan. Rivers in Rajasthan are non-perennial and receive all kinds of pollutants annually. The ground water is also depleting alarmingly due to over-exploitation, population growth and pollution. This combined problem of water scarcity and pollution cannot be managed just by conventional treatment methods, i.e. physico-chemical and biological treatment. Therefore, there is a need to go beyond ‘treatment for disposal’ towards ‘treatment for reuse’. Zero liquid discharge (ZLD) is the way forward, and its adoption is becoming essential rather than an imposition. Though the initial cost of ZLD is high, but it can be offset by framing right policies. About a year ago, the major processing units in the state stared at the dire consequence of shutting down due to the environmental degradation they created. Finding a solution was urgent to create a win–win situation for all stakeholders—industries, investors, authorities and habitants.

2 Methodology

Keeping in view of above facts, this study presents a framework to address wastewater management issues, shown in flow chart in Fig. 2. The study objectives are as follows:

1. Identification of existing problems in wastewater management in study region
2. Case study of ZLD implementation: Tiruppur Industrial cluster

3. Optimal share of wastewater discharge of member industries to CETP
4. Pricing mechanism based on concentration and flow of effluent from industries
5. Application in study region to demonstrate the methodology.

2.1 Identification of Existing Problems in Study Region

Our study region is the industrial cluster in Balotra city in Barmer district of Rajasthan, as shown in Fig. 1. There are 1500 cotton and synthetic cloth dyeing and printing units which release about 100 million litres of partially treated effluent per day into the Luni river [2]. The Balotra CETP serving the micro, small and medium enterprises (MSME) textile industrial cluster comprises 403 member industries carrying out dyeing and printing activities. During the initial visits, the following pollution-related problems were noticed [3]. Wastewater discharges from industries and CETP into Luni river, ad hoc method of wastewater allocation in which all member industries are permitted to send only an arbitrarily decided percentage of their total effluent to CETP irrespective of their size, smaller member industries bypass CETP and illegally discharge into nearby agricultural areas, leaching of untreated effluents causing contamination of underground wells and aquifers in the surrounding villages.



Fig. 1 Google map showing location of Balotra industrial cluster and the Luni river

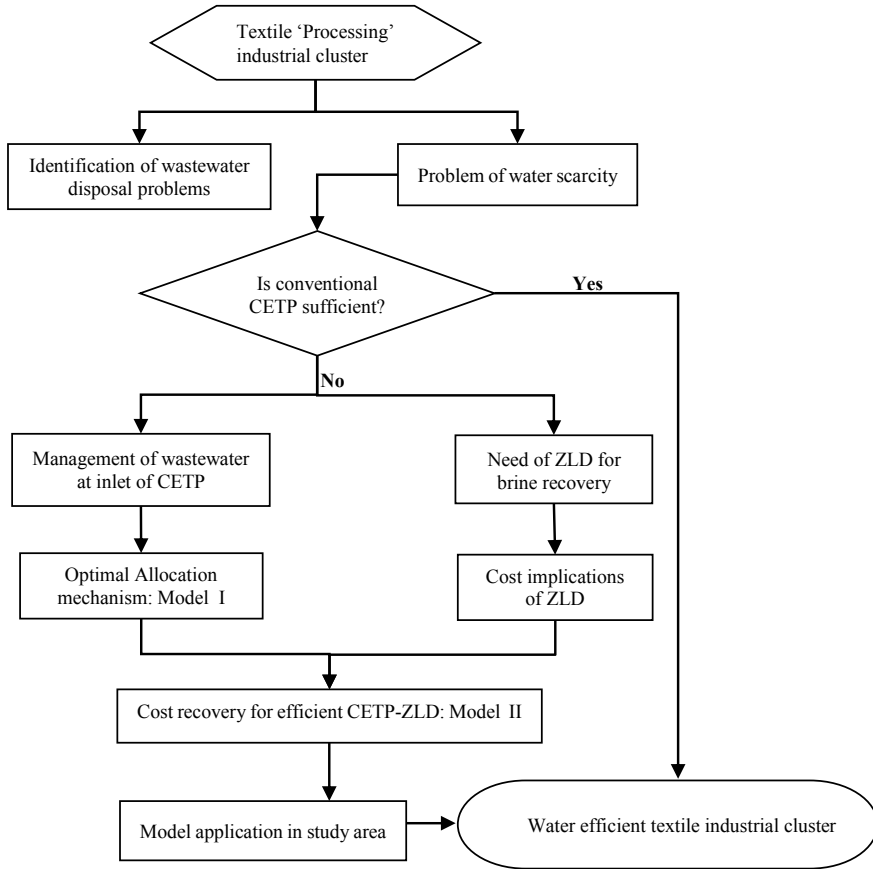


Fig. 2 Flow chart of methodology addressing environmental and operational concerns of CETP

2.2 Case Study of ZLD Implementation: Tiruppur Cluster, Tamil Nadu

ZLD refers to installation of facilities in a system which will enable recycling of permeate of membrane separation process of CETP and convert the solute of dissolved organics and inorganics into solid residue [4]. It can be achieved by adopting primary, secondary and tertiary treatment processes and polishing by filtration and sending treated water back into the process or domestic reuse (Fig. 3). The treated water is recovered from the membrane processes such as ultra-filtration (UF), nano-filtration (NF) and reverse osmosis (RO) during tertiary treatment phase, and salt is then recovered by increasing solid concentration in mechanical vapour recompressor (MVR) and then using multiple effect evaporation (MEE) with crystallization [5]. Ahirrao remarked [6] that the pollution arising from colour and high TDS brine

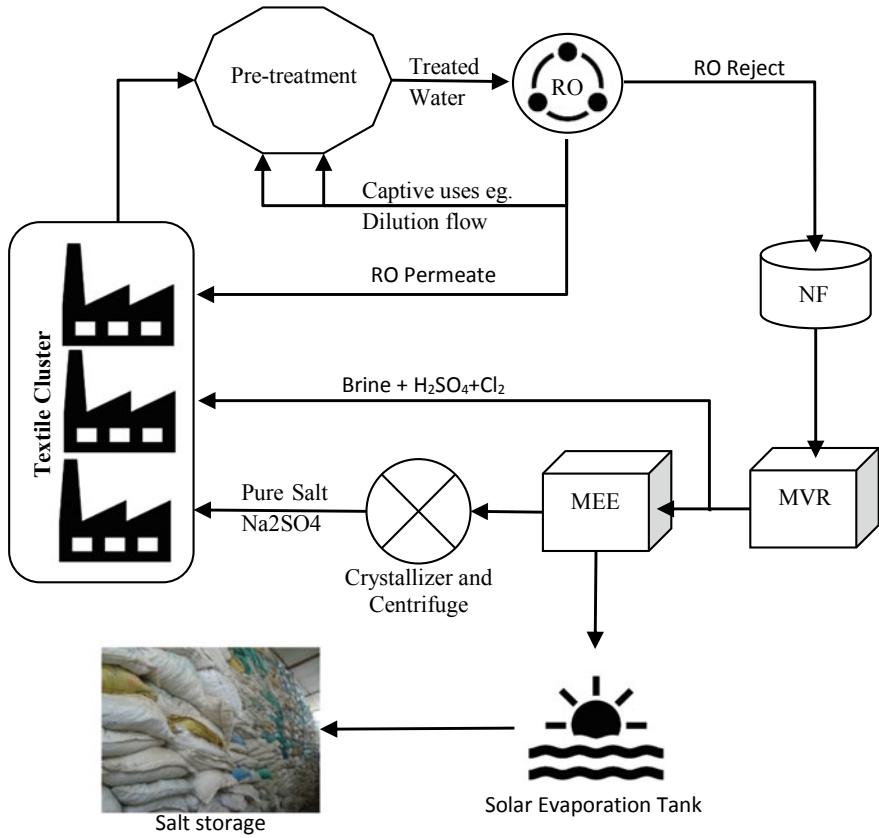


Fig. 3 Schematic diagram of unit operations and processes in ZLD treatment with proposed network for dilution flow

in the wastewater is solved by the ZLD technique of selective crystallization and recovery of Glauber’s salt and mixed salt which can reused in dyeing process.

In Tiruppur industrial cluster, there were 760 dyeing units which discharged their treated effluent through CETPs into the Noyyal river till 1997. This conventionally treated effluent contained high TDS (900–6600 mg/l) and chloride (230–2700 mg/l) and did not meet prescribed quality standards. These pollutants containing heavy metals of chromium, copper, zinc and lead got accumulated 32 km downstream in the Orathupalayam dam reservoir. This prompted the High Court to direct the dyeing units to adopt ZLD concept for RO reject management in 2006 [4]. Currently, 450 textile units have collectively set up 20 CETPs while 150 units have their own individual effluent treatment plants (IETPs). The rest of the units is shifted to Karnataka where there are no such norms. The capital cost of ETP with ZLD facilities is around Rs. 12.0–15.0 crores per MLD, operation and maintenance (O&M) cost is Rs 3000–5000, and energy consumption cost is 50% of total O&M cost. Thus, the treated

and recycled water costs approximately Rs. 120–150/cum, while the cost of water extraction from the ground or from the municipality would be between Rs. 30 and Rs. 60/cum [7]. So, to avoid migration of factories to areas where ZLD norms are not stringent, a uniform policy across different regions in India is key to the widespread adoption of ZLD if industries are to stay competitive in textile market.

2.3 Mathematical Model Formulation

A rational approach of wastewater allocation that provides the benefit of economies of scale to smaller member industries is proposed in part I model. In part II model, treatment cost recovery from the members is proposed considering both wastewater flow and concentration at CETP inlet. Treatment cost is inclusive of ZLD cost, which is arrived at from the literature review. It is assumed the all industries operate during the same hours in a day.

Part I: Wastewater Allocation Optimization Model

Let n be the number of member units served by a CETP. Then, as per the existing practice, effluent flow from industries to CETP can be expressed as follows:

$$Q = \frac{\sum_1^n r * q_i}{100} = \frac{r}{100} * \sum_1^n q_i \leq Q_0 \tag{1}$$

where r is the arbitrary allocation percentage as per ad hoc method, q_i is the effluent flow of i th industry, Q is the total inlet flow, and Q_0 is the operating capacity of CETP.

Our aim is to find the optimum effluent allocations (q_i^*, s) such that smaller players (x in number, $1 \leq x \leq n$) are allowed to release effluent at their full potential, whereas rest of the members ($n-x$) are allowed to release certain fraction f ($0 < f \leq 1$) of their full potential. Thus, the objective to maximize value of x and subsequently obtain q_x is as follows:

Max x , subject to

$$\sum_{i=1}^x q_i + f * \sum_{i=x+1}^n q_i = \sum_{i=1}^n q_i = Q \leq Q_0, q_i \leq q_{i+1} \tag{2}$$

Solution of above fractional allocation optimization can be obtained by following a stepwise procedure as shown in Fig. 4.

The optimum allocation of i th industry q_i^* will be as follows:

$$q_i^* = \begin{cases} q_i; & 1 \leq i \leq x \\ f * q_i; & x + 1 \leq i \leq n \end{cases} \tag{3}$$

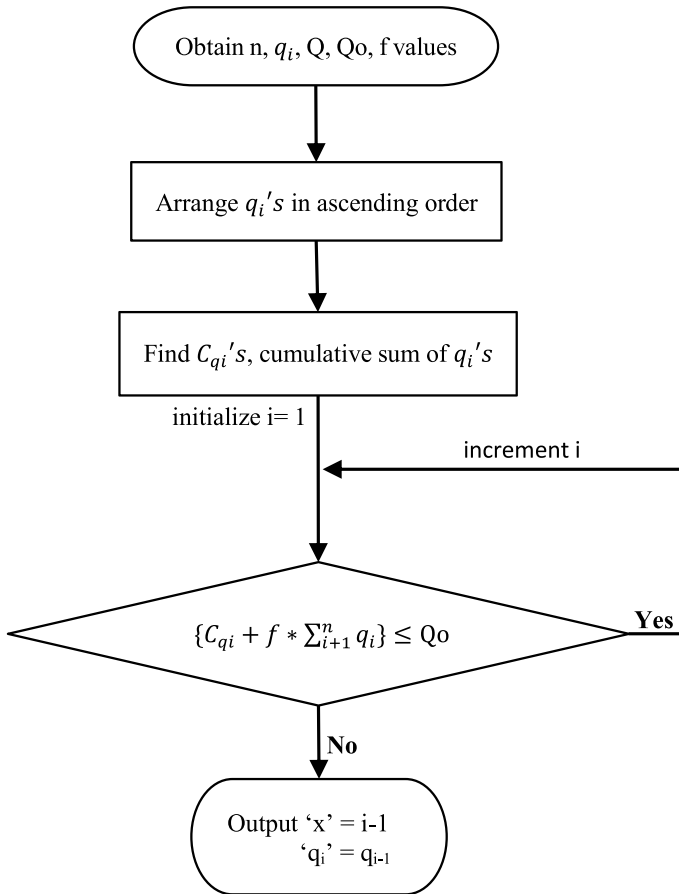


Fig. 4 Flow chart showing algorithm for finding the solution of fractional allocation equation (where, n = industries, q_i = flow of i th industry, Q = total input at CETP, Q_o = design capacity of CETP, f = percentage of fractional allocation)

Part II: Pricing Model for CETP Based on Flow and Concentration

Following conditions shown in Table 1 can exist between cost, concentration and flow.

where C_o = input design concentration of CETP; C, Q = inputs to CETP at any time, C_{mix} = combined concentration at CETP inlet, q_i = flow of i th industry, c_i = effluent concentration of i th industry, Q_d = dilution flow = $Q_d = \frac{C * Q_o^*}{C_o} - Q_o^*$, k = normal cost factor (Rs/kl), p = penalty cost factor (Rs/kl).

Table 1 Four possible conditions at CETP inlet and associated cost

Sr	Influent conditions	Cost	Remarks
1	If $C \leq C_o$ and $Q \leq Q_o$	$k \bullet Q$	Normal CETP operation cost
2	If $C \leq C_o$ and $Q \geq Q_o$	$k \bullet Q_o$	Individual q_i 's checked against the q_i^* 's and violators are identified. To manage the excess flow ($Q-Q_o$), each industry will have to store flow equal to $(q_i^* - q_i)$
3	If $C \geq C_o$ and $Q \leq Q_o$	$k \bullet Q + p \bullet Q_d$	Individual c_i 's checked against C_o , and penalty will be levied on violators in proportion to $c_i - C_o$ CETP will provide additional dilution flow Q_d such that, $Q_{mix} = Q + Q_d$, $C_{mix} = C_o$ and excess flow, $Q_{mix}-Q_o$ will be managed by CETP
4	If $C \geq C_o$ and $Q \geq Q_o$	$k \bullet Q_o + p \bullet Q_d$	Combined application of condition 2 and 3. Q_d with concentration C_o will be managed by CETP

3 Results and Discussion

Model Part I Application

For Balotra CETP, the values of variables are as follows: $n = 403$, $Q = 15.34$ MLD, $Q_o = 12$ MLD, $Q_D = 18$ MLD, $f = 0.75$, q_i values were obtained from Balotra CETP authorities. The result is 187 industries, generating wastewater below 18KLD shown in Fig. 5b, will be permitted to send discharge at full potential, while the remaining 216 industries will be permitted to send 75% of their full potential as shown Fig. 5a.

Model Part II Application

The value of k is Rs. 200/kl [7]. Value of p consists of two components, one the treatment component ($=k$) and other is the storage component corresponding to

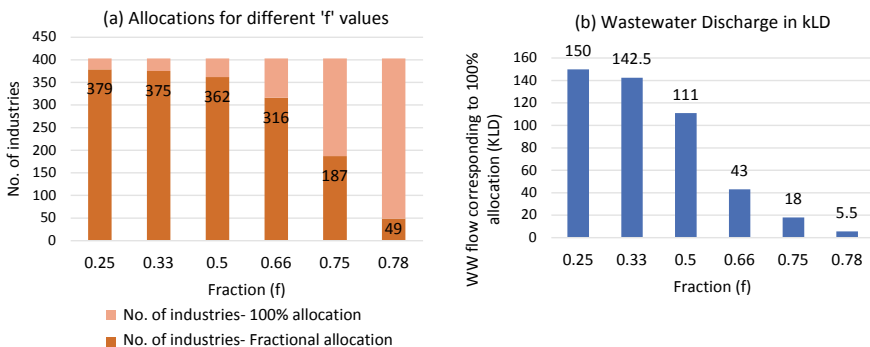


Fig. 5 Graphical representation for different f values **a** no. of industries given full allocation and **b** corresponding wastewater flow

($Q_{\text{mix}} - Q_o$). Storage cost corresponding to this value can be taken as Rs. 50/kl, so that $p = \text{Rs. } 250/\text{kl}$. The Balotra CETP design concentration for COD parameter alone was taken, i.e. $C_o = 2200 \text{ mg/l}$. For example, Industry PI-3 had sent 172.5 kld of effluent at 2349 mg/l COD concentration. Firstly, the allocated flow for PI-3 is 129.4 kld after applying model I, therefore the industry will be allowed to send only 129.4 kld to CETP, and the remaining 43.1 kld must be stored by the industry itself. As $c_i - C_o = 149 \text{ mg/l}$, it violates condition 4 of Table 1. $Q_d = 809 \text{ kld}$. Thus, PI-3 will incur per day penalty cost of $\text{Rs. } 250 \times 809 = \text{Rs. } 202,250$, in addition to the normal ZLD treatment cost of Rs. 34,500 at Rs 200/kl.

4 Conclusion

ZLD is an 'end-of-pipe' concept to mitigate the impact of wastewater pollution on the environment. The cost of the treated water recovered in the process is always higher than the cost of freshwater used from other. The use of technologically advanced equipment will reduce the cost of operation in ZLD. Consent to operate (CTO) must be given to industries on environmental grounds rather than net production of textiles. Although ZLD is a capital-intensive prospect, but its implementation will give beneficial results in longer run and the spillover effect on the environment will be nil. By using ZLD, there will be no impact on surrounding soil salinity, no groundwater pollution. Also, compliance with stringent legislative and environmental regulations can be achieved. The conservation of water resources through recovery and reuse of treated effluent and salt are the aim of ZLD. In a nutshell, the industrial water cycle is optimized, and a consistency of water supply and quality can be achieved.

References

1. MOEF&CC Notification (2016) Part II, Section 3, Sub-section (i), Environmental Protection (Protection) Fifth Amendment Rules. Ministry of Environment, Forest and Climate Change (MOEF&CC)
2. Mishra P, Soni R (2016) Analysis of dyeing and printing wastewater of Balotra textile industries. *Int J Chem Sci* 14(4):1929–1938
3. Singh AP (2018) Status report on CETPs, STPs and industrial pollution in Jodhari River (Jodhpur to Balotra, Rajasthan). National Green Tribunal (NGT), New Delhi order dated 16.03.2018
4. CPCB (2015) Guidelines on techno—economic feasibility of implementation of zero liquid discharge (ZLD) for water polluting industries, central pollution control board (CPCB). MOEF, Govt. of India, New Delhi
5. CPCB (2014–15) Report on assessment of pollution from textile dyeing units in Tirupur, Tamil Nadu and measures taken to achieve zero liquid discharge. MOEF, Bengaluru
6. Ahirrao S (2014) Zero liquid discharge solutions. In: *Industrial wastewater treatment, recycling and reuse*, 489–520
7. Sustainabilityoutlook (2015) Market outlook zero liquid discharge in indian industry, article in Sustainability Outlook magazine. Retrieved from <https://www.sustainabilityoutlook.in/content/market-outlook-zero-liquid-discharge-zld-indian-industry-755285> on 07.08.2019

A Low-Cost Decentralized Grey Water Recycling System for Toilet Flushing



N. Bhanu Sree

Abstract Water is the gifted resource which is needed by each and every living kind on this Earth. It is the part and parcel of all functions we do. The first most used resource is finding its shortage since the Industrial Revolution has been started. Water is used for many purposes where it is not required to maintain its drinking water standards for all activities. For example, toilet flushing, car washing, gardening and irrigation do not require exactly the potable standards. Relaxation on water demand and wastage can be given going for recycling. Grey water is used, and water collected from washbasin, kitchen sink and laundry activities constitutes about 33.33%. Thus, grey water collected from a residential area has given a simple treatment to make it fit to use for toilet flushing. Due to European toilet system, users even started wasting the potable water. Decentralized system confined to specific colony, i.e. individual colony is responsible for the treatment. It helps in reducing load on STP. This study concentrated on enhancing grey water aesthetic appearance by providing treatment units like aeration, two-stage filtration and disinfection.

Keywords Grey water · DO · COD · Detention time · ROF

1 Introduction

Increase in population has put great stress on energy and water resources. India is the second most populous with more than 1.35 billion. It has estimated the water demand increase from 710 BCM (Billion Cubic Metres) in 2010 to almost 1180 BCM by the year 2050 [1]. With domestic and industrial water, consumption is expected to increase almost 2.5 times. Increase in demand and wastage is making really to fight for water in between nations and states. Water after usage turns into sewage which can be classified and can be segregated into black water and grey water. Black water emerges from the toilets (urine, faeces), whereas grey water emerges from sinks, shower bath, kitchen and laundry activities [2]. A little relaxation on water demand

N. Bhanu Sree (✉)

Civil Engineering Department, Smt. S.R. Patel Engineering College, Unjha, Gujarat, India

e-mail: naragam.bhanusree@gmail.com

and wastage can be given going for recycling. Recycling is the one of the Rs. 4 concept and adopts management of wastewater by passing over some process.

The first case of grey water treatment was mentioned in 1975 by the NASA [3]. In Sweida city of Syria, 83% people were willing to use treated grey water understood by conducting house interviews [4]. As grey water measures for up to 75% of the wastewater produced in households [2], the average generation of grey water changes from country to country varying from 90 to 120 LPCD [5], Morel and Diener [2] which varies depending on the age, living standards, gender and amount of water available. A simple treatment of grey water cannot be used for drinking purpose but can be used for secondary purposes like gardening, flushing of toilets, car-bike washing and firefighting. For example, reusing grey water for irrigation in the city Los Angeles reduced 12–65% of freshwater usage annually [6]. Grey water used for toilet flushing saves 29–35% of common per capita demand. The degree of treatment depends on the quality of grey water which again depends on the source from which it is drawn as well as for the purpose it is used, but there are general characteristics that can be applicable [7]. Grey water can be classified into two categories based on pollutant loads, i.e. high and low load pollutants [8]. According to [5], grey water collected from the kitchen basin and washing machine is higher in organic and physical pollutants compared to bathroom and mixed. Grey water consists of discharges from kitchen and washing machine mostly consists of inorganic particles with very less biodegradability or not even [8]. The BOD: COD ratio of grey water is reported as 0.25–0.64 [8, 9] thus giving an idea of biodegradability. The first priority is given to improve physical parameters as the aestheticism is considered as basic for the end-user, and a considerable improvement was also made in the chemical and biological parameters. Khaldoon et al. (2011) study was conducted in the city of Sweida of Syria. The main objective of the study is to decrease the usage of potable water by constructing artificial wetland (AW), a commercial bio filter (CBF) would save 35% of drinking water for flushing of toilets, and this is also a good practice but requires large area which is not possible in urban areas. Abdel-Kader [10] constructed the mathematical model used to investigate the performance and treatment capability of rotating biological contactors (RBC) to treat the grey water. The GPS-X (version 5.0) simulation program was used in this study to simulate the proposed RBC plant.

Sand filters arranged in series 1 and 2 can reduce COD up to 90% and 84% [11] studied the long-term performance of using natural fibre-based biofilms at moderate and low organic loading rates (OLR) have been examined. Biofilms made of natural fibres (coir, ridge gourd) were similar to that of synthetic media (PVC, polyethylene) at lower OLR when operated in pulse fed mode without effluent recirculation and achieved 80–90% COD removal at HRT of 2 d. But it is not reliable in our laboratory. So, the specific objective of the study is to study of characteristics of grey water like pH, temperature, conductivity, turbidity, TDS, DO and COD studying the amount of reduction in characteristics with aeration and slow sand filtration.

2 Materials and Methods

2.1 Study Area

Gujarat is a state located at the western part of India. The major rivers are Sabarmati, Tapi, Narmada and Mahi making Gujarat yielding great amount of water. Though water scarcity is not a problem but could happen due its sharp growth in industrialization. The present study area Palanpur located in Banas kantha district with coordinates 24.17 °N 72.43 °E consists of 1.41,592 populations according to Census 2011. There is rapid increase in population since 1981 (61,300), 1991 (90,300), 2001(122,300) due to the increase in all facilities including a domestic airport at Deesa just 26 km from Palanpur town. Veer city residency is situated near Ahmadabad highway. The building consists of flushing system which utilizes large quantity of water.

2.2 Quantification and Collection of Grey Water

Before starting the experimental work, it is essential to know the amount of grey water coming out from different sources so that one will get an idea of how much to be treated and for how much system can be designed. The following two methods direct method and bucket method were easy to apply in the field for collection and also measuring the quantity.

2.2.1 Direct Method

In this method, water metre is fixed at the outlet of the drain in kitchen, washbasin, washing machine and RO filter. This not possible metre can be adjusted in between the storage tank and kitchen, washbasin, washing machine, RO filter inlets. By using this method, we can easily determine the quantity of grey water.

2.2.2 Bucket Method

In this system, quantity of grey water is collected by placing the bucket at the drain from kitchen, washbasin, washing machine and RO filter. This method is cheap, and it is applicable where the grey water is kept constant.

2.2.3 Method Followed

Bucket method is used in the study to determine the quantity. First, the outlet was determined and then a 20 L bucket is placed at all drains. The time required to fill

Table 1 Quantity of grey water from different sources

Source of grey water	Quantity (lit/day)
Washing machines	85
Kitchen sink	80
R.O. system	45
Total (from a house)	210

is noted down, measured the rate of flow of grey water at all peak times and also recorded 24 h discharge. This process was continued for one week. All the values were averaged, and finally determined the grey water can be obtained for a day. Table 1 shows house survey is conducted in each 12 houses of Veer city residence, G+3 building.

2.3 Aeration

Treatment unit's aeration, filtration and chlorination were adopted. Aeration increases the DO levels, avoids foul gases and makes user to feel comfortable. For aeration, an aquarium pump of capacity 2.5 W is used in a tank of size $25 \times 25 \times 20 \text{ cm}^3$. Initial DO of the sample is 3.2 mg/lit, and the readings were taken for 0 min, 10 min, 20 min, 30 min, 60 min, 90 min and 120 min. Subsequent readings are 3.2 mg/l, 3.6 mg/l, 4.1 mg/l, 4.5 mg/l, 5.01 mg/l, 6.2 mg/l and 6.45 mg/l. It was observed that most of the flocs settled forming a light and large sludge. Figure 1 shows aeration done for maximum time of 120 min.



Fig. 1 Aeration before and after treatment

Fig. 2 Rapid sand multimedia filter unit



2.4 Filtration

Filtration helps in removal of dissolved particles. Conventional filters based on rate of filtration are of two types: slow sand filter and rapid sand filter. Rapid sand filter filters faster than the slow sand filter. Rapid sand filter of three layers was constructed. Topmost layers consisting of sand followed by activated carbon layer finally gravel are placed for the support of top layers. Sand of effective diameter D_{10} 0.425 mm is sieved and is prepared by cleaning (separating from any impurities), and next it is oven dried for 24 h at 105 °C. The sand layer consisting of 2 cm thickness followed by activated carbon for more adsorption of dissolved particles and removal of bacteria can be processed by crushing the coal available from the market made of wood, washed with distilled water and then crushed to get fines 2 mm size. Thickness of activated carbon layer is 2 cm. These fines are bound using CaCl_2 to make layer of carbon. Gravel of size 5 cm is washed with distilled water and oven dried for 24 h @ 105 °C. The whole set-up is arranged in a plastic tank of size $25 \times 20 \times 35 \text{ cm}^3$. Figure 2 shows rapid sand multimedia filter unit. Multimedia filters use different sand layers of different sizes here, and a layer of charcoal acts as an adsorbent.

3 Results and Discussions

Chemical and physical characteristics of grey water initial and after treatment are shown in Table 2. Detention time of 90 mins for aeration is chosen as optimum time as it can be reduced to 60 min also if desired. Aeration not only decreased foulness. As seen in the figure, aeration promoted in agglomeration of the particles made the sludge light and large. Air itself acted as a coagulant. Grey water consisting of both positively charged and negatively charged ions got activated by rapid agitation using external energy source, and aeration increased the oxygen levels and could have

Table 2 Test results before and after recycling

S No.	Physical and chemical parameters	Before treatment	After treatment
1	Turbidity	78 NTU	12 NTU
2	Temperature	28 °C	22 °C
3	pH	7.6	7.3
4	Conductivity	83	25
5	TDS	584.6 mg/l	143 mg/l
6	DO	3.2 mg/lit	6.2 mg/lit
7	BOD5	66 mg/l	36 mg/l
8	COD	527 mg/l	97 mg/l

increased oxidation of some compounds resulted in flocculation. Theory behind could be ionic layer compression, and this has to be studied further. Aeration has helped in coagulation which further helped the filter from clogging and increased the filter lifetime. The initial BOD₅ and COD concentrations were 66 and 527 mg/L and show that grey water is a high strength grey water having BOD₅: COD was 0.125 which was not easily biodegradable and thus requires combination of both straining and biological treatment. Straining was done using dual media filter. Filtration helps in great reduction in COD. Biological treatment should be further proceeded in order to avoid bacterial population. Turbidity 78–12 NTU and suspended solids of the sample are considerably reduced which may not choke the pipes. Filtration not only removes total suspended particles resulting in reducing COD also removes many pathogenic organisms. Filter should be cleaned when the filtering capacity has reduced to a prefixed value and when the filter bed got exhausted by maximum absorption. The pilot plant filter has obtained a rate of filtration of 465 l/h/m² considering a peak flow of 5.16 l with a filtered flow 3.88 l in a time of 10 min. The filter ROF can be further increased by increasing the sand size. Pilot plant revealed that filter has good capacity of ROF similar to rapid sand filter which is very helpful in time saving. Table 2 helps in understanding the importance of treatment and effectiveness of aeration and filtration.

4 Conclusions

Pilot studies have revealed that recycled water has sufficient capacity to treat grey water which can be easily used for the flushing. The water also showed markable increase in DO (3.2–6.2 mg/l), BOD₅ (66–36 mg/l) and COD (527–97 mg/l). The project is to be added with the additional plumbing, extra one more pipe line is required for pumping recycled grey water and two tanks for storage of grey water and recycled grey water which is shown in Fig. 3 below drawn in AUTOCAD.

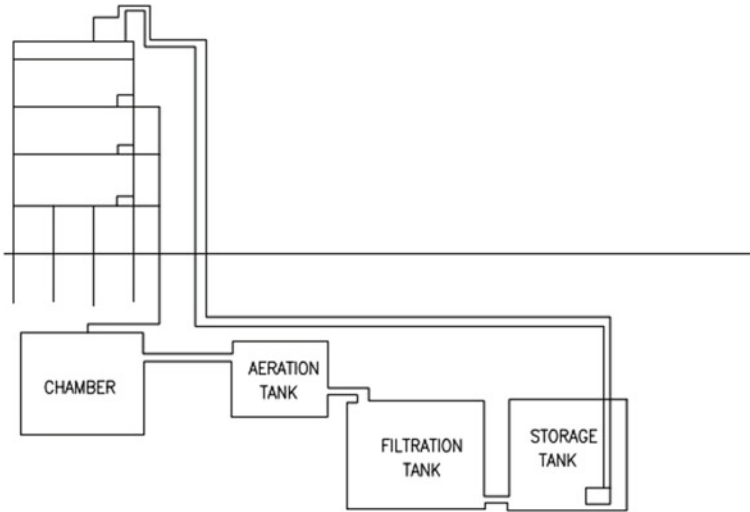


Fig. 3 Layout of decentralized grey water system

Future Scope

The following recommendations/limitations have to be concentrated more to make the system more reliable:

- Maintenance is a very big problem in a large scale, i.e. storing of grey water for long duration will produce foul gases which can be solved by providing intermediate aeration by automatic mechanical system.
- This intermediate aeration can be provided by brakes and mixing system, i.e. when vehicles apply brakes, it causes agitation in the aeration tank.
- Filters sand layers have to be checked in order to maintain non-choking.
- In India, one pipe system is followed, and this system is more adaptable when two pipe system is available. In two pipe system, grey water can be directly collected in the chamber.

References

1. NCIWRD (2000) Assessment of availability & requirement of water for diverse uses
2. Morel A, Diener S (2007) Greywater management in low and middle-income countries, review [vb1] of different treatment systems for households or neighbourhoods. Swiss Federal Institute of Aquatic Science and Technology (Eawag), Dubendorf, Switzerland
3. Hypes W, Batten C, Wilkins J (1975) Processing of combined domestic bath and laundry wastewater for reuse as commode flushing water. NASA technical note TND7937. National Aeronautics and Space Administration, Washington DC
4. Mourad KA, Berndtsson JC, Berndtsson R (2011) Potential fresh water saving using greywater in toilet flushingin Syria. *J Environ Manag* 92:2447–2453

5. Li F, Wichmann K, Otterpohl R (2009) Review of the technological approaches for grey water treatment and reuses. *Sci Total Environ* 407:3439–3449
6. Sheikh B (1993) The city of Los Angeles grey water pilot project shows safe use of grey water is possible. In: *Water management in the 90s: a time for innovation*
7. Carden K, Armitage N, Winter K, Sichone O, Rivett U (2006) Understanding the use and disposal of greywater in the non-sewered areas in South Africa. WRC Report No 1524/1/07, Water Research Commission, Pretoria, South Africa
8. Friedler E (2004) Quality of individual domestic greywater streams and its implication for on-site treatment and reuse possibilities. *Environ Technol* 25:997–1008
9. Jefferson B, Palmer A, Jeffrey P, Stuetz R, Judd S (2004) Grey water characterisation and its impact on the selection and operation of technologies for urban reuse. *Water Sci Technol* 50:157–164
10. Katukiza AY, Ronteltap M, Niwagaba CB, Kansiime F, Lens PNL (2014) *J Environ Manag* 146:131–141
11. Chanakya HN, Khuntia HK (2014) Process safety and environmental protection 9(2):186–192
12. Eriksson E, Auffarth K, Henze M, Ledin A (2002) Characteristics of grey wastewater. *Urban Water* 4(1):85–104
13. Eriksson E, Andersen HR, Madsen TS, Ledin A (2009) Greywater pollution variability and loadings. *Ecol Eng* 35:661–669
14. Abdel-Kader AM (2012) *J King Saud Univ Eng Sci* 25:89–95
15. Nolde E (2005) Greywater recycling systems in Germany—results, experiences and guidelines. *Water Sci Technol* 51:203–210
16. Mourad KA, Berndtsson JC, Berndtsson R (2011) *J Environ Manag* 92:2447–2453

Water Demand as Fuzzy Random Variable in the Analysis of Water Distribution Networks



Perna Pandey, Shilpa Dongre, and Rajesh Gupta

Abstract The analysis of water distribution networks (WDNs) involves number of parameters, some of which are uncertain and may affect the system performance. The deterministic approach considers such uncertain parameters as precisely known in the crisp value analysis. Among the various uncertain parameters, water demand at nodes which shows the major variation over the design life due to various factors including increase in population, improved way of living, fire demand, thefts, and leakages. The variation is due to combined effect of its random nature and imprecise knowledge at its values which is taken fuzzy. The various approaches in the literature consider water demand as either random or fuzzy. The present study aims to incorporate water demand as a fuzzy random variable (FRV) in the analysis of WDNs. The water demand at each node is assumed to be normally distributed with a fuzzy mean and standard deviation of $\pm 10\%$. The water demand uncertainty is represented by a triangular membership function having random demand at its kernel and $\pm 5\%$ variation as its support. The methodology is illustrated through an example network from literature. The results obtained using fuzzy random approach are compared with those obtained by fuzzy approach.

Keywords Water distribution networks · Fuzzy–random approach · Uncertainty · Water demand · Fuzzy mean

P. Pandey (✉) · S. Dongre · R. Gupta
Department of Civil Engineering, VNIT Nagpur, Nagpur 440010, India
e-mail: perna.pandey1203@gmail.com

© The Author(s), under exclusive license to Springer Nature Singapore Pte Ltd. 2021
R. Al Khaddar et al. (eds.), *Advances in Energy and Environment*, Lecture Notes in Civil Engineering 142, https://doi.org/10.1007/978-981-33-6695-4_10

103

1 Introduction

In the analysis of water distribution networks (WDN), it involves several uncertain parameters such as: (1) Pressure head requirement and future water demand at nodes which is difficult to analyze correctly. (2) Pipe roughness value. (3) Economic and environmental factors, i.e., discount rate and cost of repair of failed components etc [3]. Precise values of the parameters like future water demand and pipe roughness can be obtained when new. However, due to aging process quantifying, these values are difficult and causes some uncertainty. Hence, it is very much necessary to incorporate these uncertainties for a reliable design of WDNs.

In general, there exist two types of uncertainties, i.e., random and fuzzy. The uncertainty of random nature is caused due to natural variability and it is termed as irreducible or aleatoric uncertainty. Similarly, the uncertainty due to lack of knowledge or fuzziness is referred as reducible or epistemic uncertainty. The major difference between the two approaches is that the prior one is a probabilistic or stochastic approach while the later is possibilistic approach. The probabilistic approach is mainly statistical in nature and large reliable data is needed to define the probability distribution function (PDF) of any uncertain variable, which is treated as random variable. The approach thus suited best for such uncertain events/ processes whose occurrence is uncertain, i.e., whether the event/ process can occur or not and is based on binary characterization (either 0 or 1). However, the possibility-based approach considers uncertain parameter as fuzzy parameter and it is based upon possibility approach, thus considers, the possibility (between 0 and 1) of occurrence of an event. The uncertainty associated with lack of information is appropriate to handle with fuzzy approach. While the fuzzy random approach holds good for simultaneous representation of randomness and fuzziness for uncertainty analysis. Such uncertain parameters are together known as fuzzy random variables (FRVs).

The probabilistic approach represents the uncertain parameters by means of probability distribution function (PDF) or cumulative distribution function (CDF). From the known PDF of uncertain parameter, PDF for output variable is generated using Monte Carlo simulation (MCS), Latin hypercube sampling (LHS), etc. [2]. This requires evaluations of thousands of alternatives making the process computationally intensive. Lansey et al. [9] used chance constrained nonlinear programming to formulate single objective design problem considering nodal demands, required pressures, and roughness coefficients as an uncertain parameter. Kapelan et al. [7] proposed a robust nondominated sorting genetic algorithm II (RNSGAI), for multi-objective design considering uncertainties in nodal demands, and pipe roughness. Xu and Goulter [17] solved its model by integrating the first-order reliability method (FORM) and GRG2 optimization program, hence provided an improved design solution. Babayan et al. [1] replaced MCS by integration-based uncertainty quantification technique and solved using modified genetic algorithm (GA).

To study the effect of imprecision and uncertainty in pipe roughness coefficients and nodal demands on system performance, fuzzy sets theory adopted [13]. Gupta and Bhawe [6] have shown fuzzy uncertainty modeling to analyze the effect of uncertainty in nodal demands and pipe friction factors on pipe flows in the WDN using impact table approach. Karmakar [8] carried out hydraulic analysis with different possible combination. From these solutions, maximum and minimum values of dependent parameter were selected to form the membership function. Sivakumar et al. [18] adopted similar approach and named it as vertex approach, but this remains feasible for smaller network. Shibu and Reddy [17] used cross-entropy (CE) method for WDN analysis under fuzzy demand. Spiliotis and Tsakiris [19] opted Newton–Raphson method with fuzzy demands for WDN analysis, and Dongre and Gupta [4] obtained a reliable solution by transforming a fuzzy constrained optimization model into a deterministic model by taking the relationship between fuzzy demands and fuzzy nodal heads. Moosavian and Lence [13] opted an approximate approach for the analysis. The paper suggested that as nodal demand increases, pressure head decreases, and based on this, the maximum and minimum values of nodal demand were obtained.

For uncertainty analysis of WDN, the uncertain parameters are either treated as random or fuzzy. However, as the water demand is uncertain due to both its random nature and insufficient knowledge about the same, recently, some of the studies have considered simultaneous representation of randomness and fuzziness in the consolidate framework [5, 16]. Fuzzy random theory is observed to be one of advanced method that has been appeared as a valuable tool to deal with probabilistic problems involving fuzzy data [8]. Recently, Fu and Kapelan [5] and Shibu and Reddy [16] considered water demand as FRV in multi-objective optimization problem of minimizing the cost and maximizing the reliability. While Fu and Kapelan [5] opted GA and Shibu and Reddy [16] opted CE as optimization tool. The methodology resulted in cost-effective reliable design.

The aim of this paper is to present the uncertainty analysis of WDN through fuzzy random approach. The nodal demand is considered to be uncertain parameter and a benchmark network of two loops is solved.

2 Methodology

2.1 Basic Concept of Fuzzy Random Approach

The FRV was first discovered by Kwakernaak [9]. The outcome of the random experiments is considered as fuzzy number instead of the crisp real value. He observed that both fuzzy and random approaches are fundamentally different from each other, as fuzzy is due to lack of data while random is based upon huge statistical information. The approach holds good for uncertainties which are partially random and partially fuzzy in nature. Hence, a lot of efforts have been made [11, 12] for an individual but

simultaneous representation of both the uncertainties and is referred as fuzzy random approach and such variables are termed as fuzzy random variables (FRV) [14].

The concept of FRV is developed by combining the concept of both random and fuzzy approaches. The approach can be considered as a mapping from probability space to fuzzy numbers. This can be shown as

$$\xi:\Omega \rightarrow F(\mathfrak{R}) \tag{1}$$

In case of random approach, uncertain parameter x is shown either by probability distribution function (PDF) or cumulative distribution function (CDF). These PDF/CDF can be obtained using various approaches such as MCS, LHS, FOSM, FORM as shown in Fig. 1a. While in case of fuzzy approach, any uncertain parameter x is represented by the membership function $\mu(x)$ where its values ranges between 0 and 1. The most commonly used membership function is triangular one and is mostly represented by triplet (a, b, c) , where $[a, c]$ represents the support and $[b]$ represents the kernel of membership function. The α cut of uncertain parameter is expressed as set containing all values x having membership degree between $\alpha \in [0,1]$ as shown in Fig. 1b.

The approach first uses the probabilistic approach in order to get the improved cumulative probability spread. These new probability is spread is now been projected

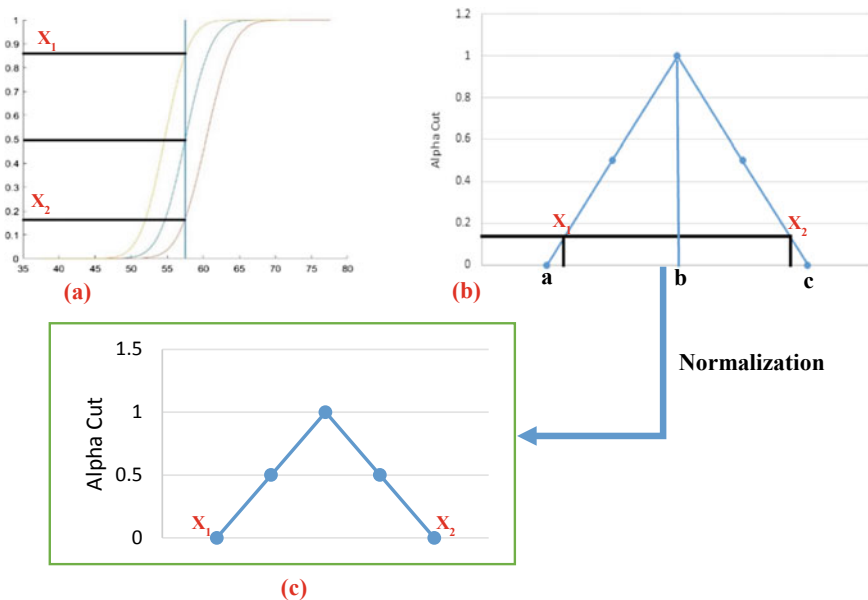


Fig. 1 Layout of fuzzy random representation. **a** CDF of input parameter drawn with the help of MCS. **b** Membership function of uncertain parameter drawn with impact table approach and the improved probability plot are shown in the same. **c** Normalized/new membership function plot considering both randomness and fuzziness

to fuzzy membership function. After the normalization, the output of the dependent parameter is achieved. The layout of same is explained in Fig. 1.

2.2 Application of Fuzzy Random Approach for Future Water Demand

Water demand being the highly uncertain parameter involved in the analysis and design of WDN, as it is affected by various factors such as population growth, climate change, socio-economic changes, etc. [14]. These factors affect the water demand forecasting accuracy. Hence, correct prediction of water demand both in short-term or long-term time horizon has become really a challenge.

Uncertainty in the water demand has to be considered while designing the system so as to have more reliable design. Probabilistic approaches consider only the random uncertainty in water demand such as, Lansey et al. [10], Kapelan et al. [7], Xu and Goulter [20] and Babayan et al. [1] used the probabilistic approach considering normally distributed PDF. Later, Revelli and Ridolfi [15], Gupta and Bhawe [6], used fuzzy approach where water demand is expressed using triangular or trapezoidal membership function. Both these approaches hold good only for individual uncertainty, i.e., either random or fuzzy. But the water demand becomes uncertain due to both random and fuzzy events. Hence, considering both simultaneously is of great importance.

The use of FRV to characterize the nodal demand can be defined as fuzzy number serves as prior knowledge in determining the parameter of PDF or CDF. For instance, the mean of the CDF of future water demand cannot be known accurately; hence, it is better shown by a fuzzy number. While solving the problem, the nodal demand at each node is considered to be normally distributed with fuzzy mean and standard deviation as 10% original demand. The fuzzy mean is represented by the triangular membership function, where kernel is having the original demand and certain deviation of this original demand as support. As shown in Fig. 1, the core of the CDF is the fuzzy mean and the lower and upper envelopes are the probability bands. These probability bands provide the cumulative probability spreads by combining both the uncertainty. With this new probability spread, the membership function is normalized again and the output of dependent parameter is obtained at various α -cut values.

A C programme is developed to carry out the analysis and it is linked to EPANET as hydraulic solver.

3 Methodology

- Decide the uncertain parameter and its uncertainty to be considered. Also, the mean and standard deviation of input uncertain parameter.
- With this mean and % uncertainty, plot the membership function for water demand.
- Plot the CDF for the water demand with the given fuzzy mean and standard deviation along with two probability bounds, through MCS or LHS. (Core of the CDF family shows the highest possibility ($\alpha = 1$) and the lower and upper bounds reveal the envelop of CDF ($\alpha = 0$), as shown in Fig. 1a)
- Obtained cumulative probability spread at most likely value 0.5 is then projected on the fuzzy membership function.
- Represent the fuzzy sets for the obtained probability spread in triangular form (a,b,c) and normalize with maximum value at 1 and minimum at 0, as shown in Fig. 1b.
- The membership function for water demand is modified with the obtained probability spread after normalization as shown in Fig. 1c.
- Obtain the membership function for output parameter (nodal heads and pipe flows) through impact table approach at different α -cut (i.e., 5 α -cut values, 0, 0.2, 0.4, 0.6, 0.8, 1).

4 Example Network

A Two-loop WDN used for the study is opted from Revelli and Ridolfi [15] as shown in Fig. 2. The network consists of a source node fixed at 100 m head and three demand nodes 2, 3, and 4. The network parameter values are given in Table 1. The direction of flow assumed is also shown in Fig. 1. The source head, nodal head, and roughness coefficient of pipes have precise value with no uncertainty. The nodal demand (q) is considered to be the uncertain. The future water demand at each node is assumed to follow normal probability distribution with fuzzy mean and standard deviation as

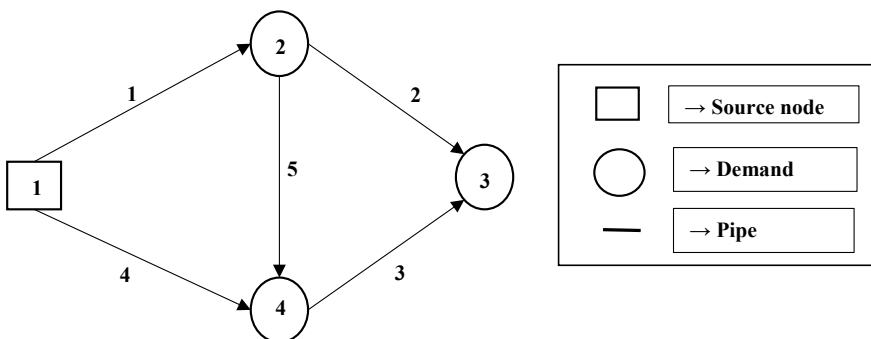


Fig. 2 Layout of two-loop water distribution network

Table 1 Pipe data of two-loop WDN

Pipe	Length (m)	Diameter(m)
1	1200	0.50
2	1100	0.50
3	1500	0.50
4	900	0.35
5	1000	0.35

Table 2 Node data of two-loop WDN

Node No.	Nodal demand (cumec)			Heads (m)
	Min	Nor	Max	
1	0	0	0	100
2	0.135	0.15	0.165	0
3	0.27	0.3	0.33	0
4	0.207	0.23	0.253	0

$\pm 10\%$ of original demand. The fuzzy mean represented as a triangular fuzzy number with kernel at its original demand and $\pm 5\%$ variation at its support, respectively.

Input Parameters

See Table 2.

5 Results and Discussion

The output of the analysis is shown in Tables 3 and 4. Table 3 shows the fuzzy and FRV values of pipe flow for all the pipes and Table 4 shows the fuzzy and FRV values of head for every demand nodes for each α -cut level. These values are used to form the membership function of the respective parameters. On comparing the results obtained by fuzzy and FRV approaches, results are found to be different. FRV considers both the uncertainty, i.e., fuzzy and random together, which leads to reduction in the spread of uncertainty. This proportionally leads to reduction in the values of dependent parameter when compared with fuzzy.

The comparison of membership functions of the discharge in all the pipes and head at demand nodes for case study are shown in Figs. 3 and 4. It can be observed

Table 3 Comparison of fuzzy and FRV values of pipe flow (lps) for different α -cut values

α -cut	Fuzzy		FRV		
	Max	Min	Max	Min	
0	Q[1] = 497.548	Q[1] = 407.085	Q[1] = 474.932	Q[1] = 429.700	
	Q[2] = 248.156	Q[2] = 194.734	Q[2] = 234.796	Q[2] = 208.083	
	Q[3] = 102.515	Q[3] = 53.463	Q[3] = 90.672	Q[3] = 66.168	
	Q[4] = 250.452	Q[4] = 204.915	Q[4] = 239.068	Q[4] = 216.300	
	Q[5] = 92.174	Q[5] = 69.458	Q[5] = 86.540	Q[5] = 75.187	
0.2	Q[1] = 488.501	Q[1] = 416.131	Q[1] = 470.409	Q[1] = 434.224	
	Q[2] = 242.812	Q[2] = 200.073	Q[2] = 232.124	Q[2] = 210.753	
	Q[3] = 97.809	Q[3] = 58.584	Q[3] = 88.272	Q[3] = 68.671	
	Q[4] = 245.899	Q[4] = 209.469	Q[4] = 236.791	Q[4] = 218.576	
	Q[5] = 89.924	Q[5] = 71.754	Q[5] = 85.410	Q[5] = 76.328	
0.4	Q[1] = 474.027	Q[1] = 430.605	Q[1] = 463.172	Q[1] = 441.461	
	Q[2] = 234.261	Q[2] = 208.617	Q[2] = 227.849	Q[2] = 215.027	
	Q[3] = 90.192	Q[3] = 66.670	Q[3] = 84.409	Q[3] = 72.650	
	Q[4] = 238.613	Q[4] = 216.755	Q[4] = 233.148	Q[4] = 222.219	
	Q[5] = 86.314	Q[5] = 75.415	Q[5] = 83.600	Q[5] = 78.151	
0.6	Q[1] = 461.001	Q[1] = 443.632	Q[1] = 456.658	Q[1] = 447.974	
	Q[2] = 226.567	Q[2] = 216.309	Q[2] = 224.002	Q[2] = 218.873	
	Q[3] = 83.245	Q[3] = 73.838	Q[3] = 80.909	Q[3] = 76.206	
	Q[4] = 232.055	Q[4] = 223.312	Q[4] = 229.870	Q[4] = 225.498	
	Q[5] = 83.056	Q[5] = 78.697	Q[5] = 81.968	Q[5] = 79.788	
0.8	Q[1] = 454.053	Q[1] = 450.579	Q[1] = 453.185	Q[1] = 451.448	
	Q[2] = 222.463	Q[2] = 220.412	Q[2] = 221.950	Q[2] = 220.925	
	Q[3] = 79.502	Q[3] = 77.621	Q[3] = 79.033	Q[3] = 78.092	
	Q[4] = 228.558	Q[4] = 226.810	Q[4] = 228.121	Q[4] = 227.247	
	Q[5] = 81.315	Q[5] = 80.443	Q[5] = 81.097	Q[5] = 80.661	
1	Q[1]= 452.316	Q[2]= 221.437	Q[3]= 78.563	Q[4]= 227.684	Q[5]= 80.87

from these figures that the results obtained through FRV are n lower side as fuzzy. The FRV is more appropriate as it combines random and fuzzy uncertainty together.

Discussion

The paper presents the uncertainty-based analysis of WDNs using fuzzy random approach. The uncertainty in the nodal demand is shown by the fuzzy random variable, where it merges the fuzzy and random uncertainty of demands. The MCS method is used for the random sampling of demand and the membership functions are characterized using impact table approach. After combining both the uncertainties, it is observed that there is reduction in the final output values of pipe flow and nodal heads when compared with fuzzy. Hence, this leads to more economical and

Table 4 Comparison of fuzzy and FRV values of head (m) for different α -cut values

α -cut	Fuzzy		FRV	
	Max	Min	Max	Min
0	H[2] = 90.000	H[2] = 85.498	H[2] = 88.946	H[2] = 86.695
	H[3] = 87.557	H[3] = 81.957	H[3] = 86.247	H[3] = 83.446
	H[4] = 88.046	H[4] = 82.665	H[4] = 86.787	H[4] = 84.096
0.2	H[2] = 89.584	H[2] = 85.983	H[2] = 88.730	H[2] = 86.929
0.2	H[3] = 87.041	H[3] = 82.560	H[3] = 85.978	H[3] = 83.737
	H[4] = 87.549	H[4] = 83.245	H[4] = 86.528	H[4] = 84.376
0.4	H[2] = 88.903	H[2] = 86.742	H[2] = 88.379	H[2] = 87.299
	H[3] = 86.193	H[3] = 83.505	H[3] = 85.542	H[3] = 84.197
	H[4] = 86.736	H[4] = 84.152	H[4] = 86.110	H[4] = 84.818
0.6	H[2] = 88.273	H[2] = 87.409	H[2] = 88.060	H[2] = 87.628
	H[3] = 85.410	H[3] = 84.334	H[3] = 85.144	H[3] = 84.606
	H[4] = 85.983	H[4] = 84.950	H[4] = 85.728	H[4] = 85.211
0.8	H[2] = 87.931	H[2] = 87.758	H[2] = 87.888	H[2] = 87.801
	H[3] = 84.984	H[3] = 84.769	H[3] = 84.930	H[3] = 84.823
	H[4] = 85.574	H[4] = 85.367	H[4] = 85.522	H[4] = 85.419
1	H[2]= 87.845	H[3]= 84.876	H[4]= 85.470	

cost-effective design even after considering the uncertainty in the input parameter. The methodology is observed to be very much useful in engaging the effect of both the uncertainties in the analysis of WDNs.

6 Conclusion

- Method is a hybrid uncertainty characterization approach considering both fuzzy and random uncertainty.
- Such hybrid approach leads to cost-effective design while considering reliability aspect.
- It can be helpful in long-term planning and design of WDN.
- One drawback of the methodology is its computational burden and excess time requirement.

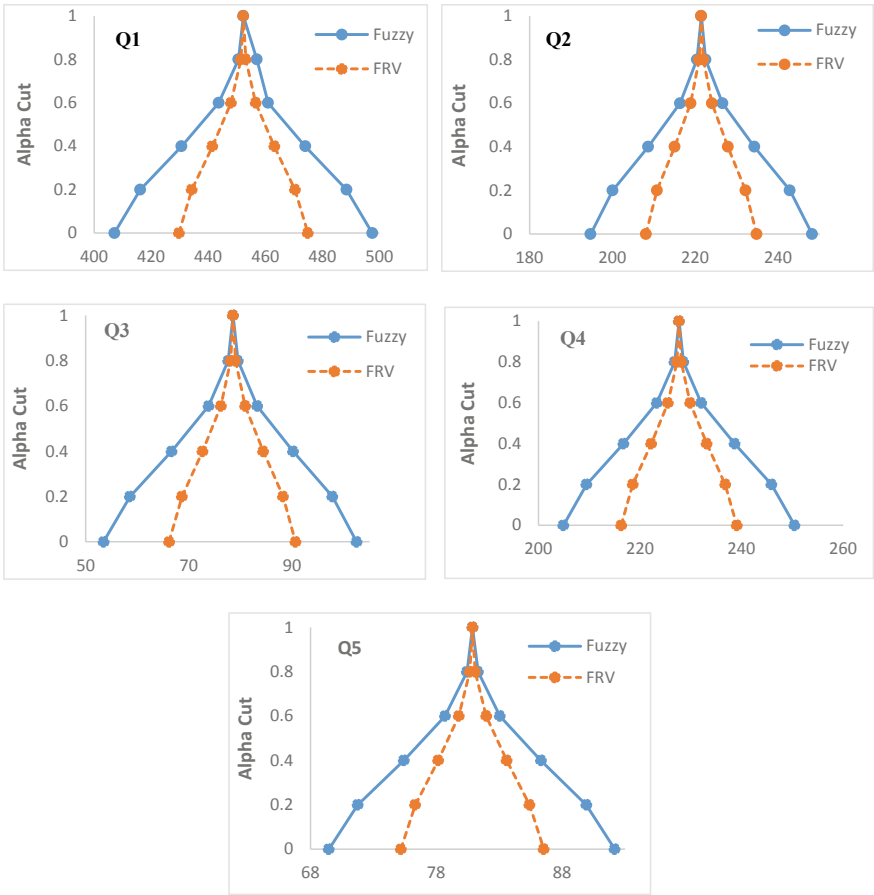


Fig. 3 Membership functions of pipe flows (lps) using fuzzy and FRV

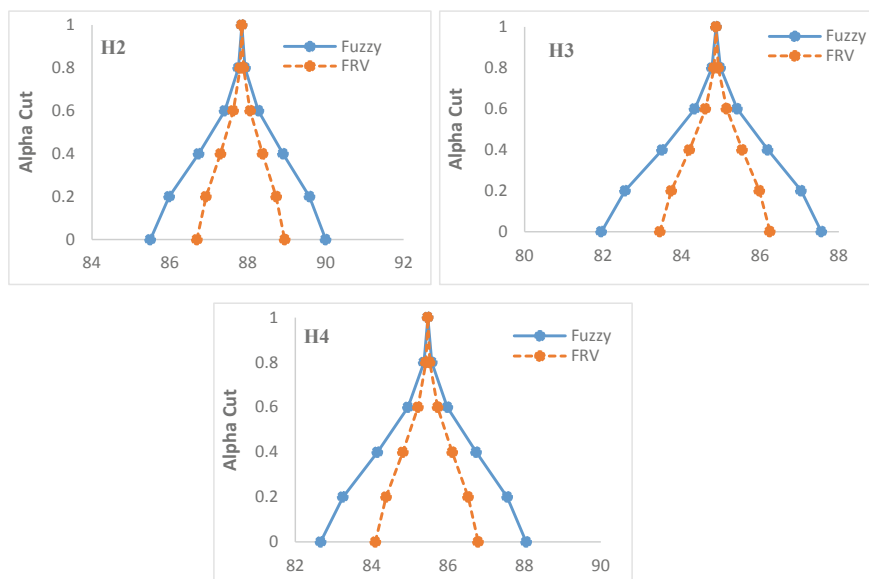


Fig. 4 Membership function of head (m) at every nodes using fuzzy and FRV

References

1. Babayan A, Kapelan Z, Savic D, Walters G (2005) Least-Cost design of water distribution networks. *J Water Resour Plann Manage ASCE* 131(5):375–382
2. Bao Y, Mays LW (1990) Model for water distribution system reliability. *J Hydr Eng* 116(9):1119–1137
3. Bhavre PR (2003) Optimal design of water distribution networks. Alpha Science International
4. Dongre SR, Gupta R (2017) Optimal design of water distribution network under hydraulic uncertainties. *ASCE-ASME J Risk Uncertainty Eng Sys Part A Civil Eng* 3(3):G4017001-1-11
5. Fu G, Kapelan Z (2011) Fuzzy probabilistic design of water distribution networks. *Water Resour Res* 47(5):1–12
6. Gupta R, Bhavre PR (2007) Fuzzy parameters in pipe network analysis. *Civ Eng Environ Syst* 24(1):33–54
7. Kapelan ZS, Savic DA, Walters GA (2005) Multiobjective design of water distribution systems under uncertainty. *Water Resour Res* 41(11):1–15
8. Karmakar S (2011) Propagation of uncertainties in water distribution systems modelling. *Desalination Water Treatment* 33(1–3):107–117
9. Kwakernaak H (1978) Fuzzy random variables-definitions and theorems. *Inf Sci* 29:1–29
10. Lansey KE, Duan N, Mays LW, Tung YK (1989) Water distribution system design under uncertainties. *J Water Resour Plann Manage ASCE* 115(5):630–645
11. Liu YK, Liu B (2003) Fuzzy random variables: A scalar expected value operator. *Fuzzy Optim Decis Making* 2(2):143–160
12. Moller B, Beer M (2004) Fuzzy randomness uncertainty in civil engineering and computational mechanics. Springer-Verlag, Berlin Heidelberg, New York
13. Moosavian N, Lence BJ (2018) Approximation of fuzzy membership functions in water distribution network analysis. *J Hydr Eng* 144(7)

14. Pandey P, Dongre S, Gupta R (2020) Probabilistic and fuzzy approaches for uncertainty consideration in water distribution networks—a review. *Water Supply* 20(1):13–27
15. Revelli R, Ridolfi L (2002) Fuzzy approach for analysis of pipe networks. *J Hydraul Eng* 128(1):93–101
16. Shibu A, Reddy MJ (2014) Optimal design of water distribution networks considering fuzzy randomness of demands using cross entropy optimization. *Water Resour Res.* 28(12):4075–4094
17. Shibu A, Reddy MJ (2011) Uncertainty analysis of water distribution networks by fuzzy -cross entropy approach. *World Acad Sci Eng Technol* 59:724–731
18. Sivakumar P, Prasad RK, Chandramouli S, Majumder S (2014) Uncertainty analysis of water distribution networks using linked EPANET-Vertex method. *Int J Innov Res Sci Eng Technol* 12:17900–17911
19. Spiliotis M, Tsakiris G (2012) Water distribution network analysis under fuzzy demands. *Civ Eng Environ Syst* 29(2):107–122
20. Xu C, Goulter IC (1999b) Reliability-based optimal design of water distribution networks. *J Water Resour Plann Manage ASCE*, 125(6):352–362

Integrating Geospatial Interpolation Techniques and TOPSIS to Identify the Plausible Regions in India to Harness Solar Energy



Aditya Kumar Dupakuntla and Harish Puppala

Abstract Energy is an essential commodity that helps in the economic growth of a country. Unfortunately, the availability of conventional sources used for the generation of electricity is reducing, which is one of the significant reasons for energy insecurity, especially in context to India. In this regard, the Indian Ministry has emphasized on the use of renewable energy to meet the increasing energy demand. Solar is one such renewable alternatives, which is being promoted in India. It is planned to extend the current installed capacity in the near future. In this regard, mapping the seasonal variation of solar radiation over the entire country would help in planning appropriate developmental activities. However, since the meteorological stations are confined to selected localities, the solar radiation received over the entire country remains unmapped. In this study, considering the solar irradiation fields of 72 discrete locations, irradiation over the entire nation is mapped using geospatial interpolation techniques. Additionally, the hierarchy of states that are relatively insensible to seasonal variations and receiving maximum radiation is determined using the TOPSIS multi-criteria decision-making technique. The findings of this study ratify that the IDW interpolation technique is most suitable for the estimation of solar radiation data. Further, the relative hierarchy of states drawn helps to plan the developmental activities optimally and to expand the solar installation capacity in the country.

Keywords Geospatial interpolation technique · Solar radiation · Mean absolute percentage error · Multi-criteria decision making · TOPSIS technique · Criteria · Alternatives

A. K. Dupakuntla · H. Puppala (✉)
Department of Civil Engineering, SoET, BML Munjal University, Gurgaon 122413, India
e-mail: harishpuppala.ce@gmail.com

© The Author(s), under exclusive license to Springer Nature Singapore Pte Ltd. 2021
R. Al Khaddar et al. (eds.), *Advances in Energy and Environment*, Lecture Notes in Civil Engineering 142, https://doi.org/10.1007/978-981-33-6695-4_11

115

1 Introduction

The role of energy in accelerating economic development and transforming the quality of life is very crucial. Fluctuations in its supply may have a detrimental effect on the nation's economy. In this regard, relying on non-renewable sources to meet the energy requirement is not admissible since the availability is limited. Therefore, various developed and developing nations emphasized on generating electricity using renewable sources. India is one such nation with a prime focus on promoting renewable sources to meet the nation's energy demand. India receives an average of 5000 trillion kWh per year. Most of the regions in the country receive radiation of 4–7 kWh per sq.m per day.¹ To take advantage of this, and in view of the energy security perspective, the Indian Ministry has been promoting the use of solar energy by giving incentives to the installation of photovoltaic modules. Solar energy is inexhaustible in a human time scale. The country's installed solar power capacity is 34.045 GW as of January 31, 2020, and is planned to harness nearly 100GW of electricity by 2022 [1]. Monitoring the solar radiation and its seasonal variation over the country before planning developmental activities would help to analyze the energy metrics.

Unfortunately, the irradiation monitoring stations are limited to specific locations. In this regard, geospatial interpolation techniques are used in this study to map the variation in seasonal solar radiation over the country. These techniques help to estimate the irradiation fields at the ungauged locations using the data available at the gauged locations. Kriging interpolation, inverse distance weight (IDW), spline, and nearest neighbor are the few of the geospatial techniques used widely in various engineering and science and applications. A brief overview of the past research works based on geospatial techniques is presented below.

Atta (2020) used kriging and inverse distance weighted techniques to assess and geographically visualize the salinities along with the river of Tigris and Diyala in Baghdad city [2]. These assessments helped in analyzing surface water quality at different locations along the river. Chatterjee and Lataye (2020) estimated the variation of surface water quality of lake Futala, Nagpur, after idol immersions [3]. The effects of different data sampling methods and interpolations methods are discussed by Kruger, Karrasch, and Bernard [4]. Hodam et al. (2017) mapped the spatial distribution of evapotranspiration over India using IDW and Kriging interpolation techniques [5]. Besides these, fluoride contamination in groundwater of the central part of Nagpur district is estimated using IDW, which helped in identifying affected areas [6].

Air pollution levels in Pune city are estimated at discrete locations using IDW, kriging, spline, and nearest neighbor techniques [7]. The 5-day soil moisture at 167 gauged stations during the period of 2010–2014 is used to prepare the surface maps of soil moisture using different spatial techniques Chen et al. [8]. Subsurface soil properties in Denmark are estimated using a kriging interpolation technique [9]. Borges et al. (2016) extended the applications of geospatial interpolation techniques to map the seasonal climatology of precipitation in central Brazil [10]. Geospatial

¹<https://mnre.gov.in/solar/current-status/> Accessed on 15–08-2020.

techniques are used to map the wind speed, solar radiation, and precipitation in Turkey at all the ungauged locations [11]. The characteristics of local-scale urban heat islands are analyzed using an integrated method of mobile measurement and interpolation methods [12].

Applications of kriging, IDW, and spline interpolation techniques in the periodic control of terrain movements in southern Poland are discussed by Lenda et al. [13]. Pavlova (2017) discussed the applications of interpolation methods in creating a digital elevation model of the Omsk region of West Siberia [14]. Findings of Pavlova (2017) ratify that Spline and IDW methods for the construction of DEMs for floodplains in Siberia [14]. The applications of geospatial interpolation techniques are extended to develop the digital elevation model of the MANIT campus in Bhopal [15]. Findings depict that IDW and spline are appropriate for a mild and steep slope, respectively. Annual average daily traffic (AADT) of Washington state is estimated using kriging interpolation and found that the estimates are close to reality [16].

Additionally, these techniques are extended to the field of energy. Ostrometzky, Bernstein, and Zussman (2019) mapped the irradiance field reconstructed from the estimated solar radiation using IDW for the New York City region [17]. Spline interpolation technique is used to map the monthly mean daily solar radiation of Tunisia at a resolution of $500\text{ m} \times 500\text{ m}$ [18]. In similar lines, Rodríguez-Amigo et al. (2017) mapped the global horizontal irradiation in Spain using IDW, spline, kriging, and natural neighbor interpolation techniques. It is found that the performance of the kriging interpolation technique is satisfactory [19]. The findings of geospatial interpolation techniques are integrated with stochastic simulation models to predict global solar radiation [20].

IDW predicts the ungauged fields by linear weighting the combination of a sample set of points in the neighborhood and the weightage of each sample depends on the distance between gauged and ungauged locations. In kriging technique, the ungauged values are estimated by fitting a mathematical function and follow a multistep process from statistical analysis of the data, variogram modeling, creating the surface. In spline interpolation, a mathematical function that minimizes overall surface curvature is chosen to estimate the ungauged parameters. From literature, it can conclusively be stated that the suitability of the geospatial interpolation technique depends on the type of parameter and the spatial distribution of gauged locations. In this regard, the solar radiation data at ungauged locations in India is mapped using various techniques, and the estimates are compared with the real field values to determine the suitable geospatial technique.

2 Methodology

Since the steps involved in geospatial interpolation techniques are evident from the literature [15], no spatial emphasis is made in this research to present the mathematical aspects associated with each of these techniques. The existing meteorological stations in India are confined to discrete locations. This impaired decision-maker to

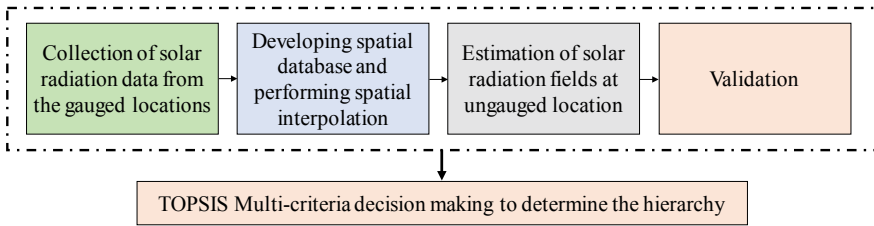


Fig. 1 Framework to find the plausible region in India to harness solar energy

consider the magnitude being received by the nearest station for an ungauged location. Any imprecision associated with this assumption will further be carried to the feasibility assessments.

In this regard, considering the solar radiation data at the gauged locations, the probable radiation received by the ungauged locations is calculated using geospatial interpolation technique. Besides mapping, for a better understanding of temporal variation in solar radiation, the analysis is performed by considering Summer, Winter, Monsoon, and Autumn seasons. Kriging, IDW, and spline interpolation techniques are used to predict solar radiation at different ungauged locations. After the spatial interpolation, the estimated fields are validated with the known fields of few localities, which are not considered for the analysis. ArcGIS Software® is used to estimate and visualize the predicted data of solar radiation fields. The performance of each technique is compared in terms of mean absolute percentage error. For better understanding, the steps involved in the analysis are shown in Fig. 1. After mapping the irradiation, the hierarchy of each state is determined using the TOPSIS multi-criteria technique by considering irradiation received in Summer, Winter, Monsoon, and Autumn and seasonal variation as the influencing criteria.

3 Analysis, Results, and Discussions

The primary objective of this study is to map the solar radiation data over the entire nation and to examine the seasonal variation. The observations thus made help in identifying the prospective regions to harness solar energy. For this analysis, daily irradiation data related to 72 monitoring stations for the year 2019 is collected using RETScreen Clean Energy Project Analysis Software.² This open-source software assists in accessing the radiation data fields from the NASA portal through the interface. Among the chosen monitoring stations, 57 monitoring stations are within the nation, and the rest 15 stations are close to the boundary of the nation. The monitoring stations within the proximity of the nation help to minimize errors during interpolation. Subsequently, the average seasonal variation of irradiation fields is

²<https://www.nrcan.gc.ca/maps-tools-publications/tools/data-analysis-software-modelling/retscreen/7465>. Accessed on 15-08-2020.

estimated for the respective weather stations. Winter season with the time window between Dec 2019 to Feb 2020, Summer season between March 2019 to May 2019, Monsoon- June 2019 to September 2019 and Autumn–October 2019 to November 2019. The spatial and temporal variation of irradiation are estimated using three different techniques, which include kriging, inverse distance weightage (IDW), and spline interpolation. From the mapped solar radiation data, as shown in Fig. 2, it is

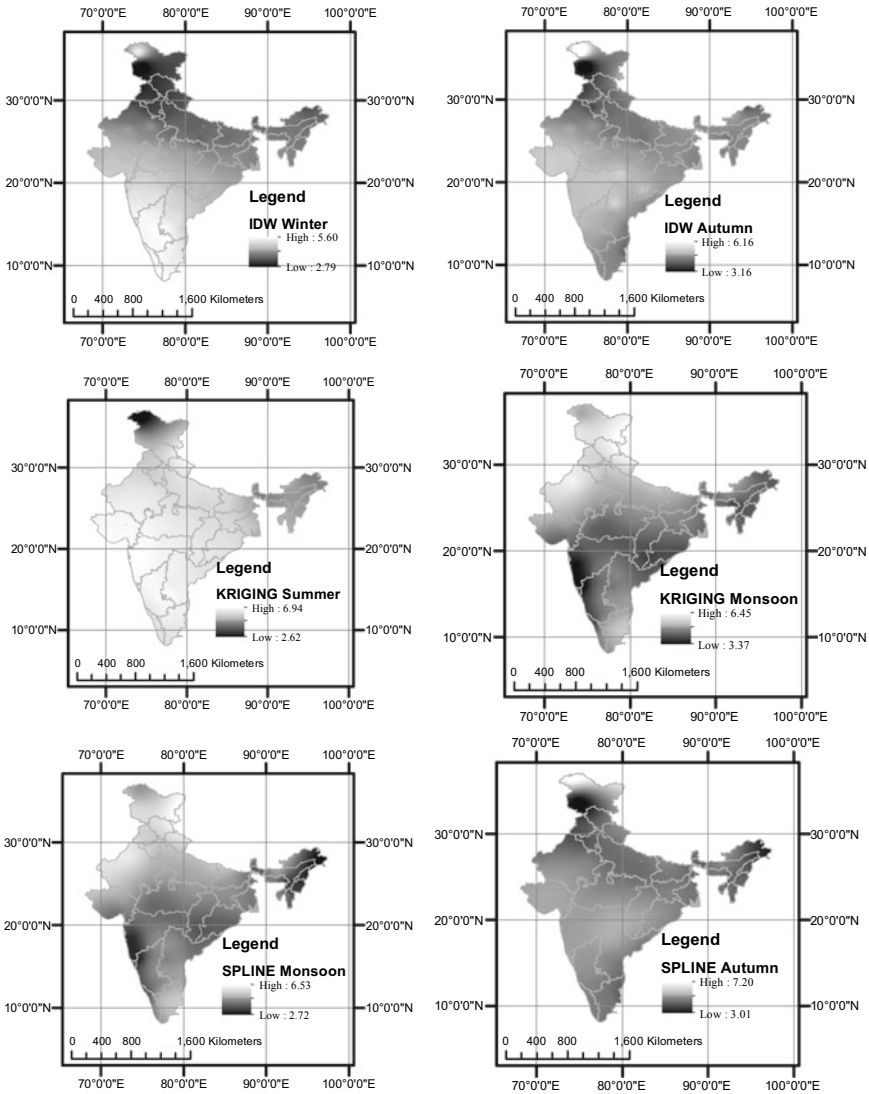


Fig. 2 Spatial variation of irradiation (KWh/m²/d) over the nation using a Inverse distance weightage b Kriging interpolation c Spline interpolation

observed that there is a notable variation in solar energy over the country. The irradiation data of six additional cities, located in six different states, is used to validate the mapped seasonal solar radiation.

From Fig. 2, it is apparent that maximum irradiation received in India during Summer is 6.94 kWh/m²/d. In contrast, the maximum irradiation received in Monsoon, Winter, and Autumn is 6.45 kWh/m²/d, 5.59 kWh/m²/d, and 5.43 kWh/m²/d, respectively. From this observation, conclusively, it can be stated that irradiation received is sensitive to seasonal changes. To expound the seasonal variation in great detail, the sensitivity of solar irradiation to seasonal changes in each of the states is evaluated in terms of standard deviation. Although the standard deviation in Assam and Arunachal Pradesh is found to be relatively less compared to other states, the maximum radiation received by these two locations is not encouraging for setting a solar plant.

Besides this, the sensitivity of irradiation is found to be significantly high in Karnataka, Uttar Pradesh, Delhi, Maharashtra, Haryana, Himachal Pradesh, Uttarakhand, Chandigarh, Punjab, Goa, Jammu, and Kashmir. Keeping in view of this seasonal variation besides considering the maximum value would help in identifying the regions in which solar projects can be promoted. Since determining the plausible region involves evaluating them on two different aspects, i.e., should receive high irradiation and seasonal variation should be relatively negligible. Evaluating the region over two different criteria is a Multi-criteria problem. Technique for Order of Preference by Similarity to Ideal Solution (TOPSIS)³ technique [21] is used in this study to determine the hierarchy.

4 Validation

The deviation of interpolated irradiation filed with the actual field values is estimated in terms of mean average percent error (MAPE). MAPE can mathematically be represented using Eq. 1. The evaluated MAPE corresponding to each of the chosen stations is presented in Table 1. It is observed that the mean absolute percentage error

Table 1 Mean absolute percentage error in the estimated solar irradiation

City	IDW	Kriging	Spline
Gorakhpur	8.67	9.41	9.31
Mahasamund	3.08	3.14	3.48
Hassan	3.96	4.64	5.36
Proddatur	2.77	2.33	2.26
Amreli	3.06	3.40	3.72
Selam	4.46	4.51	4.81

³For detailed information on TOPSIS technique please refer the study of Opricovic and Tzeng [21].

(MAPE) is within 10%, which is satisfactory.

$$\text{Mean average percent error (MAPE)} = \left| \frac{(I_{\text{int}} - I_{\text{obs}})}{I_{\text{obs}}} \right| \times 100 \quad (1)$$

where, I_{int} is the interpolated irradiation fields using IDW, kriging, and spline interpolation techniques, and I_{obs} is the observed irradiation fields obtained from RETScreen.

5 Plausible Regions to Harness Solar Energy Using TOPSIS

The region receiving maximum irradiation without any notable seasonal variations is more suitable to harness solar energy. In this regard, the irradiation received in Summer, Autumn, Winter, Monsoon, and Seasonal variation in the respective region is considered as the different criteria to evaluate the dominance of each state. Technique for Order of Preference by Similarity to Ideal Solution (TOPSIS) multi-criteria technique is used to determine the hierarchy. The relative dominance of each region is evaluated and is found that Tamil Nadu, Kerala, Assam, Arunachal Pradesh, Telangana, Andhra Pradesh, Gujarat, West Bengal, Karnataka, Jharkhand is relatively higher than the rest of the states. These states are followed by Madhya Pradesh, Chhattisgarh, Odisha, Rajasthan, Bihar, Goa, Ladakh, Uttar Pradesh, Uttarakhand, Delhi, Himachal Pradesh, Haryana, Chandigarh, Punjab, and Jammu and Kashmir. The decision-maker can consider the existing installed capacity in each of the states and further developmental actions can be taken to expand the capacity of generation.

6 Conclusions

The prospects of using geospatial interpolation techniques in mapping the geospatial parameters are reviewed. Solar irradiation of 72 monitoring stations is considered, and the spatial variation of solar irradiation over the entire nation during each season is mapped using geostatistical techniques. The obtained solar irradiation data is compared with the observed irradiation data of the respective monitoring stations. The accuracy of the mapped fields is measured in terms of mean percentage average error by considering seven additional locations chosen for validation. In view of the observed mean absolute percentage error (MAPE), it can conclusively be stated that the predicted irradiation fields using IDW interpolation are reasonable. Further, the sensitivity of irradiation to seasonal variation is evaluated in terms of standard deviation and is observed that Assam and Arunachal Pradesh relatively insensitive compared to other states. Considering irradiation received in Summer, Autumn,

Winter, Monsoon, and Seasonal variation as criteria, the cumulative score of each state is evaluated using the TOPSIS technique. The evaluated cumulative score depicts that Tamil Nadu, Kerala, Assam, Arunachal Pradesh, Telangana, Andhra Pradesh, Gujarat, West Bengal, Karnataka, Jharkhand are plausible states receiving reasonable irradiation with minimum fluctuation with seasonal changes.


References

1. Ministry of New and Renewable Energy (2019) <https://mnre.gov.in/>
2. Atta HA (2020) Assessment and geographic visualization of salinity of Tigris and Diyala Rivers in Baghdad City. *Environ Technol Innov* 17:100538
3. Chatterjee R, Lataye DH (2020) Analysis of water quality parameters and their variation for surface water using gis-based tools. In: *Applications of geomatics in civil engineering*. Springer, Singapore, pp 289–302
4. Krüger R, Karrasch P, Bernard L (2018) Evaluating spatial data acquisition and interpolation strategies for river bathymetries. In: *The annual international conference on geographic information science*. Springer, Cham, pp 3–25
5. Hodam S, Sarkar S, Marak AG, Bandyopadhyay A, Bhadra A (2017) Spatial interpolation of reference evapotranspiration in India: comparison of IDW and Kriging methods. *J Institut Eng (India) Series A* 98(4):511–524
6. Arif M, Hussain J, Hussain I, Kumar S, Bhati G (2014) GIS based inverse distance weighting spatial interpolation technique for fluoride occurrence in ground water. *Open Access Library J* 1(4):1–6
7. Kanakiya RS, Singh SK, Shah U (2015) GIS Application for spatial and temporal analysis of the air pollutants in urban area. *Int J Adv Remote Sens GIS* 4(1):1120–1129
8. Chen H, Fan L, Wu W, Liu HB (2017) Comparison of spatial interpolation methods for soil moisture and its application for monitoring drought. *Environ Monit Assess* 189(10):525
9. Firouzianbandpey S, Ibsen LB, Griffiths DV, Vahdatirad MJ, Andersen LV, Sørensen JD (2015) Effect of spatial correlation length on the interpretation of normalized CPT data using a kriging approach. *J Geotech Geoenviron Eng* 141(12):04015052
10. de Amorim Borges P, Franke J, da Anunciação YMT, Weiss H, Bernhofer C (2016) Comparison of spatial interpolation methods for the estimation of precipitation distribution in Distrito Federal Brazil. *Theor Appl Climatol* 123(1–2):335–348
11. Keskin M, Dogru AO, Balçık FB, Goksel C, Ulugtekin N, Sozen S (2015) Comparing spatial interpolation methods for mapping meteorological data in Turkey. In *Energy systems and management*. Springer, Cham, pp 33–42
12. Liu L, Lin Y, Liu J, Wang L, Wang D, Shui T et al (2017) Analysis of local-scale urban heat island characteristics using an integrated method of mobile measurement and GIS-based spatial interpolation. *Build Environ* 117:191–207
13. Lenda G, Ligas M, Lewińska P, Szafarczyk A (2016) The use of surface interpolation methods for landslides monitoring. *KSCE J Civil Eng* 20(1):188–196
14. Pavlova AI (2017) Analysis of elevation interpolation methods for creating digital elevation models. *Optoelectron Instrument Data Process* 53(2):171–177
15. Rishikeshan CA, Katiyar SK, Mahesh VV (2014) Detailed evaluation of DEM interpolation methods in GIS using DGPS data. In: *2014 international conference on computational intelligence and communication networks*. IEEE, pp 666–671
16. Shamo B, Asa E, Membah J (2015) Linear spatial interpolation and analysis of annual average daily traffic data. *J Comput Civil Eng* 29(1):04014022
17. Ostrometzky J, Bernstein A, Zussman G (2019) Irradiance field reconstruction from partial observability of solar radiation. *IEEE Geosci Remote Sens Lett* 16(11):1698–1702

18. Chelbi M, Gagnon Y, Waewsak J (2015) Solar radiation mapping using sunshine duration-based models and interpolation techniques: application to Tunisia. *Energy Convers Manage* 101:203–215
19. Rodríguez-Amigo MDC, Díez-Mediavilla M, González-Peña D, Pérez-Burgos A, Alonso-Tristán C (2017) Mathematical interpolation methods for spatial estimation of global horizontal irradiation in Castilla-León, Spain: a case study. *Sol Energy* 151:14–21
20. Jeong DI, St-Hilaire A, Gratton Y, Bélanger C, Saad C (2017) A guideline to select an estimation model of daily global solar radiation between geostatistical interpolation and stochastic simulation approaches. *Renewable Energy* 103:70–80
21. Opricovic S, Tzeng GH (2004) Compromise solution by MCDM methods: a comparative analysis of VIKOR and TOPSIS. *Eur J Oper Res* 156(2):445–455

Utilization Potential of Iron Ore Tailing Waste in Various Applications



S. R. Bharath, N. Lavanya, H. B. Bharath Kumar, R. K. Chaitra,
and Rahul Dandautiya 

Abstract Iron ore tailing (IOT) is the wastes generated during the salutariness process of iron ore concentration. These wastes are abundant in quantity, which can be utilized in many ways. In this manuscript, utilization potential of IOT as a resource and its adaptation in the replacement of different industrial raw materials have been discussed. The physico-chemical properties of IOT are one of the major factors responsible for its vast usability. Literature from eminent researchers suggested that IOT can be successfully used in the manufacturing of building blocks, replacement of fine aggregate, in powder technology, Bick manufacturing, synthesis of glass fiber, etc. In precast concrete opportune properties with respect to Portland cement can be achieved with up to 50% IOT replacement along with mineral admixtures. In spray concrete, the IOT works very well in the replacement of fine aggregate and give competitive results. The details of physical and chemical properties show that more profound applications can be researched in the future.

Keywords Iron ore tailing · Concrete · Physico-chemical properties · Sustainable · Utilization

S. R. Bharath · N. Lavanya · H. B. Bharath Kumar · R. K. Chaitra · R. Dandautiya (✉)
Atria Institute of Technology, Bengaluru, India
e-mail: rahuldandautiya@gmail.com

S. R. Bharath
e-mail: bharathsr1998@gmail.com

N. Lavanya
e-mail: lavanyanarendra33@gmail.com

H. B. Bharath Kumar
e-mail: Bharathkumarhb16@gmail.com

R. K. Chaitra
e-mail: chaitra.rk98@gmail.com

1 Introduction

The iron and steel industries are an essential assets in the national economy. The mining industry, in particular, regularly contributes a great percentage of gross domestic product (GDP) in most of the countries. However, rapid industrialization has brought about a significant deterioration in the quality of our environment. The stockpiling of tailings (waste of mining) occupies land and results in deterioration of the surrounding environment. Moreover, due to strict current environmental laws, the industries have to pay the land expropriation fee, transportation fee, and landfill fee, which increase the production cost and cause the wastages of resources.

The tailing waste from iron mining industries has been found suitable as materials for cement preparation, glass–ceramic plates, foam glass, and manufacturing of building insulation material. It is mainly due to its lightweight, good thermal insulator, chemically inert and non-toxic, bacteria-resistant, water and steam resistant, and inexpensive to transport [1]. IOT is widely used in the fabrication of foam glass, which is used in construction and many other fields because of its unique combination of properties. The use of iron ore tailings in mortars will improve its bulk density and reduced the quantity of incorporated air and similarly improves mechanical properties. The iron ore that is of extremely fins or slimes having a diameter much less than one hundred fifty is not useful and, as a result, discarded. In India, 1500–2000 million heaps of such mined ore are lost as tailings [2]. The safe disposal or valorization of such massive mineral wealth within the forms ultra fins or slimes has remained a primary unsolved and challenging problem for the Indian iron ore industry. Kudremukh Iron Ore Company Limited (KIOCL) has been undertaking its mining operation on the region of 4604.55 ha within the western ghats. It results in a discarding of 150 million tons of IOT nearby the Bhadra Dam, India. This waste has volume-wise 79% of sand debris and 19% of silt debris. Which works as an excellent sand replacement for construction activities such as constructing blocks, paver blocks, stabilized mud blocks, paving tiles, etc. [2]. Basic properties of IOT, along with possible utilization in various fields, are presented in subsequent sections of this review article.

2 Physico-Chemical Properties of Iron Tailings

IOT is the mixture of compounds firstly present in protolith minerals introduced at the time of ore processing. It includes main components such as Al_2O_3 , CaO , MgO , SiO_2 , MnO , Fe_2O_3 , etc., and small parts such as Sulphur, Phosphorus, etc. However, the principal component of IOT is hematite [3, 4]. The details of the chemical constituent's properties are summarized in Table 1.

Physical properties containing specific gravity, water content, density, void ratio, loose bulk density, water absorption, fineness modulus are presented in Table 2. The size of IOT particle is between 0.7 and 0.15 mm [5], which usually seem inline dust

Table 1 Chemical properties (%) of IOT

References	SiO ₂	CaO	Fe ₂ O ₃	Al ₂ O ₃	MnO	MgO	S	P	SO ₃	Cl	Na ₂ O	K ₂ O	TiO ₂	Fe	AlO ₃	N ₂ O
[6]	72.79	6.85	2.20	6.08	0.085	5.16	0.1	0.16	-	-	-	-	-	-	-	-
[7]	68.94	3.45	14.54	3.64	-	3.77	-	-	0.75	0.01	-	-	-	-	-	-
[5]	43.56	10.80	15.02	11.11	-	7.32	-	-	-	-	2.41	0.74	3.21	-	-	-
[8]	2.30	0.09	-	-	0.08	0.06	-	-	-	-	-	-	-	59.8	4.52	-
[9]	42.90	12.97	7.51	10.75	-	7.10	-	-	9.04	0.10	-	1.96	-	-	-	2.06

Table 2 Physical properties of iron ore tailing

Reference	Specific gravity	Density (g/cm ³)	Moisture content (%)	Void ratio	Loose bulk density (kg/m ³)	Water absorption (%)	Fineness modulus
[10]	2.91	1.71	0.3	0.7	–	–	–
[11]	3.31	–	3.9	–	1816	2.29	–
[12]	3.33	–	6	–	–	3.97	2.545
[13]	3.51	–	0.22	–	1650	–	–

in the wind, which results in dust storms and causes the utmost air pollution. [5]. The properties of IOT are makes are widely accepting for utilization in various fields.

3 Utilization of Iron Tailings

IOT is the residue separated in the production of various products from the ore. The usage of these tailings, which are considered as waste, is a big challenge for Indian iron mining industry [12]. There are two or three stages of grinding of IOT, which is essential in the use of iron ore tailings as construction materials. The chemical properties of IOT are resembles to that of ceramic materials used in construction, tile industry, and glass [4].

IOT consists of non-metallic minerals and the right amount of aluminium and silicon, which are similar to other materials useful in the construction industry; hence, it can avail the prerequisite of the above applications. From bricks to other useful applications, IOT has reached tremendous results in the usage in building materials, manufacturing of blocks, preparing cement and concrete, and also road construction materials [14].

Based on morphology, physical and chemical properties of IOT utilization have been discovered by eminent researchers which are collectively presented in Fig. 1.

3.1 Concrete

When the natural aggregate is 100% replaced by IOT, the compressive strength and workability of the material decrease. When replacing the IOT for less than 40% of the natural aggregate with standards for 90 days, the control mix was found to be comparable with it the applied steam curing for two days increased the flexural strength by up to 8% and the compressive strength of the tailing mix decreased by 11% [15]. Since the particle size is more significant than cement, it can be used as fine aggregate to form ultra-high-performance concrete, and the hardness of the

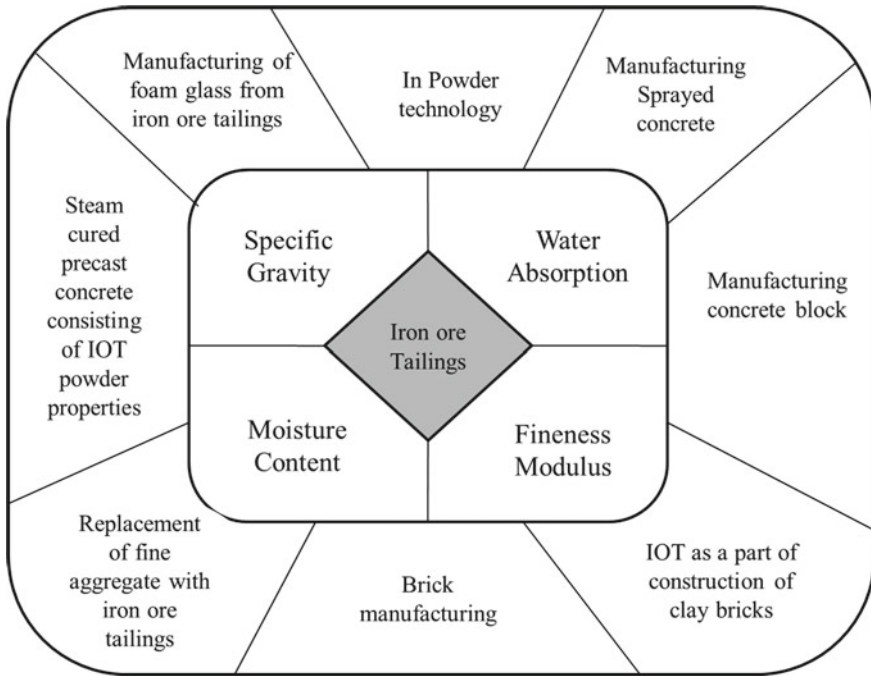


Fig. 1 Different aspects of IOT utilization

tailings observed lower than the natural sand. There is usually a strong bond between paste and aggregates and a useful link between compressive strength and porosity of Ultra-High-Performance Concrete (UHPC). Accordingly, it is inferred from the mechanical behavior of the tailings that it is possible to partially replace the iron ore tailings in natural sand to create Ultra-High-Performance Concrete (UHPC)[15].

In other research, concrete mixtures containing 25%, 50%, 75%, and 100% iron ore tailings as river sand was prepared with 0.5 water–cement ratios. Researchers work on to find the compressive and splitting tensile strength and toughness of this modified mix. They found that the IOT can be used as sand replacement in the concrete. According to the test performed, adding iron ore tailings to the concrete mix will increase the demand for water, and reduce the slump.

A concrete mix containing 25% iron ore tailings gives higher compressive strength than the reference concrete [16]. The results indicate that concrete workability decreased with a rise in the content of iron ore tailing-alccofine and that the average compressive strength was 70, 68.67, and 65Mpa at 40%, 30%, and 20%. Iron ore tailings of alccofine dosage varying the water–cement ratio of 0.35, 0.40, and 0.45, respectively. It can be used as a substitute for cement and sand because of inherent properties[11, 23].

3.2 Brick Manufacturing

There has been a lot of work and development currently in the manufacture of iron tailings building bricks. According to the literature, construction bricks can be manufactured using the hematite tailing. In one experiment, 84% of the total weight of tailings can be used in bricks, with a mass ratio of 84:10:6 that is tailing: clay: fly ash with forming water content of 12.5% and forming pressure found to be 20-MPa. The firing temperature was 980 °C for 2 h for good quality brick manufacturing [17]. The manufactured brick condition was similar to that of the Chinese fried common brick standard [22].

IOT containing high silicon is recycled in the red clay ceramic industry. By mixing iron ore tailings and two clayey materials in the range of 0–40% and 30%–70%. The resulting brick will have a compressive strength of 4.27MPa and 20.94% of water absorption. By the above property of brick, it will be better to use in sealing masonry, the bricks produced using iron ore tailings are considered as non-inert and non-dangerous and non-belligerent to the human health and also to the environment [17].

3.3 Concrete Block

Masonry is used in a wide range of construction work in a small and large structures. The inclusion of iron tailings and quarry dust in the present study indicates improved compressive strength without adjusting the water absorption. It is also said that it gives high compressive strength for 28 days of curing when only tailing is mixed. Building blocks created from mine waste are environmentally friendly as they use waste and reduce emissions from soil, land, and water. It is cost-effective too. When mines are converted into bricks, waste, and tailings will meet the demand for bricks in the metro cities [2].

3.4 Sprayed Concrete

Research has been done to compare the overall working performance of sprayed concrete with the same quantity of iron tailings replaced with natural sand. It is performed with different mix proportions of IOT. When 20% and 40% of iron tailing were replaced with natural sand, got, about C40 grade standard has been achieved. When 60% and 80% of iron tailing were replaced, natural sand got here to C30 grade standard. Then a compressive test was performed; the strength obtained was better than the natural sand. When sprayed concrete was replaced with 20% of IOT engineering requirements were achieved [7].

3.5 Precast Concrete is Steam-Cured Consisting of IOT Powder with Properties

Some experimental results show that the precast concrete constituted with 50% IOT powder shows the properties such as low chemically bound water content, low compressive strength, and low resistance to chloride ion permeability compared with Portland cement concrete. Very much alike beneficial properties of precast concrete are attained when using slag and combined mineral admixtures of IOT powder. By adding 50%, IOT powder with fly ash increases the permeability of precast concrete at 28 days. Precast concrete, when constituted along with slag and IOT powder, shows high resistance to chloride ion permeability [18].

3.6 Manufacturing of Foam Glass from Iron Tailings

Foam glass was ready, employing a higher content of iron tailing and waste glass with SiC powders used as the foaming agent. Experiments have been conducted on different phases of IOT combined with feldspar, hematite, kaolinite, and silica to manufacture foam glass. All are processed for 24.5 wt %, at 830 °C for 30 min accounted for the foaming mechanism. It comes as a material with a bulk density of 0.224 g/cm³ and flexural strength 0.53 MPa [1].

3.7 Powder Technology

3.7.1 Synthesis of Zeolite-Alpha by the Hydrothermal Method

Researchers have found out the IOT Zeolite-Alpha helps effectively softens hard water, which reduces calcium ion in water. The Zeolite-Alpha is prepared using synthesis techniques and the mixture; during alkali sintering at 850 °C IOT + Na₂CO₃ + Al₂O₃ was transformed to NaAlO₂, NaAlSiO₄, Na_{1.95}, Al_{1.95}Si_{0.05}O₄. Delicate polymerized aluminosilicates as a significant amount in distilled water. Zeolite-Alpha is obtained when the following circumstance: SiO₂/Al₂O₃ = 1.5, Na₂O/SiO₂ = 2.0, H₂O/Na₂O = 170 with the crystalline time of 24 h followed [19].

3.7.2 Synthesis of Magnetite Powder

IOT is also used for the synthesis of magnetite powder. The magnetite can be derived from solution FeCl₃ extracted from acid. The particle size of the magnetite determines magnetization. After NH₃ treatment, the tailing sample with a smaller particle size

can be collected. Iron ore tailings are subjected to HCl digestion to extract Fe_2O_3 and FeCl_3 . The FeCl_3 extracted is transformed into FeCl_2 , using NaH_4 as a reduction reagent. FeCl_2 is mixed in a molar ratio of 2:1 with the addition of an alkali solution to synthesize magnetite powder. The XRD analysis is in line with the magnetite phase formation [20]. From this, we may infer that magnetite of the correct quality can be prepared from iron ore tailings.

The IOT utilization to extract alumina from alumina rich IOT in India is also practiced. The yield percentage of iron values is currently limited to about 50%, and large quantities of residual waste are produced. Usage of the remaining iron ore tailings for the synthesis of useful products is essential. The chosen method for this process is called the leaching process [21]. The main research challenge is determining the genuinely organic and inorganic acids to accomplish the separation of iron value.

4 Conclusion

The manuscript has covered the broad-scale information, which helps the people know about the utilization potential of IOT. The formation process and properties of IOT provide the background and bases for alternative uses of iron ore tailings.

Iron tailings, although causing environmental pollution, it is the waste generated amid the removal of iron from iron ore. Utilizing IOTs in construction materials, bricks, zeolite synthesis, magnetite powder, sprayed concrete, precast concrete, foam glass will assure the reduction of environmental pollution. As we know, the entire natural resources have been ultimately used, and the awareness program for the protection of the environment has increased. Hence the possible ways to promote the efficiency of the use of IOT on a large scale are progressively growing.

The use of iron ore tailings as concrete aggregates will have positive effects on the environment for mining companies and mining communities. It would provide cheaper alternative materials to make concrete manufacturing profitable. This study evaluated the possible replacement of iron ore mine tailings produced. Appreciating the enormity of the environmental issue associated with iron ore, many have proposed new methods for using iron ore tailings for a quantitative reduction in the building industry as well as supplementing scarce conventional resources. Around 40% of replacing IOT in concrete, the result for the engineering requirement can be exceeded. In contrast, the possibility of preparing cementitious materials out of the resulted residue after iron recovery from iron ore tailings can be researched.

References

1. Yin H, Ma M, Bai J, Li Y, Zhang S, Wang F (2016) Fabrication of foam glass from iron tailings. *Mater Lett* 185:511–513. <https://doi.org/10.1016/j.matlet.2016.09.034>
2. Likhith NP, Manjunatha S, Manjunath SS, Shivakumar KM Hadimani, ShivakumaraB (2017) Manufacturing of building blocks by utilizing of iron ore tailings. *Int J Eng Sci Comput* 7(5):12274–12277
3. Mukhopadhyay S, Periyasamy M (2019) Next-generation technology for utilization of alumina rich iron ore tailings in India. *New Trends Prod Eng* 2(1):78–85. <https://doi.org/10.2478/ntp-2019-0008>
4. Zhang S, Xue X, Liu X, Duan P, Yang H, Jiang T, Wang D, Liu R (2006) Current situation and comprehensive utilization of iron ore tailing resources. *J Min Sci* 42(4):403–408
5. Li X, Wang P, Qin J, Liu Y, Qu Y, Liu J, Cao R, Zhang Y (2020) Mechanical properties of sintered ceramsite from iron ore tailings affected by two-region structure. *Constr Build Mater* 240:117919. <https://doi.org/10.1016/j.conbuildmat.2019.117919>
6. Nie YM, Xia MH, Zhang JX, Liu SX, Cui XC (2011) Experimental study of mineral polymer made from iron tailing. *Adv Mater Res* 168:730–733. <https://doi.org/10.4028/www.scientific.net/AMR.168-170.730>
7. Liu WY, Xu XL, An YY (2012) Study on the sprayed concrete with iron tailings. *Adv Mater Res* 347:1939–1943. <https://doi.org/10.4028/www.scientific.net/AMR.347-353.1939>
8. Mohanty M, Dhal NK, Patra P, Das B, Reddy PSR (2010) Phytoremediation: a novel approach for utilization of iron-ore wastes. *Rev Environ Contam Toxicol* 206:29–47. https://doi.org/10.1007/978-1-4419-6260-7_2
9. Ma BG, Cai LX, Li XG, Jian SW (2016) Utilization of iron tailings as substitute in autoclaved aerated concrete: physico-mechanical and microstructure of hydration products. *J Cleaner Produ* 127:162–171. <https://doi.org/10.1016/j.jclepro.2016.03.172>
10. Wan R, Kong D, Kang J, Yin T, Ning J, Ma J (2018) The experimental study on thermal conductivity of backfill material of ground source heat pump based on iron tailings. *Energy Build* 174:1–12. <https://doi.org/10.1016/j.enbuild.2018.06.010>
11. Bangalore Chinnappa G, Karra RC (2020) Experimental and statistical evaluations of strength properties of concrete with iron ore tailings as fine aggregate. *J Hazardous Toxic Radioactive Waste* 24(1):04019038. [https://doi.org/10.1061/\(ASCE\)HZ.2153-5515.0000480](https://doi.org/10.1061/(ASCE)HZ.2153-5515.0000480)
12. Kumar BS, Suhas R, Shet SU, Srishaila JM (2014) Utilization of iron ore tailings as replacement to fine aggregates in cement concrete pavements. *Int J Res Eng Technol* 3(7):369–376
13. Uchechukwu, EA, Ezekiel MJ (2014) Evaluation of the iron ore tailings from Itakpe in Nigeria as concrete material. *Adv Mater* 3(4):27–32. <https://doi.org/10.11648/j.am.20140304.12>
14. Bing L, Zhongying Z, Biao T, Hongbo L, Hanchi C, Zhen M (2018). Comprehensive utilization of iron tailings in China. *IOP Conf Series Earth Environ Sci* 199(4):042055. <https://doi.org/10.1088/1755-1315/199/4/042055>
15. Zhao S, Fan J, Sun W (2014) Utilization of iron ore tailings as fine aggregate in ultra-high performance concrete. *Constr Build Mater* 50:540–548. <https://doi.org/10.1016/j.conbuildmat.2013.10.019>
16. Shettima AU, Hussin MW, Ahmad Y, Mirza J (2016) Evaluation of iron ore tailings as replacement for fine aggregate in concrete. *Constr Build Mater* 120:72–79. <https://doi.org/10.1016/j.conbuildmat.2016.05.095>
17. Chen Y, Zhang Y, Chen T, Zhao Y, Bao S (2011) Preparation of eco-friendly construction bricks from hematite tailings. *Constr Build Mater* 25(4):2107–2111. <https://doi.org/10.1016/j.conbuildmat.2010.11.025>
18. Han F, Song S, Liu J, Huang S (2019) Properties of steam-cured precast Concrete containing iron tailing powder. *Powder Technol* 345:292–299. <https://doi.org/10.1016/j.powtec.2019.01.007>
19. Zhang C, Li S (2018) Utilization of iron ore tailing for the synthesis of zeolite a by hydrothermal method. *J Mater Cycles Waste Manage* 20:1605–1614. <https://doi.org/10.1007/s10163-018-0724-7>

20. Sakthivel R, Vasumathi N, Sahu D, Mishra BK (2010) Synthesis of magnetite powder from iron ore tailings. *Powder Technol* 201(2):187–190. <https://doi.org/10.1016/j.powtec.2010.03.005>
21. Sudipta M, Muthaimanoj P (2019) Next generation technology for utilization of alumina rich iron ore tailings in India. *Indian Instit Eng Sci Technol Shibpur, West Bengal, India* 2(1):78–85. <https://doi.org/10.2478/ntpe-2019-0008>
22. GB/T5101–2003 (2018) National Standard of People’s Republic of China. Standard Press of China.
23. IS 12269–9 (2013) Specification for 53 Grade Ordinary Portland. Bureau of Indian Standards

Sustainable Landfill Site Selection for Construction and Demolition Waste Management Using GIS and AHP



Bhoomi Shah 

Abstract The generation of Construction and Demolition (C&D) waste, which forms 30% of total Solid Waste, adds to the non-biodegradable component of inert waste. Majorly produced by the construction industry, this waste has a recycle value for the same industry. By proper fragmentation, treatment and disposal/recycle, demolition debris has a huge scope for application in landfilling or building non-structural elements like pavement blocks. But the current practice of mixed waste collection and disposal does not explore this potential of C&D waste. The city of Greater Mumbai is facing a crisis due to the limited availability of appropriate wasteland within the city. The authorities have stalled any new construction projects due to lack of operational dump sites. With a view to have separate landfill sites for C&D waste, and to identify the sites that could be available for the next 20–25 years, spatial analysis has been carried out in this study using ArcGIS. The criteria used for mapping sites include the buffer distance from water bodies, wells, forests, residences, heritage sites, airport, and roadways and site area. Site selection results have been processed further using Analytical Hierarchy Process (AHP) to identify and prioritize the limited number of sites that could be developed for future demands. This study would help town planning departments to identify land for waste processing and collection centers in other congested cities of India which are major contributors to Solid Waste.

Keywords Sustainability · Circular economy · Landfilling · Analytical hierarchy process

B. Shah (✉)
BITS Pilani, Rajasthan 333031, India
e-mail: h20180046@pilani.bits-pilani.ac.in

1 Introduction

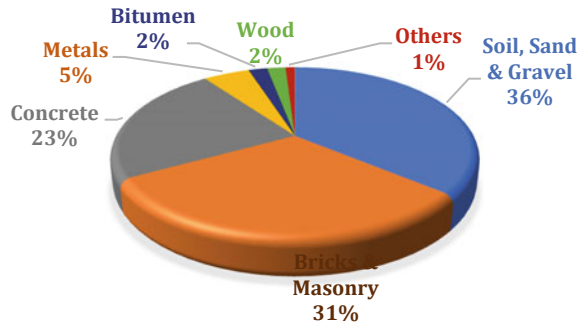
The megacity of Mumbai with a population of 13 million produces approx. 9000 MT/D of Solid Waste (SW) which is predicted to increase five-fold to 45,000 MT/D in 2041 corresponding to population growth [11]. The landfill sites currently in operation at Mulund and Deonar are packed to their full capacity. Kanjurmarg bio-reactor landfill site can process only 3000 MT/D of SW [10]. Supreme court has stalled any new construction activity in Greater Mumbai city due to the inability of local authority, i.e., MCGM to deal with and safely dispose the Solid Waste and Construction and Demolition debris. The imposed ban will continue until new Construction waste disposal sites are operational. Since construction activities are a direct generator of Construction and Demolition (C&D) waste, proper waste disposal operations including on-site processing and recycling, collection, transportation of remnants, treatment and landfilling need to be systematically planned. In order to emphasize on separate handling of Construction waste, C&D Waste Management Rules, 2016, have been formulated by Ministry of Environment, Forest and Climate Change (MOEF&CC). The ability to recycle and reuse such material requires technologically advanced methods. There is a wide scope for utilizing the recycled material in non-structural concrete, paver blocks, lower layers of road pavements, colony and rural roads, etc., which needs to be explored to form a circular economy of materials used in the construction industry. This study was undertaken to fulfil the following objectives-

- To identify suitable disposal sites for Greater Mumbai region taking into account the constraints set by MOEF&CC in Construction and Demolition Waste Management rules, 2016.
- To obtain ranking of the suitable sites for a sustainable Waste Management plan

Out of the total Solid Waste handled by Municipal Corporation of Greater Mumbai (MCGM), 30% is C&D waste which amounts to 2700 tons per day [12]. According to the C&D Waste Management Rules, 2016 [9], 'Every waste resulting from construction, re-modelling, repair and demolition of any civil structure of an individual or organization or authority' comes under the category of C&D waste. Brick bats, concrete, excavated earth, boulders, topsoil, metal and plastics, cellulosic materials, timber, lumber, roofing and sheeting scraps, crop residues, rubble, broken concrete, plaster, conduit pipes, wire, insulation, etc., are considered to be C&D waste as per National Building Code, Vol. 2, 2016 (Fig. 1). There is huge economic potential in bridging the construction materials demand-supply gap by recycling and reusing C&D waste as per Central Road Research Institute and Central Research Board [8].

Among all Multicriteria decision-making techniques, Ding et al. [3] state that AHP is effective in identification and ranking of suitable sites in a given region. Criteria selection based on regulations considering environmental, social and economic aspects has been implemented in landfill site selection. Karimi et al. [4] have applied a combination of AHP and GIS to select municipal landfill sites in Iran. The buffer distances and slope criteria maps were overlaid and standardized using fuzzy theory

Fig. 1 Typical C&D waste composition in India. *Source* Toolkit on C & D waste management rules-2016 [12]



followed by AHP to obtain landfill suitability map. A GIS-based study for locating potential landfill sites has been carried out by Colvero et al. [1] for the Goias county in Brazil. The study by Chang et al. [5] used GIS tool to identify candidate sites for landfilling based on buffer distances decided by previous studies. Fuzzy Multi-criteria Decision Making (FMCDM) was applied followed by a sensitivity analysis by Monte Carlo technique, to find the pros and cons of developing potential sites in Harlingen, South Texas. Fuzzy preference ratings were given based on the opinion of two planning experts. Rajiv Gupta et al. [6] made use of GIS tools and Fuzzy Analytical Hierarchy Process (FAHP) to rank sites for the installation of solar plant in Rajasthan state, India.

The current study is similar in terms of the tools applied. The results obtained would be useful to prioritize suitable landfill sites for C&D waste disposal, treatment, and recycling facility development.

2 Materials and Methods

For fulfilling the objectives of this study, it was required to identify available Solid Waste disposal sites subject to the constraints for developing disposal sites as laid down by the MOEF&CC. These are the criteria for site selection for Storage and Processing or Recycling Facilities for Construction and Demolition Waste mentioned under Rule 7(1) of C&D Waste Management Rules, 2016 given in Table.1 as buffer distances.

Project Phase-1: The identification of sites was done using ArcGIS 10.2, which is a Geographic Information System (GIS) tool developed by ESRI. The features as images and co-ordinates data, which geographically represent the criteria with regard to the construction of landfills, were obtained from the below sources (Table 2):

The restriction values in Table 1 were then applied to these criteria to obtain vector feature maps. All maps were produced in WGS 1984 coordinates. Next, criteria feature maps were created using buffer tool and providing the distances in

Table 1 Restrictions on the construction of landfills in India

Sr. No.	Restricted areas	Distance of buffer zone
1	Flood plains as recorded for past 100 years, CRZ, wetlands, critical habitat and eco-fragile areas	Permitted 100 m beyond HTL (CRZ regulation 2011)
2	Airport or airbase (NOC required)	10 km
3	Habitation clusters, highways	200 m
4	Forest areas, parks	200 m
5	Ponds, water supply wells	200 m
6	Rivers	100 m
7	Ground water table less than 2 m below GL	Not permitted
8	Heritage sites	500 m
9	'No development' buffer zone within selected site	500 m

Source Construction and Demolition Waste Management Rules, 2016, MOEF&CC, Govt. of India

Table 2 Geographical features as per the criteria for site selection and the data sources

Sr. No.	Feature	Data type	Data Source
1	Lakes, rivers, Forests, habitation zones	Image	Website on Mumbai Data developed by Akshay Kore
2	Airport and airbase, highways	Image	Google Earth
3	Wells, spots with GW less than 2 m below GL	Coordinates	India- WRIS (Water Resource Information System)
4	High tide line	Image	Maharashtra Remote Sensing Application Centre Coastal Zone Studies 2006
5	Heritage sites	Coordinates	Google Earth

Table 1 as input. The erase tool was used to eliminate the area within the buffer from the remaining area. Lastly, an overlay map (Fig. 2a) of all the criteria feature maps applied together was created. The void areas obtained thus became the sites suitable for landfill development. Taking only the significant areas into consideration, a final map (Fig. 2b) showing all the suitable sites thus obtained was created. The area measurement tool was used to measure the areas of each individual polygon shapefile from the suitable sites map (Fig. 2b). Along with the distances measured from highways, Table 3 shows the areas of each site.

Project Phase-2: The suitable sites were ranked based on their proximity from the features used as criteria and the area of site for selection. The Analytical Hierarchy Process (AHP), developed by Thomas Saaty [7], is a discrete multicriteria decision making process of relative ranking on absolute scales of criteria based on expert judgment. It converts the set of unrelated criteria into a system of priorities

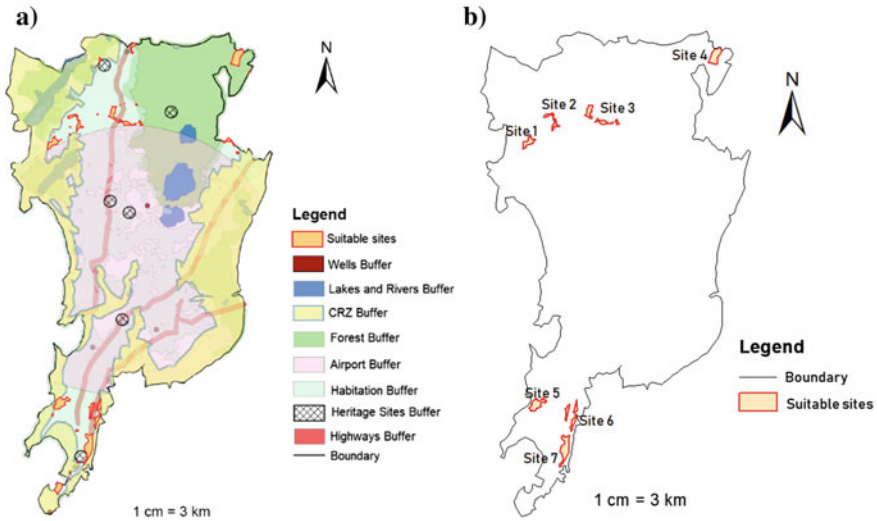


Fig. 2 a Overlay map combining all criteria feature vectors. b Map of 7 identified sites in Mumbai

Table 3 Geometrical area and distance from highways of each of the seven sites

Site No.	Area (in Ha)	Distance from road (km)
1	43	2.5
2	33	2.0
3	63	0.2
4	85	8.0
5	73	1.0
6	63	0.2
7	102	0.25

thus, reducing the problem to one-dimension. The AHP ranking of selected criteria was done on Expert Choice 11.1 software. With the objective of maximizing the appropriateness of site subject to criteria constraints, pairwise comparison was made in 2 steps: **Step 1.** Relative importance of criterion *i* in comparison with criterion *j* for each criteria pair (*i, j*). **Step 2.** Relative preference of alternative *n* in comparison with alternative *m* for each criterion *k*.

These comparisons were in the form of numerical values as per Saaty’s scale designed for AHP. The inconsistency ratio (IC) was noted to be less than 0.1 throughout the expert decision-making process. It is a measure of how inconsistent the judgements have been relative to large samples of purely random judgements.

The ranking of criteria (1–9 grades) was done by concentrating on any two criteria at a time taken from 3 experts. For example, heritage sites were considered to be more important (moderate plus-4.0) than Residential zones as they attract tourists and are historical markers of the country. To avoid aesthetical impairment and to maintain

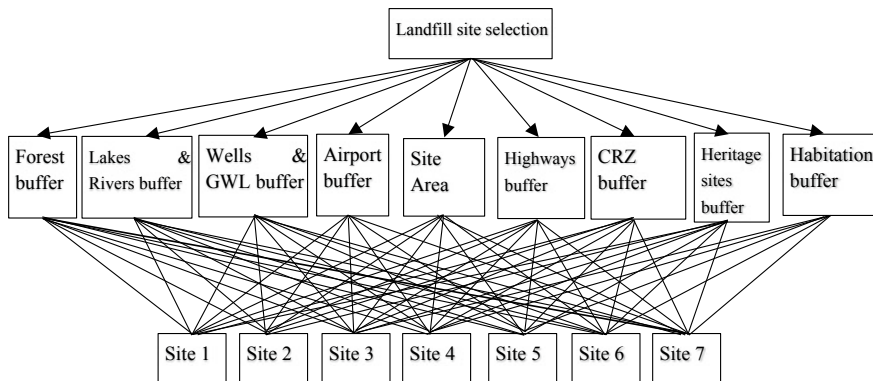


Fig. 3 Description of the hierarchy of the decision-making process

such places odor free, dump sites must be located far from them [5]. CRZ buffer and forest buffer were given equal importance as both serve as ecologically active zones. The normalized weights for the criteria were generated by the software based on the comparison matrix (Fig. 3).

For comparing the relative preference of a pair of sites with respect to a particular criterion, 1–9 grades were entered in the matrix. A check of inconsistency (<0.1) was made for each of the nine matrices. For example, based on the distance from CRZ, site 2 is moderately more important than site 1. Similarly, sites 5 and site 6 are equally important in terms of CRZ since they are equidistant from the buffer line.

3 Results and Discussion

The sites obtained are suitable since they meet all the criteria as per norms for waste disposal sites. As per opinion of experts, wells and ground water level are found to be the most important criteria affecting site selection, the least important being proximity to residential zone. This is same as the ranking taken by Karimi et al. [4] and Debishree et al. [2] for MSW. Upon synthesis based on the goal of site selection, the first three are most suitable sites and cover 260 ha, 0.59% of the total area of Mumbai city, similar to the result obtained by Ding et al. [3]. The evaluation of the results indicates that site 4 of 85 ha area ranked first in suitability (See Fig. 4) even though it is away from transportation network. Since the criteria for distance from highway had lower weight, validated as per study by Karimi et al., such a result was obtained.

Priority list of sites to be developed in future indicated that site 4 could be developed first followed by site 7, site 5, site 6, site 3, site 2, and site 1, in that order.

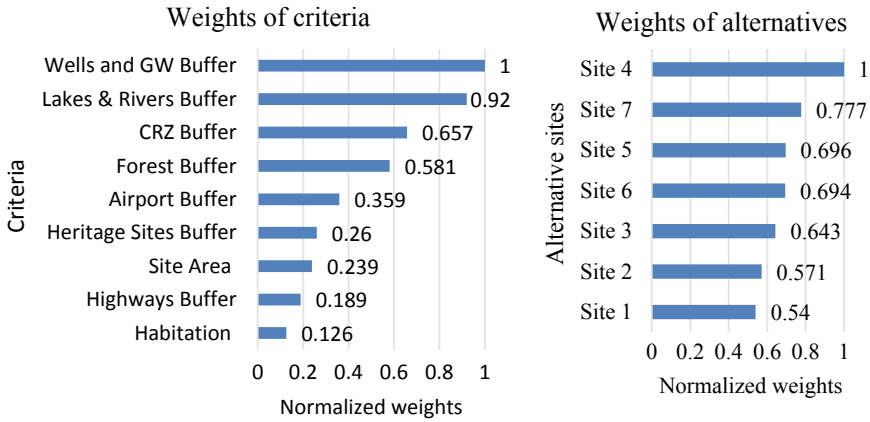


Fig. 4 Ranking and weightages obtained for seven alternative sites based on criteria weights

4 Conclusion

This study provides us with the sites which abide by the norms. The largest existing dump site in Mumbai is at Kanjurmarg of 141 ha area but only 66 ha is useable as the remnant portion does not comply with CRZ norms. The areas of first three sites are greater than 66 ha and hence are considered to serve the purpose of C&D waste disposal for next 20–25 years. The results obtained are useful as they provide sustainable sites and indicate the basis for their selection. Also, obtaining a priority list broadens the vision of town planners by giving a sustainable solution to the issue of waste disposal.

Road network connectivity must be ensured to avoid transportation issues. The ‘Not in my backyard’ syndrome comes into picture if public nuisance is created due to landfill site in a residential neighborhood. Though C&D waste is odorless inert material, its processing will produce noise. The site can be developed by keeping 500 m buffer within the boundary. Segregation of C&D waste from other MSW must be practiced if we are to make economical use of this material resource. With the help of technology in treatment, reuse and recycle of C&D waste, a major portion of the waste material will find its proper utility in the construction of less important structures, minor roads, filler material, and making paver blocks. Further reduction in waste production is possible if such technology is applied on-site itself.

This study has limitations that can be addressed in the future research. If any change occurs in the criteria weights, the decision taken is bound to change. Many factors affecting the landfill site selection are yet to be considered in this model. Site slope, soil conditions, land-use pattern, noise produced in recycling plant are few criteria which need consideration. Also, the criteria weights are calculated based on experts’ opinions.

References

Papers

1. Colvero DA, Gomes AP, Tarelho LA, Matos MA, Santos KA (2018) Use of a geographic information system to find areas for locating of municipal solid waste management facilities- Brazil, Goiás county. *J Waste Manage.* <https://doi.org/10.1016/j.wasman.2018.04.036>
2. Khan D, Samadder SR (2015) A simplified multi-criteria evaluation model for landfill site ranking and selection based on AHP and GIS. *J Environ Eng Landscape Manage* <https://doi.org/10.3846/16486897.2015.1056741>
3. Ding Z, Zhu M, Wang Y, Zhu J (2018) An AHP-GIS based model of C&D waste landfill site selection: a triangulation of critical factors. In: *Proceedings of the 21st international symposium on advancement of construction management and real estate*. Springer, Singapore, pp 163–174
4. Karimi H, Amiri S, Huang J, Karimi A (2019) Integrating GIS and multi-criteria decision analysis for landfill site selection, case study: Javanrood County in Iran. *Int J Environ Sci Technol* 16(11):7305–7318
5. Chang N, Parvathinathan G, Breeden JB (2008) Combining GIS with fuzzy multicriteria decision-making for landfill siting in a fast-growing urban region. *J Environ Manage* <https://doi.org/10.1016/j.jenvman.2007.01.011>
6. Gupta R, Puppala H, Shalini K, Integrating fuzzy AHP and GIS to prioritize sites for the solar plant installation. In: *12th international conference on fuzzy systems and knowledge discovery (FSKD)*
7. Saaty TL, *The analytic hierarchy process*. In: *Agricultural economics review*, 70. McGraw Hill, New York

Reports

8. Management of construction and demolition waste in India working subgroup report. Ministry of Housing and Urban affairs, GOI., 16th Apr. (2009).
9. Construction & demolition waste management rules. Ministry of Environment, Forest and Climate change, Govt. of India (2016)
10. Maharashtra Pollution Control Board Annual Report 2016–2017 on Implementation of Municipal Solid Waste management Rules (2016)
11. Construction & Demolition and De-silting waste (management and disposal) Municipal Corporation of Greater Mumbai guidelines (2006)
12. NPC India CD-Waste-Management-ToolKit-2017. <https://www.npcindia.org.in>

Stationary Source Emissions and Impact Assessment on Ambient Air Quality: A Case Study of Delhi Region



Debarshi Ghosh and Madhuri Kumari

Abstract Establishing equilibrium in atoms of various pollutants in atmosphere is the prime objective of environmental policies set by the governing bodies. The industries abide to environmental norms and regulations essential to control air pollution from stationary sources. Among wind, vehicle movement and industry, the latter is a major contributor to air pollution that necessitates regular monitoring. Through this study, we have attempted to analyse the contribution of stationary sources of industries to the air pollution in Delhi. The comparative study before and after nationwide lockdown due to Covid19 pandemic provides an insight into the role of organised and unorganised industry in air pollution emission. This paper portrays the decrease in air pollutants because of temporary shutdown of unorganised industry with stack emissions. However, the organised industries like power generating sector remained functional and continued to add air pollutants. This study on air pollution during lockdown contemplates an urgency to formulate provisions that will force the industries to adhere to air emission monitoring and standards. Due to restrictions of industry, the challenges persist in the detail study of combustion and plume discharge. The future scope of this study is to quantify the contribution of plume discharges from organised and unorganised industries and conduct detailed analysis of stationary sources emissions due to combustion.

Keywords Impact assessment · Air quality · Stationary source emissions · Covid19

1 Introduction

A major part of air pollution results from organised and unorganised industries through stationary source emissions. Emission from the industries is a result of combustion of various sources of fuel that emits greenhouse gases like carbon dioxide, methane, nitrous oxide and also fluorinated gases that trap heat from the sun

D. Ghosh (✉) · M. Kumari
Department of Civil Engineering, Amity School of Engineering and Technology, Noida, Uttar Pradesh, India
e-mail: debarshi.ghoshjbl@gmail.com

© The Author(s), under exclusive license to Springer Nature Singapore Pte Ltd. 2021
R. Al Khaddar et al. (eds.), *Advances in Energy and Environment*, Lecture Notes in Civil Engineering 142, https://doi.org/10.1007/978-981-33-6695-4_14

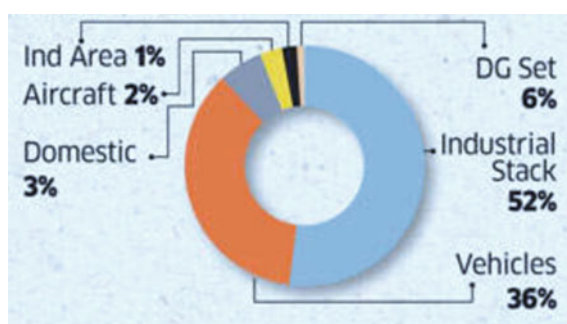
143

and atmosphere causing global warming [1]. This creates a cycle where air pollution contributes to climate change and climate change creates higher temperatures, in turn, higher temperature intensifies some types of air pollution. The air pollution leads to smog formation because of high heat and increased level of ultraviolet radiation. Smog reduces visibility, irritates the phalanx, irritate the eyes and causes respiratory distress. The conversion of $\text{NO}-\text{NO}_2$ is a major factor of smog formation. The power plants and factory emissions are one of major sources of nitrous oxide. The reaction of sunlight with oxides of nitrogen and volatile organic compounds causes the formation of ground level ozone. The deposition of oxides of nitrogen leads to acidified terrestrial and aquatic ecosystem. The consequence of which is loss of plant or fish population and change in biodiversity. The particulate matter in atmosphere causes severe alteration in natural nutrient and chemical balance of soil, air and water. National Ambient Air Quality Standards have specified standard and guidelines for monitoring the industrial emissions. Air being a transboundary element is subjected to permissible limits of being contaminated by industries, and the lack of research in the field of combustion, keep us unaware of the various unknown particles emitted from the stationary source of pollution, i.e. stack, from the industries. The comparative study before and after nationwide lockdown due to Covid19 pandemic provides an insight into the role of organised and unorganised industry in air pollution emission.

2 Study Area

Delhi NCR region is situated along the $28^\circ 24' 17''$ and $28^\circ 53' 00''$ North and longitudes of $76^\circ 50' 24''$ and $77^\circ 20' 37''$ East. The Union Territory shares borders with the States of Uttar Pradesh and Haryana with 51.90 km as maximum length and 48.48 km wide. Through many reports and news article [2, 3], the air pollution level of Delhi has been reported to be much beyond the permissible limit. A study, conducted by IIT Kanpur [4], reported that NO_x emissions are far higher at 312 tonnes per day with industrial stack accounting for 52% (Fig. 1).

Fig. 1 NO_x emissions in Delhi



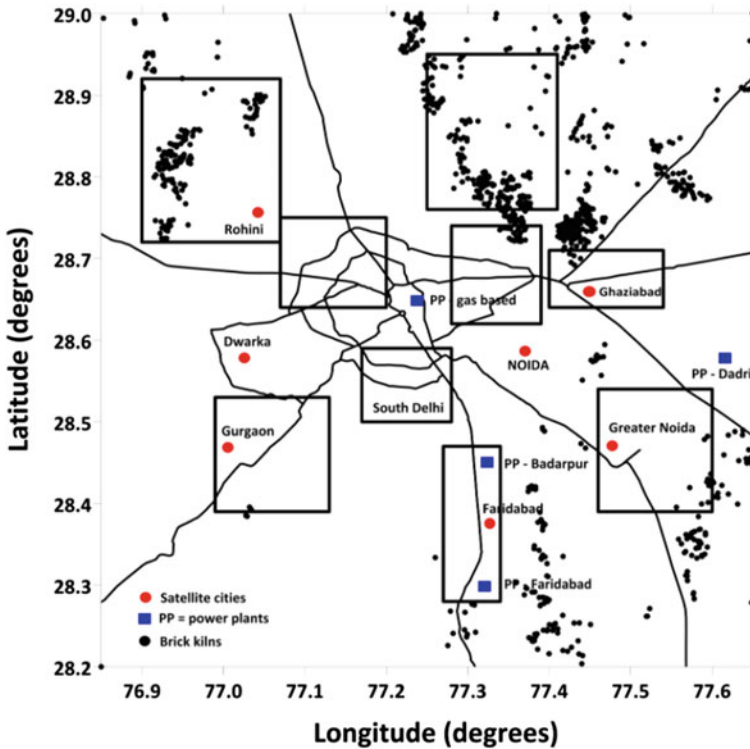


Fig. 2 Delhi and NCR region with kilns and power plants. *Source* urbanemission.info

To understand the air pollution in Delhi region, we have to consider the source of pollutions around and outside the administrative boundary of Delhi [5]. Figure 2, depicts Delhi and satellite cities with road network and location of brick kilns and power plants that are major source of NO_x emissions.

3 Ambient Air Quality of Stationary Sources

3.1 Plume Chemistry

Sulphur and Nitrogen are being major pollutants from the stationary source of air pollution. Oxidation in atmosphere is the initial reaction of these elements [6, 7]. The rate of oxidation determines the elements they react with and the products formed in gaseous phases and aqueous phase. Power stations use fossils fuels as energy source. Detail reactions study during the combustion of these fossil fuels is a major

challenge. However, the major pollutants detection and the effect of photolysis have proven to be of significance in the study of stack emission phenomenon.

Ozone layer depletion is a major cause of NO_x concentration. The water vapour present in atmosphere plays a critical role in heterogeneous oxidation of SO_2 emitted from the plume [8]. The water vapour present in the atmosphere determines the rate of change of SO_2 from one state to another and condensation to form aerosols of sulphate. Acid deposition and environmental acidification are two major contribution of SO_2 oxidation [9].

3.2 Sulphur Dioxide Chemistry in Atmosphere

Out of the total sulphur content in coal, 90% is emitted into the atmosphere as sulphur dioxide after combustion process. The reactions of sulphur dioxide in the atmosphere lead to formation of sulphur dioxide and sulphur trioxide. This sulphur dioxide mixes with water vapour and form acid rain, which is the sulphuric acid formation.

Water present in air leads to an aqueous solvent oxidation. With the ionic products of the SO_2 , it can dissolve itself in water for establishing equilibrium. Due to this establishment of equilibrium in the aqueous phase, sulphite ions (SO_2^{3-}), bisulphite ions (HSO_3^-) hydrated SO_2 ($\text{SO}_2 \cdot \text{H}_2\text{O}$) are found. NO_2 concentration being high in the emission point of stack leads to formation of $\text{O}^3(\text{P})$ by photo-dissociation process. This results in higher rate of SO_2 oxidation. But this rate of reaction decreases instantly as the dilution of plume takes place by air flow. Table 1 provides the list of chemical reactions of sulphur dioxide with atmospheric gases and sunlight [9].

Table 1 List plume gas reactions in atmosphere

Reaction	$-\Delta H^\circ$ (kJ mol ⁻¹) 25 °C	k (cm ³ molec ⁻¹ s ⁻¹)
$\text{O}_2(^1\text{A}_g) + \text{SO}_2 \rightarrow \text{SO}_4$ (biradical)	105	} 3.9×10^{-20}
$\text{O}_2(^1\text{A}_g) + \text{SO}_2 \rightarrow \text{SO}_4$ (cyclic)	~ 117	
$\text{O}_2(^1\text{A}_g) + \text{SO}_2 \rightarrow \text{SO}_3 + \text{O}^3(\text{P})$	- 56.5	
$\text{O}_2(^1\text{A}_g) + \text{SO}_2 \rightarrow \text{SO}_2(^1\Sigma_g^-) + \text{SO}_2$	94	
$\text{O}_2(^1\Sigma_g^-) + \text{SO}_2 \rightarrow \text{SO}_4$ (biradical)	167	} 6.6×10^{-16}
$\text{O}_2(^1\Sigma_g^-) + \text{SO}_2 \rightarrow \text{SO}_4$ (cyclic)	180	
$\text{O}_2(^1\Sigma_g^-) + \text{SO}_2 \rightarrow \text{SO}_3 + \text{O}^3(\text{P})$	6.3	
$\text{O}_2(^1\Sigma_g^-) + \text{SO}_2 \rightarrow \text{SO}_2 + \text{O}_2(^1\text{A}_g)$	62.8	
$\text{O}^3(\text{P}) + \text{SO}_2(+\text{M}) \rightarrow \text{SO}_3(+\text{M})$	347	5.7×10^{-14}
$\text{SO}_3 + \text{SO}_2 \rightarrow \text{O}_2 + \text{SO}_4$	241	$< 8 \times 10^{-24}$
$\text{NO}_2 + \text{SO}_2 \rightarrow \text{NO} + \text{SO}_3$	41.4	8.8×10^{-30}
$\text{NO}_3 + \text{SO}_2 \rightarrow \text{NO}_2 + \text{SO}_3$	136	$< 7 \times 10^{-21}$
$\text{ONOO} + \text{SO}_2 \rightarrow \text{NO}_2 + \text{SO}_3$	~ 126	$< 7 \times 10^{-21}$
$\text{N}_2\text{O}_5 + \text{SO}_2 \rightarrow \text{N}_2\text{O}_4 + \text{SO}_3$	100	$< 4 \times 10^{-23}$
$\text{HO}_3 + \text{SO}_2 \rightarrow \text{HO} + \text{SO}_3$	69.9	
$\text{HO}_2 + \text{SO}_2(+\text{M}) \rightarrow \text{HO}_2\text{SO}_2(+\text{M})$	29.3	$< 1 \times 10^{-18}$
$\text{CHO}_2 + \text{SO}_2 \rightarrow \text{CHO}_2\text{O} + \text{SO}_3$	~ 113	$< 1 \times 10^{-18}$
$\text{CHO}_2 + \text{SO}_2(+\text{M}) \rightarrow \text{CHO}_2\text{SO}_2(+\text{M})$	~ 130	$\sim 1.4 \times 10^{-14}$
$(\text{CH}_3)_2\text{CO}_2 + \text{SO}_2 \rightarrow (\text{CH}_3)_2\text{CO} + \text{SO}_3$	~ 109	
$(\text{CH}_3)_2\text{CO}_2 + \text{SO}_2 \rightarrow (\text{CH}_3)_2\text{CO}_2\text{SO}_2$	~ 126	$< 7.3 \times 10^{-19}$
$\text{CHO}_2\text{COO}_2 + \text{SO}_2 \rightarrow \text{CH}_3\text{CO}_2 + \text{SO}_3$	~ 138	
$\text{CHO}_2\text{COO}_2 + \text{SO}_2 \rightarrow \text{CH}_3\text{COO}_2\text{SO}_2$	~ 155	$< 7 \times 10^{-19}$
$\text{HO} + \text{SO}_2(+\text{M}) \rightarrow \text{HOSO}_2(+\text{M})$	~ 155	1.1×10^{-12}
$\text{CHO}_2 + \text{SO}_2(+\text{M}) \rightarrow \text{CH}_3\text{OSO}_2(+\text{M})$	~ 100	$\sim 5.5 \times 10^{-13}$
$\text{SO}_3 + \text{H}_2\text{O} \rightarrow \text{H}_2\text{SO}_4$	24.8	9.1×10^{-13}

3.3 Oxides of Nitrogen Chemistry in Atmosphere

The production of oxides of nitrogen ($\text{NO} + \text{NO}_2 \rightarrow \text{NO}_x$) is about 21–25 Tg NO_x every year. NO and NO_2 are emitted due to combustion process in power plants. The percentage of NO emitted during the high temperature combustion is 95% and NO_2 is 5%. During low atmospheric temperature, in places with high pollution concentration rapid oxidation of NO and NO_2 occur due to simultaneous reaction with atmospheric Oxygen. This occurs when the oxidants such as O_3 , HO_2 , OH and RO_2 are produced by photochemical reaction. This leads to the smog formation in the atmosphere at lower level. Acid deposition, acid rain and ozone formation in troposphere layer of the atmosphere are the significant hazards to human health and environment due to presence oxide of nitrogen. Nitric acid remains suspended in gas phase due to its volatile nature. The ammonium nitrate forms aerosol droplets at moderate humidity.

4 Air Quality Comparison Before and After Lockdown in Delhi Region

Through this study, we have attempted to analyse the contribution of stationary sources of industries to the air pollution in Delhi. The comparative study before and after nationwide lockdown due to Covid19 pandemic provides an insight into the role of organised and unorganised industry in air pollution emission.

The observation of one-month period from 16 March to 15 April 2020 as published by CPCB was used for the analysis [10]. The lockdown in our country was declared on 21 March 2020 and the period before this was taken as pre-lockdown and period after this date was considered as lockdown period. Several parameters were monitored in order to study the air quality of the capital city Delhi. Monitoring stations recorded a drastic change in the major pollutants of the atmosphere covering the city.

$\text{PM}_{2.5}$, PM_{10} and Nitrogen oxides were monitored and studies about to know the reduction of its level. The decrease in $\text{PM}_{2.5}$ is observed to be 46%, while PM_{10} is recorded to reduce its concentration by 50% due to this immediate pause of all outdoor activities in the city. The CO level is observed to be reduced by 37% during lockdown compared to the percentage observed pre lockdown. A considerable reduction of 56% was observed in NO_2 level. The NO_2 % decrease in the atmosphere with in the first 20 days lockdown is recorded to reduce by 75% with 24-h observation by standards set for monitoring of air quality. However, the SO_2 level drop is comparatively less as power plant industries continued operation due to the necessity is recorded to 19% in reduction. This drop in the SO_2 emission is also due to the adaptation of less polluting industry fuels such as biogas. The benzene reduction is observed to reduce by 47%. The lowest pollutant emission parameters recorded on 24-h basis are $39 \mu\text{g}/\text{m}^3$ of PM_{10} , $24 \mu\text{g}/\text{m}^3$ of $\text{PM}_{2.5}$, $15 \mu\text{g}/\text{m}^3$ of NO_2 and $10 \mu\text{g}/\text{m}^3$ of SO_2 . Figure 3 presents the comparison of various pollution parameters for pre and post lock down period in Delhi region.

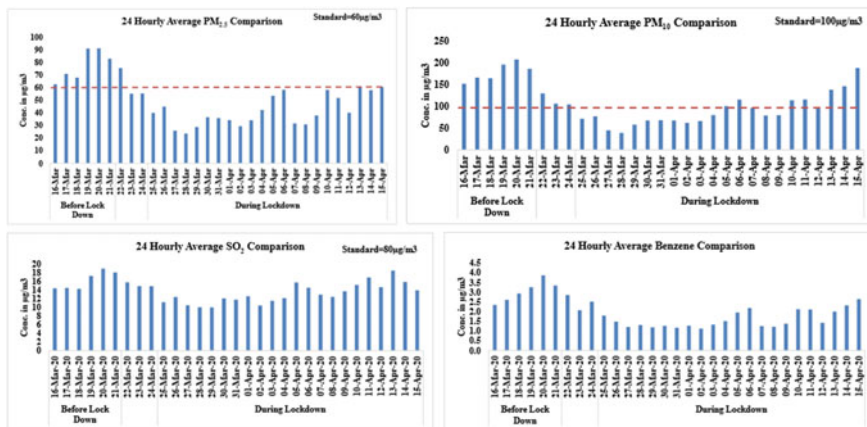


Fig. 3 24-hourly average comparison of air pollution parameters (PM_{2.5}, PM₁₀, SO₂, Benzene) for one month (16 March to 15 April 2020) in Delhi region

Because of close down of unorganised industrial activities like brick kilns along with vehicle movement led to a significant improvement in air quality.

The graph in Fig. 4 depicts the hourly concentration of PM_{2.5} and PM₁₀ for prelockdown phase 16 March 2020 to 21 March 2020 and the lockdown phase from 25 March 2020 to 15 April 2020.

A major observation recorded with respect to the PM₁₀ is that the maximum concentration amount pre-lockdown days were 244 µg/m³ at 22:00 h which declined to 127 µg/m³ and the minimum concentration amount pre-lock down was calculated to be 118 µg/m³ at 17:00 h which declined to 63 µg/m³ during the lockdown phase. For PM_{2.5}, maximum concentration pre-lockdown phase was 114 µg/m³ at 08:00 h, which was recorded to drop to 21 µg/m³ at 17:00 h during the lockdown phase. Due to restriction over the industrial activities, the maximum concentration of benzene was reduced to 49% and the minimum value was recorded to reduce by 50%. However, the SO₂ concentration was recorded to have the least reduction rate of 14% as the power plants were operational.

5 Impact Assessment

Urbanisation has accelerated the rise of industries with increase in air pollution, water pollution and fresh water scarcity and solid waste generation. The industries and vehicular movement is a major contributor of air pollution. More than 50% of SO₂ and NO_x emissions in Delhi are attributed by stationary source emissions of organised and unorganised industries. Air pollutants are majorly causing acid rain, toxic cloud formation, reduction in visibility, entrapment of heat which is further leading to the alteration of biodiversity, degradation in quality of plants, and materials. The

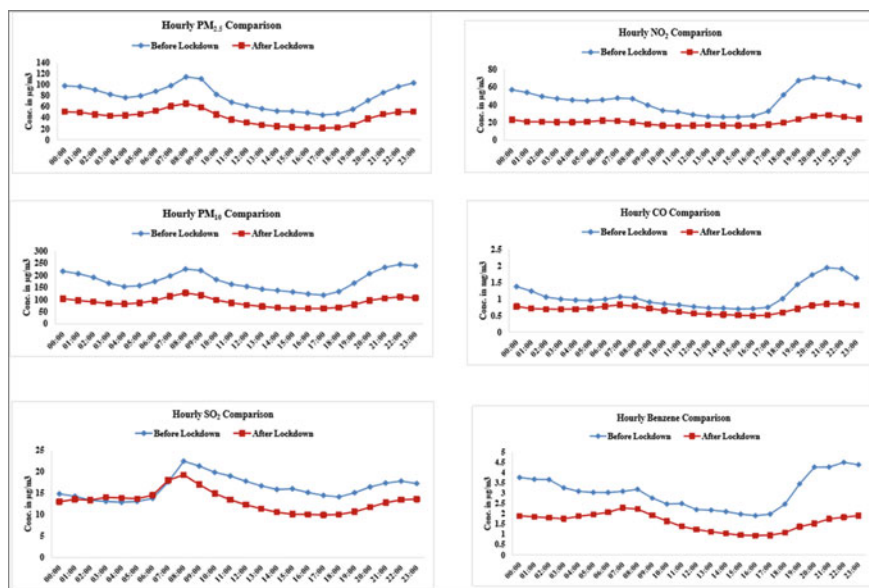


Fig. 4 Hourly comparison of air pollution parameters (PM_{2.5}, PM₁₀, SO₂, NO₂, CO, Benzene) for during lockdown and before lockdown in Delhi region

particulate matters referred as PM_{2.5} are recorded to be 114 $\mu\text{g}/\text{m}^3$ during normal working days and 21 $\mu\text{g}/\text{m}^3$ during the lockdown phase. The PM₁₀ is recorded to hold a maximum hourly value of 244 $\mu\text{g}/\text{m}^3$ during normal working days and was observed to reduce to a concentration of 127 $\mu\text{g}/\text{m}^3$ during the lock down phase. The hourly concentration of SO₂ on normal working days were observed to be 25 $\mu\text{g}/\text{m}^3$ and during the lock down, the value reduced to 19 $\mu\text{g}/\text{m}^3$. For NO₂ on normal working days, the value was observed to be 80 $\mu\text{g}/\text{m}^3$ and during the lockdown, it was recorded to reduce to 18 $\mu\text{g}/\text{m}^3$. These observations are conducted by the monitoring stations of the CPCB, Ministry of Environment and Forest and Climate Change. It is interesting to note that the SO₂ emissions have gone down by 24% which is mainly attributed to the closure of unorganised industries like brick kilns thus restricting the stack emissions. However, it is evident that the stationary source emissions from organised industries of power plants are major source of SO₂. It is the reason that the change in SO₂ level is small as compared to particulate matters. Further, it may also be noted that the level of NO₂ and CO has also decreased in atmosphere and it can also directly correlate to closure of industries contributing to air pollution through stack emissions. A major amount of the air pollution is toxic in nature. Mercury, lead, benzene and dioxins are released during gas or coal combustion of the fuel used in organised and unorganised industries, waste incineration or burning of gasoline.

6 Conclusion

This study portrays the decrease in air pollutants because of temporary shutdown of unorganised industry with stack emissions. However, the organised industries like power generating sector remained functional and continued to add air pollutants. The power generating plants are considered as red category industries as the total Greenhouse gas emission generated from these industries are 635 MTCO_{2e} approximately. This study on air pollution during lockdown contemplates an urgency to formulate provisions that will force the industries to adhere to air emission monitoring and standards [11]. Due to restrictions of industry, the challenges persist in the detail study of combustion and plume discharge. The future scope of this study is to quantify the contribution of plume discharges from organised and unorganised industries and conduct detailed analysis of stationary sources emissions due to combustion.

References

1. Martins A (2010) Industrial air emissions in Portugal: 2008 Report. WIT Trans. Ecol. Environ. 201–210. <https://doi.org/10.2495/AIR100181>
2. Sindhwani R, Goyal P (2014) Assessment of traffic-generated gaseous and particulate matter emissions and trends over Delhi (2000–2010). Atmos Pollut Res 5:438–446. <https://doi.org/10.5094/APR.2014.051>
3. Economic survey of Delhi report 2014—2015, <https://delhiplanning.nic.in>
4. Sharma M, Dikshit O Comprehensive study on air pollution and green house gases (GHGs) in Delhi
5. Hopke PK (2016) Review of receptor modeling methods for source apportionment. J Air Waste Manag Assoc 66:237–259. <https://doi.org/10.1080/10962247.2016.1140693>
6. Wang LK, Pereira NC, Hung Y Handbook on environmental engineering. Air Pollut Control Eng
7. Corio LA, Sherwell J (2000) In-stack condensible particulate matter measurements and issues. J Air Waste Manag Assoc 50:207–218. <https://doi.org/10.1080/10473289.2000.10464002>
8. Xu S (2020) Analysis of the influencing factors of industrial air pollution in Shenzhen. IOP Conf Series Earth Environ Sci 450:012094. <https://doi.org/10.1088/1755-1315/450/1/012094>
9. Hewitt CN (2001) The atmospheric chemistry of sulphur and nitrogen in power station plumes. Atmos Environ 35:1155–1170. [https://doi.org/10.1016/S1352-2310\(00\)00463-5](https://doi.org/10.1016/S1352-2310(00)00463-5)
10. Central Pollution Control Board, <https://cpcb.nic.in>
11. Henneman LRF, Liu C, Mulholland JA, Russell AG (2017) Evaluating the effectiveness of air quality regulations: A review of accountability studies and frameworks. J Air Waste Manag Assoc 67:144–172. <https://doi.org/10.1080/10962247.2016.1242518>

Use of WaterGEMS for Hydraulic Performance Assessment of Water Distribution Network: A Case Study of Dire Dawa City, Ethiopia



Bahar Adem Beker and Mitthan Lal Kansal

Abstract Hydraulic performance of a water distribution network (WDN) could be evaluated through an assessment indicating the ability of the system to meet the required quantity of water for consumers at every time and place. This study aims to assess the hydraulic performance of the water distribution network (WDN) for parts of Dire Dawa city (Zone-1) in Ethiopia. For this purpose, a combination of advanced hydraulic modeling tools (WaterGEMS V8i), GIS, and performance index is used. Bentley WaterGEMS V8i is applied for the simulation of hydraulic models, whereas the model building and the calculation of network performance indices (pressure and velocity) are carried out in ArcGIS. The output of hydraulic simulation for parameters is used as the input data for the calculation of indices. The results revealed that a higher value of pressure is observed at some nodes, which may cause leakage of water in the system. Further, the performance of WDN for pressure indices is lower for those nodes. On the other hand, the velocity index of the network is low and below the acceptance level. The minimum network performance for the velocity index is observed in the pipes of low-velocity value below the minimum standard limit. Moreover, the performance indices illustrate the problematic nodes and pipelines in the network which need improvement. Therefore, this paper suggested that appropriate measures, such as installing pressure regulating valves and changing the pipe in critical areas, can be applied to improve the hydraulic performance of the WDN for optimum network operation.

Keywords Dire Dawa · Hydraulic modeling · Hydraulic performance index · GIS · Water distribution network · WaterGEMS

B. A. Beker (✉) · M. L. Kansal
Department of Water Resources Development and Management, Indian Institute of Technology
Roorkee, Roorkee 247667, India
e-mail: baharwsee@gmail.com

M. L. Kansal
e-mail: mlk@wr.iitr.ac.in

1 Introduction

The water distribution network (WDN) is crucial for better living standards and economic development, particularly in urban areas. WDN is one of the critical hydraulic infrastructures designed to satisfy all the requirements of water for domestic, commercial, institutional, industrial, and fire demand at a given time and space with adequate pressure [1]. However, in developing countries like Ethiopia, most WDNs cannot fulfill its aim of providing sufficient water continuously due to the frequent failure of water distribution elements [2]. The first step for the design and expansion of WDN is to understand and evaluate its hydraulic performance. The evaluation of WDN performance is significant in identifying the problematic areas and elements in a network, which help the WDN in ensuring public safety, continuous operation, enhancing sustainability, and minimizing the operational as well as the maintenance costs [3]. Further, the knowledge about the actual network performance is a crucial tool to control and manage the water networks [4].

Researchers have proposed different methodologies for performance assessment of the WDN based on the three crucial aspects [5, 6]. These are (1) conceptual quality of methods, (2) the applicability of the methods, and (3) the ability of the method to translate the measurement into a correct objective. Based on the above criteria, there are two main classes of performance analysis, i.e., system performance indicators and technical performance assessment tools. The system performance indicator proposed by the International Water Association (IWA) has been one of the internationally accepted tools for evaluating the performance of water utility and applied by researchers [7–9]. Technical performance assessment tool related to the evaluation of specific aspects (e.g., water quality aspect and hydraulic behavior) of the system [10], which is typically carried out using tools like WaterNetGen (an extension of EPANET) [11]. These tools use the three-step framework [12–14], which includes the network hydraulic parameters (pressure and velocity); penalty curves, which plotted hydraulic variables against the performance index value of elements; and overall performance index of a network (the aggregate weight of performance of each element).

Nowadays, hydraulic computational tools are effectively combined with GIS tools to design, manage, and improve the efficiency of the water distribution system [15]. A combination of GIS and Hydraulic modeling tool (EPANET) has been carried out for hydraulic analysis of WDN [16], pipe replacement and performance improvement [17], for leakage management and estimation of loss in the network [18, 19]. Also, a study performed the analysis of WDNs by coupling of GIS and WaterGEMS [20]. However, no study is found that used GIS tools and WaterGEMS for assessing the hydraulic performance of WDN incorporated with technical performance tools, especially over Ethiopian cities. Therefore, the main aim of this paper is to evaluate the hydraulic performance level of WDN in Dire Dawa using a combination of hydraulic models (WaterGEMS), GIS, and hydraulic performance indices. Such

research works are necessary for proper management of water in developing countries where equitable water distribution is a challenging concern [21–23]. The problems have even worsened by rising issues of water availability, mainly due to rapid population growth and looming climate change [24, 25]. Therefore, investigating the hydraulic performance of WDN of Dire Dawa is timely research work.

2 Theoretical Background

2.1 Hydraulic Analysis in WDN

The hydraulics of flow through a WDN with a known demand should satisfy three basic principles/equations. Those are the law of conservation of mass or the continuity equation, the energy principle (conservation of energy), and loop equation. The first principle in dealing with pipe flows is the continuity of matter. It states that for an incompressible fluid, the algebraic sum of the discharge in all the pipe joining at a node, together with any external flows, is zero. Equations for each link (between nodes i and j) and each node k written as;

$$\sum_i Q_{ik} - \sum_j Q_{kj} \pm Q_k = 0 \quad (1)$$

where Q_{ik} is flow into the node k , Q_{kj} is the flow out from the node k , and Q_k is the flow consumed (-) or supplied (+) at node k . Further, the principle of conservation of energy is also satisfied and stated as the total energy of flow at two cross-sections of pipes will be the same if there is no energy loss. The total energy in terms of the head of water is expressed by the Bernoulli Eq. (2)

$$Z_1 + \frac{p_1}{\gamma} + \frac{v_1^2}{2g} = Z_2 + \frac{p_2}{\gamma} + \frac{v_2^2}{2g} + h_{l,1-2} \quad (2)$$

where Z_1 is the elevation head at cross-section 1, P_1 pressure head, γ is the unit weight of water V_1 the velocity of flow; subscripts 1 and 2 denote that the variable refers to cross-section 1 and 2; and $h_{l,1-2}$ refers head loss between two cross-section. Finally, the hydraulic flow through WDN also satisfies the loop equation that states as the algebraic sum of pressure drops around a loop must equal zero. Mathematically written as:

$$\sum \pm \Delta h_i = 0 \quad (3)$$

where Δh_i is head loss/gain the i th element of the loop.

The hydraulic equation in WDN can be calculated either in terms of unknown flow rate or in terms of the unknown head at the demand node explicitly. Recent literature

summarized the closed pipe equation solving (flows computation) of WDN into four common approaches. The selected unknown parameter characterizes them as the system equations [26]. Hardy Cross method [27] is the first, oldest, and common approaches, which adopted manual calculations. Newton–Raphson’s method [28] is the most widely used approach because it exhibits quadratic convergence. Another technique is linear theory method [29], where an applicable transformation was used to find a set of linear equations from the loop equations by determining the head in each pipe. Gradient algorithms (GA) is the method that begins with an estimation of flow in each pipe. Recently, some of hydraulic modeling software like EPANET and WaterGEMS are used the gradient algorithm for solution of pipe networks.

2.2 WaterGEMS Overview

WaterGEMS was initially developed by Company Haested method Inc. in the USA. In mid-2004, the product was commercially renamed as Bentley WaterGEMS V8i. WaterGEMS V8i is the modeling software used to design, analyze, and optimize WDN with advanced geospatial building, interoperability, and asset management [16]. It is a highly capable and dynamic simulating software that provides analysis and solutions for hydraulic and water quality modeling, fire-flow analysis, intelligent system management, and planning for system reliability, energy, and capital cost management, etc. Almost all functionalities in WaterCAD are available in WaterGEMS with an additional feature so that it is the super-set of WaterCAD.

WaterGEMS has different advantages over other hydraulic models of WDN. It is comprehensive, highly efficient, and simple to use. It has a robust design algorithm for the solution of pipe networks [17]. Furthermore, WaterGEMS has used the genetic algorithm (GA) to predict hydraulic variables in the WDN [30]. The best part of this model is the result presentation mode, which is very attractive and appealing with various graphical tools. Integration with multiple platforms graphic software (GIS tools, AutoCAD, and Micro Station tools) makes WaterGEMS highly preferable over other WDN model software, especially EPANET and Branch [15, 18].

3 Description of Study Area/Case Study/ and Existing Water Distribution Network

Dire Dawa is one of the largest and oldest urbanized centers in Ethiopia, which is considered as the study area. It has nine districts (kebeles) that cover an area of 85 km². It is located in the Awash basin to the eastern lowlands of Ethiopia with the geographical location of 41.768° to 41.891° latitude and 9.574° to 9.643° longitude direction. Dire Dawa has an elevation ranging from 1130 to 1335 m with a mean elevation of 1160 m above mean sea level [31]. Hills and steep slopes are found in

the South, whereas moderate and gentle slopes are located to the north of the city. According to the Central Statistic Authority of Ethiopia, the population of Dire Dawa by 2019 was projected to be 369,596.

From an operational point of view, the existing WDN of Dire Dawa is divided into three pressure zones (Zone I, II, and III). The zone I (Fig. 1) networks have been facing many problems compared to other zones, and since this zone is selected for this study. It includes districts 4 (Ganda Kore), and 5 (Addis Ketama) and partially covers district 3 (Kazira). The WDN of this Zone serves 123,000 residents of the city. The sources of the WDN of this Zone are groundwater located at Boren well field. The water collected from boreholes to Boren boosting station is pumped to the transfer reservoir at Sabian pumping station. From there, it is pumped to Gandboye and Entoto tanks, whose capacities are 4000 and 1000 m³, respectively. Finally, the water is distributed to the end-user by gravity from those tanks. The entire WDN of this zone has 47 km long pipeline, with the pipe diameter varying between 50 and 500 mm (PVC and DI). The pipe age is about 3–30 years.

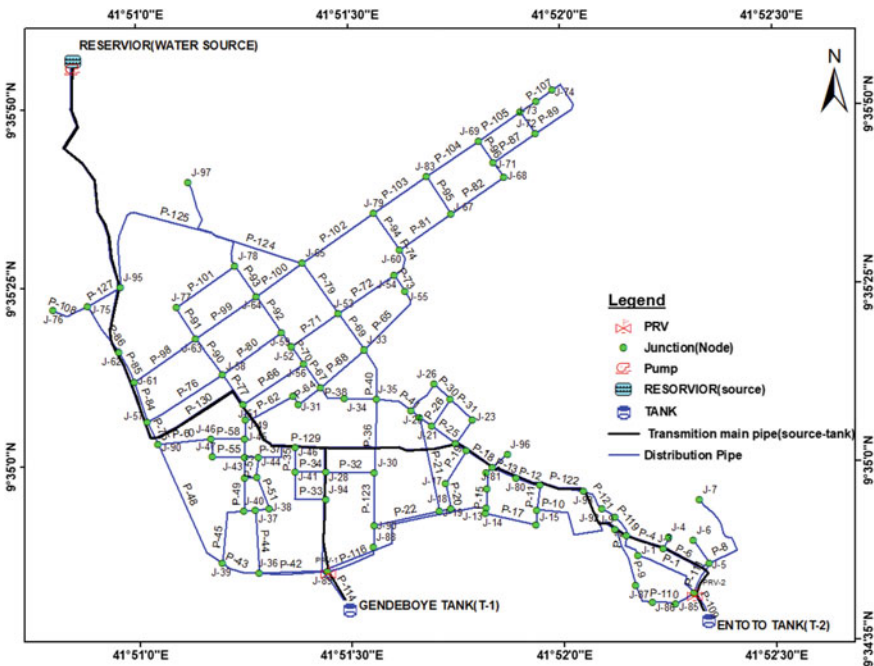


Fig. 1 Layout of Dire Dawa Water Distribution Network (Zone-I)

4 Methodology

4.1 *Hydraulic Model Building*

In this study, ArcGIS is utilized to build the water distribution network and prepare all necessary data for hydraulic simulations. The existing water distribution map (network) is obtained from the Dire Dawa Water Supply & Sewage Authority (DWSSA). Validation of the map is performed by the field visits over the study area. The validated network map is then scanned and imported to ArcGIS for georeferencing and digitalization. The layers of water distribution components (pipes, junction, tanks, reservoir, pumps, and valves) are created in ArcGIS. The input parameters viz., pipe diameter and pipe material (pipe roughness) area added to the attribute table and documented in the ArcGIS database.

The other characteristics of hydraulic elements such as pumps, tanks, and valves are also transferred to the attribute table. Only the pipes with a diameter above 90 mm in the networks are considered for the model. This simplification (skeletonization) of WDN is made to minimize the complexity of the network, thus making the model simulations more stable, accurate, and efficient [32, 33]. The length of the pipe, X -coordinate, and Y -coordinate are automatically generated in the ArcGIS environment. The elevation of the junction is a critical input data, which is assigned for each node. Contours maps of the area with required intervals are generated and verified with the data collected from the field. The topographic elevation of all nodes (reservoir, tanks, valves, and all junctions) is obtained from the elevation map in ArcGIS.

4.2 *GIS-WaterGEMS Model Transfer and Hydraulic Simulation*

GIS is a comprehensive, robust, and user-friendly software that can be integrated with the WaterGEMS, hydraulic modeling tools. For this study, ArcGIS-WaterGEMS conversion is performed using the model builder tools. These tools play a crucial role in WaterGEMS as they import and export data between ArcGIS and the model [30]. Further, different layers of network data such as diameters, elevation, pipe roughness(C) valves, tanks, and reservoirs are synchronized in the WaterGEMS model. After the constructed model is transferred to hydraulic software (WaterGEMS), the water demand and other necessary data are assigned for further analysis.

The collected data revealed that average water consumption reached 80 L per capita per day (PCD) [34]. The baseline demand for each node is allocated based on the water consumption of the node. The flow distribution method that involves lump-sum water demand distributed among the service area is used for allocating the baseline demands [26, 27]. Thiessen polygons are generated for each node in order to estimate the population under each service polygon, based on the population density data. After incorporating all the necessary data into the hydraulic model,

the simulation is performed to predict the hydraulic characteristics of WDN. Both extended period simulation (EPS) and steady-state analyses (SSA) are conducted to characterize the hydraulic parameters (pressure at each node, flow velocity in the pipes, and head loss). An EPS is carried out using the demand pattern collected from DWSSA. The final step is the calibration of the model, which intends to improve the accuracy of the models. The calibrated hydraulic parameters are transferred back to the ArcGIS database for calculation of the performance index of elements and network.

4.3 Hydraulic Performance Assessment Indices

Performance indicators are suitable measures to assess the hydraulic performance of WDN and help any decision-maker to upgrade activities to improve network performance [5]. The output of the hydraulic model (nodal pressure and velocity in pipes) is used to determine the performance index of networks and each element. The penalty curves, which plot the performance index against the pressure and velocity values, are presented in Fig. 2a and 2b, respectively. In Fig. 2a, H_{min} represents the absolute minimum pressure (no flow can be discharged), H_{des} is the minimum desired pressure head below which water consumer cannot be completely satisfied, and (H_{max}) is the maximum acceptable pressure recommended by the standard codes. The vertical axis of the penalty curves in Fig. 2a and b is divided from the minimum value of zero to the maximum value of one with 0.25 step size. The performance index of 0 (zero) denotes no service situations; 0.25 is considered unacceptable, 0.5 is acceptable, 0.75 is good, and 1(one) is considered as ideal performance. The pressure values for the penalty curve, i.e., H_{min} , H_1 , H_2 , H_3 , H_{des} , and H_{max} are considered as 0, 1.87, 7.5, 16.87, 30, and 62 m, respectively. These values are adopted based on previous studies [17, 35].

The penalty curve in Fig. 2b is for assessment of network performance using the standard limits for the velocity in the pipes. In the penalty function, the velocity values of $V_{min} = 0.3$ m/s, $V_{max} = 2.5$ m/s, $V_{opt} = 0.8$ m/s, and $V_{optu} = 1$ m/s are

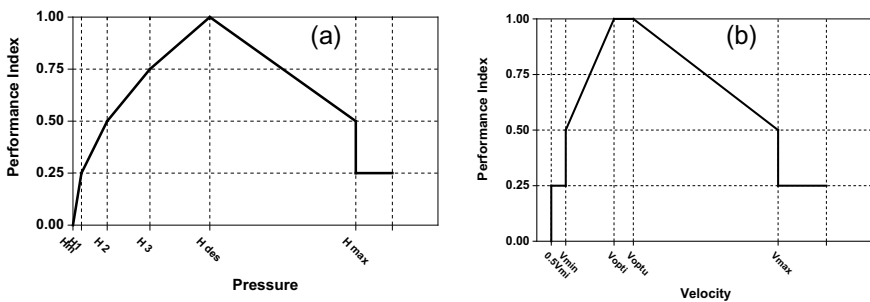


Fig. 2 a Penalty curves for nodal pressure b Penalty curves for flow velocity

considered, as per previous studies [17, 35], where V_{\min} is minimum velocity, V_{\max} is maximum velocity, V_{optl} and V_{optu} are the lower and upper bound of the optimum flow velocity, respectively.

The network performance index (generalized performance of a network) is calculated from the performance indices of elements. Two weightage functions W_1 and W_2 are applied to the performance index of each element. The performance of the network regarding nodal pressure (PI_{NP}) is assessed as follows

$$PI_{\text{NP}} = W_1(PIEP)_j = \frac{\sum_{j \in Nj} Q_j^{\text{req}} * (PIEP)_j}{\sum_{j \in Nj} Q_j^{\text{req}}} \quad (4)$$

where $(PIEP)_j$ is the performance index of an element due to pressure value at a node j , Q_j^{req} is water demand at node j , and Nj is a number of nodes in WDN. Also, the performance index due to the velocities in pipes (PI_{NV}) is calculated by the following equation,

$$PI_{\text{NV}} = W_2(PIEV)_j = \frac{\sum_{j \in NP} \bar{V}_{ij} * (PIEV)_{ij}}{\sum_{j \in NP} \bar{V}_{ij}} \quad (5)$$

where $(PIEV)_j$ is the performance index of the element due to the flow velocity in pipe ij , and NP is the pipe number. The volume of pipe ij (\bar{V}_{ij}) is expressed as,

$$\bar{V}_{ij} = \frac{\pi D_{ij}^2 L_{ij}}{4} \quad (6)$$

where, D_{ij} and L_{ij} are the diameter and the length of pipe ij , respectively. Finally, the performance index of the network and elements are manipulated in the ArcGIS for further analysis.

5 Results and Discussion

The water distribution network is evaluated based on the output of WaterGEMS and hydraulic performance indices. The result in Fig. 3a shown the nodal pressure and velocity in pipes. A significant number of demand nodes (23 out of 95 nodes) is found to have a pressure value higher than H_{\max} (62 m). The maximum pressure is observed at nodes of lower elevation. Such high pressure can be the main reason for the significant leakage problem in the pipes, which leads to a pipe burst. Also, high pressure above the maximum standard limit at the nodes may be a cause of low-performance of the networks. On the contrary, velocity is very low, i.e., below 0.3 m/s for 59 out of 134 pipes (Fig. 3a). Such a low velocity of flow in a pipeline can cause the accumulation of silt and water quality deterioration in the pipes [36].

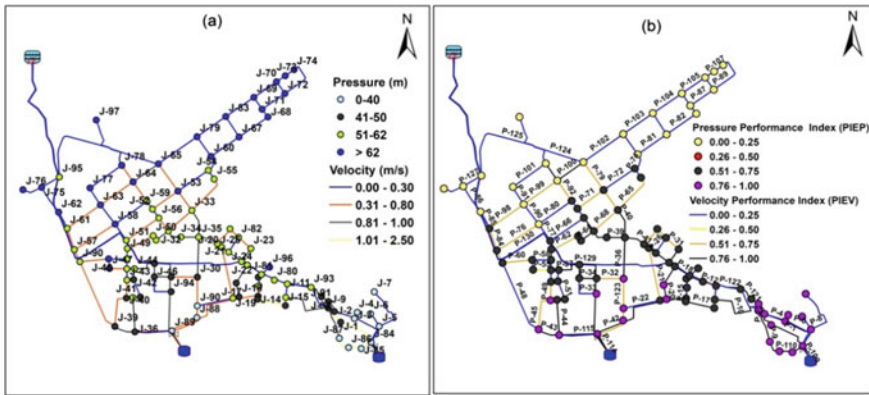


Fig. 3 a Hydraulic simulation output; b Network performance index of elements (Pressure and velocity)

The performance index of the distribution network and elements is assessed based on the proposed methodology of technical performance indices. The output of hydraulic simulation for parameters is used as the input data for the calculation of indices in ArcGIS. Figure 3b represents the performance of the network for pressure and velocity indices. The results reveal that the overall network performance for the pressure index is 0.62, which is above an acceptable level. However, a low-pressure index (below 0.5) has been found for 22 demand nodes, which is not acceptable. Higher nodal pressure above the standard limit (H_{max}) is the main reason for the low value of the pressure index. On the other hand, the overall network performance for the velocity index is 0.41, below an acceptable level of 0.5. Also, 41 out of 134 pipes performance for the velocity index in the system is below 0.25. The absolute minimum velocity out of the optimum domain is the reason for the lower velocity index value.

Obviously, in an extended period of simulation, the hydraulic variable fluctuates with time. Values of pressure for selected nodes (J-10, J-18, J-58, and J-73) reveals that maximum pressure is observed at night time when the users consume low water, and the minimum pressure is observed at peak demand period (Fig. 4a). There are fluctuations in velocity with time. The higher values at maximum water consumption period and lower at minimum consumption for selected pipes in Fig. 4b (P-6, P-47, P-100, P-103). Hence, the velocity of flow in the pipes is directly proportional to the consumption rate.

The performance index of networks is found to fluctuate with time (Fig. 5a and 5b). The minimum pressure index of 0.46 is observed at midnight, which is due to low consumption. It can be seen that during this period, the pressure at nodes is above the maximum standard limit (Fig. 5a). On the contrary, the higher pressure index value of 0.71 is observed at the peak demand period, given that the pressure nodes are in the optimum domain. Also, Fig. 5b reveals that a low value of the velocity index, i.e., 0.33, is observed during the low demand time. Hence, during the low

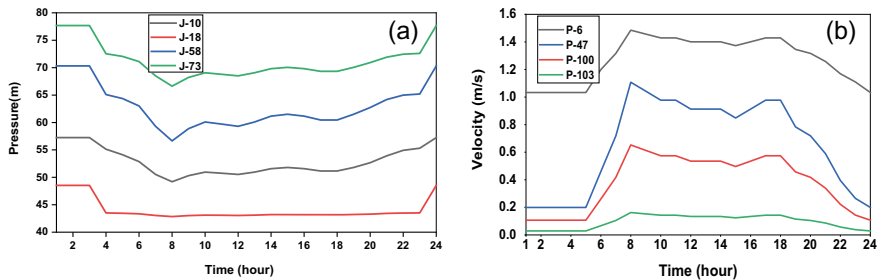


Fig. 4 a Nodal pressure for selected nodes; b Flow velocity for selected pipes

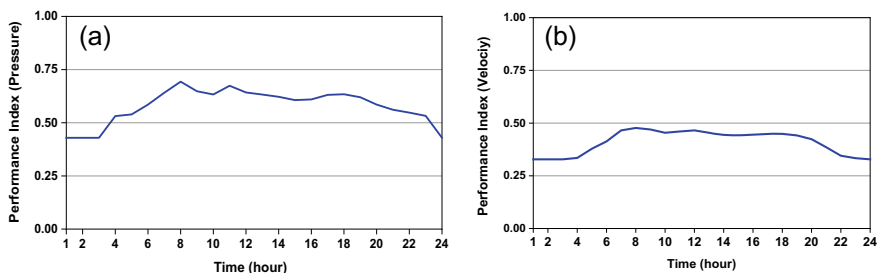


Fig. 5 a Network performance for pressure index; b Network performance for velocity index

consumption period, the flow velocities are out of the optimum range. Further, the low performance of the network may be due to poor design and weak operational management of the system. Therefore, decision-makers may consider changing the pipes, establishing or replacing valves (PRV) in the network, etc., to increase the performance in WDN.

6 Conclusions

In this paper, the hydraulic analysis and the performance evaluation of WDN for Dire Dawa city (zone-I) in Ethiopia have been presented. The analysis is carried out using a hydraulic model (WaterGEMS V8i) coupled with GIS and the technical performance indices. The hydraulic performance level of WDN is assessed using the pressure and velocity indices. The results revealed that high pressure and low velocity are observed in different areas of the network. The overall network performance for the pressure index was 0.62, which is above an acceptable level. However, lower pressure performance is observed at some nodes. Moreover, the overall performance of the network for the velocity index is 0.41, which is below the acceptable level of performance. Therefore, it is suggested that the decision-makers should be considered

appropriate strategies such as installing PRV and changing the pipes in critical areas to improve the performance of the WDN for optimum network operation.

References

1. Al-Zahrani MA (2012) Modeling and simulation of water distribution system—a case study. *Arab J Sci Eng* 39(3):1621–1636
2. Terlumun UG, Robert EO (2019) Evaluation of municipal water distribution network using watercard and watergems. *J Eng Sci* 5(2):147–156
3. Ataoui R, Ermini R (2015) Overall performance of water distribution system: a methodology. *J Appl Water Eng Res* 3(1):19–28
4. Kansal ML, Kumar A (2000) Computer-aided reliability analysis of water distribution networks. *Int J Model Simul* 20(3):264–273
5. Alegre H, Hirner W, Baptista JM, Parena R (2000) Performance indicators for water supply services. Manual of best practice series. IWA Publishing, London, UK
6. Cardoso M, Coelho S, Matos R, Alegre H (2004) Performance assessment of water supply and wastewater systems. *Urban Water J* 1(10):55–67
7. Kun R, Talib S, Redzwan G (2007) Establishment of performance indicators for water supply services industry Malaysia. *Malaysian J Civil Eng* 52(2):140–154
8. Radivojević D, Milićević D, Petrović N (2007) Technical performance indicators, IWA best practice for water mains and the first steps in Serbia. *Facta Univ-Series Arch Civil Eng* 5(2):115–124
9. Kanakoudis V, Tsitsifli S (2010) Results of an urban water distribution network performance evaluation attempt in Greece. *Urban Water J* 7(5):267–285
10. Muranho J, Ferreira A, Sousa J, Gomes A, Marques AS (2012) WaterNetGen—An EPANET extension for automatic water distribution network models generation and pipe sizing. *Water Sci Technol Water Supply* 12(1):117–123
11. Muranho J, Ferreira A, Sousa J, Gomes A, Marques AS (2014) Technical performance evaluation of water distribution networks based on EPANET. *Procedia Eng* 70:1201–1210
12. Alegre H, Coelho ST (1992) Diagnosis of hydraulic performance of water supply systems. Pipeline systems. Springer, Dordrecht, pp 247–260
13. Alegre H, Coelho ST (1995) Hydraulic performance and rehabilitation strategies. Improving efficiency and reliability in water distribution systems. Springer, Dordrecht, pp 267–282
14. Coelho S (1997) Performance indicators in water distribution through mathematical modelling. In: IWA workshop on performance indicators for transmission and distribution systems. LNEC, Lisbon, Portugal
15. Tabesh M, Delavar MR, Delkhah A (2010) Use of geospatial information system based tool for renovation and rehabilitation of water distribution systems. *Int J Environ Sci Technol* 7(1):47–58
16. Abdelbaki C, Benchaib MM, Benziada S, Mahmoudi H, Goosen M (2017) Management of a water distribution network by coupling GIS and hydraulic modeling—a case study of Chetouane in Algeria. *Appl Water Sci* 7(3):1561–1567
17. Massoud T, Zia A (2003) Dynamic management of water distribution networks based on hydraulic performance analysis of the system. *Water Supply* 3(1–2):95–10
18. Ardeshir A, Saraye M, Sabour F, Behzadian K (2006) Leakage management for water distribution system in GIS environment. In: World environmental and water resource congress 2006: examining the confluence of environmental and water concerns pp 1–10
19. Motiee H, McBean E, Motiee A (2007) Estimating physical unaccounted for water (UFW) in distribution networks using simulation models and GIS. *Urban Water J* 4(1):43–52
20. Roy PK, Konar A, Banerjee G, Paul S, Mazumdar A, Chkraborty R (2015) Development and hydraulic analysis of a proposed drinking water distribution network using Watergems and GIS. *Poll Res* 34(2):371–379

21. Swain S, Nandi S, Patel P (2018). Development of an ARIMA model for monthly rainfall forecasting over Khordha district, Odisha, India. In: *Recent findings in intelligent computing techniques*. Springer, Singapore, pp 325–331
22. Swain S, Patel P, Nandi S (2017). Application of SPI, EDI and PNPI using MSWEP precipitation data over Marathwada, India. In: *2017 IEEE international geoscience and remote sensing symposium (IGARSS)*. IEEE, pp 5505–5507
23. Dayal D, Swain S, Gautam AK, Palmate SS, Pandey A, Mishra SK (2019) Development of arima model for monthly rainfall forecasting over an Indian river basin. In: *World environmental and water resources congress 2019: watershed management, irrigation and drainage, and water resources planning and management*. ASCE, pp 264–271
24. Swain S (2017) Hydrological modeling through soil and water assessment tool in a climate change perspective—a brief review. In: *2017 2nd international conference for convergence in technology (I2CT)*. IEEE, pp 358–361
25. Swain S, Verma MK, Verma MK (2018) Streamflow estimation using SWAT model over Seonath river basin, Chhattisgarh, India. In: *Hydrologic Modeling*. Springer, Singapore, pp 659–665
26. Giustolisi O, Todini E (2009) Pipe hydraulic resistance correction in WDN analysis. *Urban Water J* 6(1):39–52
27. Cross H (1936) *Analysis of flow in networks of conduits or conductors*. University of Illinois at Urbana Champaign, College of Engineering Engineering Experiment Station, Urbana, Illinois
28. Martin DW, Peters G (1963) The application of Newton's method to network analysis by digital computer. *J Instit Water Eng* 17(2):115
29. Wood DJ, Charles COA (1972) Hydraulic network analysis using linear theory. *J Hydraul Div* 98(HY7):1157–1170
30. Bentley Systems Incorporated (2014) *WaterCAD/GEMS V8i, water distribution design and modeling, fundamentals, Version V8i (SELECT series 5)*.
31. Dire Dawa Water Supply and sewerage Authority (2014) *Final Dire Dawa water supply design review report*. Diredawa, Ethiopia
32. Perelman L, Ostfeld A (2011) Topological clustering for water distribution systems analysis. *Environ Model Softw* 26(7):969–972
33. Huang Y, Zheng F, Duan HF, Zhang T, Guo X, Zhang Q (2019) Skeletonizing pipes in series within urban water distribution systems using a transient-based method. *J Hydra Eng* 145(2):04018084
34. Ramana GV, Chekka VS (2018) Validation and examination of existing water distribution network for continuous supply of water using EPANET. *Water Resour Manage* 32(6):1993–2011
35. Tabesh M, Saber HA (2012) prioritization model for rehabilitation of water distribution networks using GIS. *Water Resour Manage* 26(1):225–241
36. Walski TM, Chase DV, Savic DA, Grayman W, Beckwith S, Koelle E (2003) *Advanced water distribution modeling and management*. Civil and Environmental Engineering and Engineering Mechanics Faculty Publications, University of Dayton, Dayton

Comparative Analysis and Prediction of Ecological Quality of Delhi



Syed Zubair, Shailendra Kumar Jain, and Shivangi Somvanshi

Abstract This study showcases the comparison of ecological quality in Delhi and also predicts the environmental quality in coming future if the anthropogenic activities continue to remain the same. A pilot study was conducted by using the remotely sensed data to develop a Geospatial Ecological Impact Index (GEII), by implementing Analytical Hierarchy Process (AHP) which incorporated vegetation, moisture content, land surface temperature, water bodies, and built-up factors of the study area to examine how much they have impacted the ecology and in what manner. The ecological changes were contrasted between the years 2016 and 2020. It was revealed through this study that the overall ecological quality has decreased over the years with an increase in the mean LST. A simulated map was also developed using the nonlinear modelling technique, i.e. artificial neural network (ANN) to ascertain the future ecological quality for the year 2024. Certainly, this study can help decision makers, urban planners, and researchers in formulating new ways to mitigate and overcome the continuous degradation of ecology.

Keywords Remote sensing · Ecological impact assessment · Delhi · ANN · AHP

1 Introduction

With the increasing growth of cities in terms of populace, geographical extent, and congestion, its environmental as well as ecological impressions pile up. The construction of various structures which occurs in forest areas, marshy lands, and agrarian regions causes the removal of the respective habitat, deterioration, and division of

S. Zubair (✉) · S. K. Jain
Amity School of Engineering & Technology, Amity University, AUUP, Noida, India
e-mail: sayyedalizubair@gmail.com

S. K. Jain
e-mail: skjain@amity.edu

S. Somvanshi
Amity Institute of Environmental Sciences, Amity University, AUUP, Noida, India
e-mail: ssomvanshi@amity.edu

the lands. The living standards in urban areas are highly consumptive, which require a lot of natural resources but also in turn generate great amounts of waste. This waste is released in the lower atmosphere, water bodies, and in the soil strata as well, all of which causes the pollution levels to increase.

The swift development of Delhi in last couple of decades has caused a remarkable decrease in the quality of the environment. Increased emissions of GHGs are a result of urban industries, emissions from vehicles using fossil fuel, and the increasing electricity demand. Burning these fossil fuels causes an increase in the concentration of air contaminants and GHG emissions. Urban greenhouse gas emissions are highly responsible for global warming and change in climate. The problem which the urban areas face is the impervious surfaces associated with the structures built, and these impervious surfaces change the actual flow of water that should have taken an optimum route. The dire repercussions of this unusual alteration are decreased volume of water which should have percolated into the soil, and also results in the increase in volume and degradation in quality of surface waters. Hence, studies have to be done by researchers in order to find out ways to preserve and protect the environment.

2 Literature Survey

Ecological changes are universal phenomena occurring naturally at different levels as part of biological reorganization. Human activities have changed the patterns of landscapes drastically worldwide and have prejudiced the environment considerably. The technique of remote sensing plays a crucial part in delivering spatial as well as temporal information/data for measuring, mapping, and observing the land use changes [1]. Urban land dynamics gives a basis for keeping a track and studying the urban land transformations [2]. To get a better understanding of the ecology of a region with respect to derive a meaningful and effective planning strategy, it is a mandate to have knowledge of the ecological structure, function, and the landscape change patterns [3]. Precise assessment of environmental and ecological factors of a region is useful for strategy developers in order to identify the ongoing circumstances of the ecological environment, and to come out with enhanced imperishable development measures [4].

Execution of remote sensing can be done in the study of Geo environmental aspect [5]. Remote sensing data was also executed in the eco-environmental evaluation of the Yellow River drainage basin [6]. Landscape level disturbance gradient was done by [3]. Remote sensing data was used multiple times for mapping the Alfios river stream changes [7]. Estimation of the area impacted by forest fires can be done using remote sensing and GIS techniques [8]. Lands affected by tanneries effluents can also be delineated [9]. In recent times remote sensing approach has been extensively employed for waterlogging and drainage assessment [10]. The estimation for temporal behavior of surface water logged areas can be done using multi-spectral and multi-temporal space borne data [11]. Use of orbital remotely sensed data combined

with GIS for analysis of the effects of manmade destruction on land as well as water bodies over a tenure has also been carried out [12]. The use of remote sensing techniques and GIS techniques can assess soil erosion dangers and vegetation parameter for soil erosion can also be modelled [13, 14]. The use of remotely sensed data in remote sensing and GIS has helped in estimating change detection of river flow along with monitoring the sedimentation in reservoirs [15–17].

The current research pertains with respect to environmental assessment, based on ecological environment of one parameter, for example, the use of vegetation index for the study of vegetation cover [18] the use of NDBI as an easy approach for fresh water body evaluation, making use of the LST calculation to evaluate the built-up heat island effect [19, 20], etc. A single ecological parameter is not responsible for the changes that occur in the environment comprehensively but depends on various factors [21] and hence, it is vital to assess the local environment using the cumulative effects of more than one ecological factor [22]. Amongst the very crucial criterion of this study is land surface temperature, which has a very important position in ecological, hydrological as well as worldwide variation [24]. Numerous attempts have been made in order to derive techniques for assessing the LST from remotely sensed evidence, and noteworthy improvements have been recorded in past few years [25–28].

2.1 Geographical Locale

Delhi is situated at the nutrient rich alluvial plains of North Indian subcontinent as a riverine city of the Yamuna river, spanning from 28° 23' 17" N to 28° 53' 00" N and 76° 50' 24" E to 77° 20' 37" E. The study area can be clearly seen in Fig. 1. It huddles near the geographical boundaries of two neighboring states, Haryana and Uttar Pradesh. It spans over an area of 1484 Km².

The city is bind from the north and east side by the Indo-Gangetic plains toward the west by Thar Desert and the Aravalli cover the southern region.

The existence of these diverse morph geological attributes depicts changes in the city's altitude which varies from 213 to 305 m. Delhi has two prime landforms, the Gangetic plains and the ridge, which is an extension to Aravalli Ranges.

3 Methodology

This pilot study was carried out in the following manner as mentioned below.

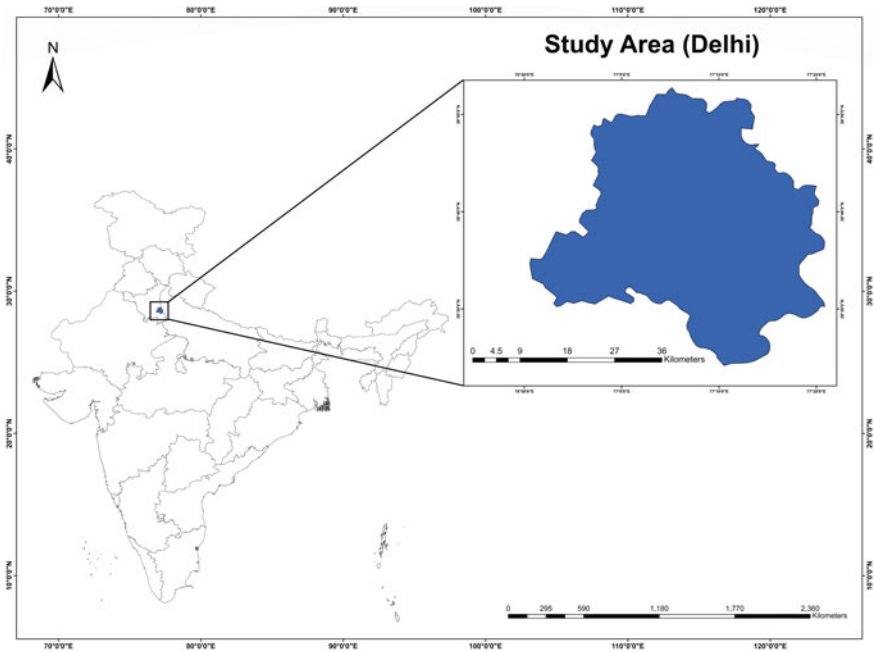


Fig. 1 Study Area

Table 1 Specifications of imagery

Satellite	Sensor	Acquisition date	Resolution (m)
Sentinel 2A	MSI	05 Feb 2016	10
Sentinel 2A	MSI	14 Feb 2020	10

3.1 Data Used

See Table 1.

3.2 Image Processing

Ever since the implementation of satellite-based recording of spectral radiance of ground objects in visible as well as NIR bands became feasible, numerous indices have been developed on the basis of certain amalgamations (addition, difference, division, and calculus based) of those bands [23]. These indices help in the recognition and observation of variations in ground surface objects from time to time. The diversity of such indices gives us an upper hand in many research fields such that

they can lower the effects of external factors, such as solar irradiance, atmospheric influence, etc. [29].

Following indices were used for the assessment of the ecology of the area:

3.2.1 Normalized Difference Moisture Index (NDMI)

NDMI is employed to assess the vegetative-based moisture concentration and water content of water bodies. It is evaluated in the form of ratio amongst the SWIR1 and NIR values.

$$\text{NDMI} = \frac{\text{NIR} - \text{MIR}}{\text{NIR} + \text{MIR}} \quad (1)$$

where MIR and NIR represent the spectral reflectance measurements recorded in the MIR (visible) and near-infrared regions, respectively.

3.2.2 Normalized Built-Up Index (NDBI)

NDBI depicting the soil quality was developed from TM bands employing the normalized difference transformation (NDX) technique [30]. The formula is:

$$\text{NDBI} = \frac{\text{MIR} - \text{NIR}}{\text{MIR} + \text{NIR}} \quad (2)$$

The NDBI provides us with swift mapping of built-up areas or bare land. Even so, this index does not effectively differentiate between the built-up and the open land areas [31–33]. This inadequacy was because of the complex spectral response created by the combination of the spectral responses of built-up regions, vegetative and bare land, mainly in terms of mixed pixels in regions having heterogeneous attributes [31].

3.2.3 Normalized Difference Vegetation Index (NDVI)

NDVI is a simple indicator that can be put in use to assess the remotely sensed measurements, frequently from a space platform, analyzing if the area being studied possesses live vegetative cover or not. NDVI necessarily falls in the range, -1 to $+1$. The NDVI is computed by using the following formula:

$$\text{NDVI} = \frac{\text{NIR} - \text{RED}}{\text{NIR} + \text{RED}} \quad (3)$$

where Red and NIR represent the spectral reflectance measurements recorded in the red (visible) and near-infrared regions, respectively [34].

3.2.4 Modified Normalized Differential Water Index (MNDWI)

MNDWI is proposed to accurately predict and assess the water characteristics. The value of MNDWI spans from -1 to $+1$ as well. MNDWI has been extensively used for analysis of waterlogging by embedding the digital elevation model and groundwater level [35].

$$\text{MNDWI} = \frac{\text{GREEN} - \text{MIR}}{\text{GREEN} + \text{MIR}} \quad (4)$$

3.2.5 Land Surface Temperature (LST)

Heat indicators put in use the surface temperatures instead [36]. Many researchers have put in use Landsat-8-based raster to evaluate land surface temperatures [37, 38].

$$\text{LST} = K_2 / \ln(K_1 / B_{10}(T_s) + 1) \quad (5)$$

where K_1 and K_2 are scaling coefficients mentioned in the metadata file of the images of all three satellites, $B_{10}(T_s)$ of $B_6(T_s)$ of Landsat-8 and Landsat (5 and 7), respectively, are the thermal radiation brightness of a blackbody at the same temperature as T_s (at satellite brightness temperature (K)), and LST is the actual temperature of the surface.

It is quite necessary to mention here that, as the dimensions of all five indices are not same, hence, in accordance to lower the effect of the ambiguity in the numerical values of the indices on the outcome, standardization was performed using Eq. (6).

$$\text{NI} = \frac{I - I_{\min}}{I_{\max} + I_{\min}} \quad (6)$$

where I is the numerical value of an index, NI is value of index after standardization, I_{\max} and I_{\min} are the max and the min values of the index.

3.3 Analytical Hierarchy Process (AHP)

Analytical Hierarchy Process is a method which gives us an edge of combining the various weighted criteria and of resolving complex complications which need to be looked upon from multiple dimensions. It allows a minimum discrepancy in judgment due to inconsistency of human decisions every time. This method was executed in three crucial parts: (a) generation of pair wise comparison matrix, (b) computation of criterion weights, and (c) estimation of consistency ratio (CR). For a swift and better estimation, easy AHP module of QGIS 2.18 was put in use for the execution of these

Table 2 Definition of numerical scales for pair-wise comparison [39]

Preference/ordinal scale	Degree of preference	Remarks
1	Equally	Factors inherit equal contribution
3	Moderately	One factor moderately favoured over other
5	Strongly	Judgement strongly favour one over other
7	Very strongly	One factor very strongly favoured over other
9	Extremely	One factor favoured over other in highest
2, 4, 6, 8	Intermediate	Compensation between weights 1,3,5,7 and 9
Reciprocals	Opposite	Refers inverse comparison

steps. Criteria and alternatives are allotted weights on a 9 point ordinal scale by the efficacy of pairwise comparison amongst them, as mentioned in Table 2 [39]. CR is referred as the ratio between the consistency index (CI) and random index (RI). Where RI is the consistency index of a randomly generated pair-wise comparison matrix. RI was put together based on a number of random samples [40].

Calculation of CI is done in the following way;

$$CI = \frac{\lambda_{max} - n}{n - 1} \tag{7}$$

where λ_{max} = biggest Eigen value of the matrix, n = number of parameters (in this study, $n = 5$).

3.4 Development of GEII

The five important indices/factors pertaining to the survival of humans, i.e. green cover, moisture, surface heat, built-up, and water body are crucial parameters of the environmental conditions. Hence, they were and are often employed to assess ecosystems [41]. Hence, the geospatial ecological impact index (GEII) was developed and expressed as a function of these five parameters/indices that is:

$$GEII = f(G, W, T, M, \text{ and } B) \tag{8}$$

where G is vegetation, W is water body, T is surface temperature, M is moisture content, and B is built-up. GEII maps for all the years were prepared by employing weights generated through AHP to integrate the above mentioned five indices.

3.5 *Ecological Impact Change Identification:*

The ecological change detection in the study area was implemented after developing the GEII for respective years, 2016 and 2020. A pixel-based contrast technique was put in use to produce the changes in reflectance values using ArcGIS 10.5, and later, these changed reflectance values were implemented to interpret the changes in ecological impact grades efficiently. GEII image pairs of year 2016–2020 were analyzed to assess the quantitative as well as qualitative characteristics of the change in the subsequent years.

3.6 *GEII Simulation Modelling Using ANN*

Forecasting the ecological impact incorporates assessing the variations in GEII spectral maps between the two time frames (here, 2016 and 2020) and deducing these changes into future change estimation [42]. In this study, QGIS 2.18 software was put in use for simulation and GEII change prediction modelling. In QGIS 2.18, the Molusce plugin does the simulation and forecast. ANN model was used in this study for ecological impact forecast, as it gives results with less ambiguity, is reliable and hence is much preferred by researchers.

4 Results and Discussion

Year-wise comparison of various Indices and GEII is mentioned in the below given Table 3. This year wise comparison will better differentiate in the ecological quality of Delhi. After comparing the change in 5 indices (which represent the five ecological parameters) and GEII of both the years, it was evident that the trend of GEII/ecological quality is upwards, which indicates that the local ecology has been adversely affected. The average value of GEII elevated from 2.01 in 2016 to 2.45 in 2020.

The maps of the five indices prepared after the analysis and assessment of remotely sensed data for the years 2016 and 2020 are as shown in Figs. 2 and 3 (Table 4).

To analyze reasonableness of the index efficiently, the GEII of respective years was grouped into 5 categories, representing 5 grades (Very High, High, Medium, Low

Table 3 The average change of 5 indices and GEII of the study area

Year	NDMI	NDBI	NDVI	MNDWI	LST	GEII
2016	0.48	0.074	0.41	0.61	18.04	2.01
2020	0.39	0.087	0.48	0.57	19.54	2.45

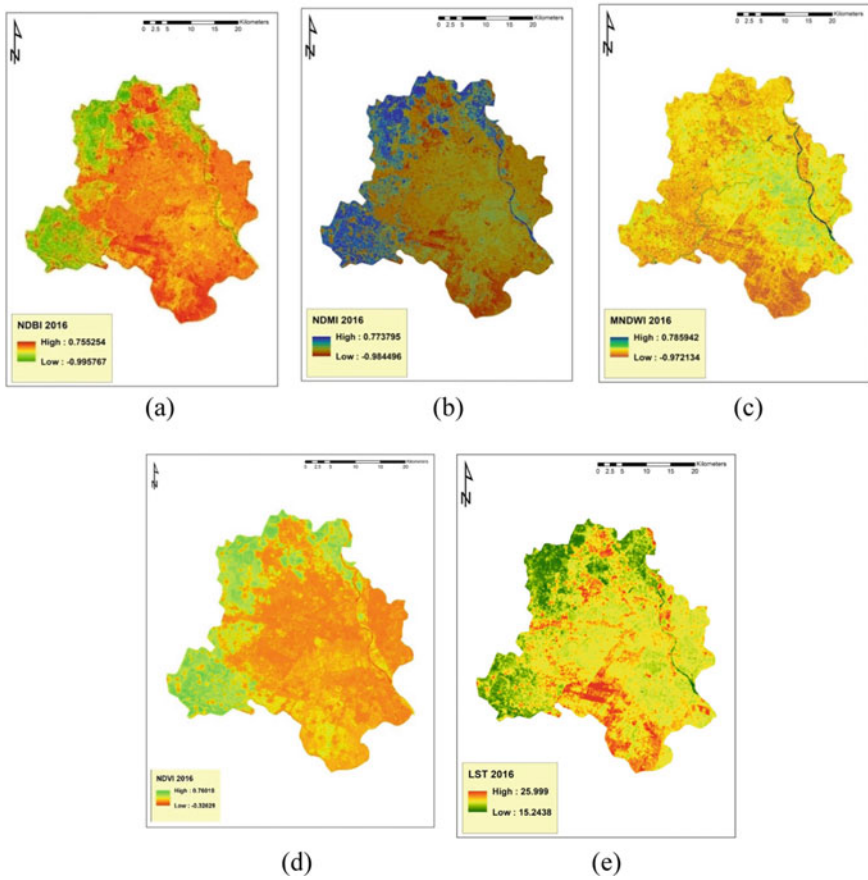


Fig. 2 Maps of the five indices 2016

and Least Impact) of ecological environment (Fig. 4). This grading gave a better and easy way to determine that the southern part of Delhi is most affected (Table 5).

4.1 GEII Prediction Modelling:

GEII spectral maps of 2016 and 2020 were set as input data to predict the 2024 ecological impact map. The prediction was carried out by using the Molusce plugin in QGIS 2.18. As per the assessment carried out, it was found that the ecological impact will get adverse by the year 2024 and high impact and moderate impact zones will expand and hold 23.50% and 41.96% of Delhi’s area respectively (Table 6). This on the go predicted map clearly depicts that, if the prevailing conditions continue, then the ecological quality of Delhi will worsen (Fig. 5).

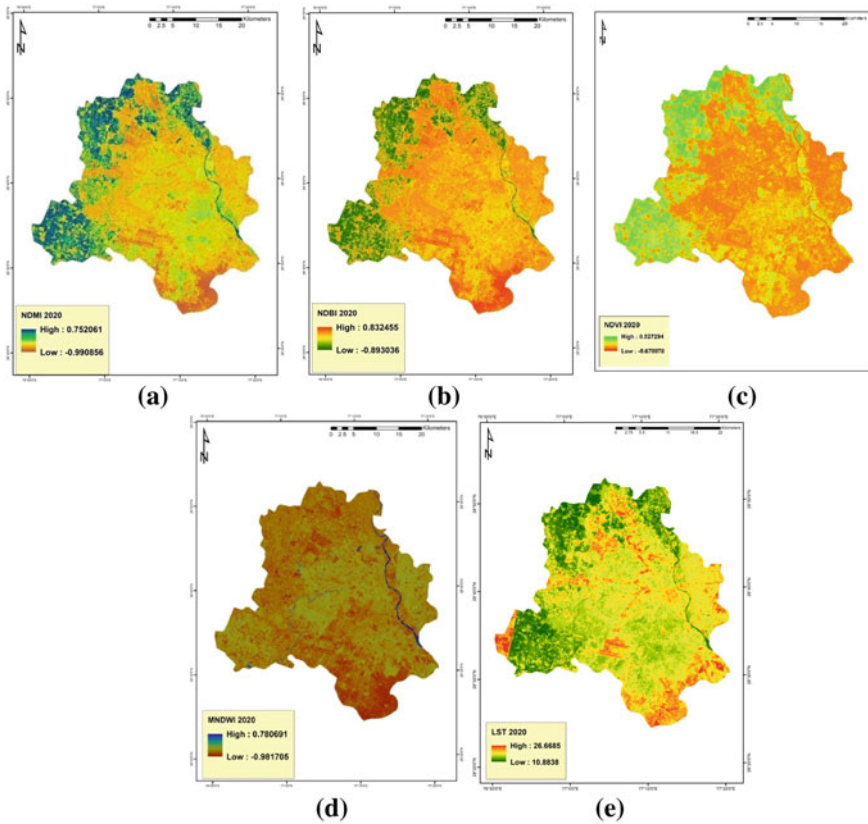


Fig. 3 Maps of the five indices 2020

Table 4 Weighted linear combination (WLC)

S. No.	Index name	Weights	
		2016	2020
1	NDMI	0.241	0.07
2	NDBI	0.206	0.206
3	NDVI	0.189	0.138
4	MNDWI	0.265	0.152
5	LST	0.099	0.433

5 Conclusion

It was also clearly revealed from the outcomes of the study that the phenomenon of urbanization is causing serious and long lasting impacts on the ecology. The predicted GEII map for the year 2024 can be looked upon as an alarm which is continuously

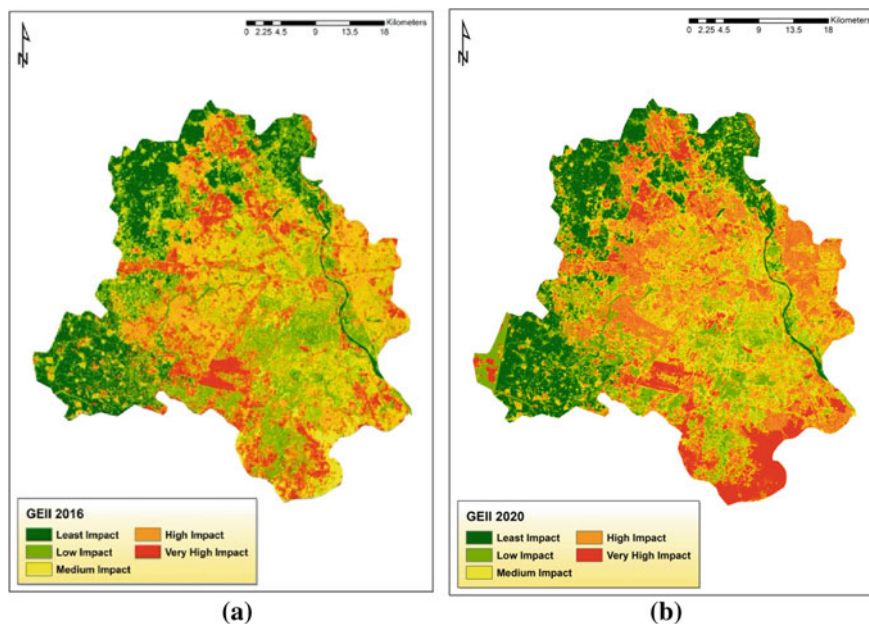


Fig. 4 Ecological impact zones for 2016 and 2020

Table 5 Area and proportion of ecological grade of Delhi

GEII (ecological impact)	2016		2020	
	Area (km ²)	Area (%)	Area (km ²)	Area (%)
Least impact	236.83	15.96	229.26	15.45
Low impact	408.39	27.52	318.43	21.46
Moderate impact	373.93	25.20	376.48	25.37
High impact	211.31	14.24	235.49	15.87
Very high impact	253.54	17.08	324.34	21.86
Total	1484	100	1484	100

Table 6 Area and proportion of simulated ecological grade

GEII (ecological impact)	2024	
	Area (km ²)	Area (%)
Least impact	317.68	21.41
Low impact	151.30	10.20
Moderate impact	622.72	41.96
High impact	348.80	23.50
Very high impact	43.50	2.93
Total	1484.00	100

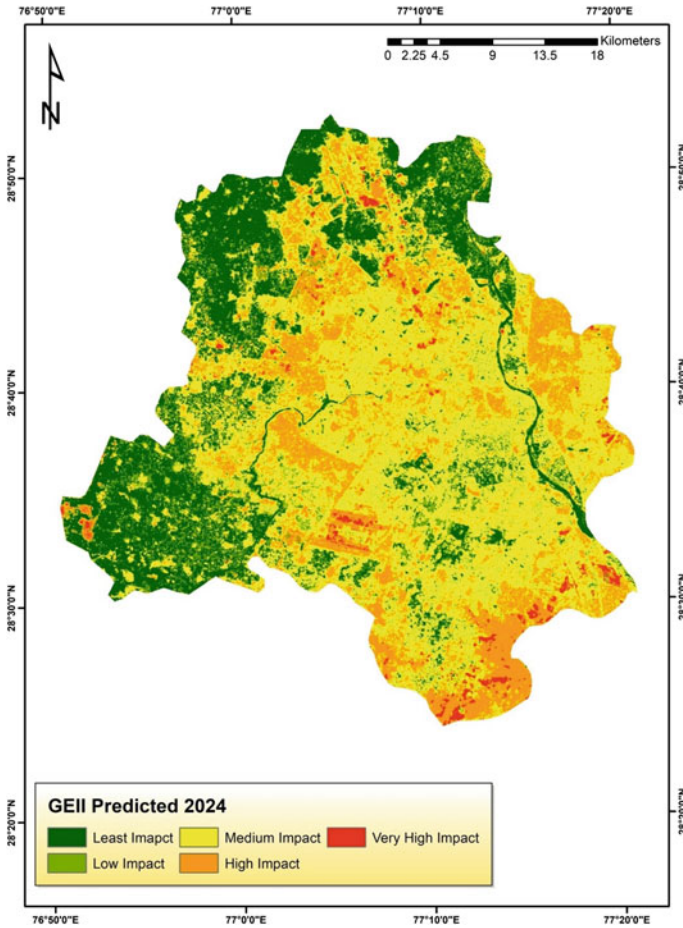


Fig. 5 Predicted map of ecological impact zones for 2024

ticking. The predicted map can help urban planners and decision-makers to mitigate and resolve the problems associated with increasing urbanization in transition zones. Henceforth, this study manifests the urgency and seriousness for closely keeping an eye on the rural-to-urban transformation, which will eventually help the decision-making authorities for recognizing the critical areas that act as a hotspot for increasing urbanization. In order to lower the adverse effects of urban sprawl, the government needs to adopt better urban planning and management ventures/techniques. This combined analysis of increasing levels of urbanization along with the ecological attributes justifies the present environmental position of Delhi.

References

1. Niyogi D et al (2018) The impact of land cover and land use change on the Indian monsoon region hydroclimate. pp 553–575. https://doi.org/10.1007/978-3-319-67474-2_25
2. Angel S, Parent J, Civco D (2007) Urban sprawl metrics: An analysis of global urban expansion using GIS. In: American society for photogrammetry and remote sensing—ASPRS annual conference 2007: identifying geospatial solutions, vol 1, pp 22–33
3. Sinha RK, Sharma A (2006) Landscape level disturbance gradient analysis in Daltonganj south forest division. *J Indian Soc Remote Sens* 34(3):233–243. <https://doi.org/10.1007/BF02990652>
4. Guo H, Zhang B, Bai Y, He X (2017) Ecological environment assessment based on remote sensing in Zhengzhou. In: IOP conference series earth environment science, vol 94(1). <https://doi.org/10.1088/1755-1315/94/1/012190>
5. Trivedi RK, Chourasia LP, Singh DK (2006) Application of remote sensing in the study of geo-environmental aspects of Rajghat DAM project. *J Indian Soc Remote Sens* 34(3):309–317. <https://doi.org/10.1007/BF02990659>
6. Tang UW, Wang ZS (2007) Influences of urban forms on traffic-induced noise and air pollution: results from a modelling system. *Environ Model Softw* 22(12):1750–1764. <https://doi.org/10.1016/j.envsoft.2007.02.003>
7. Nikolakopoulos KG, Vaiopoulos DA, Skianis GA (2007) Use of multitemporal remote sensing data for mapping the Alfios River network changes from 1977 to 2000. *Geocarto Int* 22(4):251–271. <https://doi.org/10.1080/10106040701204727>
8. Kunwar P, Kachhwaha TS (2003) Spatial distribution of area affected by forest fire in Uttaranchal using remote sensing and GIS techniques. *J Indian Soc Remote Sens* 31(3):145–148. <https://doi.org/10.1007/BF03030821>
9. Dwivedi RS, Sreenivas K, Ramana KV, Sujatha G, Sharma KL (2006) Delineation of lands affected by Tanneries' Effluents: a remote sensing and GIS approach. *J Indian Soc Remote Sens* 34(1):95–100. <https://doi.org/10.1007/BF02990751>
10. Goyal VC, Jain SK, Pareek N (2005) Water logging and drainage assessment in Ravi-Tawi Irrigation command (J&K) using remote sensing approach. *J Indian Soc Remote Sens*. 33(1):7–15. <https://doi.org/10.1007/BF02989986>
11. Dwivedi RS, Ramana KV, Sreenivas K (2007) Temporal behavior of surface waterlogged areas using spaceborne multispectral multitemporal measurements. *J Indian Soc Remote Sens* 35(2):173–184. <https://doi.org/10.1007/BF02990781>
12. Rout DK, Parida PK, Behera G (2005) Man-made disaster-a case study of NALCO Ash-pond in the Angul district, Orissa using remote sensing and GIS technique. *J Indian Soc Remote Sens* 33(2):291–295. <https://doi.org/10.1007/BF02990048>
13. Kunwar TS, Kachhwaha P, Assessment soil erosion hazard through remote sensing and GIS technique in Kuthlar Gad Sub-watershed, Almora District, Uttar Pradesh, pp 212–215
14. de Asis AM, Omasa K (2007) Estimation of vegetation parameter for modeling soil erosion using linear spectral mixture analysis of landsat ETM data. *ISPRS J Photogram Remote Sens* 62(4):309–324. <https://doi.org/10.1016/j.isprsjprs.2007.05.013>
15. Das JD, Dutta T, Saraf AK (2007) Remote sensing and GIS application in change detection of the Barak River channel, N.E. India. *J Indian Soc Remote Sens* 35(4):301–312. <https://doi.org/10.1007/BF02990786>
16. Durbude DG, Purandara BK (2005) Assessment of sedimentation in the Lingankakki reservoir using remote sensing. *J Indian Soc Remote Sens* 33(4):503–509. <https://doi.org/10.1007/BF02990735>
17. Rathore DS, Choudhary A, Agarwal PK (2006) Assessment of sedimentation in Harakud reservoir using digital remote sensing technique. *J Indian Soc Remote Sens* 34(4):377–383. <https://doi.org/10.1007/BF02990922>
18. Ochoa-Gaona S, Kampichler C, de Jong BHJ, Hernandez S, Geissen V, Huerta E (2010) A multi-criterion index for the evaluation of local tropical forest conditions in Mexico. *For. Ecol. Manage.* 260(5):618–627. <https://doi.org/10.1016/j.foreco.2010.05.018>

19. Xu H, Wen X, Ding F (2009) Urban expansion and heat island dynamics in the Quanzhou region, China. *IEEE J Sel Top Appl Earth Obs Remote Sens* 2(2):74–79. <https://doi.org/10.1109/JSTARS.2009.2023088>
20. Chen A, Sun R, Chen L Studies on urban heat island from a landscape pattern view: a review. *Shengtai Xuebao/Acta Ecol Sin* 32(14):4553–4565. <https://doi.org/10.5846/stxb201106280965>
21. Wen XL, Xu H-Q, Remote sensing analysis of impact of Fuzhou city expansion on water quality of Lower Minjiang River, China. *Sci Geogr Sin* 30(4):624–629
22. Xu H (2013) “Remote sensing evaluation index of regional ecological environment change. *Chinese Environ Sci*
23. Somvanshi SS, Kunwar P, Tomar S, Singh M (2018) Comparative statistical analysis of the quality of image enhancement techniques. *Int J. Image Data Fusion* 9(2):131–151. <https://doi.org/10.1080/19479832.2017.1355336>
24. Zhang Z, He G (2013) Generation of Landsat surface temperature product for China, 2000–2010. *Int J Remote Sens* 34(20):7369–7375. <https://doi.org/10.1080/01431161.2013.820368>
25. Weng Q, Fu P (2014) Modeling annual parameters of clear-sky land surface temperature variations and evaluating the impact of cloud cover using time series of Landsat TIR data. *Remote Sens Environ* 140:267–278. <https://doi.org/10.1016/j.rse.2013.09.002>
26. Weng Q, Fu P, Gao F (2014) Generating daily land surface temperature at Landsat resolution by fusing Landsat and MODIS data. *Remote Sens Environ.* 145:55–67. <https://doi.org/10.1016/j.rse.2014.02.003>
27. Roy DP et al (2014) Landsat-8: science and product vision for terrestrial global change research. *Remote Sens Environ* 145:154–172
28. Huang C, Goward SN, Masek JG, Thomas N, Zhu Z, Vogelmann JE (2010) An automated approach for reconstructing recent forest disturbance history using dense Landsat time series stacks. *Remote Sens Environ* 114(1):183–198. <https://doi.org/10.1016/j.rse.2009.08.017>
29. Girard M-C, Girard C (2003) Processing of remote sensing data. CRC Press Taylor Fr. Gr., p 508
30. Rogers AS, Kearney MS (2004) Reducing signature variability in unmixing coastal marsh Thematic Mapper scenes using spectral indices. *Int J Remote Sens* 25(12):2317–2335. <https://doi.org/10.1080/01431160310001618103>
31. He C, Shi P, Xie D, Zhao Y (2010) Improving the normalized difference built-up index to map urban built-up areas using a semiautomatic segmentation approach. *Remote Sens Lett* 1(4):213–221. <https://doi.org/10.1080/01431161.2010.481681>
32. Zha Y, Gao J, Ni S (2003) Use of normalized difference built-up index in automatically mapping urban areas from TM imagery. *Int J Remote Sens* 24(3):583–594. <https://doi.org/10.1080/01431160304987>
33. Sukrisyanti (2007) Evaluasi Indeks Urban Pada Citra Landsat Multitemporal Dalam Ekstraksi Kepadatan Bangunan. *J Ris Geol dan Pertamb* 17(1):1. <https://doi.org/10.14203/risetgeotam2007.v17.153>
34. Ruíz AAB (2015) Measuring vegetation. *NASA Earth Observat* 3(2):54–67
35. Zubair S, UIWafa B, Somvanshi SS, Kumari M, Comparative analysis of different satellite based water indices for the assessment of water bodies. In: National conference on recent trends in environmental pollution & disaster risk reduction
36. Li F, Chang Q, Shen J (2015) Ecological environment of the loess plateau gully areas of remote sensing dynamic monitoring. Taking Shaanxi Province as an example in. *Chinese J Appl Ecol* 3811–3817
37. Li H et al Evaluation of the VIIRS and MODIS LST products in an arid area of Northwest China. *Remote Sens Environ* 142:111–121. <https://doi.org/10.1016/j.rse.2013.11.014>
38. Liu F (2012) Retrieval of surface temperature by remote sensing
39. Saaty TL (1977) A scaling method for priorities in hierarchical structures. *J Math Psychol* 15(3):234–281. [https://doi.org/10.1016/0022-2496\(77\)90033-5](https://doi.org/10.1016/0022-2496(77)90033-5)
40. Saaty TL (2000) Fundamentals of decision making and priority theory with the analytic. p 478

41. Song HM, Xue L (2016) Dynamic monitoring and analysis of ecological environment in Weinan City, Northwest China based on RSEI model. *Chinese J Appl Ecol* 27(12):3913–3919. <https://doi.org/10.13287/j.1001-9332.201612.024>
42. Eastman JR, IDRISI Taiga: guide to gis and image processing, p 342.

Defluoridation of Drinking Water–Fluoride Wars



G. Gayathri, M. Beulah, H. J. Pallavi, and K. Sarath Chandra

Abstract Fluorine is also known as two-edged sword. At lower doses, it influences tooth by inhibiting tooth caries, while in high doses, it causes dental and skeletal fluorosis. It is known that some quantity of fluoride is important for the formation of tooth enamel and mineralization in tissues. The present work aims at providing safe and potable water to rural areas where this element has created a menace. This work also suggests the use of few adsorbents such as paddy husk and coir pith which are affordable and removes fluorine to greater extent. The study concludes that materials which are used as adsorbents and can be safely inculcated as fluorine removal adsorbents which help people to have safe potable water.

Keywords Fluorine · Potable water · Ground water · Contamination

1 Introduction

Fluorine is the most electronegative element in the periodic table and has much impact confiding on its application. The component is transfigured together in distinction with compounds that are electrovalent and covalent. By growing the size of the apatite crystals and their solubility, low doses of fluoride stimulate the skeletal system. Approximately, 95% of the fluoride is in hard tissues and even after other bone constituents have achieved a steady state, it seeks to be in harden indurate [1].

Health impacts from prolonged intake of fluoride-contaminated water are:

G. Gayathri (✉) · H. J. Pallavi
Department of Civil Engineering, ACS College of Engineering, Bengaluru, India
e-mail: gayathri.jayaram30@gmail.com

H. J. Pallavi
e-mail: pallavij16@gmail.com

M. Beulah · K. Sarath Chandra
Department of Civil Engineering, Christ Deemed To Be University, Bengaluru, India
e-mail: m.beulah@christuniversity.com

K. Sarath Chandra
e-mail: sarathchandra.k@christuniversity.in

- < .5 mg/L: dental problem
- 0.5–1.5 mg/L: inhibits dental health
- 1.5–4.0 mg/L: dental fluorosis;

The furnishing of fluoride free (<1.5 mg/L) potable water can curtail the pathological state associated to fluoride malignancy [2]. The supply of water from rivers for drinking to the residents of distant villages is impervious due to the huge capital obligation for changing technology. The easy and affordable strategy to have secure drinking water is the therapy of high fluoride polluted(>1.5 mg/L) ground water. Accordingly, the defluoridation of potable water is the only feasible alternative choice to get the better of immoderate fluoride in drinking water [3]. Lots of work has been conducted on various methods of extracting fluoride from water and detection of fluoride as the root of fluorosis [4].

The methods are.

- (1) Precipitation–coagulation.
- (2) Sorption
- (3) Ion-exchange
- (4) Membrane separation
- (5) Electrochemical methods.

In India, fluoride in the water affects Tamilnadu, Uttar Pradesh, Andhra Pradesh, Bihar, Chhattisgarh, Haryana, Orissa, Rajasthan, Madhyapradesh, Punjab, Karnataka, and West Bengal. This involves about 10,000 villages impacting 35 million people [5]. In the table below, the fluoride content of the water in some villages is given.

There are multiple causes of water accumulation of fluoride concentration. Tilling up of shallow aquifers has contributed to low levels of groundwater, so that aquifers containing excessive fluoride are in volume [6] (Table 1).

Fluoride Distribution in Karnataka State

In Karnataka, in ground water, fluoride varies from 0 to 8 mg /l. Groundwater usually displays values within the acceptable limits of the Bureau of Indian Drinking Water

Table 1 Fluoride concentration in distinct states of India [2]

Place	Fluoride in PPM
Himachal Pradesh	0.2–6.5
Jammu and Kashmir	0.2–18
Rajasthan	>1.5
Haryana	0.2–0.6
Bihar	0.35–15
Orissa	8.2–13
Maharashtra	0.7–6.0
West Bengal	12.0
Chhattisgarh	15–20

Table 2 Concentration distribution of fluoride in Karnataka

Place	Fluoride in mg/lit
Gulbarga	4.6
Raichur	4.18
Bellary	3.32
Tumkur	1.82
Chitradurga	2.29
Kolar	2.21

Requirements from the districts of Belgaum, Bidar, Dakshina Kannada, chickamagalur, Kodagu, Hassan, Udupi, Shimoga, and Uttara Karnataka. Parts of the Bellary, Bijapur, Chitradurga and Gulbarga, Kolar, Mandya, Mysore, and Raichur districts have elevated levels of fluoride content above the permitted limits [7] (Table 2).

Sources of Fluoride and Optimum Intake

There is no across the board optimal level for the daily intake of fluoride that enhances shielding against tooth decay while diminishing other risks, but the permissible limit is 0.05–0.07 mg of fluoride. Sources of fluoride for human consumption include tea, meat, fish, cereals, and fruits. Fluoride is also imbibed from toothpaste and other oral solutions. The concentration of fluoride in farm crops and other foodstuffs is listed below in Table 3. Though fluoride ingestion into the body is through various sources, the optimum intake can be achieved by limiting its levels in water rather than in food. Therein lies the importance of defluoridation of drinking water. High fluoride impacts have been reported in ground waters of over 23 countries. The problem of acute fluorosis in 19 states is faced by developed and developing countries, including India. Fluorine is one of the most common inorganic natural pollutants present in ground water in India (Table 3).

In India the need of the hour is defluoridation rather fluoridation. In thousands of villages in our country, fluoride level is so high that the water is unsafe to drink. More than 25 million people in our country are affected by fluorosis [8]. Using some materials as adsorbents like Amla was performed & inferred it can be a effective adsorbent [9]. Bagasse dust (BD), bagasse flyash (BF), aluminum treated bagasse flyash (ABF), buffalo bone powder (BP) and clam shell powder is used for ground-water containing fluoride (SP) [4]. One of the inborn substitutes for defluoridation of water is *Moringa Oleifera*., optimal dose of adsorbent was determined. From the

Table 3 Fluoride concentrations (mg/g or mg/kg) in agricultural crops and other edible items [3]

Food	Amount (g)	Fluoride (mg)	Food item	Amount (Kg)	Fluoride (mg)
Rice	100	3.5	Wheat	1	4.6
Tea	100	1.41	Rice uncooked	1	5.9
Coffee	100	5.0	Apple	1	5.7
Noodles	100	4.6	Rock salts	1	200–250

results obtained, it can be concluded that *Moringa Oleifera* can become an affordable alternative for defluoridation of water [10].

2 Materials and Methods

The present work aims at emerging an affordable and safe method of defluoridation which can reach any common lame person. Affordable and non-toxic adsorbents that are locally available are used and batch tests are performed. Husk Paddy powder. Coir pith powder of mixed different proportions is used for conducting experiments.

2.1 Physical and Chemical Characteristics of Adsorbents

Paddy husk. An enhanced adsorbent paddy husk is used as an adsorbent in this present work [11]. The impact of different parameters like adsorbent dosage, pH, initial concentration of fluoride ions, contact duration, presence of other interfering anions was studied [13].

Coir pith. The coir pith is the soft component that connects the coir fiber in the husk. The structure and properties of the coir pith vary depending on the maturity of the coconut, the method of unsheathing and disposal, the time period between extraction, usage, and environmental factors.



The Advantages of Coir Pith Are

- High water holding capacity
- Excellent moisture retention
- Greater physical resiliency.
- Excellent aeration providing enhanced root penetration.

2.2 Methodology

Paddy husk was crushed in a grinder to get a uniform grain size 1.6–1.8 mm. Sieve analysis was performed to obtain the size consistency. Coir pith was crushed in a grinder to get a steady grain size of 1.6–1.8 mm.

Batch Experiments

50 ml of water was applied to the specified concentration of adsorbent. The initial CF concentration was about 2.5 mg/l. The mixture was perturbed by the application of magnetic stirrer and fluoride concentration was determined using SPADN method. The investigation is recurred at various time interims for two adsorbents in application. The results are compiled and charted. It is floated that the initial fluoride strength substantially turned down and nearer to the allowable standards (Figs. 1 and 2).

At different time intervals and different flow rates, batch measurements are performed. In batch tests, the length of time for which non-toxic and inexpensive adsorbents are used is the only parameter monitored (Fig. 3).

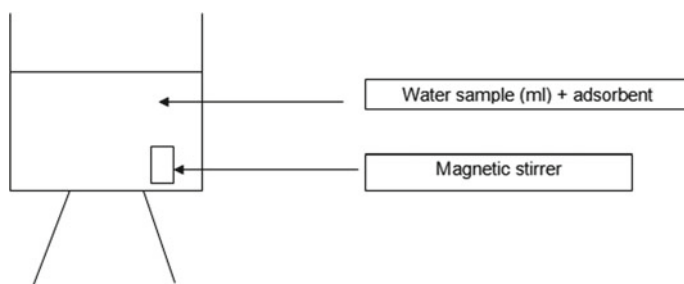


Fig. 1 Batch experiment, experimental setup

Fig. 2 Spectrophotometer
UV



Fig. 3 Magnetic stirrer

3 Results and Discussions

This work concludes the defluoridation of water which included a detailed study and assessment and application of different adsorbents to contain fluoride in drinking water.

3.1 Results of Batch Experiments

Paddy husk 1.6–1.8 mm grain powder was taken and fluoride was analyzed and found that 1 gm of paddy husk powder decreased from 2.5 to 0.95 mg/l. As a material for defluoridation, paddy husk may also be used. But it slightly imparts colour to the defluoridated water that has not been taken and certified to undergo batch processing. Different quantities of paddy husk powder of 0.5 and 1 gm were added and a batch process was conducted. Fluoride was tested and it reduced by 0.5 gm of paddy husk powder from 2.5 to 1.15 mg/l.

Coir pith powder 1.6–1.8 mm grain powder was taken and allowed to undergo batch experiment. Various amounts of 0.5 gm and 1 gm of coir pith powder were added and the batch process was performed. Fluoride in 0.5 gm of coir pith powder was measured and decreased from 2.5 to 1.4 mg/l. Fluoride was calculated in 1 gm of coir pith powder and the decrease was observed from 2.5 to 0.9 mg/l. Coir pith may thus also be used as a material for defluoridation. However, it imparts color slightly to flourine removed water, which is not detrimental to health, but color removal methods can be suggested (Tables 4 and 5).

Table 4 Batch experiment results using paddy husk as adsorbent

Sl. No.	Initial Cf in mg/l	Final Cf in mg/l		Adsorbents/paddy husk (g)		Time in sec
1	2.5	2.4	1.26	0.5	1.0	900
2	2.5	1.8	1.1	0.5	1.0	1800
3	2.5	1.71	1.0	0.5	1.0	2700
4	2.5	1.15	0.95	0.5	1.0	3600

Table 5 Batch experiment results using coir pith as adsorbent

Sl. No.	Initial Cf in mg/l	Final Cf in mg/l		Adsorbents /coir Pith (g)		Time in s
1	2.5	2.2	1.5	0.5	1.0	900
2	2.5	1.7	1.3	0.5	1.0	1800
3	2.5	1.5	1.0	0.5	1.0	2700
4	2.5	1.4	0.9	0.5	1.0	3600

3.2 Results of All Used Adsorbents Are Graphically Tabulated as Follows

The above figure shows the fluoride intensity in water, Where Cf decreased rapidly for about 15 min and for 60 min steadily reached a constant value. By using a higher dose of adsorbent and performing a batch experiment, a constant value of 1.4 mg / hence coir pith can be used as one of the adsorbents for the defluoridation of drinking water. But, after the defluoridation process, it imparts color along with little turbidity. By using activated charcoal, rice bran, rice husk and bran and husk mixture, various techniques have been developed and suggested by Researchers for color removal (Figs. 4 and 5).

The above figure indicates that the fluoride concentration rapidly decreased for 15 min when particle 1.6–1.8 mm paddy husk was used and batch testing was

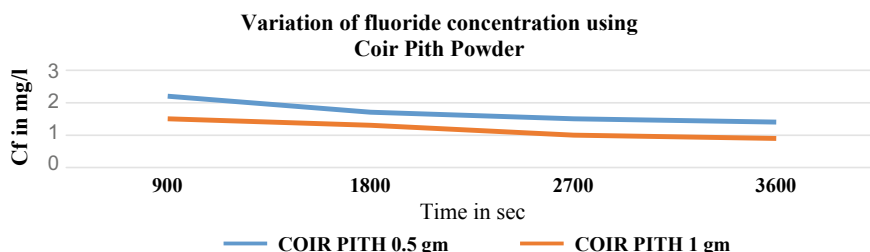


Fig. 4 Differentiation of fluoride intensity in water Cf in batch investigation with time t. Cf = 2.5 mg/l, particle size = 1.6–1.8 mm, added adsorbent mass = 0.5 g, 1.0 g, 1.5 g. adsorbent-coir pith

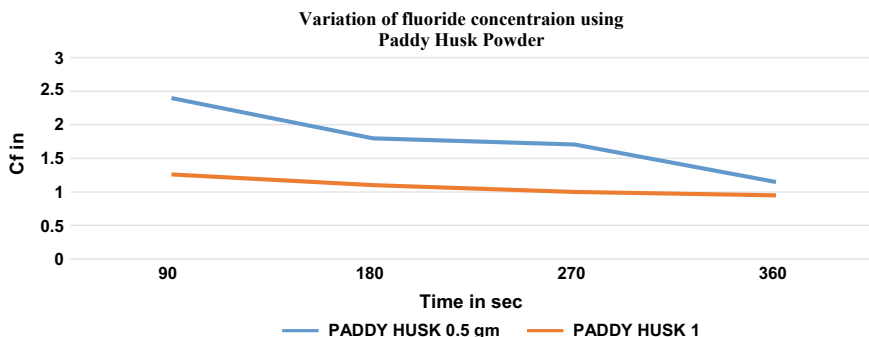


Fig. 5 Differentiation of fluoride intensity in water C_f in a batch investigation with time t . $C_f = 2.5$ mg/l, particle size = 1.6–1.8 mm, added adsorbent mass = 0.5 g, 1.0 g, 1.5 g. Paddy husk is adsorbent

performed and obtained a constant value of 1.1 mg/l at 2900 s. After defluoridation, the water achieved a constant value with an initial concentration of 2.5 mg/l, indicating that it could be used as a defluoridating agent. In grammes, weights of distinct proportions were introduced and variation was observed. During the process, the water is defluoridated but methods are to be developed for color removal.

4 Conclusions

The aim of this work is to establish a rural-level system for drinking water defluoridation. Several methods for extracting fluorine have been developed that require costly and sophisticated equipment. These cannot be met by the common man at the rural stage. Consequently, an attempt was made to test the defluoridation study. Thus, also in rural areas, fluorine removal is feasible at a significantly affordable rate. The removal capability has also improved as the particle size has improved. This technique is readily available for simple adsorbents. Paddy husk and coir pith have been shown to be efficient for defluoridation. When used as an adsorbent, the fluoride concentration has decreased and is therefore sufficient for this phase.

The desirable grain size of coir pith powder was obtained and it was found to be a cost-implementative method of minimizing drinking water fluorine. In addition, both adsorbents with the greatest defloridizing potential are ideally matched to the adsorbent used in the batch experiment. However, for defluoridation, all adsorbents may be used, but methods for color removal and turbidity must be created.

Therefore, this research can show that many such adsorbents can be used for drinking water defluoridation. At domestic and rural levels, this can be used. The method is so simple that no expensive, non-available chemical substances are needed. Fuel is not required, and this is eco-friendly. Such methods of using adsorbents are both non-toxic and safe.

References

1. Poonam M, Vijeyta S, Deepmala V, Chauhan OP, Rai GK (2018) Physico-chemical properties of Chakiya variety of Amla (*Emblicaofficinalis*) and effect of different dehydration methods on quality of powder
2. Gayathri G, Kumar Raju BC, Dinesh SR (2017) Defluoridation of ground water using low cost adsorbents. 10(05): 967–972. ISSN 0974–5904
3. Pali S, Godbole BJ, Sudame AM (2013) Removal of fluoride from aqueous solution by using low cost adsorbent. Int J Innov Res Sci Eng Technol 2(7)
4. Parlikar AS, Mokashi SS (2013) Defluoridation of water by *Moringaoleifera*-a natural adsorbent. Int J Eng Sci Innov Technol (IJESIT) 2(5)
5. Koteswara R, Mallikarjun M (2014) Effective low cost adsorbents for removal of fluoride from water. 3(6)
6. Prosanta KD, Afroza A, Md. Abdul M (2014) Physico-chemical characterization and product development from turmeric (*Curcuma Longa*) germplasm available in South Western Region of Bangladesh. 4(1):484–494
7. Santhi D, UmayoruBhagan V, LekshmanaSarma R (2005) Defluoridation of drinking water using locally available low cost adsorbents. J Ind Pollut Control 21(2):397–400
8. Bulusu (1979) Fluorides in water-defluoridation methods and their limitations. J Inst Eng 60:2–6.
9. Gupta N, Gupta V, Singh AP, Singh RP (2014) Defluoridation of groundwater using low cost adsorbent like bagasse dust, aluminum treated bagasse flyash, bone powder and shell powder. Bonfring Int J Indus Eng Manage Sci 4(2)
10. APHA (2000) Standard methods for examination of water and wastewater, 18th edn. American Public Health Association, Washington DC
11. Jamode AV, Sapkal VS, Jamode VS (2004) Uptake of fluoride ions using leaf powder of *Ficusreligiosa*. J Inst Wat Works Ass 36:19–22

A Review of Electric Power Generation from Solar Ponds Using Organic Rankine Cycle and Air Turbine



Gaurav Mittal, Desh Bandhu Singh, Gaurav Singh, and Navneet Kumar

Abstract Salinity gradient solar ponds have high thermal capacity and collect and store thermal energy for long duration of time. Thermal energy in solar ponds, at temperature less than 90 °C, is low grade energy. Several researchers have explored the possibility of using organic Rankine cycle and air turbine for efficient conversion of thermal energy of solar pond into electrical energy. This paper reviews various approaches that have been proposed in this direction. It is noted that the solar-to-electrical conversion efficiency of these systems is low and it has discouraged large-scale commercialization of these systems. Improvements in the design of solar ponds for enhanced capturing of solar energy can potentially make them economical for cogeneration of heat and electricity.

Keywords Solar pond · Electric power · ORC · Air turbine · Solar energy

1 Introduction

Solar ponds collect solar radiation and also store it as thermal energy for long duration of time [1, 2]. In salinity gradient solar ponds (SGSP), salt concentration gradient is established in the pond and salinity decreases from close to saturation (approximately 20%) at the bottom to very low value at the top. The purpose of establishing salt gradient is to have higher density at the bottom of the pond and thereby inhibit free convection even when favorable temperature gradient is established by absorption of solar radiation. Since water is opaque to infrared radiation, infrared part of the

G. Mittal · D. B. Singh (✉)

Department of Mechanical Engineering, Graphic Era Deemed to be University, Bell Road, Clement Town, Dehradun, Uttarakhand 248002, India
e-mail: Deshbandhusingh.me@geu.ac.in

G. Singh

School of Basic and Applied Science, Galgotias University, Plot 2, Sec-17 A, Yamuna Expressway, Greater Noida, India

G. Singh · N. Kumar

Galgotias College of Engineering and Technology, Plot No. 1, G.B. Nagar Knowledge Park II, Greater Noida, Uttar Pradesh 201306, India

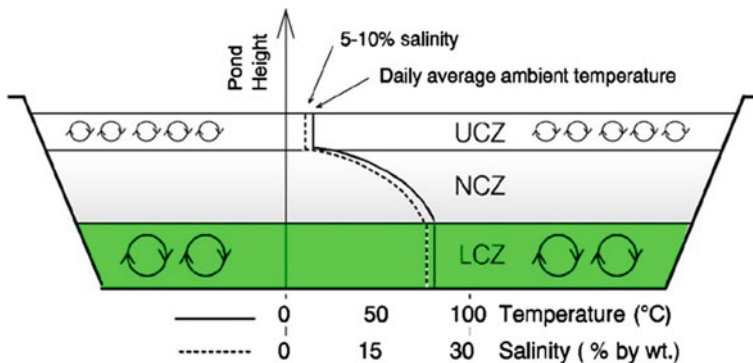


Fig. 1 Salinity gradient solar pond [2]

solar radiation is absorbed by the top layers of water and lost to the surrounding by convection, radiation, and evaporation. However, a part of the radiation in the ultraviolet and visible region is absorbed and stored as thermal energy by the bottom layers of water.

Non-convecting SGPS consists of three zones, namely lower convective zone (LCZ), non-convective zone (NCZ), and upper convective zone (UCZ), as shown in Fig. 1. The heat loss from the bottom LCZ is avoided by the NCZ which remains more or less stagnant despite of the temperature gradient due to the density gradient established by the gradient in salinity. The temperature at the bottom of the pond can reach up to 90 °C and the temperature difference between the top and the bottom can be 50–0 °C. Solar ponds are attractive only in low to moderate latitudes [3, 4] because they are like horizontal solar collectors.

Since solar ponds constitute source of low grade thermal energy, the power generation approach is different from the approach used with fossil fuels-based power cycles. In order to produce electric power from solar ponds, extensive research has been done. Potential methods include use of organic Rankine cycle, solar chimney integrated with air turbine [5], and thermoelectric generators. Ding et al. [6], Kasaeian et al. [7], and Karthick et al. [8] recently reviewed some of these configurations. In the following, the approaches for solar pond power plant (SPPP) based on ORC and air turbines are reviewed.

2 Solar Pond Power Plant Using Organic Rankine Cycle

2.1 Organic Rankine Cycle

The peak temperature realized in a solar pond is less than 100 °C, making it appropriate for Rankine cycles that are based on organic fluids having low boiling point

such as propane, isobutane, and R134a. In contrast with steam cycle, these fluids are able to evaporate at much lower temperature and pressure. Rankine cycles based on these fluids are called organic Rankine cycles (ORC) and have been amply reviewed for applications with low-grade thermal energy [9, 10]. The configuration of the SGPS provides both source and sink for an ORC. The UCZ zone serves the purpose of cold sink for the condenser, while the hot LCZ zone supplies thermal energy to the boiler. In the closed cycle, the working fluid is expanded in the turbine, condensed in the condenser, and finally pumped to the boiler [11].

Research on solar pond-based ORCs started in Israel in 1970s, and many power plants based on this concept were built and operated across the world demonstrating ORC as a successful concept to produce electricity from solar ponds. Notable among the plants that were built are 5 MW-250,000 m² SPPP at Beith Ha'arava, Israel [12]; 15 kW-1600 m² plant at Alice Springs, Australia; 150 kW-7000 m² SPPP at EinBokek, Israel [13] and 70 kW-3350 m² SPPP at El Paso, USA.

The thermal efficiency of a solar pond is in the range of 15–25%. This is defined as the ratio of the thermal energy captured by the pond to the incident solar radiation. Assuming a temperature difference of 60 °C between the LCZ and UCZ, an efficiency of 20% for the solar pond heat extraction and an efficiency of 70% of Carnot efficiency for the ORC, the theoretical solar-to-electric conversion efficiency turns out to be 2.5% at best. Practically, solar-to-electric conversion efficiency of 0.8–2% is realized [14]. Owing to the low efficiency, the concern of economic viability of solar pond-based ORCs has attracted much attention over the years.

Nearly half a century ago, Bectel [15] explored a solar pond power plant with a pond area of 1 km² using F-11 as the working fluid. In comparison with a traditional power plant of same power, the cost of the SPPP was estimated to be five times greater [15]. Khalil et al. [4] investigated the prospects of using an SPPP for production of electricity in Jordan. A model was described to optimize an SPPP system for climatic conditions of Jordan. An ORC analysis was conducted with R134a, and it was determined that a pond of 1.5 km² surface area could produce 5 MW electricity. However, the cost of electricity generation using the SPPP was estimated to be around double of the cost of traditional power plant system. It is clear that more favorable economics is required for SPPP to be widely successful.

2.2 *Enhancing Efficiency of ORC-Based SPPP*

One thrust of current research is regarding improving the efficiency of solar ponds by reducing thermal losses and increasing solar ponds' ability to store thermal energy. This direction includes the concept of cover for solar ponds [16], liner selection, and geometry optimization and has been reviewed by Kasaeian et al. [7]. Another direction deals with consideration of the thermodynamic cycle which is discussed below.

Ziapour et al. [17] proposed and theoretically examined the design of a large-scale SPPP. In their proposal, multiple ORC systems and two-phase closed thermosyphons

were used to produce electricity. The power plant models considered by them are shown in Fig. 2. The arrangements differ in the method of energy extraction from solar pond. In Fig. 2a, pumps are used to transfer water from LCZ and UCZ to evaporator and condenser of the ORC, respectively. The heat transfer fluid (brine) remains in single phase. The mode of operation can be called ‘active’ due to use of pumps. This approach was widely used for plants at El Paso and Beith Ha’arava. In Fig. 2b, thermal energy of the LCZ is transferred by thermosyphons without need of a pump. The heat transfer fluid in the thermosyphon undergoes phase change and therefore involves two-phase heat transfer. The mode is ‘passive’ due to the absence of pump. Ziapour et al. [17] pointed out that the single-phase method of heat transfer has the drawbacks of requiring pumping power and bigger heat exchanger in contrast to the two-phase thermosyphon method.

In addition, for big solar ponds, the required amount of thermal energy removal rate from the hot brine in the LCZ may be so large that one thermosyphon may fail to provide the energy from the LCZ to the boiler. Therefore, many thermosyphons may be necessary and thus, a system comprising of several thermosyphons and ORC units may be incorporated as shown in Fig. 3. Within this framework, Ziapour et al. [17] also considered incorporation of regenerators (internal heat exchanger) between ORC units. These regenerators were placed to transfer energy from turbine exit side of one ORC unit to the pump exit side of adjacent ORC unit. By such approach, the working fluid of one cycle gets cooled prior to flowing into the condenser and the fluid of the neighboring cycle gets preheated prior to flowing into the evaporator. This approach reduces the amount of water that needs to be pumped from the UCZ, resulting in a decrease in the pump work. At the same time, preheating of the working fluid also makes boiling in evaporator more efficient. Ziapour et al. [17] considered a union of ten ORC units that were fed from the pond by using ten thermosyphons. In addition, the ORC units were connected together like a chain with the help of regenerators, as shown in Fig. 3. They simulated and compared the two-phase closed thermosyphon system with the single-phase pump-based method and demonstrated that the overall thermal efficiency of the SPPP was highest by using both internal regenerative heat exchangers and thermosyphons. Their work also suggested that

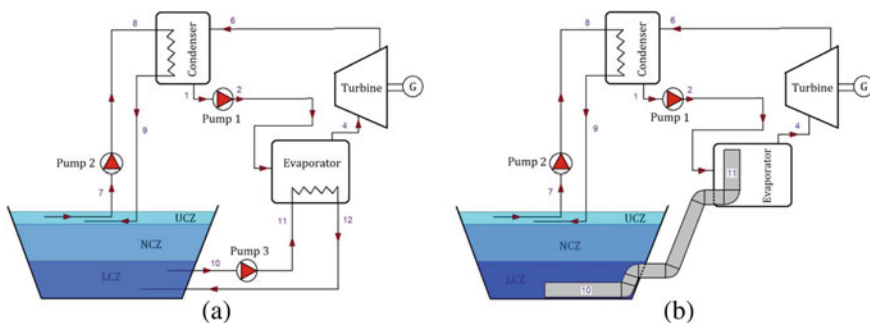
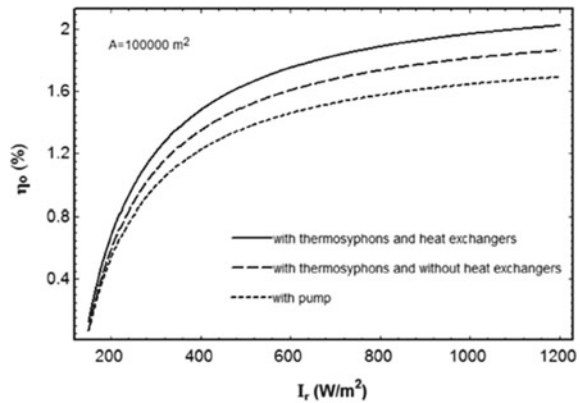


Fig. 2 Models of SPPP **a** active mode with pump and **b** passive mode utilizing thermosyphons [17, 18]

Fig. 5 Variation of overall efficiency versus radiation for different configurations [17]



Subsequently, an exergoeconomic analysis was conducted for the SPPP based on two-phase closed thermosyphon (TPCT) design and the ‘active’ pump design [18]. In both cases, evaporators were shown to have the smallest values of exergoeconomic factor and the largest values of total cost rate was attributed to turbines. In the overall scheme, the exergoeconomic factor, the total cost rate, and the cost per unit of power produced were more favorable for the thermosyphon-based system than the pump-based system. Therefore, systems based on thermosyphons were recommended [18].

Ziapour et al. [19] also used a thermoelectric generator (TEG) in place of condenser of the ORC with the idea of improving the efficiency of the system. Two models of SPPP were considered. One (Model 1) was based on employing TEG in the condenser of the ORC without any heat exchanger, and the other (Model 2) used TEG along with a heat exchanger, as shown in Fig. 6. These systems were explored

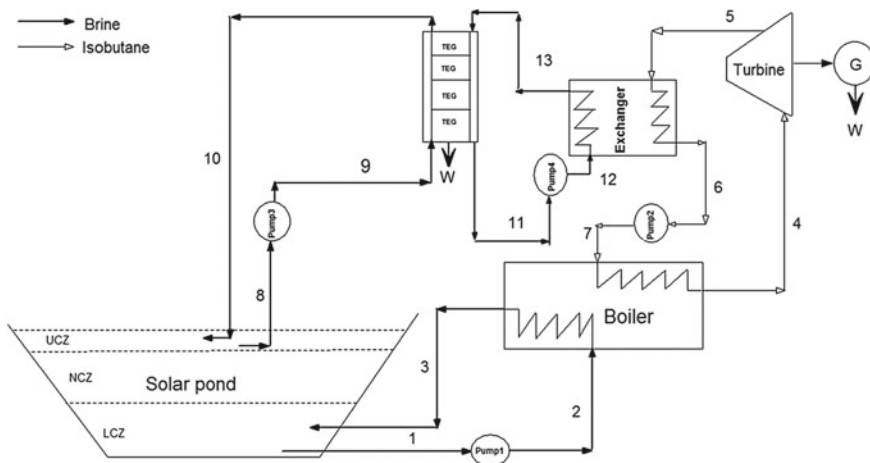


Fig. 6 SPPP using thermoelectric generator (TEG) and heat exchanger [19]

computationally by using the climatic conditions of the Beach of Urmia Lake in Iran. Under the same conditions, Model 1 had slightly higher efficiency than Model 2. For both models using TEG at $TT_{LLCCLL} = 90\text{ }^{\circ}\text{C}$, the overall solar-to-electric efficiency of the SPPP was approximately 0.2% greater than ORC without TEG.

In order to determine the ideal cycle for power production from the solar pond, Zeynali et al. [20] investigated the efficiency of an ORC, trilateral flash cycle (TFC) as well as altered systems with an open feed liquid heater (FLH) and an internal heat exchanger (IHE) for a variety of working fluids. The systems considered by them are shown in Fig. 7. The results indicated that the efficiency of the ORC was always greater than that of TFC. The regenerative ORC using R123 as the working fluid had the highest output power and performance among all the studied cycles when both open FLH and IHE were integrated into the system. La Rocca et al. [21] analyzed a model of a solar pond for power production based on ORC. The model was validated by using climate data from Palermo city, Italy. Their study investigated use of R123 and R245.

An integrated system consisting of a solar pond, flat-plate collectors, and an ORC based on ammonia as the working fluid was modeled to investigate the thermal and electrical efficiency as well as the performance of hydrogen generation, as shown in Fig. 8 [22]. In this arrangement, solar pond assists the flat-plate collectors. It plays an important role and increases the thermal performance of the system by increasing the temperature of the inlet water to the solar collectors. It was presented that a substantial amount of electrical energy can be produced by the system by rapidly increasing the temperature of the water. The power produced by the model system was subsequently utilized for producing hydrogen by an electrolysis system. Substantial amount of hydrogen was generated as the ultimate output of the model system. An advantage of such an integrated system is that the surplus thermal energy in summer can be utilized to produce hydrogen for later use. It was shown that the water electrolysis system can reach hydrogen generation rate of 2.25 kg per day.

3 SPPP Using Solar Chimney and Air Turbine

Akbarzadeh et al. [5] examined the idea of combining a solar chimney with a SGSP for producing power in the salt-affected areas of northern Victoria in Australia. The concept is shown in Fig. 9. In Fig. 9, air in the chimney is heated by using the thermal energy from the LCZ of the solar pond. The chimney on the right side arrangement uses a heat exchanger, while that on the left side incorporates spray nozzles. The latter arrangement would also require make up water to compensate for evaporation.

Based on the investigation [5], several benefits that can be realized from such integration are listed below, owing to the intrinsic heat storage ability of a solar pond. It was argued that solar ponds have large thermal capacity which depends primarily on the size of LCZ. Consequently, if thermal energy is continuously extracted on a rainy day with overcast sky even at a rate of 15% of the average daily solar insolation,

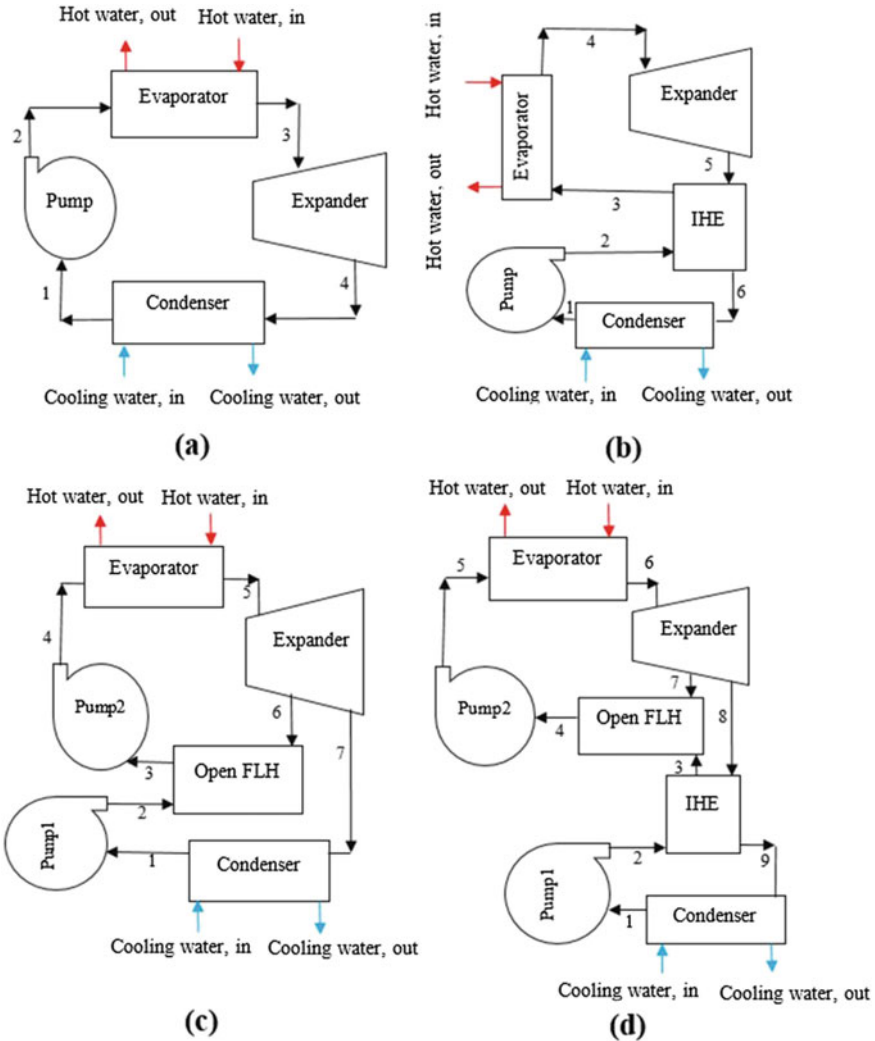


Fig. 7 Diagram of **a** simple ORC and TFC, **b** regenerative ORC with internal heat exchanger, **c** regenerative ORC and TFC with open feed liquid heater, and **d** regenerative ORC with IHE and FLH [20]

the temperature decrease of the LCZ in a day will be less than 0.5 °C. Therefore, the plant can operate without significant decrease in power generation even over many rainy days.

An initial experimental exploration using a small model chimney, integrated with a solar pond, was conducted at RMIT University in 2002. It demonstrated a low response time of few minutes for delivery of thermal energy from pond to the air stream in the chimney [5].

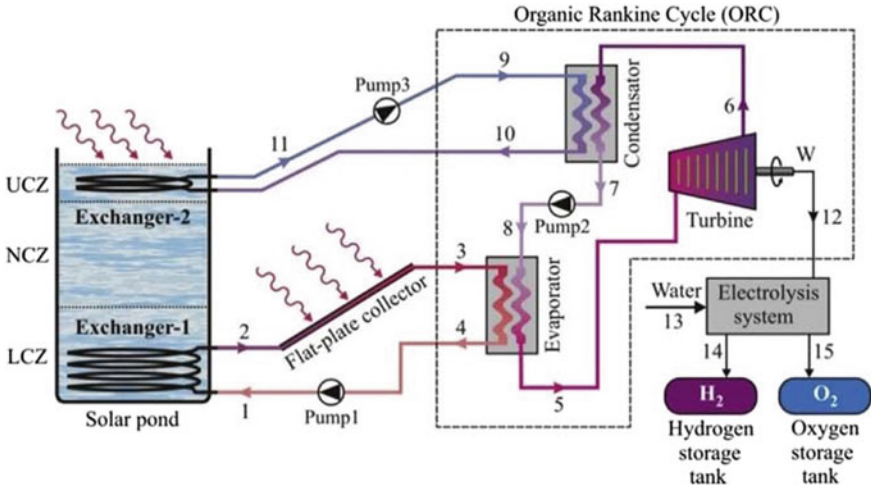


Fig. 8 Schematic of the integrated system [22]

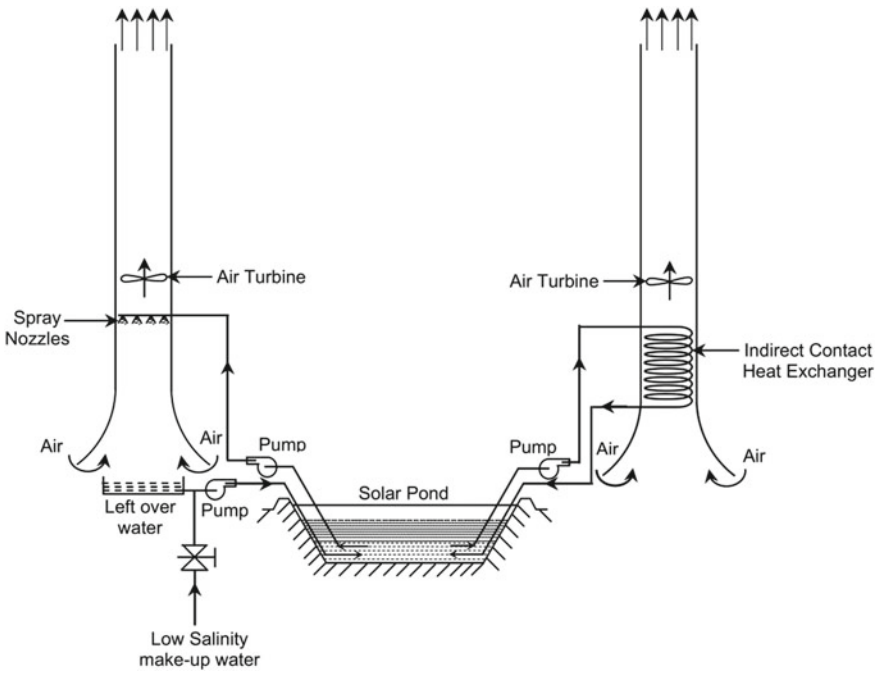


Fig. 9 Concept for integrating a chimney and air turbine with a solar pond [5]

The system can therefore generate electricity intermittently at any time of the day. Such flexibility is due to the fast response of the system and inherent heat storage capability of a solar pond [5]. Another important factor is the simplicity of the system. Unlike an ORC-based plant, the proposed plant has few moving parts. A preliminary design was also described for a demonstration SPPP having a pond of area 60,000 mm^2 with depth of 3 m and a 10 m diameter chimney having a height of 200 m [5].

However, concern arises due to low efficiency of such system. The efficiency is substantially lower than the Carnot efficiency for same temperatures unless very tall chimneys are employed. For their proposed system, having a chimney of 10 m diameter and 200 m height, a thermal to mechanical conversion efficiency of only 0.4% was predicted [5].

With the objective of night time operation of a solar chimney power plant, a mathematical investigation for a power system integrating solar pond and solar chimney power plant was done [23]. It was determined that the integrated solar system comprising of a daytime solar chimney power plant of 5 MW and a properly dimensioned solar pond can generate power in excess of 2.21 MW during night. On the basis of performance and cost factors, a combination of a solar chimney power plant of 5 MW and 1.4 km^2 solar pond was advocated.

4 Concluding Remarks

A comprehensive review of solar ponds for electric power generation has been done by incorporating organic Rankine cycle (ORC) and air turbine. Based on the present study, it has been concluded that most of the work in the area of solar pond application for electrical power generation was of computational or prototype based at best. Enormous cost has prevented researchers from experimental work and no air turbine-based SPPP has ever been constructed in practice. Indeed, solar ponds offer advantage of large thermal mass. However, the efficiency of a SPPP system is in the range of 2% for ORC and less than 0.5% for air turbine. Gains in efficiency are possible by various approaches including the use of thermosyphon for heat extraction, regenerative ORC, integration of TEG with ORC, and proper choice of working fluid. The gains, however, do not seem to be game changers. An ORC-based SPPP is more practical for large-scale solar pond. However, the economics of electricity generation using solar ponds does not seem to be favorable. Significant advances in the design of solar pond that can increase its efficiency can potentially make solar ponds attractive in hybrid systems where cogeneration of heat and electricity is required.

References

1. Tabor H, Doron B (1986) Solar ponds-lessons learned from the 150 kW(e) power plant. EinBoqek. Proceedings of the ASME Solar Energy Div, Anaheim, California
2. Singh R, Tundee S, Akbarzadeh A (2011) Electric power generation from solar pond using combined thermosyphon and thermoelectric modules. *Sol Energy* 85:371–378
3. Kalogirou SA (2014) *Solar energy engineering: processes and systems*, Second edition, Academic Press
4. Khalil RA, Jubran BA, Faqir NM (1997) Optimization of solar pond electrical power generation system. *Energy Conver Manage* 38(8):787–798
5. Akbarzadeh A, Johnson P, Singh R (2009) Examining potential benefits of combining a chimney with a salinity gradient solar pond for production of power in salt affected areas. *Sol Energy* 83:1345–1359
6. Ding LC, Akbarzadeh A, Tan L (2018) A review of power generation with thermoelectric system and its alternative with solar ponds. *Renewable Sustainable Energy Rev* 81:799–812
7. Kasaean A, Sharifi S, Yan WM (2018) Novel achievements in the development of solar ponds: a review. *Sol Energy* 174:189–206
8. Karthick K, Suresh S, Muaaz M, Hussain MD, Ali HM, Sujith Kumar CS (2019) Evaluation of solar thermal system configurations for thermoelectric generator applications: a critical review *Sol Energy* 188:111–142
9. Orosz M, Dicks R (2017) Solar thermal powered organic rankine cycles, organic rankine cycle (ORC) power systems. Elsevier, 569–612
10. Zhai H, An Q, Shi L, Lemort V, Quoilin S (2016) Categorization and analysis of heat sources for organic rankine cycle systems. *Renew Sustain Energy Rev* 64:790–805
11. Tchanché BF, Lambrinos G, Frangoudakis A, Papadakis G (2011) Low-grade heat conversion into power using organic Rankine cycle: a review of various applications. *Renewable Sustainable Energy Rev* 15(8):3963–3979
12. Tabor HZ, Doron B (1990) The Beith Ha'Arava 5 MW(e) Solar Pond Power Plant (SPPP)-Progress report. *Sol Energy* 45(4):247–253
13. Tabor H (1981) Solar ponds. *Sol Energy* 27(3):181–194
14. Bronicki LY, Robert AM (2001) *Solar ponds*, encyclopedia of physical science and technology. Academic Press, New York
15. Corporation B (1975) Technical and economic assessment of the prospects for electrical power generation by use of solar ponds. Report to the U.S. Energy Research and Development Administration, Washington, D.C.
16. Ruskowitz JA, Suárez F, Tyler SW, Childress AE (2014) Evaporation suppression and solar energy collection in a salt-gradient solar pond. *Sol Energy* 99:36–46
17. Ziapour BM, Shokrnia M, Naseri M (2016) Comparatively study between single-phase and two-phase modes of energy extraction in a salinity-gradient solar pond power plant. *Energy* 111:126–136
18. Ziapour BM, Shokrnia M (2017) Exergoeconomic analysis of the salinity-gradient solar pond power plants using two-phase closed thermosyphon: a comparative study. *Appl Therm Eng* 115:123–133
19. Ziapour BM, Saadat M, Palideh V, Afzal S (2017) Power generation enhancement in a salinity-gradient solar pond power plant using thermoelectric generator. *Energy Conversion Manage* 136(2017):283–293
20. Zeynali A, Akbari A, Khalilian M (2019) Investigation of the performance of modified organic Rankine cycles (ORCs) and modified trilateral flash cycles (TFCs) assisted by a solar pond. *Sol Energy* 182:361–381
21. Rocca VL, Morale M, Peri G, Scaccianocce G (2017) A solar pond for feeding a thermoelectric generator or an organic Rankine cycle system. *Int J Heat Technol* 35:435–441

22. Erden M, Karakilcik M, Dincer I (2017) Performance investigation of hydrogen production by the flat-plate collectors assisted by a solar pond. *Int J Hydrogen Energy* 42:2522–2529
23. Zhou X, Yang J, Xiao B, Li J (2009) Night operation of solar chimney power system using solar ponds for heat storage. *Int J Glob Energy* (31):193–207

Major Flows for Lead (Pb) Within an Academic Campus



Akash Agarwal, Amit Kumar, and Sanyam Dangayach

Abstract This study attempts to understand the major mass flows of lead and processes associated with it in an academic campus. The campus of MNIT Jaipur has been analysed using a combination of data obtained from field sampling and literature review. The main processes under consideration are private household (PHH), wastewater treatment plant (WWTP), planetary boundary layer and different types of soil cover. The major flows for lead identified within the campus are inputs to the PHHs, municipal solid waste from households being transferred to outside of the system and the sewage sludge from WWTP to forest and other soil.

Keywords Material flow analysis · Heavy metals · Lead · Urban contamination · Academic campus

1 Introduction

Mass flows associated with a system can be investigated with material flow analysis. Material flow analysis (MFA) is a systematic assessment of the flows and stocks of materials within a system. The system is defined in space and time [2]. Because of the law of the conservation of matter, the results of an MFA can be controlled by a simple material balance comparing all inputs, stocks and outputs of a process. MFA as a method is very useful for resource management, waste management and environmental management. A freeware, STAN, has been developed by Technical University of Vienna for modelling material flow analysis. It includes a graphic user interface and Sankey diagrams [5].

Lead is a heavy metal and has been found to be carcinogenic in humans. Exposure to high levels of lead can cause anaemia, weakness, kidney and brain damage [4]. Exposure to infants at concentrations considered low has been found to affect behaviour and intelligence. The effects include reduced attention span, increased antisocial behaviour and reduced educational attainment [10]. One route for lead

A. Agarwal · A. Kumar (✉) · S. Dangayach
Department of Civil Engineering, Malaviya National Institute of Technology Jaipur, Jaipur
302017, India
e-mail: amitrathi.ucf@gmail.com

to enter drinking water is through plumbing material that contain lead [9]. Lead has been used industrially in the production of gasoline, ceramic products, paints, metal alloys, batteries and solder. The use of tetra ethyl lead as an anti-knocking agent in gasoline led to automobiles being major contributors of lead emissions to the atmosphere [4]. After leaded motor vehicle fuels were phased out in 1995, the contribution of air emissions of lead from the transportation sector, and particularly the automotive sector, greatly declined.

2 Methodology

In this study, the lead flow within the MNIT campus area is based on the flows and stocks similar to the analysis performed for Bunz Valley [2]. The MNIT has a campus of 317 acres which is covered with buildings, roads, sports ground, parks, etc. Total population of the campus has been taken as 7710. As per the estimations made using Google Earth, the area covered by buildings and roads constitutes approximately 27.4 percent and is considered as urban area. The area covered in MNIT by residential areas is about 87 acres, landscaping soil is about 202 acres, and forest soil is about 28 acres, respectively. The main processes that have been considered are PHH, WWTP, planetary boundary layer, sewer system and different types of soil cover.

In the process PHH, import goods that are relevant include petrol and diesel and consumer goods such stabilizers, electronics, kitchen utensils and toys. Input flows for lead are considered from consumer goods only. The emissions from this system include those from the vehicular emissions, sewage and MSW.

In the process WWTP, while input is wastewater, the outputs are treated wastewater, sewage sludge and some gaseous emissions. Hence, all the lead is assumed to leave the WWTP in sewage sludge and treated wastewater. The quantities of treated wastewater and sludge are calculated based on the information provided by the plant operator regarding the input flows and concentrations and the technology employed. The concentration of lead in influent and effluent wastewater and sludge are determined by taking samples from the treatment plant and testing them in the laboratory at MNIT.

The exchange of lead between anthropogenic activities and the atmosphere is represented by the process of planetary boundary layer. The lowest layer of the atmosphere is represented by the planetary boundary layer. The height of PBL has been considered as 500 m for the analysis. For this study, it has been assumed that all the lead emitted from the campus falls back in this area only, and there is no exchange of lead with the atmosphere from the adjoining regions. For the amount deposited on different kinds of soils, fixed ratios have been assumed from the literature [2].

The sewer system in MNIT receives water from PHHs and the sewage from the various departments and laboratories. The lead concentration in the influent to WWTP was determined by field sampling. Afterwards, performing a mass balance on the sewer system, it was possible to estimate the approximate loading of lead from various laboratories in the campus.

For MNIT, since all the effluent from WWTP is used for irrigation purpose, it was assumed that all wastewater goes to the landscaping soil. The sludge from the treatment plant is discarded in open areas within the campus referred to as forest soils in the study. A separate drain is provided in MNIT for total run-off. The run-off factors adopted in case of urban, landscaping and forests are 0.6, 0.2 and 0.1, respectively.

Finally, an attempt is made to balance the flows around various processes considered in the study. The STAN software developed by Vienna University of technology was used to balance the flows of lead through various processes [6]. The system boundary was chosen based on the physical boundaries of the sites. A period of one year was selected as analysis period and calculations were performed according to the deposition and flows within one year.

3 Result and Discussion

The lead concentrations in the different processes including PHHs, WWTP, PBL, landscaping, forest soil and total run-off were reported. The calculations for PHH are shown in Table 1. The total lead flow in exhaust gas, sewage and MSW is 0.454 kg/year, 9.17 kg/year and 24.59 kg/year, respectively.

Table 1 Material flow for PHH

Description	Units	MNIT	Remarks
<i>Household sewage</i>			
No. of inhabitants	Capita	7710	
Lead emission per person	gm Pb/capita/year	1.19	[3]
Total lead flow	Kg Pb/year	9.1749	
<i>Municipal solid waste (MSW)</i>			
Rate of municipal waste generation	Kg/capita/year	146	[1]
Lead concentration in MSW	gPb/kg MSW	0.0218425	[8]
Total lead flow	kgPb/year	24.58722855	
<i>Exhaust gas</i>			
No. of cars	Number	250	
Mileage	Km/car/year	8030	Taking average mileage as 22kmpl and 1 L consumption per day (informal survey)
Gasoline consumption	l/km	0.045	
Lead content in gasoline	mg Pb/l	5	[7]
Total lead flow	Kg Pb/year	0.45168	

The calculations for WWTP are shown in Table 2. The total lead flow to the WWTP is estimated to be 28.6 kg/year. The total lead flow from the WWTP through effluent and sludge is 4.0 kg/year and 24.6 kg/year, respectively.

The calculations for planetary boundary layer are shown in Table 3. The deposition in forest and other soil is 0.13 kg/year. The deposition in landscaping soil is 0.05 kg/year, and deposition in urban soil is 0.27 kg/year.

The calculations for total run-off are shown in Table 4. The mass flows for lead through run-off from urban areas, landscaping and forest soils are 0.16 kg/year, 0.81 kg/year and 2.47 kg/year, respectively.

For various processes, mass balance was performed using STAN software. For PHHs, major emissions of lead are through municipal solid waste, which directly flows out of the system (Fig. 1). Using mass balance, total input of lead to the households can be estimated as 34.2 kg/year. As all the measurements have some

Table 2 Material flow in WWTP

Description	Units	MNIT	Remarks
<i>WWTP input</i>			
Wastewater flow	L/Year	4.09E + 08	Assuming 80% is converted to sewage
Lead concentration	µg/L	70	Data from MNIT WWTP
Total lead concentration	Kg Pb/Year	28.616	
<i>WWTP output</i>			
Purified water flow	L/Year	4.09E + 08	
Lead concentration	Mg/L	9.8	Data from MNIT WWTP
Total lead flow	Kg Pb/Year	4.008	
<i>Sewage sludge</i>			
Sludge Flow	Kg dry/Year	26,858.16	Calculations done By formulae
Lead concentration	Mg pb/Kgdry	916.22	Data from MNIT WWTP
Total lead flow	Kg Pb/Year	24.608	

Table 3 Material flow from planetary boundary layer

Description	Units	MNIT 0.4518			Remarks
		Landscaping	Forest Soil	Urban	
Total lead flow (through emission to the atmosphere)	Kg Pb/Year				
Deposition ratio		3	1	5	
Deposition values		0.294	0.098	0.49	
Surface	Ha	11.28	81.83	35.143	
Deposition	Kg Pb/Year	3.31	8.019	17.2207	
		0.0524	0.126879	0.272	Adjusted As Per Area

Table 4 Material flow in total run-off

Description	Units	MNIT			Remarks
		Forest	Landscaping	Urban	
Deposition from PBL	Kg Pb/year	0.126879	0.0524	0.272	
Deposition from WWTP	Kg Pb/year	24.61	4.01	–	
Run-off factor		0.1	0.2	0.6	Sandy soil assumed
Run-off	Kg Pb/year	2.47368	0.81248	0.1634	
Change in stock	Kg Pb/year	22.26312	3.248	0.1088	

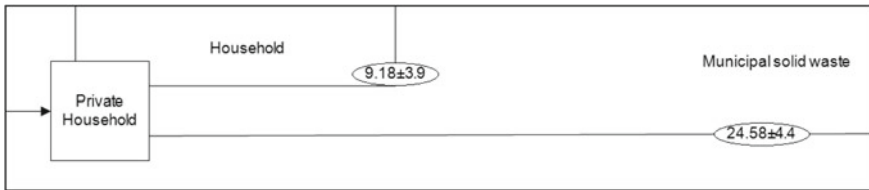


Fig. 1 Flow balance for the process of PHH

uncertainty associated with them, the uncertainties were provided to all the calculated flows while providing input to STAN software. As a result, uncertainty can be observed for all the values in STAN.

Mass balances for sewer system and WWTP are shown in Fig. 2. Total flow to the WWTP is about 28.6 kg/year which is much more than the total lead flow from households. It is suspected that remaining lead flows may be coming from laboratories in the campus. For the WWTP, major emissions of lead occur through

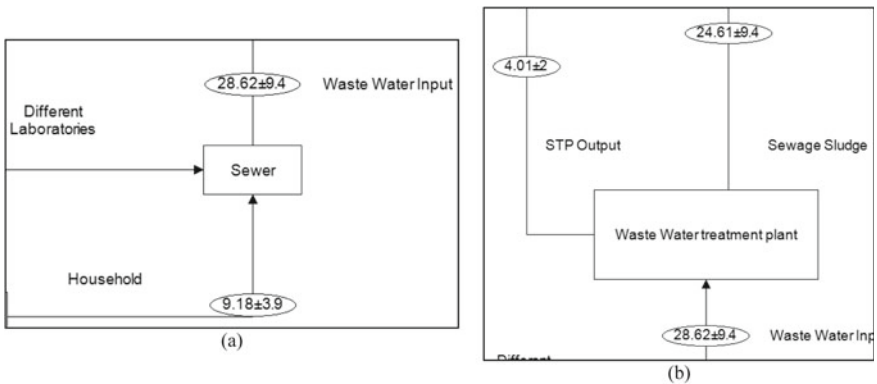


Fig. 2 Mass balance for sewer system and WWTP

sewage sludge. For other process, e.g. planetary boundary layer, soils and storm water, the flows are not significant. It is also important to note here that the estimations made in the study are approximate and have uncertainty associated with them. When these numbers were provided into STAN for modelling, the uncertainty was considered based on the procedure adopted to estimate a value.

4 Conclusions

The study attempts to quantify lead flows in the campus of MNIT Jaipur and identify major flows associated with the system. The major flows identified are input flow to PHH, lead flow through municipal solid waste from PHH to outside the system, flow by wastewater input to WWTP and flow by sewage sludge from WWTP to forest soil. These flows are 34.2, 24.6, 28.6 and 24.6 kg/year. Another major finding of the study is the loading of lead from institute laboratories to the treatment plant. There is major difference between the quantities of total lead flow exiting from PHH through sewer system and that estimated for input to WWTP. Consequently, it can be deduced that there is another substantial flow of lead to WWTP from other sources. Another significant flow of lead is by sewage sludge from WWTP to forest soil. As the sludge is continuously being deposited onto the soil, it may lead to increase in stock of lead already existing in the soil. This, in turn, may lead to increased concentration of lead in the soil and increased risk to human health.

Acknowledgements The authors are thankful to TEQIP-III office at MNIT Jaipur for providing funds for this study. Thanks are also due to Material Research Centre at MNIT Jaipur for providing services regarding analysis of heavy metals.

References

1. Bhat RA, Dar SA, Dar DA, Dar G (2018) Municipal solid waste generation and current scenario of its management in India. *Int J Adv Res Sci Eng* 7:419–431
2. Brunner PH, Rechberger H (2004) *Practical handbook of material flow analysis*. Lewis Publishers, Boca Raton, FL, USA
3. Buzier R, Tusseau-Vuillemin M-H, dit Meriadec CM, Rousselot O, Mouchel J-M (2006) Trace metal speciation and fluxes within a major French wastewater treatment plant: impact of the successive treatments stages. *Chemosphere* 65:2419–2426
4. CDC (2020) Childhood lead poisoning prevention: source of lead
5. Cencic O, Rechberger H (2008) Material flow analysis with software STAN. In: *EnviroInfo*, pp 440–447
6. Cencic O, Rechberger H (2008) Material flow analysis with software STAN. *J Environ Eng Manag* 18:3–7
7. ICCT India: Fuels: diesel and gasoline/transport policy
8. Sharma A, Ganguly R, Gupta AK (2019) Characterization and energy generation potential of municipal solid waste from nonengineered landfill sites in Himachal Pradesh, India. *J*

Hazardous Toxic Radioact Waste 23:1–15. [https://doi.org/10.1061/\(ASCE\)HZ.2153-5515.0000442](https://doi.org/10.1061/(ASCE)HZ.2153-5515.0000442)

9. WHO (2008) Guidelines for drinking-water quality WHO Library Geneva
10. WHO (2020) Lead poisoning and health

Comparative Analysis of Different Vegetation Indices of Noida City Using Landsat Data



Richa Sharma, Lolita Pradhan, Maya Kumari, and Prodyut Bhattacharya

Abstract Noida is a part of National Capital Territory (NCT) of Delhi and is rapidly expanding. With high rates of urbanization in the form of skyscrapers, industrialization, and dense population, the city is under enormous pressure. Increasing environmental pollution and waste generation, along with urban heat island effects, has made the city more vulnerable to climate change impacts. Monitoring and studying the urban green cover of the city is one of the solutions to the aggravating challenges. Inputs from such detailed analysis are important for sustainable city planning. The present work explores five spectral indices to study the vegetation status of the city between 2011 and 2019, namely NDBI, GARI, SAVI, GSAVI, and NDVI. Temporal examination of NDBI from year 2011 to 2019 indicates overall rise in the built-up area of the city. The appropriateness of the indices was assessed using six image quality measures like mean absolute deviation (MAD), correlation coefficient (CC), root mean square error (RMSE), standard deviation (SD), ERGAS, and mean absolute percentage error (MAPE), respectively. Quantitative evaluation of the performance of the four vegetation indices was performed on the enhanced images to select the most appropriate vegetation index that can be used to study urban vegetation status. The analysis of the six quality parameters reveals that SAVI is much sensitive to urban greenness than other vegetation indices with respect to urban areas.

Keywords NDBI · GARI · SAVI · GSAVI · NDVI

R. Sharma (✉) · L. Pradhan · M. Kumari
Amity School of Natural Resources & Sustainable Development, Amity University, Uttar Pradesh, Sector-125, Noida, India
e-mail: richasharma1987@gmail.com

L. Pradhan
e-mail: pradhanlolita2013@gmail.com

M. Kumari
e-mail: maya.84s@gmail.com

P. Bhattacharya
School of Environmental Management, Block 'A', Guru Gobind Singh Indraprastha University, New Delhi, India
e-mail: prodyutbhattacharya@yahoo.com

1 Introduction

Cities have always been important centers of human development, commercial activities, technological innovation and home to migrating populations. With rapid conurbation, urban cities are under tremendous stress of environmental pollution, waste management, and limited resources. These problems are further intensified by climate change and its impacts. With proper city planning, urban centers can be managed to help reduce the unwanted consequences of global environmental challenges [6].

Urban vegetation can be an important part of the solution when striving for sustainable development of cities. Urban green spaces help in reducing energy use, reducing burden on fossil fuel-based energy requirement for cooling or heating spaces [8]. These also help in increasing natural infiltration of water into the ground, recharging ground water levels. Urban trees also act as carbon sinks, thereby mitigating impacts of global warming [2]. Apart from these, these green spaces also provide aesthetic and cultural benefits to the city dwellers [5].

Therefore, it is imperative to study and monitor urban vegetation to understand land use/land cover dynamics. Monitoring spatial and temporal changes in vegetation linked with urbanization provides an important input for sustainable city planning. The benefits of the urban green spaces can be maximized when such large-scale analysis is available for the cities to the urban planners.

Remote sensed data is one of the most preferred approaches these days to study terrestrial vegetation and to arrive at solutions for effective urban green space management. Satellite-based remote sensing has several advantages such as cost effectiveness, high spatial resolution, and availability of long time series data. A large body of work exists on several vegetation indices (VI) derived using satellite imageries based on the wavelengths of light absorbed and reflected by vegetation. These indices are used in a number of applications and provide accurate and precise information on vegetation structure and dynamics.

Different indices have been used to assess urban vegetation. Normalized difference vegetation index (NDVI) is one of the most preferred indices to study vegetation cover of an area. Guha et al. [4] used NDVI to study vegetation cover in Raipur city, India. Anchang et al. [1] employed soil-adjusted vegetation index (SAVI) to monitor urban vegetation in an African city. Scudiero et al. [10] applied the green atmospherically resistant index (GARI) to assess vegetation in Western San Joaquin Valley, California, USA.

The first objective of the present work is to study five spectral indices for Noida city, namely normalized difference built-up index (NDBI), green atmospherically resistant index (GARI), soil-adjusted vegetation index (SAVI), green soil-adjusted vegetation index (GSAVI), and normalized difference vegetation index (NDVI). The second objective is to highlight the most appropriate index that can be used for studying urban vegetation using different image quality parameters.

2 Study Area

New Okhla Industrial Development Authority abbreviated as Noida is under the district of Gautam Buddha Nagar, Uttar Pradesh (Fig. 1). Noida was formulated by Uttar Pradesh government on April, 19, 1976 which is now a part of National Capital Territory (NCT) of Delhi.

The latitudinal and longitudinal extension of this city is 28.57°N 77.32°E . The city is surrounded by two rivers—Yamuna river in north and northwest and Hindon river in northeast, east, and southeast of the city. The hot and dry climatic weather condition is found in Noida city where temperatures range between maximum 45°C and minimum 28°C . From June to September month monsoons are generally predominated. Because of the cold waves of Himalayan Regions, winters are very cold here and the maximum and minimum temperature varies from 3 to 10°C .

Every year huge amount of money is spent for the development of the city. After Mumbai, Noida is famous for its skyscrapers. Noida is highly integrated town where it offers residential, commercial, and industrial structure. In the last 10 years, Noida has also become a hub of different software and hardware companies and is well connected by metro, rail, and road.

3 Data and Methods

The general methodology of the paper is illustrated through Fig. 2.

3.1 Satellite Data

The details of the remote sensed data is given in Table 1.

3.2 Image Preprocessing

The Landsat images of 2011 and 2019 were used as primary data for deriving spectral indices. The temporal images were recorded under uniform atmospheric condition and image preprocessing was applied before processing spectral indices.

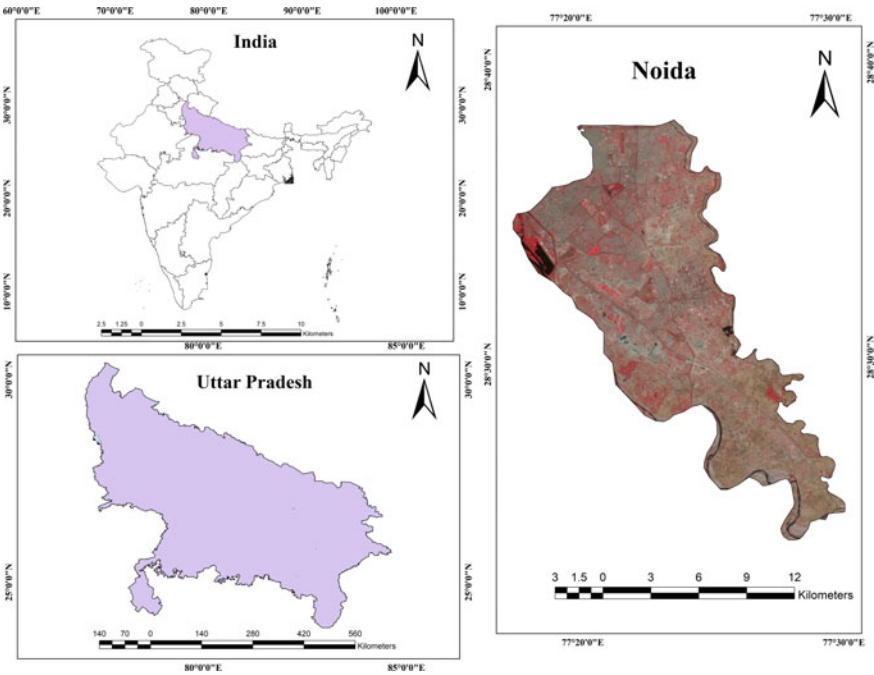


Fig. 1 Study area map

Table 1 Satellite data

S. N.	Data type	Acquisition date	Source
1	LANDSAT 4-5TM	16 January, 2011	USGS
2	LANDSAT 8 OLI	23 February, 2019	USGS

3.3 Spectral Indices

Spectral indices aid in distinguishing between various types of land cover. A vegetation index provides both quantitative as well as qualitative evaluation of vegetation density of an area. There are variety of such different indices that measure wavelength of the incoming solar insolation in visible as well as near-infrared portion of the spectrum and quantify vegetation biomass for each pixel in the satellite imagery. A detailed analysis of the spectral response for a vegetation class can also be used to distinguish between healthy and stressed vegetation. The present work limits to analysis of the following five spectral indices:

- Normalized difference built-up index (NDBI)
- Green atmospherically resistant index (GARI)
- Green soil-adjusted vegetation index (GSAVI)

- Soil-adjusted vegetation index (SAVI)
- Normalized difference vegetation index (NDVI).

3.3.1 Normalized Difference Built-Up Index (NDBI)

Normalized difference built-up index (NDBI) is a spectral index that highlights the built-up area and ranges from +1 to -1 [18]. NDBI is derived using the below equation, where SWIR is short-wave infrared, and NIR is near-infrared spectral band.

$$\text{NDBI} = (\text{SWIR} - \text{NIR}) / (\text{SWIR} + \text{NIR})$$

3.3.2 Green Atmospherically Resistant Index (GARI)

Green atmospherically resistant index (GARI) is highly responsive to chlorophyll concentrations and can counter the effects of atmospheric interference in satellite imagery [3]. GARI is derived using the below equation, where NIR is near-infrared, GREEN is the green, BLUE is the blue, and RED is red spectral band of the dataset.

$$\text{GARI} = \{\text{NIR} - [\text{Green} - (\text{Blue} - \text{Red})]\} / \{\text{NIR} + [\text{Green} - (\text{Blue} - \text{Red})]\}$$

3.3.3 Soil-Adjusted Vegetation Index (SAVI)

SAVI is used for monitoring both soil and vegetation. NDVI and SAVI are almost the similar indices but the difference is that SAVI is used for only low vegetation coverage of less than 40%. The formula of SAVI is

$$\text{SAVI} = [(\text{NIR} - \text{Red}) / (\text{NIR} + \text{Red} + L)] * (1 + L)$$

where $L = 0.5$ where L is a correction factor that ranges from 0 (very high vegetation) to 1 (very low vegetation) [16]. The value 0.5 is for intermediate vegetation cover which is used in the present work. NIR is near-infrared and RED is the red spectral band of the dataset.

3.3.4 Green Soil-Adjusted Vegetation Index (GSAVI)

Green soil vegetation index (GSAVI) is similar to SAVI where the vegetation is highlighted. This index was designed with color infrared photography for the nitrogen estimation [13]. The formula of GSAVI is

$$\text{GSAVI} = \left[\frac{\text{NIR} - \text{green}}{\text{NIR} + \text{green} + L} \right] * (1 + L), \text{ where } L = 0.5$$

NIR is near-infrared and GREEN is the green spectral band of the dataset. L is a correction factor that ranges from 0 (very high vegetation) to 1 (very low vegetation).

3.3.5 Normalized Difference Vegetation Index (NDVI)

In normalized difference vegetation index (NDVI), NIR band reflects the vegetation strongly and red band absorbs the vegetation. NDVI ranges between -1 and $+1$ and the values which are very close to $+1$ there is a high possibility of dense vegetation and the value is near to -1 , it indicates no vegetation [9]. NDVI uses the ratio of red (R) and near-infrared (NIR) spectral bands

$$\text{NDVI} = (\text{NIR} - \text{Red}) / (\text{NIR} + \text{Red})$$

3.4 Image Quality Measures

The appropriateness of the indices was judged using six quality indicators like mean absolute deviation (MAD), correlation coefficient (CC), root mean square error (RMSE), ERGAS, standard deviation (SD), and mean absolute percentage error (MAPE), respectively [11] (Table 2).

All the spectral indices were derived using ArcGIS10.1 software. The enhanced images values were examined using six statistical parameters in reference to the standard false color composite (FCC) values.

4 Results and Discussion

In recent decades, exponentially expanding population and urbanization has prompted an unplanned and unsustainable urban sprawl, an emerging major threat in Noida. The dynamic nature of urban growth makes it little difficult to measure greenness extent around it. Temporal examination of NDBI from year 2011 to 2019 indicated overall rise in the built-up area. In 2011, the NDBI value ranged between -0.43 and 0.44 while in 2019 the maximum value reached to 0.66 indicating huge expansion of urban area. By 2011, almost whole of northern and central Noida got urbanized. However, in 2019 most of southern part of Noida which is agricultural area is in process of urban development and areas along the Noida Expressway have urbanized [11].

The green space in urban area are like lungs of the city as they support exchange of gases and keeps microclimate cooler. The remote sensing-based spectral indices

Table 2 Image quality indicators

S. N	Quality indicator	Mathematical expression	Interpretation
1	Mean absolute deviation (MAD)	$MAD = \frac{\sum_{i=1}^n A_i - F_i }{n}$ Where A_i and F_i are the pixel values of the original and enhanced image, respectively, and n is the number of observations	Image is of better quality when MAD values are less
2	Correlation coefficient (C_c)	$C_c = \frac{\sum_{i=1}^n (x_i - \bar{x})(y_i - \bar{y})}{\sqrt{\sum_{i=1}^n (x_i - \bar{x})^2} \sqrt{\sum_{i=1}^n (y_i - \bar{y})^2}}$ Where x_i, y_i are the gray values of homologous pixel synthesized image and real high-resolution image [7]	Values range between 0 and 1. C_c equal to 1 implies that both images are same, value corresponding to 0 implies they are dissimilar and value corresponding to -1 implies a negative correlation
3	Root mean square error (RMSE)	$RMSE = \sqrt{\sum \frac{(y_{pred} - y_{ref})^2}{N}}$ Where Y_{pred} is the gray value of the enhanced image and Y_{ref} is the gray value of the original image. N is the no. of observations	Values on the lower side indicate a good fit with minimum errors
4	ERGAS	$ERGAS = 100 \frac{h}{l} \sqrt{\frac{1}{n} \sum_{i=1}^n \left(\frac{RMSE}{Mean}\right)^2}$ Where h and l are spatial resolution of Reference and Enhanced images, respectively; N is the number of bands	Higher values indicate aberration, whereas lower values indicate no distortion in the two images
5	Standard deviation (SD)	$\sigma = \sqrt{\frac{1}{N} \sum_{i=1}^N (x_i - \bar{x})^2}$ Where x_i is the data vector and \bar{x} is the mean value and N is the total number of observations	Image is of better quality when SD values are less
6	Mean absolute percentage error (MAPE)	$MAPE = \frac{\sum_{i=1}^n \left \frac{A_i - F_i}{A_i} \right }{n} \times 100$ Where A_i and F_i are the pixel values of the original and fused image, respectively, and N is the total number of observations	Image is of better quality when MAPE values are less

Table 3 Descriptive statistics of vegetation indices

	GARI		GSAVI		SAVI		NDVI	
	2011	2019	2011	2019	2011	2019	2011	2019
Minimum	-1.03	-2.99	-0.24	-0.33	-0.34	-0.36	-0.23	-0.24
Maximum	0.98	0.98	0.41	0.49	0.72	0.84	0.48	0.56
Mean	0.91	0.95	0.38	0.43	0.69	0.78	0.42	0.51

discriminate between the vegetation and non-vegetation. But in areas like Noida where mixed pixels of urban and vegetation are common, it is very difficult to study vegetation. Therefore, certain constants or adjustment factors are applied to suppress the reflectance of other land uses and highlight vegetation cover.

The statistics of various indices used in the study is summarized below (Table 3).

4.1 Analysis of Image Quality Measures

Multispectral images of Landsat were enhanced with respect to vegetation using NDVI, SAVI, GSAVI, and GARI, with an objective to select the most appropriate vegetation index that can be used to study urban vegetation. The corresponding maps of various spectral indices are demonstrated in Figs. 3, 4, 5, 6 and 7. Qualitative evaluation (i.e., ocular interpretation) may not be always sufficient for final assessments as it may include aberrations that cannot be just discriminated visually [17]. Therefore, it is imperative to quantitatively assess images and respective indices. The six quality indicators (Table 2) were employed to all the images, and the results are recorded in Table 4. These indices were equated and evaluated using RMSE, MAD, CC, ERGAS, SD, and MAPE between FCC (green, red, and NIR) of the multispectral image and enhanced images through vegetation indices [13].

The results indicate highest correlation coefficient of the NDVI image indicating similarity between the reference and the enhanced image. For all other indicators, lower values imply better image quality. Values of RMSE, ERGAS [15], MAPE, SD, and MAD on the lower side suggest line of best fit, with minimum errors. The results indicate that SAVI is much sensitive to urban greenness than other vegetation indices, viz. GSAVI, GARI, and NDVI with respect to urban areas.

5 Conclusion

To delineate vegetation using remotely sensed data in an urban region, which is very often affected by the mixed pixels because of the dense built-up, especially city like Noida requires atmospheric correction. The vegetation spectral indices can provide a useful aid to monitor vegetation status at various scales. The present results indicate

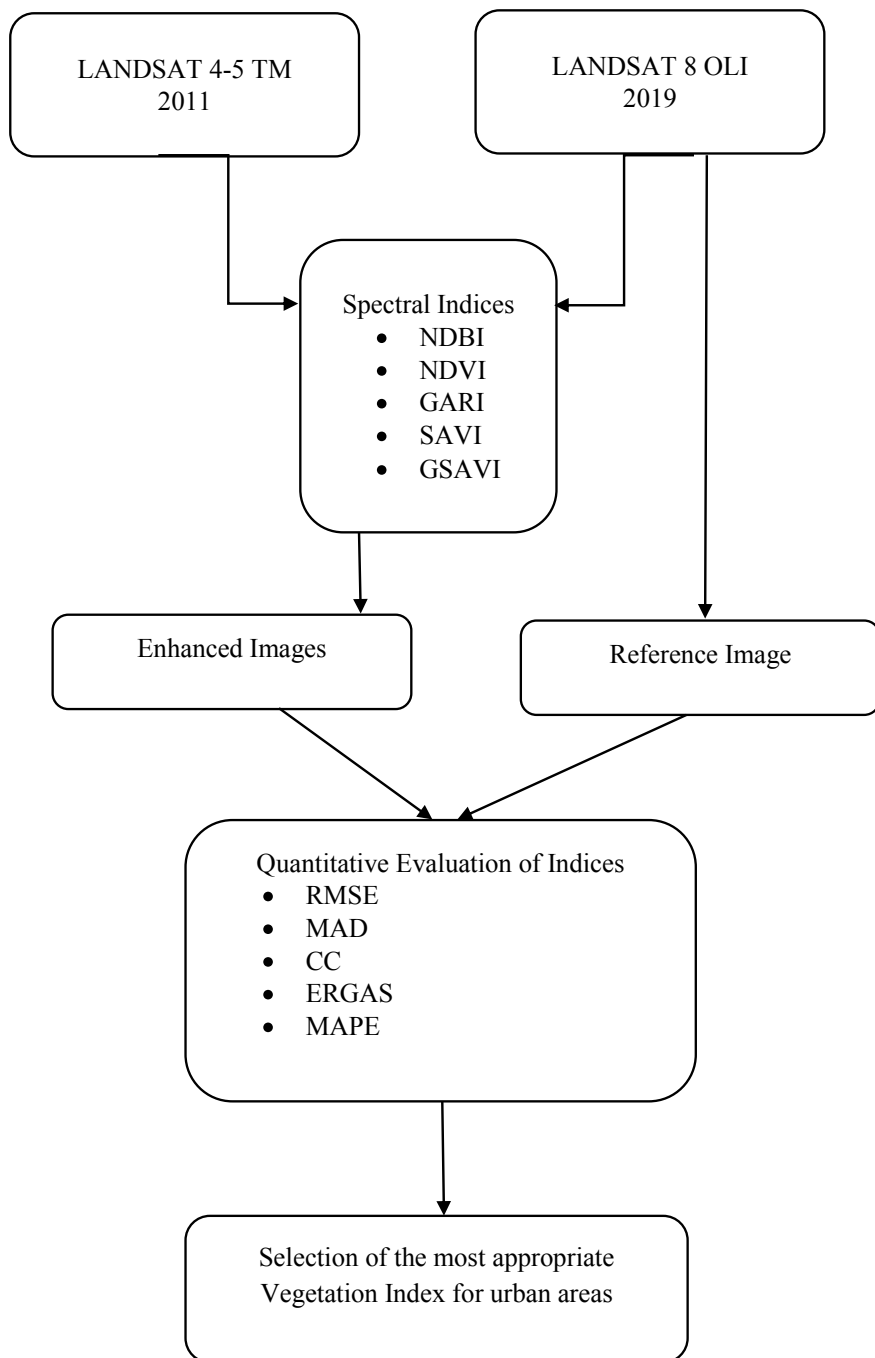


Fig. 2 Methodology flowchart

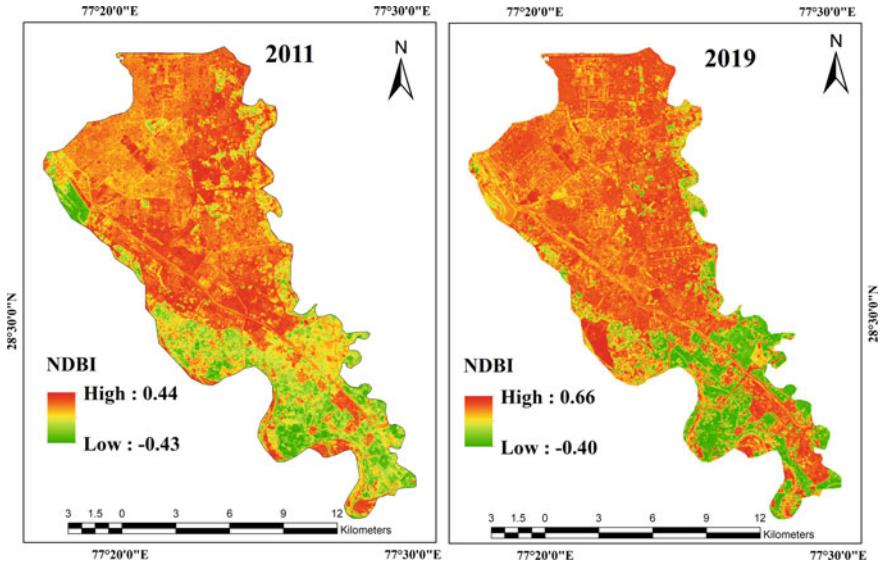


Fig. 3 Normalized difference built-up index map (NDBI)

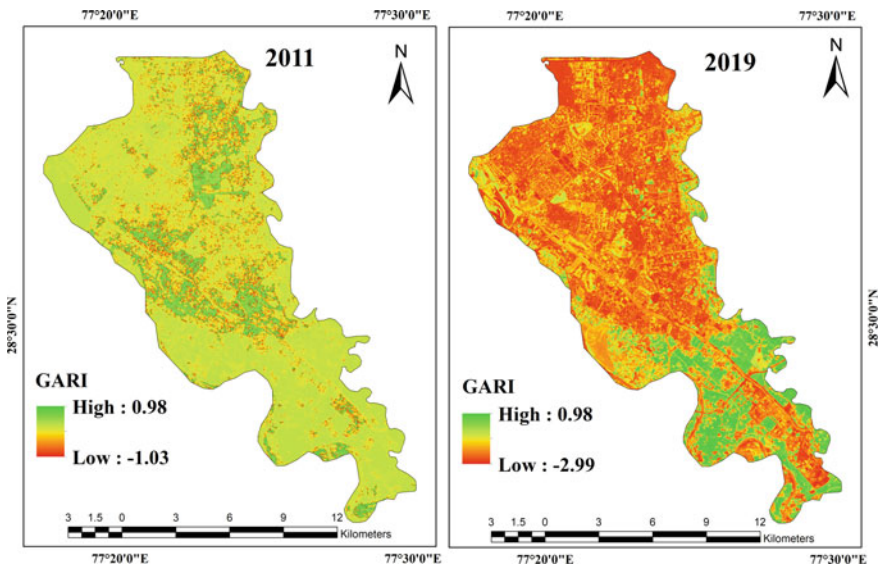


Fig. 4 Green atmospherically resistant index map (GARI)

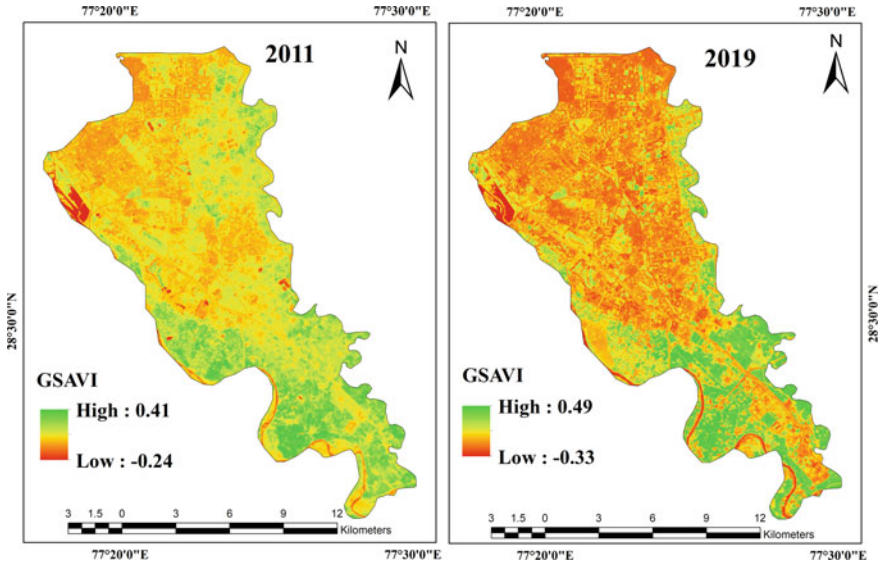


Fig. 5 Green soil-adjusted vegetation index map (GSAVI)

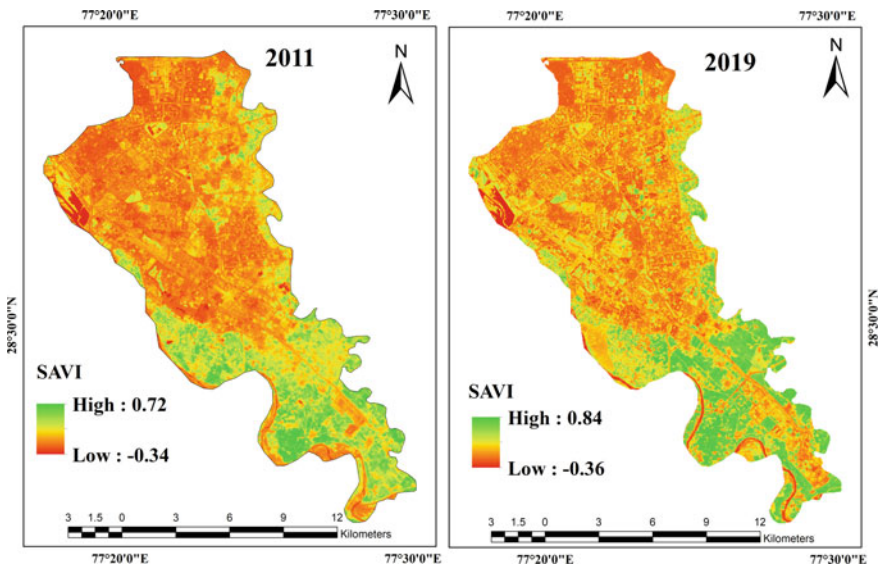


Fig. 6 Soil-adjusted vegetation index map (SAVI)

Table 4 Comparison results of enhanced images

Vegetation indices	RMSE	MAD	CC	ERGAS	SD	MAPE
NDVI	9779.34	9777.52	0.567	865,565.48	0.06	0.20
SAVI	9779.08	9777.24	0.0116	577,048.45	0.00	0.00
GARI	9779.62	9777.81	-0.5942	36,710,268.29	0.09	0.298
GSAVI	9779.34	9777.56	0.1418	996,634.40	0.05	0.181

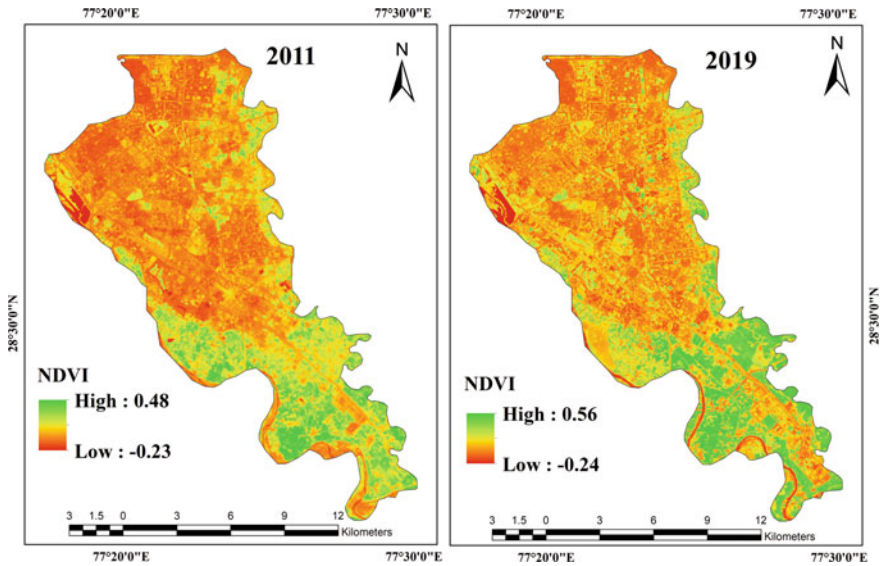


Fig. 7 Normalized difference vegetation index map (NDVI)

that SAVI is one of the most appropriate indicators of assessing and monitoring urban vegetation. SAVI is less sensitive to other land uses such a built-up and soil as compared to other vegetation indices.

References

1. Anchang JY, Ananga EO, Pu R (2016) An efficient unsupervised index based approach for mapping urban vegetation from IKONOS imagery. *Int J Appl Earth Obs Geoinf* 50:211
2. Chen WY (2015) The role of urban green infrastructure in offsetting carbon emissions in 35 major Chinese cities: a nationwide estimate. *Cities* 44:112–120
3. Gitelson A, Kaufman Y, Merzylak M (1996) Use of a green channel in remote sensing of global vegetation from EOS-MODIS. *Remote Sens Environ* 58:289–298
4. Guha S, Govil H, Mukherjee S (2017) Dynamic analysis and ecological evaluation of urban heat islands in Raipur city India. *J Appl Remote Sensing* 11(3):36020

5. Huang L, Li J, Zhao D, Zhu J (2008) A fieldwork study on the diurnal changes of urban microclimate in four types of ground cover and urban heat island of Nanjing China. *Building Environ* 43(1):7–17
6. Hunt A, Watkins P (2011) Climate change impacts and adaptation in cities: a review of the literature. *Climatic Change* 104:13–49
7. Karathanassi V, Kolokousis P, Ioannidou S (2007) A comparison study on fusion methods using evaluation indicators. *Int J Remote Sens* 28(10):2309–2341
8. Nowak DJ, Greenfield EJ (2018) Declining urban and community tree cover in the United States. *Urban Forest Urban Greening* 32:32–55
9. Rouse JW (1974) Monitoring the vernal advancement of retrogradation of natural vegetation. NASA/GSFG Type III Final Report 371
10. Scudiero E, Skaggs TH, Corwin DL (2014) Regional scale soil salinity evaluation using Landsat 7, Western San Joaquin Valley, California, USA. *Geoderma Reg* 2:82–90
11. Sharma R, Pradhan L, Kumari M, Bhattacharya P (2021) Assessing urban heat islands and thermal comfort in Noida City using geospatial technology. *Urban Clim* 35:100751
12. Somvanshi SS, Kunwar P, Tomar S, Singh M (2017) Comparative statistical analysis of the quality of image enhancement techniques. *Int J Image Data Fusion* 9(2):131–151
13. Somvanshi SS, Kumari M (2020) Comparative analysis of different vegetation indices with respect to atmospheric particulate pollution using sentinel data. *Appl Comput Geosci* 100032
14. Sripada RP, Heiniger RW, White JG, Meijer AD (2006) Aerial colour infrared photography for determining early in-season nitrogen requirements in corn. *Agron J* 98(4):968–977
15. Wald L (2000) Quality of high resolution synthesised images: Is there a simple criterion? In: Ranchin T, Wald L (eds) *Proceedings of the third conference “fusion of earth data: merging point measurements, raster maps and remotely sensed images*. Sophia Antipolis, France, January 26–28, 2000, published by SEE/URISCA, Nice, France, 99–103
16. Xue J, Su B (2017) Significant remote sensing vegetation indices: a review of developments and applications. *J Sensors* 17
17. Yilmaz V, Gungor O (2016) Determining the optimum image fusion method for better interpretation of the surface of the Earth. *Norwegian J Geograp* 70(2):69–81
18. Zha Y, Gao J, Ni S (2003) Use of normalized difference built-up index in automatically mapping urban areas from TM imagery. *Int J Remote Sens* 24(3):583–594

Review of Biomass Technologies and Practices for Cooking in India



Harshika Kumari

Abstract The growing apprehension for the environment and sustainable development has led to global concern for the renewable energies and bioenergy in particular. In the past few years, there has been noteworthy improvement in renewable energy technologies beside decline in its expenditure. Biomass has been one of the most essential energy sources for the mankind ever since the dawn of development, yet its significance dwindled after the increase in exploit of coal and oil in the late nineteenth century. Taking into consideration the benefits biomass offers, there has been a renaissance of awareness in the last few years in biomass energy. It is renewable, commonly accessible along with being carbon neutral and has the prospective to offer considerable prolific service in the rural areas. India being an agricultural-based country has a variety of fuel woods which plays an imperative function in household and industrial sectors. Biomass provides 40% of the whole energy requirement of the country apart from giving food, hay, and wood. Biofuels, which include wood, crop residue and dung cake, account for 67% of the total energy utilization in country and are the main resource for cooking in the rural areas and are also used in agroprocessing industries, small-scale enterprises, and in the agricultural estate. This paper gives an overview of biomass prospective in India and the technologies to utilize biomass as a clean and sustainable fuel to meet the cooking energy demand for India.

Keywords Biomass · Cookstoves · Energy · Fuels · India

1 Introduction

Energy is a fundamental necessity for socioeconomic growth. Biomass has been used ever since millennia for meeting various individual necessities. Biomass has been dominating the global energy supply since the middle of the nineteenth century [1]. Availability of biomass in large quantity and scarcity of fossil fuel, coal, oil, and gas lead to large use of biomass as the fuel. The overall consumption of biomass energy

H. Kumari (✉)

Dr. Akhilesh Das Gupta Institute of Technology & Management, New Delhi, Delhi, India
e-mail: harshika@niecdelhi.ac.in; harshikaiitd@yahoo.co.in

has risen unabatedly in precedent two decades. Biomass can be converted into liquid fuels and gaseous fuels, electrical energy and processed heat to give clean energy services and to supplement the conventional energy in meeting energy needs of the country in an equitable way and ensuring access to clean fuels to all. Biomass is an environmental friendly and a renewable resource.

Biomass is renewable organic matter which can be classified into two types, woody and non-woody biomass. Woody biomass is the biological degradable part of any material, product, or wastes obtained from vegetable materials, plantations, and forests. Non-woody biomass is obtained from farming and agro-industrial residues, industrial wastes, and animal and community wastes. Biomass growth takes place when soils have sufficient nutrients and moisture. Due to the benefits that biomass offers there has been a resurrection of attention in the biomass energy as apart from being renewable and extensively accessible it is also carbon neutral.

The economy is rising per year and the nation is aspirant to become a foremost runner in the power sector in the world. But the insufficient growth in employment and rise in poverty with the escalating rural–urban split are matters of solemn worry and attention for our policymakers. There is a straight association amid economic growth and energy consumption. If India has to attain its objective of becoming a principal financial supremacy, the country will have to work on renewable energy sector to viaduct the rising gap between demand and supply of energy. To meet the projected demand of energy in the coming years, the import will increase and it will place a great burden on the nation's foreign exchange resources. For the strengthening of energy security, the diversification of the energy mix is required which will lead to accelerated harnessing of renewable energy resources that are competent of obtaining a wide band of necessities hence contributing to the nationwide power security with economic development and environmental security. The miscellany of sources of biomass is certainly high. In most of the countries, the available quantum of biomass energy is high but it is only used for heating purpose. By 2050, it has been estimated that 15–50% of the world's primary energy will be met by the biomass. Presently around 10% of the world's primary energy is obtained from biomass [2]. Among the variety of available renewable energy resources, bioenergy is the prospect future fuel and feed stock for the country.

2 Available Cooking Fuels in India

In developing nation, it is projected that, almost 70% of the household use biofuels for cooking [2]. A large number of populations in rural remote areas cook their foodstuff on unvented open fire leading to poor thermal efficiency, which also releases high level of pollutants and result in stern physical condition and health issues for women and children [3]. It is established that the biomass fuels are extensively used in area where the low-income people's lives and the availability of clean fuel are neither affordable nor sufficient. Biomass is found in nature in the form of forests, wastelands, and widespread lands and is also grown by water and soil management

in agricultural lands. India has a huge biomass reserve in the form of wasteland which is presently being not utilized resourcefully. The biomass energy in India is double the fossil fuel energy consumed per annum [4]. The utilization efficiency of the available biomass must be examined and calculated as all the biomass that grows is not readily obtainable for utilization. The accessible land for biomass production is 9.6–36.5 Mha under available diverse conditions [5].

Wide ranges of fuels have been used for cooking in India. The details of these cooking fuels are given below.

2.1 Wood: Acacia (Keekar) and Eucalyptus (Safeda)

In India, 49% people used firewood for cooking. The common firewood are acacia, eucalyptus, and mango wood. Acacia is a tree which is small in size and commonly found grown on the sides of road and barren land. Since it is easily found in all parts of India, it is one of the most ordinarily used biomass fuel in India. Another popular wood use for cooking in India is eucalyptus, which is found in large number in Karnataka, Haryana, Punjab, Uttar Pradesh and Maharashtra. Eucalyptus trees can be easily grown along the roadsides, railway tracks and can be cultivated in farm forestry along with other crops. Eucalyptus has high heating values and animals do not browse it. Due to its high commercial value Ministry of Environment and Forestry is promoting its plantation [6].

2.2 Dung Cakes

Dung cakes are mainly prepared from dungs of cow, buffalo, cattle, and camels by mixing little quantity of crop residue with the dung after which it is sun dried. Dung cakes are usually used in the villages and semi-urban areas in the country. Haryana and Uttar Pradesh are the two states having the maximum use of dung cake as a fuel. Overall 8% of people in India use dung cakes for cooking.

2.3 Crop Residues: Mustard Stalk, Arahar Stalk, Rice Straw

The crop residue is used by 8.9% of the households in India. Crop residues are obtained in the form of stalk, straw, husk and fibrous material after the main crop has been extracted in the field. These are the left over fraction of the energy crops grown in an agricultural land. Based on the type of crop grown in an area, the crop residue will vary from one field land to another. In general rice straw, wheat straw, arahar stalk, mustard stalk, cotton stalk, jute stalk, tobacco stalk, and various pulse stalks are used as crop residues in India.

2.4 Kerosene

Kerosene is a liquid fuel that is considered a cleaner fuel in comparison with the solid biomass fuels is used in traditional or improved biomass cookstoves. The main advantage of the kerosene is its easier transportation and distribution. It has high calorific value than any other traditional biomass fuels. But it is used by only 2.9% of population in India [7].

2.5 Liquefied Petroleum Gas (LPG)

LPG is mainly marketed and distributed by Indian Oil Corporation, Hindustan Petroleum, and Bharat Petroleum group as famous name of 'Indane', 'HP' and 'Bharat' respectively, in 14.2 kg per cylinder. It consists of 80% butane and 20% propane. Presently 28.5% people are using it for cooking in India.

2.6 Biogas

Biogas is a clean gaseous fuel that can be used for cooking as well as lighting. It is used by 0.4% of households in India. It is produced from dungs of animals and other wastes of animals by the process of anaerobic digestion. Biogas is composed of 60% methane, 30% CO₂, and 2% H₂ with traces of nitrogen, ammonia, nitrogen, and hydrogen sulfide. Biogas plants are mostly constructed in the rural areas where a large number of cattle and animals are found to continuously supply the dung and animal waste needed to make slurry to run a biogas plant.

2.7 Coal, Lignite, Charcoal

In India, 1.4% households are using coal, charcoal, and lignite for cooking. Coal is a sedimentary rock and it is a compound blend of organic and inorganic material that include mixed liquid and gas and solids of allothigenic plus authigenic origin. Coal has forever been inexpensive fuel in terms of its cost per joule of energy. Lignite is the lower grade of coal, which is typically used for cooking. Coal is made from biomass in the absence of air in airtight condition. When biomass remains underground for thousands of years, the volatile matter in them is evaporated and it is condensed to a solid that has twice the density of biomass and this results into the formation of charcoal. At present, Indian uses one-third of charcoal for cooking and the major part that is about three quarters of charcoal is used in industries like jewelry making, silk reeling, laundries, and other small-scale industries.

3 Consumption Pattern of Cooking Fuels

There is a constant increase in energy demand due to the rising population and prosperity. Most of the thermal energy demand is from the residential sector in India for cooking. So, accordingly the utilization of commercial (electricity, LPG, etc.) and non-commercial (biomass) is made.

In India, biomass contribution is approximately a third of the total energy and it is mostly used in rural households for cooking and heating (rural—90% and urban—40%). It is also used by conventional and artisan industries [8, 9]. Wood fuels supply around 56% of the entire biomass energy. The absolute consumption of biomass energy has however risen unabatedly during past two decades, growing at an annual rate of over 2% [10, 11] (Fig. 1).

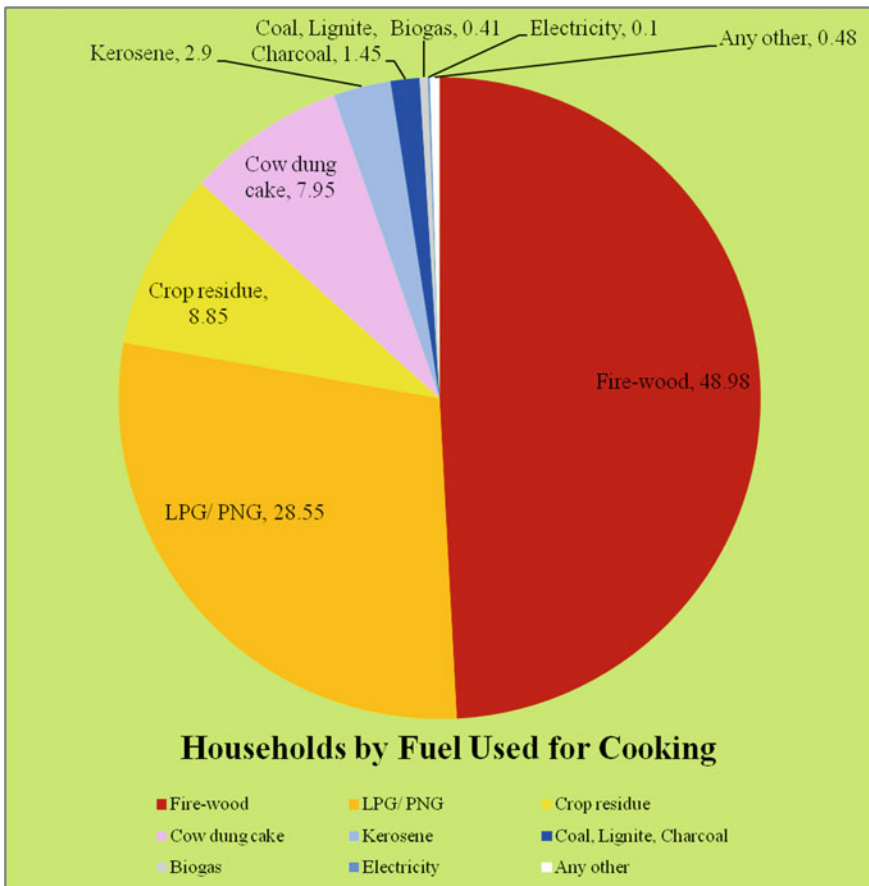


Fig. 1 Distribution of households cooking fuel used in India [7]

Table 1 Distribution of households in India based on fuel used for cooking

Fuel used for cooking	Total (%)	Total (%)	Rural (%)	Rural (%)	Urban (%)	Urban (%)
	2001	2011	2001	2011	2001	2011
Firewood	52.5	49.0	64.1	62.5	22.7	20.1
Crop residue	10.0	8.9	13.1	12.3	2.1	1.4
Cow dung cakes	9.8	8.0	12.8	10.9	2.0	1.7
Coal, charcoal, lignite	2.0	1.4	1.1	0.8	4.6	2.9
Kerosene	6.5	2.9	1.6	0.7	19.2	7.5
LPG/ PNG	17.5	28.5	5.7	11.4	48.0	65.0
Electricity	0.2	0.1	0.1	0.1	0.3	0.2
Biogas	0.4	0.4	0.5	0.4	0.4	0.4
Any other	0.6	0.5	0.8	0.6	0.2	0.2
No cooking	0.3	0.3	0.2	0.2	0.6	0.5

According to the Census of India (2011), a lot of households still rely on firewood fuel for cooking (Table 1), and approximately 20% rely on different forms of biomass fuels. Around 80–90% of the rural households are reliant on biomass fuels for cooking and heating. In comparison with this, urban households utilize much cleaner fuels like LPG and kerosene which account for 48% and 19%, respectively. Comparison of rural and urban data for household cooking in the year 2001 and 2011 is shown in Table 1.

Approximately, 166 million households that are 67% of households in the country continue to use solid fuels as their main resource for cooking. The consumption of commercial fuels is increasing in the urban areas, but population in rural areas still consumes the solid fuels [7, 12].

The main barriers in sustainable growth of biomass is short of commercial requirement of wood for energy, insufficient financial incentives, low production of plantations, terrain tenurial barriers, and lack of organizations to incorporate biomass production and utilization.

4 Clean and Sustainable Energy from Biomass

There is various clean biomass conversion technology which is widely available and used for conversion of raw biomass into clean energy such as electricity or gaseous, liquid and solid fuels. These conversion technologies will help in supplying various energy needs of the people. Some of the main technologies for power generation that is being promoted in India are gasification, liquidification, combustion, cogeneration, and biomethanation which are discussed below.

4.1 Gasification of Biomass

India being an agriculture-based country has enormous potential for employing biogas technologies which is now well recognized in India [13]. 0.037m^3 of biogas can be produced from a kilogram of dung. Biogas can be produced from sources other than animal dung like dropping of poultry, marine plants, water hyacinth garbage, sewage and municipal and industrial wastes, and other biowastes. Biogas has extra significance in contrast to the majority of the clean energy alternatives since it is also a way of waste management and it makes the community to be self-sufficient in energy, as the amount and value of the output is completely reliant on the utilization and maintenance of the biogas plant users.

India has a 40 year old biogas program. Community-based biogas plants can meet the requirement of the community by processing dung from the households with 3–5 animals. In the last four decades, the illustration of MNRE with a number of research and development made in the country with the allocated funds has led India in becoming a global player in the expansion of biomass gasification systems intended for high-grade heat and power. In 1981 in India, National Project on Biogas development started the widespread dissemination of biogas plants. There are approximately five million individual and community level biogas plants in India as of 2016 [14]. It is estimated that whole installed capacity of biomass gasification-based power in India is about 140 MW out of total of 2600 MW of biomass power generation.

Gasification is a two-step course. During the first step, biomass undergoes incomplete combustion to produce gas and charcoal, and in the second step, charcoal reduces the product gas to a flammable producer gas which consists of carbon monoxide and hydrogen with traces of additional gases like nitrogen. The producer gas can be utilized in internal combustion engines for mechanical applications such as milling or lifting water, and for electricity production whilst joined with generators. Directly it can be used for cooking in a burner to provide process heat. The readily offered capacities for gasifiers are from 20 kW to 2000 kW.

Biogas plant has a number of vital challenges to face which can be resolved by taking into consideration the following points

- (i) Provide grants, incentives, and subsidies for the encouragement of biogas plants for development, advertising, and maintenance.
- (ii) Pilot model for venture for biogas plants for rural biogas entrepreneurs.
- (iii) Endow in research and development to cut down the cost of biogas bottling and packaging.
- (iv) Organize demonstrations that exemplify the practice of using biogas and bring awareness to the masses to employ it.
- (v) Develop ease of access to consumer finance for biogas plant.

4.2 *Briquetting and Cogeneration of Biomass*

Briquette is a lump of condensed biomass with amplified volumetric calorific value for consumption as fuel. Such briquettes are similar to woody biomass which has high ash content and relatively steady with extended shelf life. Biomass like rice straw or rice husk, wheat husk, sawdust, jute stick, and bagasse can be used for briquetting. Presently biomass briquetting is a well-known technology with local mechanized ability in Asian countries like India, china Korea, Japan, Taiwan, Thailand, Malaysia, and Bangladesh. Biomass briquettes prepared by manual processes are generally used for domestic cooking, while briquettes created through mechanical processes is used in boilers and furnaces [15]. The pace of increase of briquetting technology in India is insignificant.

Cogeneration is a technology to produce both heat and power simultaneously in a process industry like sugar mills, rice mills and paper mills [16]. The accessible biomass is projected at 500 million metric tonnes per annum with 18000 MW potential of Cogeneration power. Therefore there is copious prospect for wider employment of bagasse-based cogeneration in the one of the major cane producing country like India.

4.3 *Liquefaction of Biomass*

The common liquid fuels produced from biomass are ethanol and methanol. Ethanol is produced by the process of fermentation of sugars obtained from sugarcane and maize. Methanol is produced by a thermochemical procedure by means of lingo cellulose. These two technologies in India are in the research and development phase; however, it offers huge possibility in the transportation division. These biofuels are being produced for transportation on an extremely huge scale in Brazil and can be efficiently substituted for petrol.

Biodiesel being an eco-friendly fuel can substitute diesel fuel which is prepared from biorenewable sources like vegetable oils (edible or non-edible oil) and animal fats. The natural oils and fats obtained from them are combination of many triglycerides [17]. Since India is undersupplied in edible oils, non-edible oil possibly will be a better choice for production of biodiesel. Biodiesel is obtained by transesterification process of oil obtained from the plant. In India *Jatropha curcas* has been acknowledged as the main tree-borne oilseed (TBO) for production of biodiesel as it is non-edible oil and is available all through the country. The ability of *Jatropha curcas* to recuperate degraded or dry lands, as of which the underprivileged mostly derive their food, by improving land's water preservation ability, makes it furthermore fitting for upgradation of soil resources. Currently, in India, there are six biodiesel plants with combined annual production capacity of 650 million liters of biodiesel per year [18, 19].

4.4 Improved Cookstoves with Biomass as Fuel

For effective biomass utilization, improved cookstoves programs have been initiated in most of the Asian countries. The National Program on Improved Cookstove (NPIC) was launched in April 1985 in India, under which 30.6 million units were planned by the end of March 1997. The success of this program and demand for improved cookstoves led to more comprehensive National Biomass Cookstoves Initiative (NBCI) in 2009. Jain et al. in 2018, have mentioned in their paper that less than 1% of rural households were only making use of improved cookstoves and 14% of households were aware of their subsistence, demonstrating less awareness among the non-users [20]. Unnat Chulha Abhiyan was launched in 2014 to initiate offer for subsidies ranging from INR 300 to 800 per improved cookstoves with the aim of deploying 2.75 million improved cookstoves by March 2017 with a finances of INR 294 crores but the scheme had met only 1.3% of its objective by March 2017, with much of the finances having lapsed unutilized [14].

The traditional biomass cookstoves are generally sludge built cylinder by three faintly raised stands on which tools rest. The efficiency of the traditional biomass cookstoves is only 5–10%, emitting greenhouse gases, danger of firing, and produce health vulnerability in kitchens [21]. The improved biomass cookstoves reduce the consumption of biomass resources and lower the household expenses on biomass, and it also cuts down the time required for assortment of fuel and most importantly reduces the indoor air pollution [22, 23]. The improved biomass cookstove is estimated to save 40–60% of fuel compared to traditional biomass cookstoves. Incentives are provided for construction, maintenance, dealership, and publicity, technical backup, and training for the improved cookstoves [24].

Sharma et al. in 1990 emphasized the strategy on adoption and large-scale propagation of improved cookstoves to work on the health parameter of rural women and to lessen the consumption of firewood [25]. Apart from the health impact, inefficient cookstoves require extended cooking hours up to 5–8 h per day on cooking with 20% of that time dedicated for the gathering of fuel. There are several health related issues like asthma, respiratory diseases and shortened lung functions, problem in breathing, stinging eyes, low birth weight, and sinus problem coupled with the application of biomass cookstoves. Keeping in mind the above aspects, the scientific community around the globe made immense struggle to improve the cooking environment and it was supported by the lawmakers, NGOs, World Bank, etc., to decrease the environmental pollution, health hazardous, deforestation, and global warming [26, 27]. But there are some barriers to above given bioenergy technology which is given below in Table 2.

A multifuel, multistakeholder, and multipronged nationwide policy that mull over not only the delivery side, but also the requirement, aspiration, and priority of the patrons will promise a sustainable conversion toward clean and inexpensive cooking energy entrée for all [28, 29].

Table 2 Bioenergy technology and its barriers

Bioenergy technology	Barriers to bioenergy technology
Family biogas	High installment rate Technical hindrance for obtaining funding
Community biogas	Insufficient dung Low capacity utilization of system Large investment requirement Lack of institute to implement, plan and maintain biogas
Biomass gasifiers	Land accessibility and sustainable biomass availability Requirement of multifeed system Uncertain land tenure Absence of institute to enable community participation Biomass gestation period
Improved cookstoves	Lack of user education No quality control Diminutive time period of cookstoves Low performance of cookstoves

5 Conclusion

Sustainable exploitation of biomass as clean and cost-effective energy has a prospective to work as a means for sustainable development for rural sector. The vital aspect of sustainable harnessing of biomass energy resource is its preservation by escalating the end use consumption efficiency. If appropriately harnessed and designed bioenergy systems offer enormous amount of environmental and socio economic advantages. Better coordination between existing institutions is required to avoid replication of research. Biomass generation, biomass conservation and adept change of biomass to clean bio fuels are requisite to extend the accessibility of clean and renewable fuel in India.

References

1. UNDP/WEC (2001) World energy assessment: energy and the challenges of sustainability. United Nations development Programme. United Nations Department of Economic and Social Affairs, World Energy Council, New York, USA
2. WHO (2006) Fuel for life: household energy and health. Geneva
3. Smith KR, Dutta K (2011) Cooking with gas, editorial. *Energy Sustainable Dev* 15:115–116
4. Kumari H (2016) Rethinking biomass cookstoves innovations and issues. *IJRASET* 4:608–613
5. Jagadish KS (2003) Bioenergy for India: prospects, problems and tasks. *Energy Sustainable Develop* 7:28–34
6. O'Neal D (2007) Guide to designing retained heat cookers. HELPS International Addison, TX; U. S. Environmental Protection Agency, Washington DC
7. Census of India (2011) Ministry of home affairs. Government of India, New Delhi
8. NCAER (1992) Evaluation survey of household biogas plants set up during seventh five year plan. National Council for Applied Economic Research, New Delhi

9. Sinha CS, Ramana PV and Joshi V (1994) Rural energy planning in India: designing effective intervention strategies. *Energy Policy* 22(5)
10. FAO (2001) Global forest resources assessment 2000. Main Report. Food and Agriculture Organization of the United Nations, Rome
11. TERI (1997) Rural and renewable energy: perspectives from developing countries. New Delhi, India
12. Viswanathan B, Kavi Kumar KS (2005) Cooking fuel use patterns in India: 1983–2000. *Energy Policy* 33:1021–1036
13. Desai BG (2018) CO₂ emissions—Drivers across time and countries. *Curr. Sci.* 115:386–387
14. MNRE (2017) Annual Report 2016–2017
15. Chen L, Xing L, Han L (2009) Renewable energy from agro-residues in China: Solid biofuels and biomass briquetting technology. *Renew Sustain Energy Rev.* 13:2689–2695
16. Nzotcha U, Kenfack J (2019) Contribution of the wood-processing industry for sustainable power generation: viability of biomass-fuelled cogeneration in Sub-Saharan Africa. *Biomass Bioenergy* 120:324–331
17. Biodiesel Industries Australia Pty Ltd (2003) Response to: Environment Australia National Standard for Biodiesel. Discussion Paper No. 6
18. Pramanik K (2003) Properties and use of *Jatropha curcas* oil and diesel fuel blends in compression ignition engine. *Renewable Energy* 28:239–248
19. Chisti Y (2008) Biodiesel from microalgae beats bioethanol. *Trends Biotechnol* 26:126–131
20. Jain A, Tripathi S, Mani S, Patnaik S, Shahidi T, Ganesan K (2018) Access to clean cooking energy and electricity 2018—Survey of states. Council for Energy, Environment and Water
21. Masera OR, Diaz R, Berrueta V (2005) From cookstoves to cooking system: the integrated program on sustainable household energy use in Mexico. *Energy Sust. Dev.* 9:25–36
22. Panwar NL, Kaushik SC, Kothari S (2011) Role of renewable energy sources in environmental protection: a review. *Renew Sustain Energy Rev* 15:1513–1524
23. Zhang H, Ye X, Cheng T, Chen J, Yang X, Wang L et al (2008) A laboratory study of agricultural crop residue combustion in China: emission factors and emission inventory. *Atmos Environ* 42:8432–8441
24. Venkataraman C, Sagar AD, Habib G, Lam N, Smith KR (2010) The Indian National Initiative for advanced biomass cookstoves: the benefits of clean combustion. *Energy Sustainable Develop* 14:63–72
25. Smith KR, Ahuja DR (1990) Toward a greenhouse equivalence index: the total exposure analogy. *Climatic Change* 7:1–7
26. World Health Organization (2017) Available online: <https://www.who.int/globalchange/resources/countries/en>
27. International Renewable Energy Agency (2016) Available online: <https://www.irena.org/publications/2016/Oct/Renewable-Energy-in-Cities>
28. PPAC (2019) Import of LNG: Historical. Ministry of Petroleum and Natural Gas, Government of India
29. NITI Aayog (2017) Draft National Energy Policy NITI Aayog

Present Status, Conservation, and Management of Wetlands in India



Vandana Shan, S. K. Singh, and A. K. Haritash

Abstract Among various types of aquatic ecosystems, wetland is highly productive and efficient one which provides direct as well as indirect services to human beings. And these services of wetland ecosystem account around fifty percent of the overall global ecosystem values and ranks first among all of them. The ever-growing needs for freshwater have exerted great pressure on wetland ecosystem. Also, in last few decades, a bunch of activities such as accelerated urbanization, industrialization, technological advancement in agricultural sectors along with changed land use pattern have unfortunately threatened the uniqueness of wetlands and affected their ecological, economical, and biological identity. Due to various natural and anthropogenic activities, wetland occupied areas throughout the world are decreasing and declining its water quality. Indian wetlands cover around 4.1 million hectares (excluding irrigated agricultural lands, rivers, and streams) of land area, from which 1.5 million hectares are natural and 2.6 million hectares are man-made. Interest in sustainable use and adaptive management of wetlands has increased in the last few years. Based on the available information, wetlands are facing problems like inadequate information and uneven management of these valuable systems. A conceptual framework is highly required for wetland management which should include all the major issues affecting the wetland status, trends, management scenario and related responses, technical input and data management, respectively. This paper mainly reviews the present status, conservation and management plans for Indian wetlands concentrating on various threats and their possible sources to wetland regions and also focuses to investigate major factors responsible for overutilization of wetland wealth and various management practices for their present and future usage in sustainable way.

Keywords Wetland · Threats · Conservation · Sustainable use · Management plans

V. Shan (✉) · S. K. Singh · A. K. Haritash

Department of Environmental Engineering, Delhi Technological University, New Delhi, Delhi, India

e-mail: vandanashan@dce.ac.in

1 Introduction

Water is most important commodity which sustains life on planet earth. Even a large part of earth surface is covered with water but a very less amount of water is accessible for human use. And that amount of water is available in various lentic (lakes, ponds) and lotic (stream, river) ecosystems. Wetlands are one of the highly productive and valuable ecosystems among them. Wetlands are transitional zone between permanently wet (water) and generally dry environment (land), where water is usually found closed to the surface and soil is temporarily or permanently covered with shallow water [31]. According to Indian context, Ramsar Convention [40] stated about various water bodies (natural and anthropogenic) like rivers, lakes, mangroves, ponds, agricultural fields, water reservoirs, canals, etc. This is also one of the most biologically diverse ecosystems on the earth surface as it provides natural habitats to wide varieties of plant and animal species [16]. Wetlands are freshwater resources and provide many ecological, economic, cultural, aesthetical and supportive services that are important for human society [51]. In addition, wetlands provide feeding, resting, and breeding place for wildlife and are important habitat for water fowl and various migratory birds [41]. In recent years, there has been increasing recognition of wetlands in context of providing various regulating, provisioning, supporting, and cultural services. Inland water is known the most endangered ecosystem on the earth and it is predicted that more 50% of the world's wetlands would have been vanished by 2030. Increasing demand of water use is due to increasing rate of population growth, so uphill task to protect and conserve our ecosystem resources for their sustainable use. Even after all these, services providing wetlands are under the threat of extinction or degraded by poor management and unsustainable use which ultimately declined their benefits significantly. Wetlands, being the most threatened habitats of the world, are facing tremendous anthropogenic pressures posing degradation in quality and quantity of water resources [17] and the catchments areas found in their vicinity. Burgeoning human population, unplanned urbanization [12], changes in land use/land cover [10, 15] at large scale, fast-moving activities and continued overexploitation of resources has drastically reduced in number of wetland resources in India. A number of significant losses like hydrological alterations, lowering in water table, contamination of underground water resources with organic and inorganic pollutants, sprout of water borne diseases [24, 35], etc. have been observed. In order to conserve wetland productivity and biodiversity, sustainable use of its resources is highly required by human beings. To understand the vitality of these ecosystems need of advance research is highly required in planning and implementation of a national strategy. And this can only be possible by collective efforts and collaboration of planners, managers, owners, occupiers, and stakeholders. The scientific knowledge further will lead in setting priorities and in framing appropriate planning processes to achieve sustainable approach/results in conservation of these productive ecosystems and help in mitigation of pollution. In addition more research emphasis on the physical, socio-economic, and institutional factors is needed which directly influence present wetlands

conditions and their use [28]. The present paper includes the wetland values, distribution in varied geographical conditions, threats, conservation of wetlands, and their sustainable management plans.

2 Global Wetlands Scenario

97.5% of the total water in the hydrosphere is situated in the oceans as saline water that constitutes two-thirds of the earth's surface [47]. Wetlands constituted nearly 6.4% of the earth's surface which includes bogs, fens, swamps, and flood plains with 30%, 26%, 20%, and 15%, respectively (Table 1). The water resource distribution throughout the world and continentwise distribution is given in Tables 1 and 2, respectively [9, 47]. Wetlands are distributed globally in each continents of world except Antarctica (Fig. 1.) where bog, fen, freshwater marsh, bog, swamp forest, mire, and peat lands are types of palustrine, lacustrine have lakes, pans, and saline wetlands and estuarine represents coastal wetlands [26].

According to recent report published by the Economics of Ecosystems and Biodiversity (TEEB), the world has lost around half of its wetlands in just the last 100 years,

Table 1 Global water resources distribution

Water resource	Area (millionsq.km)	Volume (mill.cu.km)	Total water (%)	Freshwater (%)
Ocean	361	1338	97.47	–
Freshwater	–	35	2.53	–
Ice	16	24	1.76	69.1390
Ground water	–	10.5	0.76	30.0710
Lakes (excluding saline lakes)	1.5	0.09	0.007	0.2769
Rivers	–	0.02	0.0002	0.0079
Wetlands (Marshes, swamps, lagoons, flood plains, etc.)	2.6	0.1	0.0001	0.0039

Table 2 Freshwater resources distribution in continents

Freshwater type	Africa	Europe	Asia	Australia	North America	South America
Lakes	30,000	2027	27,782	154	25,623	913
Rivers	195	80	565	25	250	1000
Reservoirs	1240	422	1350	38	950	286
Groundwater	5,500,000	1,600,000	7,800,000	1,200,000	4,300,000	3,000,000
Wetlands	341,000	–	925,000	4,000	180,000	1,232,000

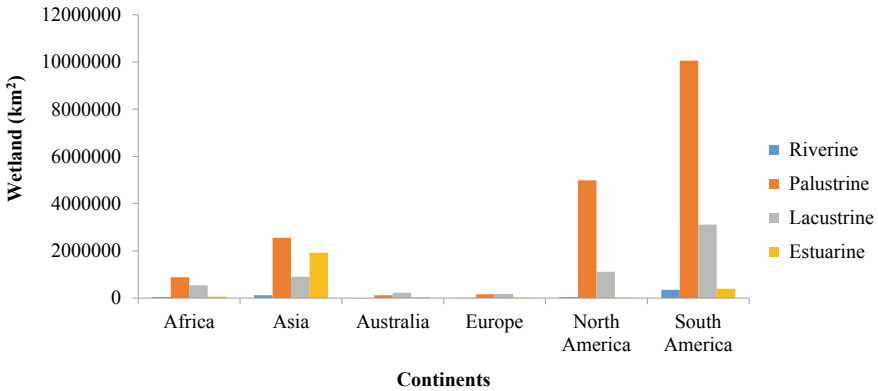


Fig. 1 Wetland area distribution in various continents except Antarctica

Table 3 Wetland density (km²) excluding reservoirs and Ramsar sites [26] and wetland loss (%) [10] in various continents

Continent	Wetland density (km ²)	Wetland loss (%)
Africa	0.051	43
Asia	0.085	83.7
Australia	0.051	44.3
Europe	0.037	71
North America	0.25	36.5
South America	0.094	NA

and it was found that out of 25 million square kilometers of wetlands that existed in 1900 just 12.8 million square kilometers now remain. The rate of destruction varies geographically and is higher in East Asia with annual rate of 1.6% per year. Wetland losses have been found larger and faster for inland wetlands as compared to coastal wetlands. As compared to Europe and North America, the rate of wetland loss has observed high in Asia with fast and large-scale conversion [10]. Table 3 represents wetland density (km²) excluding reservoirs and Ramsar sites [26] and percentage wetland loss [10] in various continents.

3 Indian Scenario

Most of the Indian wetlands have depth below six meter. And presently most of Indian lakes are being degraded by the problems of siltation and encroachment. Some of them are Wullar lake of Kashmir, Chilka lake in Orissa, Kolleru lake in Andhra Pradesh, and man-made Sukhna lake in Chandigarh. In last two decades, the water holding capacity of most of these lakes has also decreased. The other most important reason for degradation of water quality in most popular lakes of country, Srinagar’s

Table 4 Indian wetland distribution according to wetland inventories of India

Sr. No.	Inventory list	Year	Total wetlands		Total wetlands	
			Natural	Anthropogenic	Natural	Anthropogenic
1	WWF and AWB	1989 & 1993	Not identified	–	58.3	–
2	MoEF, GoI	1990	2167	65,253	1.45	2.59
3	Wetlands of India (Space Applications Center)	1998	1815	49,249	1.45	2.27

Source [15, 50]

Dal lake and Loktak lake of Manipur is eutrophication (nutrient enrichment) and weed infestation which have threatened the ecological functioning and biodiversity of these lakes. In Harike lake (Punjab), water hyacinth is spreading at alarming rate and infested about 75% of the wetland area. Extensive and unsustainable utilization of natural resources, for example, (excessive fishing) in the catchment areas of wetlands has created noticeable nuisance to aquatic life (waterfowls) in this lake. Loktak lake situated in southern part of Manipur valley is the largest natural lake in eastern India which is seriously threatened due to unwisely use of resources in its catchment and unplanned land use practices. Most of the lake is choked with various invasive species, e.g., *Eichhornia crassipes*, *Typha angustata*, *Hydrilla verticillata*, and *chara* spp. Problems of increased pollution, loss of biological diversity and available natural resources and reduction in water-spread areas are mainly resulted by various anthropogenic activities. The water-spread area and number of water bird species (pelicans, storks, and flamingos) of Kaliveli (Tamil Nadu) have reduced mainly due to encroachment by paddy fields and poaching for meat, respectively, and resulted in their migration. A number of lakes have also shrunk on account of repossession for agriculture, e.g., Kolleru lake of Andhra Pradesh, Deepar beel of Assam, Pyagpur and Sitadwar Jheels of Uttar Pradesh, and Hokarsar lake of Kashmir (Table 4).

4 Distributions and Classification of Wetlands in India

India comprises a large geographical spread and varied topography along with wide range of weather conditions which support large and highly diverse wetland classes with unique characteristics. Indian climate ranges from cold arid Laddakh to the warm arid Rajasthan, with a coastline of over 7500 km, with its major river systems and mountains. In India, most of the Indian wetlands are linked with famous rivers, Ganges, Cauvery, Krishna, Godavari, Tapti, and their tributaries directly or indirectly linked with major river systems and their tributaries. About 1–5% of geographical

Table 5 Aerial estimates of typewise national wetland inventory and assessment

Sr. No.	Wetland type	Wetland area (ha)	Wetland area (%)
1	River/stream	5,258,385	34.5
2	Reservoir/barrage	2,479,754	16.2
3	Intertidal mud flat	2,413,642	15.8
4	Tank/pond	1,310,443	8.6
5	Lake/pond	729,532	4.8
6	Wetlands	555,557	3.6
7	Mangrove	471,407	3.1
8	Waterlogged-natural	316,091	2.1
9	Aquaculture pond	287,232	1.9
10	Lagoon	248,277	1.6
11	Creek	206,698	1.4
12	Salt marsh	161,144	1.1
13	Salt pan	148,913	1.0
14	Coral reef	142,003	0.9
15	Waterlogged-man-made	135,704	0.9
16	High-altitude wetland	124,263	0.8
17	Ox-bow lakes/cutoff meander	104,124	0.7
18	Riverine wetland	91,682	0.6
19	Sand/beach	63,033	0.4
20	Salt pan-inland	13,698	0.1
	Total	15,260,572	100

Source National Wetland Atlas, Space Applications Centre, ISRO, Ahmedabad, March 2013

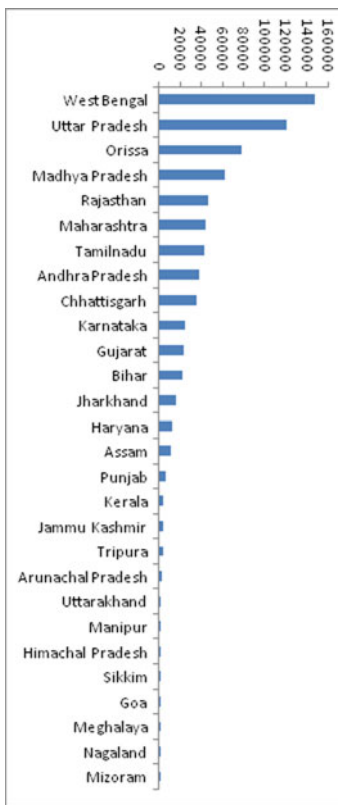
region of country is occupied by wetlands alone. India is at fifth position in category of mega biodiversity zone (MoEF 2010) (Table 5).

Of an estimated 4.1 million hectares (excluding irrigated agricultural lands, rivers, and streams) of wetlands, 1.5 million hectares are natural and 2.6 are man-made, while 6750 km² areas of coastal wetlands are mainly occupied by mangroves. Indian wetlands are mainly classified in two main categories, inland and coastal wetlands according to definition devised under the Ramsar Convention and these are further divided into two categories as: natural and man-made. Ox-bow lakes, high-altitude wetlands, riverine wetlands, and waterlogged area, river/stream are natural inland wetland and creeks, sand/beach, intertidal mud flats, salt marsh, mangroves, and coral reefs comes under the category of coastal natural wetlands (Table 6).

However reservoir/barrages, tanks/ponds, salt pans, and aquaculture ponds are examples of inland man-made wetlands and coastal man-made wetlands category, respectively. Majority of man-made wetlands are found in regions of South India in form of tanks and these tanks have constructed in each and every village for human consumption and besides this act as resting, nesting, and breeding site for a variety of

Table 6 Statewise number of wetlands in India [5]

Sr. No.	State	No. of wetlands
1	West Bengal	147,826
2	Uttar Pradesh	121,242
3	Orissa	78,440
4	Madhya Pradesh	62,618
5	Rajasthan	46,748
6	Maharashtra	44,714
7	Tamil Nadu	42,978
8	Andhra Pradesh	38,514
9	Chhattisgarh	35,534
10	Karnataka	25,276
11	Gujarat	23,891
12	Bihar	21,998
13	Jharkhand	15,690
14	Haryana	11,970
15	Assam	11,178
16	Punjab	6430
17	Kerala	4354
18	Jammu Kashmir	3651
19	Tripura	3415
20	Arunachal Pradesh	2653
21	Uttarakhand	994
22	Manipur	708
23	Himachal Pradesh	641
24	Sikkim	553
25	Goa	550
26	Meghalaya	426
27	Nagaland	421
28	Mizoram	234



avifauna. Statewise wetland distribution in India follows the trend of Lakshadweep > Andaman and Nicobar Islands > Daman and Diu > Gujarat > Puducherry > West Bengal > Assam with 96.12%, 18.52%, 18.46%, 17.56%, 12.88%, 12.48%, 9.74%, respectively, with maximum geographical area to minimum geographical area in different union territories and states. States like Mizoram, Haryana, Delhi, Sikkim, Nagaland, and Meghalaya the extents of wetland are less than 1.5% [46].

The total estimated wetland area in India is 15260572 ha [46] (Table 5) which turns out to be 4.63% of the geographic area. The summary area statistics shows that inland: natural wetlands dominate with about 43% followed by inland: man-made

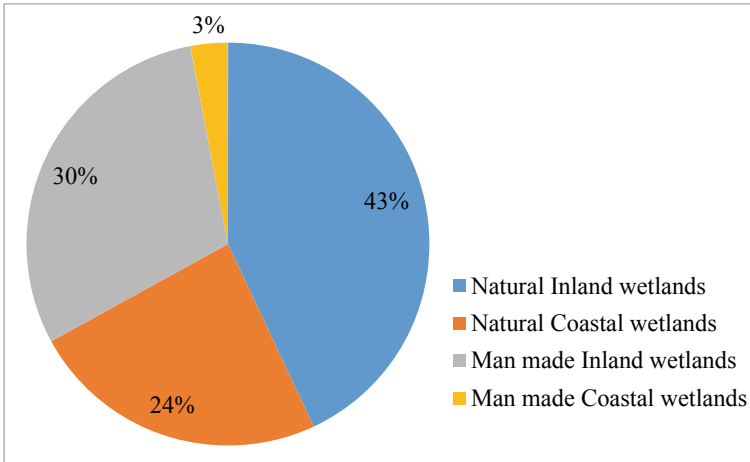


Fig. 2 Categorywise distribution of wetlands in India. (Source Aerial estimates of national wetland inventory and assessment based on Resource sat- 1 LISS-III data on 1: 50,000 scale)

wetlands (30%) and coastal: natural wetlands (Fig. 2). The sizewise distribution of wetlands (Fig. 3) reveals that large size wetlands (> 10,000 ha) constitute 49% followed by the wetland between 100 and 10,000 ha (37%).

Typewise statistics (Table 7) reveals that river/stream is the dominate type with 34.5% of the wetland area followed by reservoir/barrage (16.3%), intertidal mudflat (15.8%), and lagoon (8.6%). Rest of the each wetland type comprised less than 5% of wetland area.

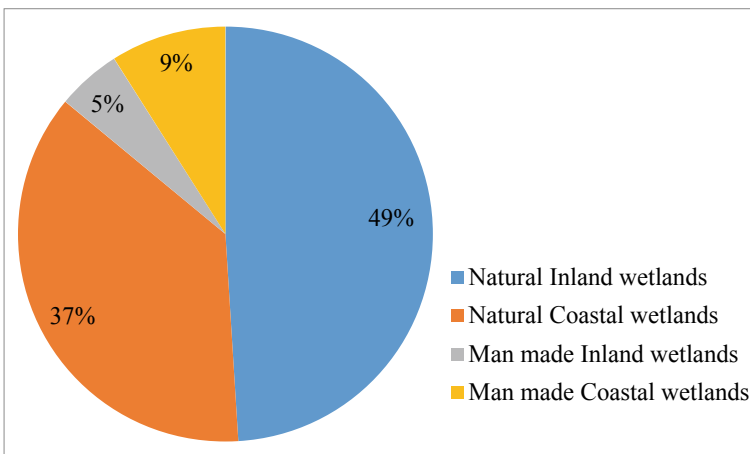


Fig. 3 Sizewise distribution of wetlands in India. (Source Aerial estimates of typewise national wetland inventory and assessment based on Resource sat- 1 LISS-III data on 1: 50,000 scale)

Table 7 Types of wetlands in Indian states and union territories*

State code	State	Wetland Type																	Wetland Total							
		Geographic Area																	Sub-total (a2, 2b)							
		1101	1102	1103	1104	1105	1106	1107	1201	1202	1203	1204	1205	1206	1207	1208	1209	1210	2101	2102						
Lake/pond	Open water/lake/pond	Shallow water/lake/pond	Wetland	Wetland (Natural)	Reservoir/Storage	Wetland (Artificial)	Wetland (Artificial)	Wetland (Artificial)	Wetland (Artificial)	Wetland (Artificial)	Wetland (Artificial)	Wetland (Artificial)	Wetland (Artificial)	Wetland (Artificial)	Wetland (Artificial)	Wetland (Artificial)	Wetland (Artificial)	Wetland (Artificial)	Wetland (Artificial)	Wetland (Artificial)						
35	Andhra Pradesh	8249	45	-	-	-	671	230	16	-	56	1777	10653	12399	6029	66101	49378	-	-	-	15215	94	15289			
28	Andhra Pradesh	25045	2443	-	-	214	35839	40489	20167	478	47407	9594	15891	3167	4062	41446	-	1725	240674	142996	18037	144153				
18	Assam	87658	18	520	11422	-	8146	13484	164	95	-	-	-	-	-	-	-	-	-	-	154609	1119	155728			
24	Gujarat	197481	23150	6	-	-	4258	47141	63764	2833	544	-	-	-	-	-	-	-	-	-	758291	6081	764372			
6	Haryana	49663	801	24	-	-	2118	34878	296408	8012	4822	336	-	-	-	-	-	-	-	-	384627	1782	402629			
4	Chhattisgarh	114	160	-	-	-	-	167	-	14	-	-	-	-	-	-	-	-	-	-	341	9	350			
22	Chhattisgarh	15194	-	26	-	-	174	17988	90389	40226	240	-	-	-	-	-	-	-	-	-	310143	2923	337966			
25	Dadra & Nagar Haveli	112	-	-	-	-	-	380	125	88	24	-	204	1054	57	63	-	-	-	-	2058	10	2068			
26	Dadra & Nagar Haveli	487	-	-	-	-	-	732	1286	13	-	-	-	-	-	-	-	-	-	-	2011	39	2070			
7	Daman	2966	49	-	-	-	-	380	1074	479	260	228	-	-	-	-	-	-	-	-	2470	301	2771			
30	Goa	3702	499	6	-	-	-	982	2363	396	17	41	-	-	-	-	-	-	-	-	2929	167	3137			
24	Gujarat	197481	23150	6	-	-	20660	278877	248979	73873	13951	1295	22289	149898	6508	2360565	144268	90475	33547	90878	882	3468242	9708	3474950		
6	Haryana	49663	801	24	-	-	-	412	13025	1775	3319	-	-	-	-	-	-	-	-	-	31949	1029	42478			
2	Himachal Pradesh	55673	52	-	-	-	-	47	55558	41817	134	30	-	-	-	-	-	-	-	-	98052	471	98466			
1	Jammu & Kashmir	22211	1762	-	-	-	-	-	23197	25132	6	-	-	-	-	-	-	-	-	-	339261	2540	391501			
20	Jharkhand	79714	3204	83	-	-	1629	231	97843	48177	5688	61	8	-	-	-	-	-	-	-	158824	13227	170631			
29	Karnataka	107191	638	-	-	-	1051	2845	197331	213327	222010	2403	-	-	-	-	-	-	-	-	812	2799	629712	13864	643576	
32	Kerala	38863	2643	-	-	-	440	20395	65362	26167	2435	-	-	-	-	-	-	-	-	-	157998	2939	160998			
31	Lakshadweep	828	-	-	-	-	-	-	-	-	-	-	-	-	-	-	-	-	-	-	79386	0	79386			
23	Madhya Pradesh	30814	206	93	-	-	7	157	31526	392455	64768	-	-	-	-	-	-	-	-	-	773214	44952	818166			
27	Maharashtra	307748	9003	15	-	-	2	284	289730	380135	206669	310	-	-	-	-	-	-	-	-	7025	71	992854	21668	1014522	
14	Manipur	22227	30123	64	-	-	-	8252	16627	866	187	-	-	-	-	-	-	-	-	-	2643	6395	541	6346		
17	Meghalaya	22420	501	461	-	-	1272	1028	24881	1582	150	5	-	-	-	-	-	-	-	-	29820	146	29968			
15	Mizoram	21087	185	-	-	-	-	-	-	-	-	-	-	-	-	-	-	-	-	-	-	13842	146	13988		
21	Nagaland	16521	3	9	-	-	-	423	19254	1847	41	-	-	-	-	-	-	-	-	-	21277	267	21544			
13	Odisha	153845	712	728	-	-	860	12925	223522	189972	29341	934	-	-	-	-	-	-	-	-	21396	1992	624700	66174	690904	
34	Puducherry	492	1120	-	-	-	-	20	2113	-	867	-	-	-	-	-	-	-	-	-	194	6391	144	6338		
3	Punjab	50562	1934	373	-	-	306	3032	59864	11858	3256	1341	-	-	-	-	-	-	-	-	-	8124	5049	86283		
8	Rajasthan	84269	38269	-	-	-	-	10856	342270	190600	151027	7636	12243	-	-	-	-	-	-	-	-	748191	34123	782314		
11	Sikkim	7096	15	-	-	-	-	-	4311	-	-	-	-	-	-	-	-	-	-	-	-	7196	281	7477		
33	Tamil Nadu	134049	136991	-	-	-	127	2928	136078	56149	27913	10811	-	-	-	-	-	-	-	-	3399	22889	10790	842620	10294	902520
16	Tripura	11040	387	-	-	-	-	2846	7420	3320	186	-	-	-	-	-	-	-	-	-	-	14559	2983	17542		
5	Uttarakhand	53566	2081	63	142	-	9	80133	20319	108	211	-	-	-	-	-	-	-	-	-	-	103666	816	103882		
9	Uttar Pradesh	240928	122531	5171	-	-	6100	76263	607315	105641	32363	83094	-	-	-	-	-	-	-	-	-	1148178	97352	1242510		
19	West Bengal	88005	58654	19550	82	3664	8664	56603	559392	22672	20470	1435	71	-	-	-	-	-	-	-	-	4866	1557	96290	138707	1107907
Total		3297467	729532	104124	124283	91082	316991	525888	2481987	1310443	135704	157974	16098	246044	266088	63033	241642	161144	471407	142003	148913	287232	1479015	558557	15266072	

Source [47]

Distribution of different types of wetlands in Indian states and union territories is given in Table 6.

5 Significance of Wetlands

Wetlands are obligate biodiversity support system and habitats for a wide range of rare, endangered, and threatened species of flora and fauna. They are well known as kidney of landscape and buffer zone. Besides this, wetlands provide various provisional, regulating, cultural, and supportive services [39] as discussed below.

5.1 Provisioning Services

Wetland ecosystems provide a large variety of natural products like food grain, fruits, raw materials for industries, timber, and firewood production and also provide resources for medicinal, ornamental, and genetic use. Also, these are known buffer zone which help in storage of storm water and retention of excess water during flood. Wetlands also provide water for domestic, industrial, and agricultural use. A number of well-known Indian lakes, e.g., Kolleru (Andhra Pradesh); Vembanad (Kerala) Chilka (Orissa); Khabartal (Bihar); Loktak (Manipur); Nalsarovar (Gujarat); Nainital (Uttarakhand); Dal lake (Jammu and Kashmir); Deepor Beel (Assam); and Carambolim (Goa), are main source of domestic, agricultural, and irrigational services and also provide tourism, fisheries, and recreational services [22]. Due to extraction of medicine from medicinal plants and other materials from biota, they are also having biochemical importance.

5.2 Regulating Services

Wetlands are highly important in maintaining essential ecological processes and life support systems. As a large source of and sink of greenhouse gases, they help in carbon sequestration and also useful in regulating local and regional temperature. They also influence other climatic conditions like gaseous exchange and precipitation. During excess rainfall, they keep proper continuous hydrological flow, maintaining water quality, and enhancing ecosystem productivity for both, humankind as well as for aquatic biota. Wetlands are the main primary source for recharging ground water aquifers by storing excess rainwater. They are known as natural filters as they remove a large amount of organic and inorganic contaminants from water, consisting harmful pathogens (bacteria and viruses) from waste water and sewage and heavy metals and hazardous waste generated from industries. They act as a buffer zone during periods of excessive rainfall and absorb suspended impurities like solids and

nutrient under soil surface. In addition, they are useful in erosion regulation, natural hazard regulation, and pollination. Wetlands are habitat of a number of native and migratory bird species as these provide resting and nesting place to them. Rann of Kutch, coastal areas in Gujarat, and Bharatpur wild life sanctuary in Rajasthan are well-known habitat of around 1200–1300 species of migratory birds (equivalent to 24% of total Indian bird species [1] from western and European countries during winter season.

5.3 Cultural and Amenity Services

Cultural service is the broad term used for spiritual interest which wetlands provide such as inspirational approach toward human culture, spiritual enrichment, intellectual development, science and education, cultural and historic information, religious experience, and education throughout recreation. It comprises knowledge systems, social relations, aesthetic values, and appreciation of nature. Pushkar lake (Rajasthan) and Ramappa lake (Telangana) are closely related to the local culture. Wetlands are becoming an increasingly important economic resource which offers chances for outdoor recreation and environment friendly tourism. Besides providing an aesthetic experience for the privileged, ecotourism helped out in alleviating poverty in major regions of the world and proven success for enhancing human well-being.

5.4 Supporting Services

Wetlands provide habitat for a large species of flora and fauna and support their biological and genetic diversity. Soil formation and reservation, biomass generation, atmospheric oxygen production, nutrient and water cycling, and serving habitat are some of supporting services which are provided by wetlands to large variety of plants and animal species for their entire life time. In regime of wetlands, plants flourish and produce a variety of products. Wetlands play an important role in supporting food chains which further help in maintaining ecological balance in nature [23]. Majority of water ecosystems in India support a large biological diversity of almost all taxonomic groups (flora and fauna). A rich species biodiversity of endemic and endangered species are preserved and supported by freshwater ecosystems in southern India. Loktak lake in North eastern region is nesting and breeding ground for endangered Sangai [44] and supports 75 and 120 species of phytoplanktons and rotifers, respectively, and Western Ghats provides habitat to around 24% of endemic aquatic plants species. Due to highly divergent ecological characteristics, the capital Delhi has achieved second most position after Nairobi. During winter season, more > 450 bird species are observed in Delhi alone. Red-crested pochards, white-tailed lapwing, great white pelicans; and Orphean warbler are some of these migratory birds species usually sighted in capital region [25].

6 Threats to Wetlands

India is second most populous country of the world and yet constitutes very little portion (around 2.4%) of the earth's surface. Wetlands are one of the most threatened habitats of the world that are subjected to both human and natural forces. Hydrologic cycle, rising sea level, natural succession, sedimentation, subsidence, drought, hurricanes, weed infestation, and soil erosion are some of natural processes which influence proper functioning of wetland. Wetland's spatial extent, due to rising sea level, is dependent on local factors. Due to burgeoning population and increasing anthropogenic activities (industrial and agricultural), Indian wetlands are facing great pressure of their extinction and degradation. Improper use of watersheds, large-scale change in land use cover and constructional projects have all caused dramatically reduction in wetland resources in our country. Extinction and degradation of highly useful wetlands result in various environmental and ecological issues, which directly affect the social and economic prosperity of associated population [34]. It has been estimated that in every single minute, one hectare of the world's wetlands is turning degenerated.

6.1 Urbanization

Wetlands situated near urban areas are facing expanding developmental pressure for various man-made activities. Urban wetlands are major source of freshwater supplies for public. Open land/wetland situated in urban center or suburban centers is treated as wasteland and transformed into various development activities. Local governments are responsible for zoning wetlands for light industry or residential housing. Urban wetlands have become ineffective in maintaining water quality and flood abatement due to various ongoing developmental activities in adjoining uplands. Urban development and industrial development have declined the wetlands area and due to poor water holding capacity of concrete, water runoff from the land surface and increase the risk of flood [38] due to increasing the flow rate of rivers after heavy rainfall. Also, various pollutants bring together with increased runoff and degrade water quality. Effluents from industries and untreated sewage from sewage treatment plants [6, 27] are usually dumped in wetland which leads to various disease causing microorganisms [24].

6.2 Anthropogenic Activities

Various man-made activities are responsible for deterioration of water quality [12] in lake and in catchment areas. Direct disposal of untreated sewage waste and solid waste is highly responsible for water quality deterioration in wetlands [37]. Direct

and indirect disposal of solid waste (biodegradable and toxic non-biodegradable) and immersion of idols have affected the physical, chemical, and biological properties of water in wetlands. Bathing, washing clothes, recreation, and navigation with motorized boats also affect the biota in wetlands. Exploitation of biological and physical resources of lakes and wetlands by dredging, harvesting of aquatic crop and vegetation, and fishing have caused interminable ecological and economic losses. Due to unmanaged urban, agricultural and industrial activities, wetlands have been depleted and altered causing their completely loss [32, 41]. Most of the human settlements are situated in catchment areas of urban and suburban wetlands and lakes which are facing both liquid and solid waste from these regions. In urban areas, large amount of pollutants and waste find their ways through storm water. But in rural areas, due to presence of natural vegetation in catchment area is facing different level of stress. Catchment devoid of vegetation, caused by excessive grazing and cultivation of vegetation, is highly susceptible for soil erosion. Due to soil erosion, upper fertile soil moves with runoff. In agricultural catchments, the degradation is caused due to excessive addition of fertilizers and non-biodegradable pesticides and silts due to surface and subsurface runoff.

6.3 Agricultural Activities

Increased population and advanced civilization have reduced vast stretches of wetlands, lakes, and floodplains of rivers and converted them into paddy fields with substantially increased in their spatial extent in India [14]. Due to easy access of water, the rich Gangetic floodplains are known highly rich cultivated regions all over the world. About 34,000 ha in Kolleru lake have been lost in Andhra Pradesh due to transformation of natural wetlands into agricultural land. Due to increased agricultural activities to support large number of population, excessive synthetic fertilizers are being used last few years which move with surface run off in wetlands and nearby water resources and caused enrichment of lake (Eutrophication) [4, 33]. In last twenty years, the irrigated land has been increased by 1506 km², showing approximately 50% increase in the area [3]. In last few decades, increasing water demand to irrigate crops in water deficient regions has been increased considerably leading to large number of canals, dams, and reservoirs construction resulting in advanced irrigation pattern and altered wetland hydrology in India. Hydrology of the wetland is significantly altered due to construction of a large number of reservoirs, dams, and canal in water scare regions. In certain extent, construction of reservoirs, dams, and canals increased economic prosperity of nation by converting wetlands and mangrove forests into pisciculture and aquaculture ponds instead their altered physiological and ecological characteristics.

6.4 *Hydrologic Activities*

Diversion of streams and rivers flow by constructing dams and reservoirs for water transportation to downstream arid zones for irrigation has changed the direction of water flow and drainage pattern which have substantially degraded the wetlands of that particular region. For example, in Gujarat, water drain from western Himalayan mountains in Satluj river is diverted via canal system to the dry zones of the state along with the neighboring state Rajasthan for providing water for irrigation to cash crops which have altered in the physicochemical characteristics of the soil and created various ecological problems like invasion of alien plant species, salinization, water scarcity in regional zones, and elimination of culturally sustainable life styles. Change in hydrological regime caused by human interference has resulted in changes in natural drainage [18]. Natural drainage of water bodies has also altered due to many anthropogenic activities in their catchment areas. Due to isolation of rivers and lakes from their flood plain zones lead to lower in water tables, decreased groundwater recharge and also increased human activities in flood plain zones caused increased flooding potential in lower zones due to faster flood water drainage. Migratory birds which usually visit to Bharatpur bird sanctuary have to force for alternate water bodies, e.g., Bhindawas Bird Sanctuary for nesting and breeding [20]. Moreover, change in structural, functional characteristics, and value of wetlands has transformed hydrology in urban and rural regions.

6.5 *Change in Land Use Cover*

Changed land use pattern has resulted in degradation of wetlands [8, 37] and decreased availability and production of a variety of valuable resources like fuel, fodder, fishes, medicine, honey, shell fish, and various chemicals. Along with this economic harm, a number of problems related to changes in land use have also been accelerated like accumulation of silt in bottom water bodies, soil erosion, and water pollution with unwanted wastes. Excessive and over withdrawal of ground water has decreased the water table level by 1.5 to 2.0 m making the situation worse in most of the regions. Change in hydrological conditions further resulted in increased soil erosion which eliminated a number of wetlands in directly in urban regions by filling them. Excessive ground water withdrawal has further raised the problems of soil salinity with reduced crop production which significantly accelerated the economic loss to the nation.

6.6 Deforestation

Major changes in water quality and quantity were observed in last few decades mainly due to deforestation. The rate of degradation of wetlands was noticed faster and larger as compared to forests. Removal of large number of plants and trees in the catchment area leads to removal of fertile soil and soil deposition over bottom surface of various water bodies. Mangroves, special type of wetlands, are being replaced to obtain farming lands and formation of fish ponds for rearing fishes, are significantly affecting their ecological properties. Mangrove forests are valued for their direct and indirect uses [2]. Altered land use pattern and advanced pisciculture have substituted large mangrove region into agricultural land and affected hydrology of wetlands.

6.7 Pollution

Only one-third of the total domestic wastewater generated from urban areas in India is treated and rest untreated is disposed in various natural and man-made water reservoirs affecting their water quality. River Yamuna passes through six big cities and a huge amount of untreated sewage and industrial waste is dumped daily in this river. A large proportion of untreated sewage and wastewater from metro city, Delhi, alone is discharged into Yamuna river which constitutes 78 percent of the total pollution load that flows every day in the river. Also, Bellandur lake in Bengaluru is also facing the problem related to industrial effluents discharged from nearby industries leading to increased problems of eutrophication in lake [33]. Excessive accumulation of nutrients in lakes has polluted freshwater by decreasing oxygen content and created nuisance and make them dead after some time [42]. Point source (emanating from an identifiable source like sewage and industrial effluent) and non-point sources (emanating from a diffuse source like agriculture and urban areas) are two main prominent sources for wetland pollution. A number of lakes and wetlands have lost due to improper and excessive use of their resources without their conservation [45].

6.8 Invasive Species

Introduction of invasive or alien species has threatened many of Indian wetlands by clogging water ways and fast uptake of nutrients in comparison to their native Indian species. Water hyacinth and salvinia are examples of mostly invaded exotic plant species. Due to changed habitats, these invasive plants species grow fast over native plants. Due to fast uptake of nutrients by exotic species, wetlands have lost a large number of native species of animals and plants. In late 1960, the problem of weed infestation in India has raised with free floating species of salvinia in Kakki reservoir of Kerala.

6.9 Climate Change

In reports of UNESCO [48] it was stated that climate change is expected to become main driver causing drastic change and loss in wetland ecosystems. Due to change in climatic conditions, water level has risen in Tsomoriri lake in Laddakh, due to which important breeding islands of various endangered migratory birds species would be submerged leading to their extinction. It was estimated that 1 m rise in sea water due to climate change will disappear coastal and saline wetlands with 84% and 13%, respectively. A number of climatic conditions, viz. change in rainfall pattern, fluctuated storms frequency; increased air temperature; unexpected droughts, and floods; excessive greenhouse gases (CO₂, CH₄, CFCs, etc.) concentration; and sea level rise, have also affected the ecological functioning of wetlands. Climate change acts both, boon and curse for wetlands. Paddy fields are also a type of wetlands and a large source of methane, a green house gas causing global warming. Rapidly increasing population in India has caused change in the landscape and topography, which is continuously affecting the water and wetland resources and making the regions less habitable by humans, animals.

7 Ramsar Sites in India

The Ramsar Convention is an intergovernmental treaty including 171 contracting parties. The main objective of convention is conservation and sustainable use of all wetlands at local, regional, and national level [36] and advice various contracting parties to produce wetland inventories, to adopt various wetland policies, to conduct research and monitoring within wetland areas. 2323 wetland sites were described in Ramsar list contributing over 248 million hectares throughout the world with their International importance. In 1981, India became signatory to the Ramsar Convention, mainly on the Waterfowl Habitat. Chilika lagoon and Keoladeo National Park in Orissa and Rajasthan states were designated first two Ramsar sites in India in 1981 significantly based on waterfowl habitats. In 2012, total 26 wetlands have been designated as Ramsar sites in India with maximum number in 2002. As India has various types of wetlands depending on their size, area, and importance, there are some criteria of selection of sites for Ramsar designation. India has 27 sites designated as Wetlands of International Importance (Ramsar Sites), with a surface area of 689, 131 ha in 2019. But on January 28, 2020, Ramsar Convention declared ten more new wetland sites, Nandur Madhameshwar of Maharashtra, Keshopur-Miani, Beas Conservation Reserve and Nangal from Punjab, and Nawabganj, Parvati Agra, Saman, Samaspur, Sandi, and Sarsai Nawar are from Uttar Pradesh as sites of national importance from India with surface area of 1,067,939 ha.

8 Conservation of Wetlands

Conservation is management of resources to maximize efficiency of use, minimize wastage and preservation for future. In India efforts to conserve wetlands had begun in 1987 and still various attempts are being done for wetland protection and conservation with the government's help using biological methods instead of engineering methods. It was observed that initiation of national wetland-mapping project provided an integrated approach on conservation. Various national committees were constituted for recommending the government regarding implementation of appropriate policies and management plans for conservation of wetlands, mangroves, and coral reefs. Steering committees should be set in each state including representatives from various government and non-government departments, research institutions, and universities for successful execution of these policies.

8.1 Ramsar Convention

The Ramsar convention is named after the name of city Ramsar in Iran where the convention was ratified in 1971. Main aim of the convention was to aware nations for conservation and wise use of wetlands without affecting its quality and quantity. India is also signatory to the Ramsar convention. Presently, India has 37 sites designated as Wetlands of International Importance (Ramsar sites).

8.2 National Wetland Conservation Programme (NWCP)

National Wetland Conservation Programme was implemented in 1985. The main aim of the plan is to set effective policies and guidelines for conservation and management of wetlands in the country to avoid their loss and deterioration. Several lakes were covered under this program. 115 wetlands were identified from 24 states and 2 union territories of India for their conservation and management. But due to differences noticed in implementing activities needed for conservation of wetlands and lakes, a distinct National Lake Conservation Plan was started for restoration and conservation of urban and suburban lakes degraded by man-made activities. According to Ministry of Environment and Forests [29], under this plan, only 10 lakes were recognized initially for their conservation and management.

8.3 *The Central Wetlands (Conservation and Management) Rules*

They were introduced in 2010 for effective management and preservation of wetlands across the country. According to new rules in 2017, state government has authority to keep an eye on prohibited activities in wetland areas along with their identification and notification.

8.4 *National Environment Policy 2006*

National Environment Policy, 2006, first time noticed the wetlands degradation due to various anthropogenic and natural factors and no proper legislative system for conservation of wetland were regulated in the country. So it was highly recommended to enforce legal system for identification and management of valuable wetlands, to avoid their further degradation and increase their restoration [28]. Further, the policy advocated in developing a national inventory of such wetlands implemented a wide spectrum of policies and plans for wetland conservation and their environmental impact assessment (EIA). Central government notified the Wetlands (Conservation and Management) Rules, 2010 based on the directives of National Environment Policy, 2006 and recommendations made by National Forest Commission and under the chairmanship of Secretary, Environment and Forest, Central Wetlands Regulatory Authority (CWRA) has been constituted. Besides this, for examining management action plans of newly identified wetlands, an Expert Group on Wetlands (EGOW) has also been constituted. The rules put restrictions on the activities such as reclamation, setting up industries in vicinity, discharge of untreated effluents, manufacture or storage of hazardous substances, any permanent construction, and solid waste dumping within the wetlands.

8.5 *National Plan for Conservation of Aquatic Ecosystems (NPCA)*

NPCA plan was initiated for both wetlands and lakes and implemented in 2015 by merging National Wetlands Conservation Programme (NWCP) and the National Lake Conservation Plan (NLCP). This plan was sponsored by center. Its main objective is to provide strong policy framework to State Governments for their effective management.

8.6 Education and Capacity Building

The meaning of capacity building is increase in knowledge, skills and attitudes of people and their development at individual, organizational, and institutional level. Ministry of Environment and Forests has noticed that proper trained manpower in different fields, viz. research institutions, economic and social administrative is required for effective management and conservation of wetlands. Conservation of rivers and lake is a multidisciplinary course, sponsored by MoEF, at Indian Institute of Technology, Roorkee, with various coordinating departments like hydrology, civil engineering, and management, for capacity building of state, local, and central government officers for conservation of water bodies and their ecology.

8.7 Legal and Regulatory Framework

In India, a number of policy and legislative measures (Table 8) influenced wetland conservation directly or indirectly.

Provisions under these acts/stringent laws include conservation, restoration of ecologically sensitive regions along with protection of water quality and increasing the biodiversity of flora and fauna in various environmental ecosystems (terrestrial and aquatic) of country.

Table 8 Indian legal and regulatory framework

Sr. No.	Legal framework/stringent law	Year
1	National Policy And Macro level Action Strategy on Biodiversity	1999
2	National Conservation Strategy and Policy Statement on Environment and Development	1992
3	Wildlife (Protection) Amendment Act	1991
4	Coastal Zone Regulation Notification	1991
5	Environmental (Protection) Act	1986
6	Forest (Conservation act)	1980
7	Maritime Zone of India (Regulation and fishing by foreign vessels) Act	1980
8	Water (Prevention and Control of Pollution) Act	1977
9	Territorial Water, Continental Shelf, Exclusive Economic Zone and other Marine Zones Act	1976
10	Water (Prevention and Control of Pollution) Act	1974
11	Wildlife (Protection) Act	1972
12	The Indian Forest Act	1927

9 Conclusion

The present study concludes that the wetlands are backbone of economy and human society as these ecosystems provides a large extent of services to mankind and help in keeping ecological balance with human needs. But now current status of wetlands is matter of concern that must be discussed, understood, and acted upon to ensure their protection, restoration, and conservation. For this, an integrated approach in terms of planning, execution, and monitoring of various wetland regions should be practiced along with effective collaboration with, experts in hydrologist, watershed management, ecologist, economist, planners, and decision makers for their proper management of resources as well as efficient and sustainable use. Awareness for wetland restoration and their conservation at local level is prerequisite condition. Public awareness by educational programs about the wetland importance in rural areas, colleges, schools, and among local people should be practiced to spread awareness about importance of wetlands and their need for conservation. Present study also stated that the various conservation and management plans practiced by government so far, for large National and Ramsar sites, were resulted likely to be ineffective and unrealistic to meet the desired goals. Small wetlands were totally neglected under these government conservation plans. So a common whole of government policy should be exercised for conservation of both, large as well as small wetlands by decentralizing power of center to states along with district too. Only proper care and efficient management of wetlands can ensure its sustainability otherwise continued mismanagement and depletion of the same will dead to crisis for life on this planet.

References

1. Agarwal M (2011) Migratory birds in India: migratory birds dwindling. *Nature*.
2. Ahmad N (1980) Some aspects of economic resources of Sundarban mangrove forest of Bangladesh. In *Asian Symposium on Mangrove Environment, Research and Management*, Kuala Lumpur (Malaysia), pp 25–29
3. Anon (1994) World Development Report. World Bank Development report. pp 254
4. Badar B, Romshoo SA, Khan MA (2013) Modelling catchment hydrological responses in a Himalayan Lake as a function of changing land use and land cover. *J Earth Syst Sci* 122:433–449
5. Bassi N, Kumar MD, Sharma A, Pardha-Saradhi P (2014) Status of wetlands in India: a review of extent, ecosystem benefits, threats and management strategies. *J Hydrol Regional Stud* 1(2):1–9
6. Brraich OS, Jangu S (2016) Comparative account of accumulation of heavy metals and structural alterations in scales of five fish species from Harike Wetland. *India. Iranian J Ichthyol* 3(4):275–282
7. Central Pollution Control Board, CPCB (2008) Status of Water Quality in India (2007) New Delhi: Central Pollution Control Board. Ministry of Environment and Forests, Government of India
8. Chitra, KP (2016). How Kerala is destroying its wetlands, amendment to kerala conservation of paddy land & wetland Act 2008. *Economic and Political Weekly*. 51(22). <https://www.epw.in/journal/2016/22/reports-states/how-kerala-destroying-itswetlands.html>

9. Clarke R (1994) The pollution of lakes and reservoirs (UNEP environmental library, no. 12). Nairobi, Kenya: United National Environment Programme
10. Davidson NC (2014) How much wetland has the world lost? Long-term and recent trends in global wetland area. *Marine Freshwater Res* 16:65 (10):934–41
11. Farooq M, Muslim M (2014) Dynamics and forecasting of population growth and urban expansion in Srinagar City-A Geospatial Approach. *Int. Arch Photogramm Rem Sens Spatial Inf Sci* 40:709–716
12. Farooq R, Chauhan R, Mir MF (2018) Deterioration of water quality of Anchar Lake as indicated by analysis of various water quality parameters. *Int J Adv Res Sci Eng* 7:2551–2558
13. Fazal S, Amin A (2011) Impact of urban land transformation on water bodies in Srinagar City, India. *J Environ Protec* 2:142–153
14. Foote AL, Pandey S, Krogman NT (1996) Processes of wetland loss in India. *Environ Conserv* 23:45–54
15. Garg JK, Singh TS, Murthy TV (1998) Wetlands of India. SAC, Indian Space Research Organisation, Ahmedabad
16. Ghermandi A, van den Bergh JCJM, Brander LM, Nunes PAD (2008) The economic value of wetland conservation and creation: a meta-analysis. [Working Paper 79]. Fondazione Eni Enrico Mattei, Milan, Italy
17. Gopal B (2014) Wetland conservation for biodiversity and ecosystem services needs a shift in land and water resources policies. Published by the National Institute of Ecology Japan, Policy brief, p 16
18. Gopal B (1982) Ecology and Management of freshwater wetlands in India. In: Proceedings of the International Scientific Workshop (SCOPE-UNEP) on ecosystem dynamics in Freshwater Wetlands and Shallow water bodies, pp 127–162. Centre for International projects, GKNT, Moscow, USSR
19. Gopal B, Sengupta M, Dalwani R, Srivastava SK (2010) Conservation and Management of lakes-an Indian perspective. Ministry of Environment & Forests, p 22. National River Conservation Directorate, Paryavaran Bhavan, CG O Complex, Lodhi Road, New Delhi, India
20. Haritash AK, Shan V, Singh P, Singh SK (2015) Preliminary investigation of environmental status of Bhindawas Bird Sanctuary. *Int J Eng Res Technol* 4(3):53–56
21. IUCN (1994) IUCN Red List categories. World Conservation Union, Gland, Switzerland
22. Jain CK, Singhal DC, Sharma MK (2007) Estimating nutrient loadings using chemical mass balance approach. *Environ Monit. Assess* 134(1–3):385–396
23. Juliano K, Simonovic SP (1999) The Impact of Wetlands on Flood Control in the Red River Valley. University of Manitoba, Manitoba, Canada, Natural Resource Institute
24. Kumar G, Kaur A (2018) Status of Wetlands in Punjab: a review on policy frameworks. *Asian J Multidimens Res* 7(10):169–177
25. Lalchandani N (2012) Green zones packed as avian guests flocked. *The Times of India* December, 4
26. Lehner B, Döll P (2004) Development and validation of a global database of lakes, reservoirs and wetlands. *J Hydrol* 296:1–22
27. Mabwoga SO, Chawla A, Thukral AK (2010) Assessment of water quality parameters of the Harike Wetland in India, a Ramsar Site, using IRS LISS IV satellite data. *Environ Monitor Assess* 170(1–4):117–128
28. Ministry of Environment and Forests (MoEF) (2006) National Environmental Policy. MoEF, Government of India, New Delhi
29. Ministry of Environment and Forests (MoEF) (2007) Conservation of Wetlands in India: A Profile (Approach and Guidelines). MoEF, Government of India, New Delhi
30. Ministry of Environment and Forests (MoEF) (2012) Annual Report 2011–2012. MoEF, Government of India, New Delhi. Ministry of Environment and Forests (MoEF), n.d. Wetlands of India: a directory. New Delhi: MoEF, Government of India
31. Mitsch WI, Gosselink IG (1986) Wetlands. Wiley Publication. Van Nostrand Reinhold, New York

32. MoEF [Ministry of Environment and Forests], Government of India (2010) National Wetland Atlas. Kerala, Space Application Centre, ISRO, Ahmedabad, p 146p
33. Nune S (2016) Wetlands in India: Significance, Threats & Conservation
34. Prasad SN, Ramachandra TV, Ahalya N, Sengupta T, Kumar A, Tiwari AK, Vijayan VS, Vijayan L (2002) Conservation of wetlands of India-a review. *Tropical Ecol* 43(1):173–186
35. Ramachandra TV (2001) Restoration and management strategies of wetlands in developing countries. Secretariat R. The list of wetlands of international importance, In The Secretariat of the Convention on Wetlands, Gland, Switzerland, p 2013
36. Ramsar CS (2007) River basin management: integrating wetland conservation and wise use into river basin management, Ramsar Handbooks for the Wise Use of Wetlands, vol. 7. In Ramsar Convention Secretariat, Gland, Switzerland, p 62
37. Rashid I, Romshoo SA, Amin M, Khanday SA, Chauhan P (2017) Linking human-biophysical interactions with the trophic status of Dal Lake, Kashmir Himalaya. India. *Limnologica*. 62:84–96
38. Romshoo SA, Altaf S, Rashid I, Dar RA (2017) Climatic, geomorphic and anthropogenic drivers of the 2014 extreme flooding in the Jhelum basin of Kashmir. India. *Geomatics Natl Hazards Risk*. 9:224–248
39. Russi D, ten Brink P, Farmer A, Badura T, Coates D, Förster J, Kumar R, Davidson N (2013) The Economics of Ecosystems and Biodiversity for Water and Wetlands. London and Brussels. Ramsar Secretariat, IEEP
40. Secretariat R (2013) The List of Wetlands of International Importance. The Secretariat of the Convention on Wetlands, Gland, Switzerland
41. Shan V, Singh SK, Haritash AK (2017) Major ions chemistry of surface water in Bhindawas Wetland. Haryana. *Int J* 5(1):117–121
42. Shan V, Singh SK, Haritash AK (2020) Water crisis in the Asian Countries: Status and Future Trends, Resilience, Response, and Risk in Water Systems, 173–194
43. Sharma BK (2009) b) Diversity of rotifers (Rotifera, Eurotatoria) of Loktak lake, Manipur. North-Eastern India. *Trop. Ecol*. 50(2):277–285
44. Sharma BK (2009) Composition, abundance and ecology of phytoplankton communities of Loktak lake, Manipur. India. *J. Threat. Taxa* 1(8):401–410
45. Singh SK, Shan V (2017) Biodiversity and its conservation. In: Environmental studies New Delhi: Bharti Publications
46. Space Applications Centre (SAC) (2011) National Wetland Atlas. SAC, Indian Space Research Organisation, Ahmedabad
47. UNEP (1994) The pollution of lakes and reservoirs. United Nations Environmental Programme, UNEP Environmental Library NO.12, Nairobi, Kenya, pp 3–24
48. United Nations Educational, Scientific and Cultural Organization (UNESCO) (2007) Case studies on climate change and world heritage. UNESCO World Heritage Centre, France
49. United Nations Environmental Programme, UNEP (1994) The pollution of lakes and reservoirs. Environmental Library No. 12, Nairobi, Kenya. pp 9–33
50. World Wide Fund for Nature (WWF) and Asian Wetland Bureau (AWB) (1993) Directory of Indian Wetlands. World Wide Fund for Nature and Asian Wetland Bureau, New Delhi and Kuala Lumpur
51. Zedler JB (2003) Wetlands at your service: reducing impacts of agriculture at the watershed scale. *Front Ecol Environ* 1:65–72

Annual Rainfall Prediction Using Artificial Neural Networks



Anjaney Singh , Amit Dua , and A. P. Singh 

Abstract The hydrological cycle depends primarily on rainfall. It is of utmost importance to measure and predict accurately the spatial and temporal distribution of rainfall for countries flourishing agricultural growth. However, developing and implementing rainfall predictive models is one of the most challenging problems due to its highly nonlinear characteristics. The prediction of rainfall has been observed to deviate from the real data because of dependence on a large number of complex parameters and involving high uncertainty. Artificial neural network (ANN) is a pioneering approach, which facilitates a computationally intelligent system to possess humanlike expertise, adapt itself, and attempt to acquire to do better in varying environments so that decisions become useful for planning and management. Unlike conventional artificial intelligence techniques, the guiding principle of soft computing such as ANN is to achieve tolerance for inaccuracy, uncertainty, robustness, and partial truth to realize tractability and a better understanding of reality. Rainfall is one of nature's greatest gifts which has become even more important in the states like Rajasthan which has historically been a water-deficient state with only 1% of the country's water resources available in 10.4% geographical area. It is thus a major concern to identify any trends for rainfall and predict it accordingly so that it would give greater insight among the people and would help the planners, administration, technicians, researchers, and NGOs engaged in the decision-making process of water conservation to make sustainable development and management. Therefore, this paper deals with a case study of annual rainfall prediction in the Chittorgarh district of Rajasthan by taking 53 years of historical rainfall data of Chittorgarh for training the ANN. The ANN has also been validated with another set of data of 13 years. The transfer function used for all three layers of ANN was the radial basis transfer function (RADBAS). The number of iterations involved in the process has been taken as 100,000 which finally leads to achieving a mean square error of 0.005 during the training process of the normalized data. The current manuscript presents

A. Singh (✉) · A. Dua

Department of CS & IS, Birla Institute of Technology and Science, Pilani, India

e-mail: asinghbits5@gmail.com

A. P. Singh

Department of Civil Engineering, Birla Institute of Technology and Science, Pilani, India

the comparison of the network predicted outputs with the actual rainfall data. The results depict that the proposed network model can efficiently scale to other parts of the country and can prove to be a great asset.

Keywords Artificial neural network · Seasonal rainfall forecast

1 Introduction

It is the need of the hour to dexterously use the modeling techniques to efficiently use water resources. Accurate prediction of precipitation can only be possible when the ground conditions and other physical parameters are taken into consideration. Most hydrological processes comprise a high degree of temporal and spatial variation and are further pursued by the nonlinear variation in physical processes and uncertainty in data measurement. Hence, one can make use of ANN, which predicts outputs without the physics being explicitly provided to it. ANNs have been widely used in the estimation of the values of variables in various hydrological processes including water quantity and quality, rainfall-runoff modeling, reservoir sizing and operations management, precipitation forecasting, time series analysis, as described by ASCE Task Committee reports [1, 4]. Some of these studies deal with the estimation of flow rate [7, 8], modeling of precipitation and runoff [2, 10, 13, 15], hydrologic time series modeling [9, 11], and sediment transport prediction [3]. Thus, the modeling of the system by making use of artificial neural networks (ANN) is more effective than traditional systems.

Chittorgarh is an ancient town, located in the state of Rajasthan. It is on the Berach River, a tributary of the Banas, and is well known for its bravery in the Indian subcontinent. The Chittorgarh district is one of the districts in the southern part of the state which is the 14th largest district by population and contains the largest forest area. The Chittorgarh district area falls in the Banas catchment (52%), Chambal catchment (27%), and Mahi catchment (21%). However, this study deals with a watershed falling under the Banas catchment of Chittorgarh district which covers the maximum geographical area of the district. In Chittorgarh district, five Panchayat Samities of Bhadesar, Chittorgarh, Gangrar, Kapasan, and Rashmi fall completely (100%) in the Banas catchment and the remaining nine Panchayat Samities partly fall in different catchments of Banas, Chambal, and Mahi. The water divides run between Chambal and Mahi in Arnod and Pratapgarh, between Mahi and Banas in Chhoti Sadri and Bari Sadri, and between Chambal and Banas in Nimbahera and Begun Panchayat Samities. It is interesting to know that part of the water runoff of Chittorgarh district flows through Jakham and Mahi to the Arabian Sea in the west while a major part flows to the Bay of Bengal through Berach, Banas, Chambal, Yamuna, and the Ganges River in the east [17]. The Berach River originates in the hills of the Udaipur district. The study which tries to develop an ANN model to predict rainfall will be useful for making efficient use of water resources in the future. It would also be useful in predicting the groundwater levels, crop planting

decisions, and reservoir water resource allocation and decide upon a strategy for the years to come. The river water level of the Berach River would also depend on the rainfall and runoff in the region. Hence, the forecast of future rainfall can be helpful for making efficient operating decisions.

In this study, ANN, one of the artificial intelligence techniques, is used to forecast rainfall. ANN consists of connected neurons in different layers to best emulate the human brain through nonlinear mathematical modeling. Its architecture deals with the number of nodes, connectivity pattern between nodes, the methodology used to determine weights, suitable activation functions, backpropagation error estimation process, etc. Artificial neural networks are generally classified on the basis of the direction of the flow of information and processing mechanism. For example, in the case of a feed-forward network, the nodes are specified in layers, each of which may single or multiple nodes. Information is transmitted from an input layer to the output layer because nodes of one layer are linked to nodes of the next layer. Also, the nodes in a given layer do not connect with the other nodes of the same layer. Thus, the output value of a node in a layer is determined using the inputs coming from the preceding layers and the respective weights assigned for the i th node of the preceding layer to the j th node of the next layer.

In most networks, the input layer receives the input variables (the rainfall for the previous years in this case). The rainfall at a place can be dependent on various factors such as physiographical features, rainfall pattern, latitude, and longitude. Thus, the number of nodes can be decided based on the availability of data. Once such information is fixed, target (output) values can be predicted. Thus, the input layer serves as providing information to the network in a transparent manner. The output layer is the final layer that provides the predicted value of the network. The various hidden layers and the number of nodes in each hidden layer are determined by repeated statistical and experimental analysis. The weights corresponding to the link are corrected in each epoch by the gradient descent process is the heart of the training process.

As far as district Chittorgarh's physiographical features are concerned, it is traversed by linear to arcuate hills, dissected plateaus, buried pediments, ravines, valley fills, and isolated small alluvial plains. As far as land utilization pattern is concerned, it reveals about 18% forest land and about 40% cultivated land. The wind is prominent in the months of April to July with higher speed occasionally up to 60–70 km per hour. The temperature ranges between 0.2 and 46 °C with humidity levels up to 62%. The annual average wind speed is 6 km/h, humidity 41–62%, and potential evapo-transpiration about 1635 mm. The average intensity of annual rainfall occurs at 772 mm in about 33 monsoon days in a year. In the last 22 years (1997–2019), the average annual rainfall varied between 410 mm (2002) and 1029 mm (1994). The lowest rainfall year was 1981 (368 mm) after independence. It was also low in the year 2002 (393 mm).

In this paper, an attempt has been made to predict rainfall using ANN, the basic principle of which has been discussed in the subsequent section.

2 Basic Principles of the Neural Networks

ANN is a powerful parallel computing system involving a large number of processing elements that work on principles similar to the biological neural networks. It constitutes primarily three components, namely nodes, link weights, and activation functions.

ANN is a powerful statistical modeling technique that can be used for solving problems with nonlinear properties. Various researchers have used ANN for solving nonlinear problems in various domains [1, 5, 6, 16, 18].

The nodes are connected to each other through links which are also called synapses. There is a weight factor associated with each synapse. These networks are trained with the help of available past data so that a given set of inputs can produce better target outputs, with high accuracy and least error. However, it depends on the availability of past data used for prediction target values.

2.1 Feed-Forward Backpropagation Neural Networks (FFNN)

The feed-forward three-layered ANN has various nodes in each layer. The nodes process information at the input layer and present the result as the output to the layer through each node. The weights assigned to each link affect the outcome of that node as they signify the signal strength between the nodes. The number of input and output parameters determines the neurons in the input and output layers, respectively. The current work uses the FFNN for prediction.

The input layer, hidden layers, and output layer together with the weights associated with every connection are depicted in Fig. 1. As observed, the nodes are connected between adjacent layers and within a particular layer, they are not connected among each other.

2.2 Radial Basis Neural Networks (RBNN)

RBNN uses the radial basis functions (RBF) that work on distance criteria and is extensively used for interpolation. RBF are used in place of sigmoid transfer function in all three layers either nonlinearly with hidden layers or linearly with the output layer.

RBF networks are advantageous over the feed-forward networks, especially when local minima is being locked while performing the analysis. When the input lies within the localized region of input space, the hidden layer functions generate a nonzero response. The term localized receptive field network is also used extensively for them [12]. RBNN uses radial fixed shape function for input transformation [8].

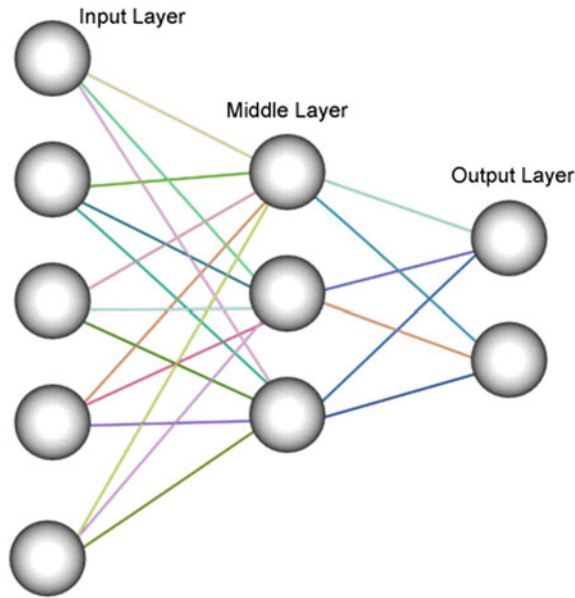


Fig. 1 General structure of three-layered FFNN

The RBF works as a regressor after eliminating the nonlinearity from the multidimensional output space. These regressors are implemented by the output layer with adjustments possible only in the corresponding weights. The least-square method is used to determine parameters and optimally converge. The trial-and-error technique is used with the different number of iterations to achieve the best spread over constants in the RBNN models. RBNN model is depicted in Fig. 2.

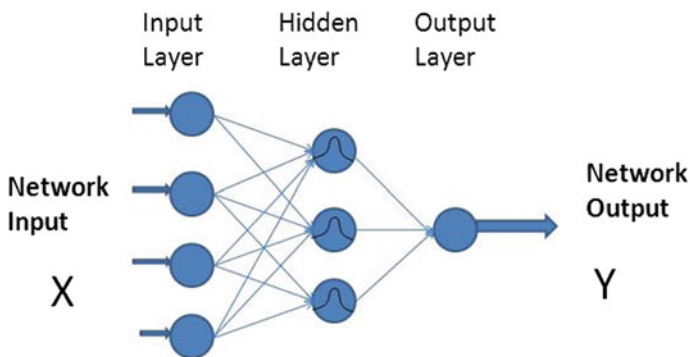


Fig. 2 General structure of a RBNN

3 Application of the Ann Model

3.1 Definition of Study Area

Yearly rainfall data from 1939 to 2019 at Chittorgarh town are used in this study. The yearly rainfall data were taken from Irrigation Division-1, Chittorgarh district. The minimum yearly rainfall was 326.4 mm in 1952 and the maximum rainfall was 1475 mm in 1945. The average yearly rainfall was found to be 816.3 mm. The average intensity of annual rainfall occurs at 772 mm in about 33 monsoon days in a year.

3.2 Application of Feed-Forward Backpropagation Neural Networks

At the start of the experimentation, the input and output variables were normalized between 0.1 and 0.9. This was done before the training phase using the following equation:

$$\alpha_{\text{norm}} = 0.8 \times \frac{(\alpha - \alpha_{\text{min}})}{(\alpha_{\text{max}} - \alpha_{\text{min}})} + 0.1 \quad (1)$$

In Eq. (1), α_{norm} denotes the normalized value of the input parameter, α denotes the observed value of the parameter with α_{min} , α_{max} signifying the minimum and maximum values of the corresponding parameters, respectively.

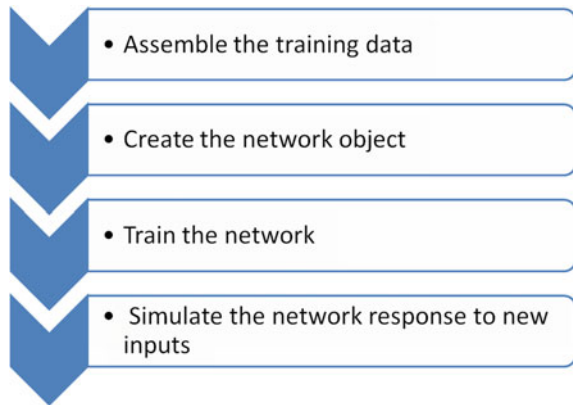
The networks can be exposed to under fitting and over fitting when too few or too many nodes in hidden layers are considered. The primary reason for these problems is the high sensitivity of the network. Several combinations were tested for hidden layers and nodes in these layers to attain the optimum configuration of the network. In order to reach an optimum amount of hidden layer nodes, different numbers of nodes are tested. Finally, three layers with two hidden layers have been considered to analyze the problem. The rainfall data in the past four years have been considered as the input data and the fifth year rainfall data have been used as output. The program has been initialized with the function ‘initlay’ and the performance function has been evaluated using mean square error (MSE). The ‘traincgf’ is used as the training function of the process using MATLAB version 7 [14].

The backpropagation uses the gradient to adjust the weights such that the gradient is negative. The adjusted weights make sure that the performance function decreases sharply. Even though the function decreases sharply along with the negative of the gradient, it does not always result in the fastest convergence. The conjugate gradient algorithm is utilized that produces the quickest convergence by searching along the conjugate direction. The experiments prove that the conjugate gradient algorithm works better than the steepest descent algorithm.

Table 1 Summary of ANN data for rainfall prediction

Training period (years)	53 years
Test period (years)	13 years
No. of layers	3 (including 2 hidden)
Transfer function used	Radial basis
No. of iterations	100,000
Mean square error for the normalized training data	0.005
Mean square error for the normalized data during the test period	0.2677

Fig. 3 Flowchart used for developing the ANN model



In this case study, annual rainfall prediction in the Chittorgarh district of Rajasthan has been made by taking 53 years of historical rainfall data of Chittorgarh for training the ANN which has been further tested for another 13 years [17]. The transfer function used for all three layers of ANN was the radial basis transfer function (RADBAS). The number of iterations involved in the process has been taken as 1,00,000 which finally leads to achieve a mean square error of 0.005 during the training process of the normalized data. The important parameters of the ANN model have been summarized in Table 1 and the flowchart used for developing the ANN model is illustrated in Fig. 3.

4 Results and Discussions

The results obtained during training as well as the test period are given in the form of scatter plots as shown in Figs. 4 and 5. In the end, network predicted outputs were compared with the actual rainfall data to evaluate performance of the network.

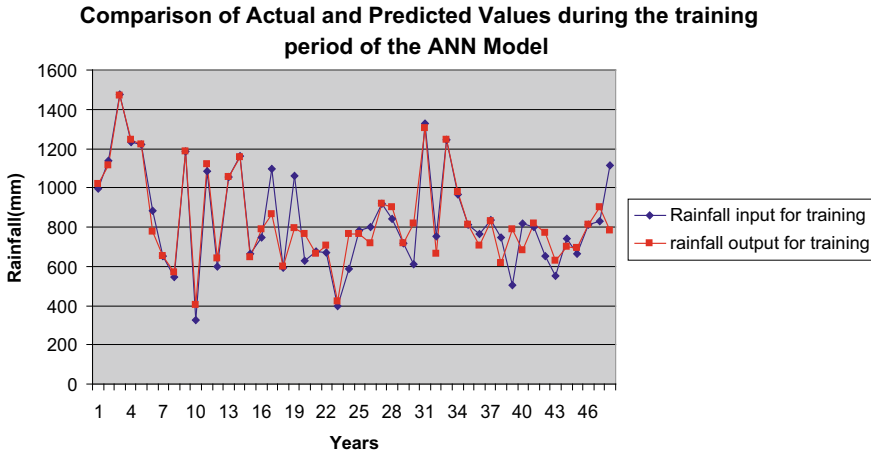


Fig. 4 Comparison of input and output during the training period

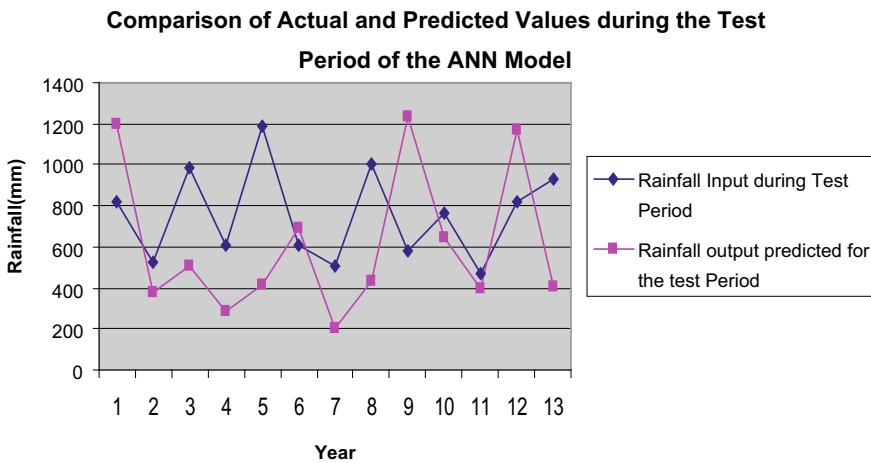


Fig. 5 Comparison of actual and predicted values during the test period

4.1 Training

Once the network weights and biases have been assigned, training of the network can be performed. It can be trained using different algorithms: approximation (nonlinear regression) function, pattern classification, pattern association, and so on. The training process should be initiated by feeding a set of network inputs (p) and target outputs (t). While running the algorithm of training, the weighing factors and biases of the network are adjusted in an iterative manner using the backpropagation

algorithm to minimize the network performance function net.performFcn . Generally, in the feed-forward networks, performance is evaluated using mean square error (MSE), which is defined as the average squared error between the network outputs (a) and the target outputs (t).

Figure 4 shows a comparative plot of our input and output rainfall values during the course of the training period of the ANN model used. The mean square error achieved was 0.005. The training was done for a period of 53 years taking the immediate previous four values as the input for the values. The number of iterations used was 100,000. To train the system to the required level of accuracy, more relevant data are required. The further scope for this study includes obtaining the data and improving the accuracy of the system in order to be able to use it for real-life prediction and validation.

4.2 Testing

Figure 5 shows a comparative plot of the actual and predicted values obtained for the test period of the ANN model. The testing was done for a duration of 13 years. The mean square error of the normalized error achieved during the testing period was 0.2677. The values predicted by the model are quite close to the actual values for the second, sixth, eleventh, and twelfth year. For the other years, the rainfall predicted by the model showed greater variability. This can be attributed to insufficient training data (53 years).

The high variability in the actual and predicted values during the test period can be attributed to the short duration of the training period. The training was done only for 53 years due to the lack of sufficient rainfall data for the Chittorgarh region. Another reason that can cause such variability would be that the data retrieved from the source might not have been very accurate. This affects the result considerably as the more reliable the data provided to the ANN model, the better the output it can predict.

The training rate used for the purpose of the training was 0.5 and the required goal was set as 0.005 or in other words a 0.5% margin was allowed for error in prediction. The number of neurons used in the different layers was determined by a trial-and-error approach. Simulation results reveal that artificial neural network techniques are promising and efficient which provide relatively better performance compared to the error goal that was set. However, the predicted result can be more accurate if the artificial neural network is trained with more input and output parameters in the training phase.

5 Conclusion

This study explores the application of an artificial neural network model to predict rainfall in the Chittorgarh district of Rajasthan, India. Therefore, this paper deals with a case study of annual rainfall prediction in Chittorgarh district of Rajasthan using ANN by taking a total of 53 years of historical rainfall data that has been used to train the ANN which has been further tested for another set of data of 13 years. The transfer function used for all three layers of ANN was the radial basis transfer function (RADBAS). The number of iterations involved in the process has been taken as 100,000 which finally leads to achieving a mean square error of 0.005 during the training process of the normalized data. Though the historical data has been used to analyze the outcome using NNtools, it would be better if various factors such as physiographical features, rainfall pattern over the years with seasonality, air temperature and saturation pressure, humidity in the atmosphere, latitude, and longitude specific information are incorporated in the input layer to predict the rainfall in much more generalized manner. Such a generalized prediction model using artificial intelligence techniques will help water managers to take appropriate decisions to a greater extent.

References

1. Abhishek K, Kumar A, Ranjan R, Kumar S (2012) A rainfall prediction model using artificial neural network. In: 2012 IEEE control and system graduate research colloquium. IEEE, pp 82–87
2. Antar MA, Ellassiouti I, Alam MN (2006) Rainfall-runoff modelling using artificial neural Networks technique: a Blue Nile catchment case study. *Hydrol Process* 20:1201–1216
3. Agarwal A, Mishra SK, Ram S, Singh JK (2006) Simulation of runoff and sediment yield using artificial neural networks. *Biosyst Eng* 94(4):597–613
4. ASCE Task Committee on Application of Artificial Neural Networks in Hydrology (2000) Artificial neural networks in hydrology i: preliminary concepts *J Hydrol Eng* 5(2):115–123
5. Chattopadhyay S (2007) Feed forward Artificial Neural Network model to predict the average summer-monsoon rainfall in India. *Acta Geophys* 55(3):369–382
6. Dao DV, Ly HB, Trinh SH, Le TT, Pham BT (2019) Artificial intelligence approaches for prediction of compressive strength of geopolymer concrete. *Materials* 12(6):983
7. Dibike YB, Solomatine DP (2001) River flow forecasting using artificial neural networks. *Phys Chem Earth (B)* 26:1–7
8. Firat M, Gungor M (2007) River flow estimation using feed forward and radial basis neural network approaches. In: Proceedings of international congress on river basin management. Antalya, Turkey, March 22–24, p 599–611
9. French MN, Krajewski WF, Cuykendal RR (1992) Rainfall forecasting in space and time using a neural network. *J. Hydrol. Amsterdam* 137:1–37
10. Kumar AR, Sudheer KP, Jain SK, Agarwal PK (2005) Rainfall-runoff modelling using artificial neural Networks: comparison of network types. *Hydrol Process* 19:1277–1291
11. Lachtermacher G, Fuller JD (1994) Backpropagation in hydrological time series forecasting. In: Hipel KW et al (eds) *Stochastic and statistical methods in hydrology and environmental engineering time series analysis in hydrology and environmental engineering*, vol 3. Kluwer, Dordrecht, The, Netherlands, pp 229–242

12. Lee GC, Chang SH (2003) Radial basis function networks applied to DNBR calculation in digital core protection systems. *Ann Nucl Energy* 30:1561–1572
13. Luk CK, Ball JE, Sharma A (2001) An application of artificial neural networks for precipitation forecasting. *Math Comput Modeling* 33:683–693
14. MATLAB (2004) Documentation neural network toolbox help, Version 7.0, Release 14. The Math Works, Inc.
15. Sajikumar N, Thandaveswara BS (1999) A non-linear rainfall–runoff model using an artificial neural network. *J Hydrol* 216:32–55
16. Salimi AH, Masoompour Samakosh J, Sharifi E, Hassanvand MR, Noori A, von Rautenkranz H (2019) Optimized artificial neural networks-based methods for statistical downscaling of gridded precipitation data. *Water* 11(8):1653
17. Tanwar BS (2004) A study on water resource management for District Chittorgarh, Birla Corporation Limited Chittorgarh, p 45–60
18. Wagale M, Singh AP, Singh A (2016) Neural networks approach for evaluating quality of service in public transportation in rural areas. In: 2016 1st India international conference on information processing (IICIP). IEEE, pp 1–5